

Cardiovascular Regenerative Medicine

Tissue Engineering and Clinical
Applications

Vahid Serpooshan
Sean M. Wu
Editors

 Springer

Cardiovascular Regenerative Medicine

Vahid Serpooshan • Sean M. Wu
Editors

Cardiovascular Regenerative Medicine

Tissue Engineering and Clinical
Applications

 Springer

Editors

Vahid Serpooshan
Department of Biomedical Engineering
Emory University School of Medicine
and Georgia Institute of Technology
Atlanta, GA
USA

Sean M. Wu
Cardiovascular Institute and
Department of Medicine,
Division of Cardiovascular Medicine,
Stanford University
Stanford, CA
USA

Department of Pediatrics
Emory University School of Medicine
Atlanta, GA
USA

Children's Healthcare of Atlanta
Atlanta, GA
USA

ISBN 978-3-030-20046-6 ISBN 978-3-030-20047-3 (eBook)
<https://doi.org/10.1007/978-3-030-20047-3>

© Springer Nature Switzerland AG 2019

This work is subject to copyright. All rights are reserved by the Publisher, whether the whole or part of the material is concerned, specifically the rights of translation, reprinting, reuse of illustrations, recitation, broadcasting, reproduction on microfilms or in any other physical way, and transmission or information storage and retrieval, electronic adaptation, computer software, or by similar or dissimilar methodology now known or hereafter developed.

The use of general descriptive names, registered names, trademarks, service marks, etc. in this publication does not imply, even in the absence of a specific statement, that such names are exempt from the relevant protective laws and regulations and therefore free for general use.

The publisher, the authors, and the editors are safe to assume that the advice and information in this book are believed to be true and accurate at the date of publication. Neither the publisher nor the authors or the editors give a warranty, express or implied, with respect to the material contained herein or for any errors or omissions that may have been made. The publisher remains neutral with regard to jurisdictional claims in published maps and institutional affiliations.

This Springer imprint is published by the registered company Springer Nature Switzerland AG
The registered company address is: Gewerbestrasse 11, 6330 Cham, Switzerland

Cardiovascular Regenerative Medicine: An Introduction

In the past decades, the progress made in cardiovascular regenerative medicine has been nothing but spectacular. From an improved understanding of how the heart develops in the earliest stages of fetal development to barriers that prevents an adult cardiomyocytes to undergo cell division, we have come a long way to identify potential therapeutic strategies that can mediate the repair and regeneration of the mammalian heart. While much scientific progress has been celebrated and showcased at research conferences and in published studies, the stark reality remains that cardiovascular disease is the number one cause of death in the Western world with rapidly rising incidence in developing countries such as China and India. Given this, the interest in developing new therapies for treating, if not curing, damaged hearts remains strong.

Therapeutic approaches to treat cardiovascular diseases span a broad spectrum from small molecules/drugs (least invasive) to heart transplant (most invasive). Unfortunately, while drugs have helped improve the quality-of-life of patients with heart failure, they have not significantly alter the overall course of disease. On the other hand, heart transplant is life saving and provides a durable solution to heart failure, the number of hearts available for transplant is limited to roughly 2200 per year in the U.S. and this number has not changed significantly in the past three–four decades. Given that there are in excess of 100,000 patients waiting and dying while on the heart transplant waitlist, there is a great need to find innovative solutions to stem the rising tide of mortality due to heart failure. Hence, cardiovascular investigators have actively sought new therapeutic strategies that fills this large void between these two therapeutic extremes.

With the discovery of stem cells from tissue/resident sources, early human embryos, and more recently induced from somatic cells by the over-expression of key pluripotent transcription factors, many investigators have turned to using stem cell-derived cardiac cells as the therapeutic agent to help repair and regenerate lost heart tissue. The remarkable potential for stem cells to differentiate into cardiac cells has naturally led to the interest in applying these different types of stem cells in clinical studies. The transplantation of autologous adult derived stem cells to treat heart disease has received significant attention in the past 15 years and is a topic that will be addressed in Chap. 9. In parallel, the rapidly expanding field of bioengineering has taken notice of the possibility of creating new cardiac tissues or even replacement organs using stem cell-derived cardiac cells. The convergence of stem

cell biology and bioengineering may represent one of the greatest synergy for generating new therapy for cardiovascular diseases and improving the care of heart disease patients. Given the numerous advances that have been made in this area, we have chosen to devote a number of Chaps. 3, 4, 5, and 6 to this topic.

Among the different stem cells types that are being explored, induced pluripotent stem cells (iPSCs) has received significant attention due to the lesser concerns ethically compare with human embryonic stem cells (ESCs) and greater differentiation potential into various cardiac cell types compare with autologous stem cells from the blood, bone marrow, or adipose tissues. Indeed, these iPSC cells derived from human carrying specific genetic mutation has been actively explored by cardiovascular investigators in a strategy akin to “disease-in-a-dish”. In Chaps. 1 and 2, the use of iPSC to model arrhythmia, sarcomeric gene mutation with contractile defect, and metabolic syndrome will be discussed. The use of patient/disease-specific iPSC has raised the exciting prospect for being able to deliver personalized treatment in a way that meets the intent of precision medicine. Indeed, numerous studies have now shown the faithful recapitulation of cardiac disease phenotype in the *in vitro* differentiated iPSC-derived cardiomyocytes and endothelial cells. Furthermore, the use of these disease models for high throughput drug discovery will be highlighted in Chap. 2, since there is no longer a limitation on the number of cardiac cells available for screening hundreds of thousands of compounds at a time.

While iPSC-derived cardiac cells show significant promise as a drug discovery and disease modeling platform, they represent another source of stem cells that may be used for autologous cell-based therapy. Thus far, very few clinical studies have utilized human iPSC as the cell source due to concerns for teratoma formation, low rate of cell engraftment, and toxicity from potentially lethal arrhythmia. Fortunately, there has been no reported incidence of teratoma formation when human ESC/iPSC-derived cardiac cells were injected into hearts of large animal models. However, the size of the transplanted cell graft is generally small and declines in size over time. Notably, there was an extremely high incidence of ventricular tachycardia in non-human primates that receiving iPSC-CM injection. To overcome this challenge, cardiovascular investigator have turn to creating engineered tissue that can be perfused and integrated to connect with the host. The hope is that these engineered tissues will be better aligned and organized so that their arrhythmogenic potential will be reduced as well. This strategy will be explored in Chaps. 8 and 9 on engineering of cardiac patch for regenerative medicine.

Aside from the goal of remuscularization of the damaged heart, it has been shown that some improvement in cardiac function may be achieved when the adverse remodeling of the heart can be prevented after myocardial infarction. This was originally shown in an unique surgical procedure where the latissimus dorsi muscle of the patient is resected and used as a flap to wrap around the epicardial surface of the infarcted region of the heart. This was intended to prevent the aneurysmal ballooning of that region of the heart and promote normal pump function of the left ventricle. Subsequent studies have found that much if not all of the benefit from this invasive surgical procedure can be recapitulated by injection of biomaterials into the infarcted regions. A number of biomaterials such as fibrin, alginate, and

decellularized cardiac matrix have been studied in recent year. These studies will be discussed in Chap. 10 on injectable hydrogel biomaterial for treatment of myocardial infarction.

Beyond the treatment of adult cardiac diseases, a special consideration needs to be given to the treatment of pediatric patients with congenital heart diseases. As detailed in Chap. 11, the treatment of children with congenital heart diseases has been particularly challenging due to the severity of their disease, the need for continued growth during childhood, and the complexity of their cardiac anatomy. Furthermore, the number of patients available for clinical study is generally small so conclusions are harder to reach when the error bars for studies are large. Nevertheless, significant advances have been made in generating engineered heart valves and vascular grafts for surgical and percutaneous repair of children with heart disease. These advances will be covered in Chap. 11 on regenerative medicine for the treatment of congenita heart diseases.

In summary, we hope this book will illustrate both the challenges and excitement of regenerative medicine and tissue engineering for cardiovascular applications. By incorporating advances in stem cell biology, biomaterials, and high through put drug screen, we hope that new therapies for children and adults with heart disease will be available in the near future.

Stanford, CA, USA
Atlanta, GA, USA

Sean M. Wu
Vahid Serpooshan

Contents

1	Tissue-Engineered Stem Cell Models of Cardiovascular Diseases	1
	Christopher W. Anderson, Jiesi Luo, Lorenzo R. Sewanan, Mehmet H. Kural, Muhammad Riaz, Jinkyu Park, Yan Huang, Laura E. Niklason, Stuart G. Campbell, and Yibing Qyang	
2	Phenotypic Screening of iPSC-Derived Cardiomyocytes for Cardiotoxicity Testing and Therapeutic Target Discovery	19
	Arne A. N. Bruyneel, Tyler Muser, Vaidya Parthasarathy, Dries Feyen, and Mark Mercola	
3	Decellularized Extracellular Matrix-Based Cardiovascular Tissue Engineering	35
	Kristin M. French and Michael E. Davis	
4	3D Bioprinting of Cardiovascular Tissue Constructs: Cardiac Bioinks	63
	Martin L. Tomov, Andrea Theus, Rithvik Sarasani, Huyun Chen, and Vahid Serpooshan	
5	Nanobiomaterial Advances in Cardiovascular Tissue Engineering	79
	Michael J. Hill, Morteza Mahmoudi, and Parisa P. S. S. Abadi	
6	Bioengineering 3D Cardiac Microtissues Using Bioassembly	107
	Longjun Gu, Jinghan Feng, Donghui Zhang, and Pu Chen	
7	From Bench to Clinic: Translation of Cardiovascular Tissue Engineering Products to Clinical Applications	125
	Amanda N. Steele and Y. Joseph Woo	
8	Cardiac Patch-Based Therapies of Ischemic Heart Injuries	141
	Wuqiang Zhu, Danielle Pretorius, and Jianyi Zhang	
9	Cell-Based Cardiovascular Regenerative Therapies	173
	Ray P. Prajnamitra, Yuan-Yuan Cheng, Li-Lun Chen, and Patrick C. H. Hsieh	
10	Injectable Hydrogels to Treat Myocardial Infarction	185
	Miranda D. Diaz and Karen L. Christman	

11 Regenerative Medicine for the Treatment of Congenital Heart Disease 207
Elda Dzilic, Stefanie Doppler, Rüdiger Lange, and Markus Krane

12 Cardiovascular Regenerative Medicine: Challenges, Perspectives, and Future Directions 223
Sean M. Wu and Vahid Serpooshan

Index 227

Contributors

Parisa P. S. S. Abadi, Ph.D. Department of Mechanical Engineering-Engineering Mechanics, Michigan Technological University, Houghton, MI, USA

Department of Biomedical Engineering, Department of Materials Science and Engineering, Michigan Technological University, Houghton, MI, USA

Christopher W. Anderson, Ph.D. Vascular Biology and Therapeutics Program, Yale University, New Haven, CT, USA

Department of Pathology, Yale University, New Haven, CT, USA

Arne A. N. Bruyneel, Ph.D. Cardiovascular Institute and the Department of Medicine, Stanford University, Stanford, CA, USA

Stuart G. Campbell, Ph.D. Department of Biomedical Engineering, Yale University, New Haven, CT, USA

Yale Stem Cell Center, New Haven, CT, USA

Huyun Chen Wallace H. Coulter Department of Biomedical Engineering, Emory University School of Medicine and Georgia Institute of Technology, Atlanta, GA, USA

Li-Lun Chen, Ph.D. Institute of Biomedical Sciences, Academia Sinica, Taipei, Taiwan

Pu Chen, Ph.D. Department of Biomedical Engineering, School of Basic Medical Sciences, Wuhan University, Wuhan, China

Institute of Hepatobiliary Diseases of Wuhan University, Transplant Center of Wuhan University, Hubei Key Laboratory of Medical Technology on Transplantation, Wuhan, China

Yuan-Yuan Cheng, Ph.D. Institute of Biomedical Sciences, Academia Sinica, Taipei, Taiwan

Karen L. Christman, Ph.D. Department of Bioengineering, University of California, San Diego, La Jolla, CA, USA

Sanford Consortium for Regenerative Medicine, San Diego, La Jolla, CA, USA

Michael E. Davis, Ph.D. Wallace H. Coulter Department of Biomedical Engineering, Emory University, Atlanta, GA, USA

Division of Cardiology, Emory University School of Medicine, Atlanta, GA, USA

Miranda D. Diaz, Ph.D. Department of Bioengineering, University of California, San Diego, La Jolla, CA, USA

Sanford Consortium for Regenerative Medicine, San Diego, La Jolla, CA, USA

Stefanie Doppler, M.D. Department of Cardiovascular Surgery, German Heart Center Munich at the Technische Universität München, Munich, Germany

Insure (Institute for Translational Cardiac Surgery), Department of Cardiovascular Surgery, German Heart Center, Technische Universität München, Munich, Germany

Elda Dzilic, M.D. Department of Cardiovascular Surgery, German Heart Center Munich at the Technische Universität München, Munich, Germany

Insure (Institute for Translational Cardiac Surgery), Department of Cardiovascular Surgery, German Heart Center, Technische Universität München, Munich, Germany

Jinghan Feng, Ph.D. Department of Biomedical Engineering, School of Basic Medical Sciences, Wuhan University, Wuhan, China

Institute of Hepatobiliary Diseases of Wuhan University, Transplant Center of Wuhan University, Hubei Key Laboratory of Medical Technology on Transplantation, Wuhan, China

Dries Feyen, Ph.D. Cardiovascular Institute and the Department of Medicine, Stanford University, Stanford, CA, USA

Kristin M. French, Ph.D. Internal Medicine, Cardiology, University of Texas Southwestern Medical Center, Dallas, TX, USA

Longjun Gu, Ph.D. Department of Biomedical Engineering, School of Basic Medical Sciences, Wuhan University, Wuhan, China

Institute of Hepatobiliary Diseases of Wuhan University, Transplant Center of Wuhan University, Hubei Key Laboratory of Medical Technology on Transplantation, Wuhan, China

Michael J. Hill, Ph.D. Department of Mechanical Engineering-Engineering Mechanics, Michigan Technological University, Houghton, MI, USA

Patrick C. H. Hsieh, M.D., Ph.D. Institute of Biomedical Sciences, Academia Sinica, Taipei, Taiwan

Yan Huang, Ph.D. Vascular Biology and Therapeutics Program, Yale University, New Haven, CT, USA

Department of Internal Medicine, Section of Cardiovascular Medicine, Yale Cardiovascular Research Center, Yale School of Medicine, New Haven, CT, USA

Markus Krane, M.D. Department of Cardiovascular Surgery, German Heart Center Munich at the Technische Universität München, Munich, Germany

Insure (Institute for Translational Cardiac Surgery), Department of Cardiovascular Surgery, German Heart Center, Technische Universität München, Munich, Germany
DZHK (German Center for Cardiovascular Research), Partner Site Munich Heart Alliance, Munich, Germany

Mehmet H. Kural, Ph.D. Department of Biomedical Engineering, Yale University, New Haven, CT, USA

Department of Anesthesiology, Yale University, New Haven, CT, USA

Rüdiger Lange, M.D. Department of Cardiovascular Surgery, German Heart Center Munich at the Technische Universität München, Munich, Germany

DZHK (German Center for Cardiovascular Research), Partner Site Munich Heart Alliance, Munich, Germany

Jiesi Luo, Ph.D. Vascular Biology and Therapeutics Program, Yale University, New Haven, CT, USA

Department of Internal Medicine, Section of Cardiovascular Medicine, Yale Cardiovascular Research Center, Yale School of Medicine, New Haven, CT, USA

Morteza Mahmoudi, Ph.D. Department of Anesthesiology, Brigham and Women's Hospital, Harvard Medical School, Boston, MA, USA

Precision Health Program, Department of Radiology, College of Human Medicine, Michigan State University, East Lansing, MI, USA

Mark Mercola, Ph.D. Cardiovascular Institute and the Department of Medicine, Stanford University, Stanford, CA, USA

Tyler Muser, B.S. Cardiovascular Institute and the Department of Medicine, Stanford University, Stanford, CA, USA

Laura E. Niklason, M.D., Ph.D. Vascular Biology and Therapeutics Program, Yale University, New Haven, CT, USA

Department of Biomedical Engineering, Yale University, New Haven, CT, USA

Department of Anesthesiology, Yale University, New Haven, CT, USA

Yale Stem Cell Center, New Haven, CT, USA

Jinkyu Park, Ph.D. Vascular Biology and Therapeutics Program, Yale University, New Haven, CT, USA

Department of Internal Medicine, Section of Cardiovascular Medicine, Yale Cardiovascular Research Center, Yale School of Medicine, New Haven, CT, USA

Vaidya Parthasarathy, Ph.D. Cardiovascular Institute and the Department of Medicine, Stanford University, Stanford, CA, USA

Ray P. Prajnamitra, Ph.D. Institute of Biomedical Sciences, Academia Sinica, Taipei, Taiwan

Danielle Pretorius Department of Biomedical Engineering, School of Medicine, School of Engineering, University of Alabama at Birmingham, Birmingham, AL, USA

Yibing Qyang, Ph.D. Vascular Biology and Therapeutics Program, Yale University, New Haven, CT, USA

Department of Pathology, Yale University, New Haven, CT, USA

Department of Internal Medicine, Section of Cardiovascular Medicine, Yale Cardiovascular Research Center, Yale School of Medicine, New Haven, CT, USA

Yale Stem Cell Center, New Haven, CT, USA

Muhammad Riaz, Ph.D. Vascular Biology and Therapeutics Program, Yale University, New Haven, CT, USA

Department of Internal Medicine, Section of Cardiovascular Medicine, Yale Cardiovascular Research Center, Yale School of Medicine, New Haven, CT, USA

Rithvik Sarasani Scheller College of Business, Georgia Institute of Technology, Atlanta, GA, USA

Vahid Serpooshan, Ph.D. Department of Biomedical Engineering, Emory University School of Medicine and Georgia Institute of Technology, Atlanta, GA, USA

Department of Pediatrics, Emory University School of Medicine, Atlanta, GA, USA

Children's Healthcare of Atlanta, Atlanta, GA, USA

Lorenzo R. Sewanan, Ph.D. Department of Biomedical Engineering, Yale University, New Haven, CT, USA

Amanda N. Steele, Ph.D. Department of Cardiothoracic Surgery, Stanford University, Stanford, CA, USA

Department of Bioengineering, Stanford University, Stanford, CA, USA

Andrea Theus, M.S. Wallace H. Coulter Department of Biomedical Engineering, Emory University School of Medicine and Georgia Institute of Technology, Atlanta, GA, USA

Martin L. Tomov, Ph.D. Wallace H. Coulter Department of Biomedical Engineering, Emory University School of Medicine and Georgia Institute of Technology, Atlanta, GA, USA

Y. Joseph Woo, M.D. Department of Cardiothoracic Surgery, Stanford University, Stanford, CA, USA

Department of Bioengineering, Stanford University, Stanford, CA, USA

Sean M. Wu, M.D., Ph.D. Cardiovascular Institute and Department of Medicine, Division of Cardiovascular Medicine, Stanford University, Stanford, CA, USA

Institute of Stem Cell Biology and Regenerative Medicine, Stanford, CA, USA
Department of Medicine, Division of Cardiovascular Medicine, Stanford University,
Stanford, CA, USA

Donghui Zhang, Ph.D. College of Life Sciences, Hubei University, Wuhan, China

Jianyi Zhang, M.D., Ph.D. Department of Biomedical Engineering, School of
Medicine, School of Engineering, University of Alabama at Birmingham,
Birmingham, AL, USA

Wuqiang Zhu, Ph.D. Department of Biomedical Engineering, School of Medicine,
School of Engineering, University of Alabama at Birmingham, Birmingham, AL,
USA



Tissue-Engineered Stem Cell Models of Cardiovascular Diseases

1

Christopher W. Anderson, Jiesi Luo, Lorenzo R. Sewanan, Mehmet H. Kural, Muhammad Riaz, Jinkyu Park, Yan Huang, Laura E. Niklason, Stuart G. Campbell, and Yibing Qyang

Authors “Christopher W. Anderson, Jiesi Luo, Lorenzo R. Sewanan, and Mehmet Kural” contributed equally to this work.

C. W. Anderson

Vascular Biology and Therapeutics Program, Yale University, New Haven, CT, USA

Department of Pathology, Yale University, New Haven, CT, USA

e-mail: Christopher.w.anderson@yale.edu

J. Luo · M. Riaz · J. Park · Y. Huang

Vascular Biology and Therapeutics Program, Yale University, New Haven, CT, USA

Department of Internal Medicine, Section of Cardiovascular Medicine, Yale Cardiovascular Research Center, Yale School of Medicine, New Haven, CT, USA

e-mail: jiesi.luo@yale.edu; muhhammad.riaz@yale.edu; jinkyu.park@yale.edu; yan.huang@yale.edu

L. R. Sewanan

Department of Biomedical Engineering, Yale University, New Haven, CT, USA

e-mail: lorenzo.sewanan@yale.edu

M. H. Kural

Department of Biomedical Engineering, Yale University, New Haven, CT, USA

Department of Anesthesiology, Yale University, New Haven, CT, USA

e-mail: mehmet.kural@yale.edu

L. E. Niklason

Vascular Biology and Therapeutics Program, Yale University, New Haven, CT, USA

Department of Biomedical Engineering, Yale University, New Haven, CT, USA

Department of Anesthesiology, Yale University, New Haven, CT, USA

Yale Stem Cell Center, New Haven, CT, USA

e-mail: laura.niklason@yale.edu

S. G. Campbell

Department of Biomedical Engineering, Yale University, New Haven, CT, USA

Yale Stem Cell Center, New Haven, CT, USA

e-mail: stuart.campbell@yale.edu

Y. Qyang (✉)

Vascular Biology and Therapeutics Program, Yale University, New Haven, CT, USA

Department of Pathology, Yale University, New Haven, CT, USA

Department of Internal Medicine, Section of Cardiovascular Medicine, Yale Cardiovascular Research Center, Yale School of Medicine, New Haven, CT, USA

Yale Stem Cell Center, New Haven, CT, USA

e-mail: yibing.qyang@yale.edu

Introduction

In vitro disease modeling can provide compelling insights into the molecular underpinnings of various pathological conditions. Traditionally, researchers have used two-dimensional (2D) cell culture methods to elucidate the molecular mechanisms that drive diseases. However, this method of cell culture fails to recapitulate the complex, three-dimensional (3D) microenvironment that is present in vivo. Recently, tissue-engineered models have been generated to create culture systems that better recapitulate the complex 3D microenvironments found in living tissue. By using these engineered models, more relevant data may be produced to unravel the molecular underpinnings of disease states and potentially translate into new therapeutic strategies. In this chapter, we will discuss engineered tissue models for studying cardiovascular diseases and some of the insights gained through using these complex, 3D models.

Enabling Technology: Induced Pluripotent Stem Cells

Pluripotent stem cells are defined as those which are capable of self-renewal, and differentiation into multiple somatic cell lineages [1]. One of the first types of stem cells for biological research were embryonic stem cells (ESCs). ESCs are cells derived from the inner cell mass of the blastocyst that retain the ability to derive cells from all three germ layers [1, 2]. One appealing trait of ESCs is that they are capable of being expanded in culture indefinitely. Because the establishment of an ESC line requires the destruction of the developing human embryo, the national dialogue surrounding this issue ultimately restricted progress in ESC research in that there could be no new ESC lines generated with federal funds as declared by the Dickey-Wicker amendment in 1996, which is still in effect to this day [3]. ESCs have been crucial in understanding basic biology surrounding pluripotency; however, current laws surrounding the legality of using public funds on new lines has

severely limited the genetic diversity that can be studied with this cell type. In 2007, Shinya Yamanaka described successful reprogramming of human somatic cells into a pluripotent state by using retroviral transduction of what have become known as the Yamanaka factors (Oct3/4, c-MYC, Klf4, Sox-2) that behave similarly to ESCs in both its phenotype and transcriptome expression patterns [4]. These induced pluripotent stem cells (iPSCs) have allowed for the study of patient-specific cellular models of genetic and acquired cardiovascular diseases. Furthermore, by combining the ample, renewable supply of these iPSCs with emerging technologies from the field of tissue engineering, increasingly complex models of human physiology and pathophysiology which capture the complexity of primary human tissues can be created. It is the hope that these complex, stem-cell-derived models will provide insight into the mechanisms underlying cardiovascular disease and potential therapeutic strategies.

Cardiac Disease Models

Differentiation Protocols

Widely employed protocols for differentiation of ESCs into cardiomyocytes *in vitro* have been largely based on observations of cardiac development pathways *in vivo* (Fig. 1.1). During development, heart tissue is initially formed from the brachyury⁺ lateral plate mesoderm. The developing heart is initially in a relatively simplistic structure known as the cardiac crescent. Through a series of complex contortions performed by Isl1⁺ cardiac progenitor cells, populating the first and second heart

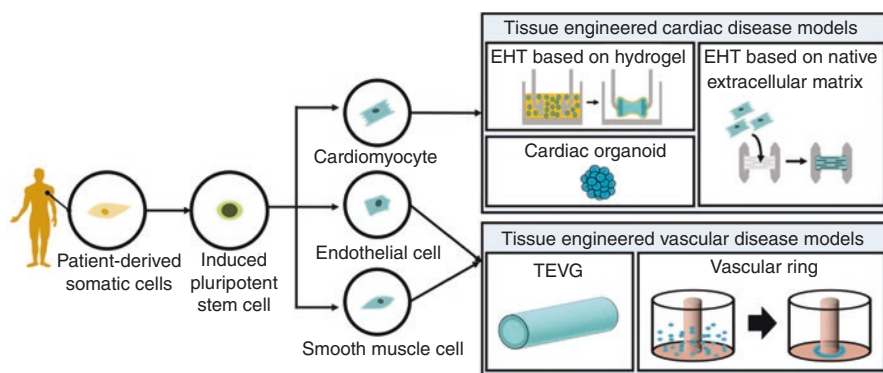


Fig. 1.1 Production of patient specific cardiovascular disease models. This schematic depicts the workflow of how clinical models can be produced from patient cells. Somatic cells may be derived from a noninvasive source such as cord blood and reprogrammed into induced pluripotent stem cells (iPSC) [4]. From here, the new iPSC line can be expanded indefinitely and differentiated into the different cell lineages relevant to the cardiovascular system [47, 56, 67]. Finally, these cells will be incorporated into one of a variety of engineered tissue designs as 3D culture models for study [8, 66, 68, 69]

fields, the four-chambered geometry of the postnatal heart is gradually formed. Several key pathways have been found to be involved in differentiation of mesoderm into cardiac cells. These include that of Wnt, activin/Nodal/TGF β , BMP, and FGF signaling cascades. A typical protocol for cardiac differentiation may include the following basic steps: (1) Pluripotent cell differentiation into cardiac mesoderm (brachyury⁺) cells through upregulation of Bmp4, Nodal/activin A, and Wnt/ β -catenin signaling cascades; (2) subsequent inhibition of both Wnt/ β -catenin and Nodal/activin A to yield cardiac progenitor (Isl1⁺) cells; (3) continued inhibition of Wnt/ β -catenin and addition of FGF to induce differentiation into cardiomyocytes; (4) addition of Wnt/ β -catenin, IGF, NRG, FGF1, Notch1, periostin to support further proliferation of early stage cardiomyocytes [5].

Design Strategies for Engineered Heart Tissue

Engineered heart tissues (EHTs) offer a novel method for studying various cardiac pathologies *in vitro*. EHTs have recently begun to be exploited to model genetic disorders such as hypertrophic cardiomyopathy (HCM) and dilated cardiomyopathy (DCM) and acquired disorders such as arrhythmias, drug-induced cardiac dysfunction, and fibrosis [6]. EHTs foster a 3D cellular landscape that allows for more complex and physiologically relevant interactions between cells, matrix architecture, and functional conditions such as anisotropic conduction, afterload, and preload when compared to traditional 2D culture environments [7]. These 3D conformations also allow for more robust functional characterization than what is possible in a 2D monolayer. Furthermore, as discussed below, increased maturation of iPSC-CMs toward adult-like phenotypes has been achieved only in biomimetic 3D engineered heart tissues, a critical consideration in modeling many cardiac diseases.

EHTs may be produced in a variety of ways including seeding cardiomyocytes onto an existing biomaterial scaffold, stacking cell sheet monolayers, or incorporating them into a hydrogel that can be molded into the desired shape [8–10]. Each strategy for generating EHTs has unique attributes that make them suited for varied clinical and research applications. Broadly, strategies for preparation of engineered heart tissues use one of three methodologies: (1) hydrogel-based tissue models; (2) fibrous, solid-state scaffolds seeded with cells; and (3) self-assembly of tissue organoids. Each model has its own unique advantages and drawbacks which must be considered when selecting the most appropriate design to build a given disease model.

Hydrogel-Based Engineered Heart Tissues

Fibrin/fibrinogen-based cell suspensions have been used by a variety of labs for cardiac tissue generation [7, 11, 12]. An advantage of using a gel-based design strategy for production of engineered heart tissue is versatile fabrication. The malleability of the hydrogel design provides this versatility to generate EHTs of complex patterns and shapes that can be modified based on the intended use. However, some

mechanical input is needed to coax growing fibers to align within the gel. Cells are generally suspended in the hydrogel and can be cast into customized molds to produce the desired shape. Although there is no inherent topography within these gels for cardiomyocyte fibers to align with, mechanical stress during the development period has been shown to increase fiber alignment within these tissues [11, 12]. Cardiomyocytes naturally align themselves along the plane where the stress is being applied, an important consideration in the measurement and analysis of cardiac contractility.

Fibrous Scaffolds

Natural or fabricated solid scaffolds offer a greater degree of control of the cellular arrangements within the tissue as compared to gel-based design strategies. One such design for performing in vitro testing of engineered tissues utilizes native extracellular matrix (ECM) as a scaffold for seeding iPSC-derived cardiomyocytes [8]. The native scaffold provides naturally aligned fibers that ensure seeded myocardial cells to align in a controlled direction for more standardized force output [8]. Another strategy that holds great promise is the use of electrospun scaffolds, which can be created from various ECM materials but embodying characteristics of tissues such as fiber geometry, anisotropy, porosity, and additional tunable characteristics. Further advancement of these techniques have allowed researchers recently to create even miniature ventricles and heart valves for in vitro studies [13–15].

Engineered Heart Tissue Self-Assembly

Organoid technology has been used to produce self-assembling organ-like structures where all of the relevant cell types are represented in the tissue [16]. However, these tissue structures do not recapitulate the complex, hierarchal physical structures seen in vivo. Therefore, these strategies for generating heart tissues are better suited for dissection of paracrine effects of diseased cells during pathological and normal development [17, 18].

Molecular Maturity of Cardiovascular Stem Cell Models

Despite their promise in modeling human disease, stem-cell-derived cardiomyocytes show some limitations due to their relatively immature phenotypes. It has been noted that current protocols for generating cardiomyocytes from pluripotent cells yield cardiac cells whose physical, metabolic, and electrical characteristics more closely resemble that of neonatal cardiomyocytes rather than what is found in adult myocardium [12, 19, 20]. This question of cellular maturity raises a notable issue when looking at both research and clinical applications of these iPSC-CMs. The neonatal transcriptional profile may throw into question results obtained from molecular and pharmacological data extracted from drug screening and various experimental perturbations [21]. For example, some pathological hypertrophy markers are associated with upregulation of fetal genes, including ANP, BNP, α -skeletal actin, and MHC [22]. It is for these reasons that cardiac maturation is a very active area of investigation.

Mature cardiomyocytes display several prominent phenotypes such as an elongated rod shape, gap junction expression and the formation of robust sarcomere, t-tubule, and intercalated disk structures. Each of these factors will directly influence the electrical and physical characteristics of the cells within a given tissue [23, 24]. Additionally, excitation-contraction coupling are a very important factor for proper cardiomyocyte function [25]. Stem-cell-derived cardiomyocytes do not immediately display these phenotypes, though long-term studies of implanted cells in animal models showed these cells do have the capacity to reach maturity if the proper environmental cues are presented [26].

Alternatively, researchers are also working toward developing methods to mature stem-cell-derived cardiomyocytes *in vitro* (Fig. 1.2). As mentioned before, 3D systems have opened many avenues to manipulate these cells in ways that were not possible with traditional 2D cultures. EHTs can be leveraged for maturation of myocardium in addition to simple characterization. Biomimetic strategies to coax out phenotypes closer to what is seen in mature myocardium have shown great promise with neonatal rat cardiomyocytes [11]. When developing hiPSC-CM-derived EHTs, researchers have specifically turned to mechanical and electrical stimulation which are present in the heart during development and throughout life. Manipulating these parameters has become an area of great interest for maturing stem-cell-derived cardiomyocytes [24, 27, 28]. The Murray group, for example, generated collagen-gel-based hiPSC-derived cardiomyocyte tissues that were subjected to static tensile

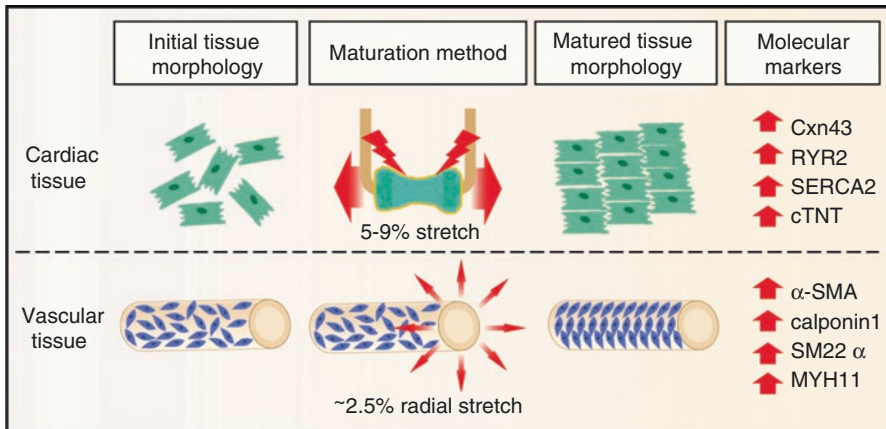


Fig. 1.2 General approaches for maturation of engineered cardiovascular tissues. A schematic diagram of strategies employed for maturing pluripotent stem-cell-derived cardiovascular cells (cardiomyocytes; green) (vascular smooth muscle cells; blue). Cardiac tissue maturation protocols generally employ mechanical stretching and/or electrical stimulation, similar to what is experienced during systole and diastole *in vivo* [24, 29]. These strategies have demonstrated an improved alignment of cardiomyocytes in the tissue parallel to the applied force and/or electrical current [70, 71]. This is accompanied by a transcriptomic shift closer to what is seen in mature cardiac tissue. Similarly, mechanical cyclic stretching of vascular smooth muscle cells allows for the alignment of these cells perpendicularly to the applied force in addition to transcriptome shifts toward maturity benchmarks [68]

force alone or in conjunction with electrical stimulation [24]. They found that compounding these cues lead to an additive effect for increased force output of the tissue. Additionally, they noted an increase in expression of sarcoplasmic reticulum proteins RYR2 and SERCA2 which further indicate molecular maturation of the cardiomyocytes. Co-culturing cardiomyocytes with fibroblasts aided in remodeling of the EHT and likely provide paracrine signals that aid in cardiac maturation [12]. Co-culturing with human foreskin fibroblasts led to a significant increase in contractile output of the EHT, although it was noted that the optimal seeding ratio varied between stem cell lines. Another major contributing factor to the maturity of these tissues is the media composition used to provide nutrients. Zimmerman et al. described a serum free media that helps push the transcriptional profile of differentiated cardiomyocytes closer to that of adult myocardium and functionally resulted in a positive force frequency response. Aside from nutrient composition, the availability of those nutrients throughout the tissue is vital for proper maturation of the EHT [10]. Using dynamic culturing conditions, where the media was constantly agitated and better able to penetrate the thickness of the tissue, was shown to increase contractile force of the EHTs [10]. This observation was shown to be linked to nutrient availability through a noted increase in mTOR signaling pathway activation in the dynamic condition. Although more refinement of protocols is needed to produce fully mature myocardium, great strides have been made in this effort and reliable data has been collected from these methods [29]. Bouchard et al. recently demonstrated that gradually increasing pacing frequency of engineered heart tissues from 2 to 6 Hz during a 2 week training regimen while undergoing auxotonic contractions achieved an unprecedented level of contractility and molecular maturity of the iPSC-derived cardiomyocytes [29]. As investigators continue to improve and standardize the metabolic, electrical, mechanical, and other microenvironmental conditions for maturing iPSC-CMs during culture, iPSC-CMs will continue to gain relevance and applicability for applications such as disease modeling and regenerative medicine.

Disease Models of Genetic Cardiac Disorders

Since iPSCs can be readily derived from individual patients and furthermore, edited via techniques such as TALEN and CRISPR/Cas9 prior to differentiation into cardiomyocytes, they hold great promise in unraveling underpinnings of genetic cardiac disease and in allowing therapeutic strategies to be screened in an in vitro setting with high relevance to human biology (Fig. 1.3). While the application of engineered heart tissues to genetic cardiac disease is still an emerging approach, several studies have revealed the promise of this technology in understanding pathologies such as hypertrophic cardiomyopathy (HCM) and dilated cardiomyopathy (DCM). Though iPSC-CMs have been used more generally in 2D systems to model cardiac disease as comprehensively reviewed in previous works [30, 31], we focus here on papers that have specifically looked at tissue-engineered models of genetic cardiac diseases.

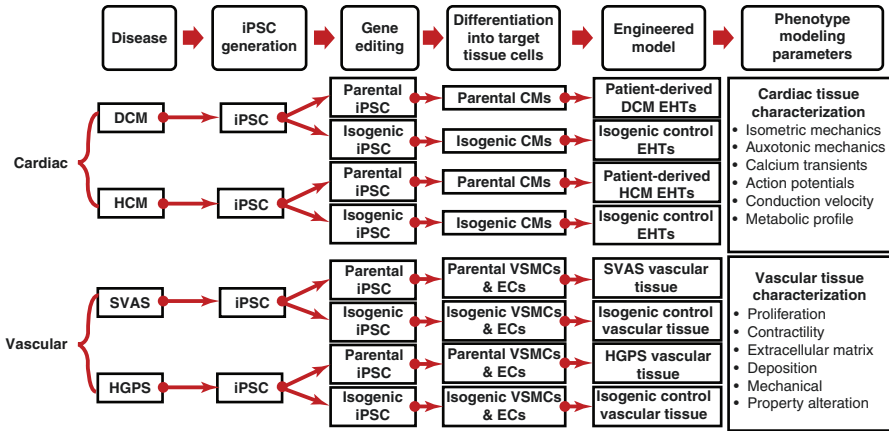


Fig. 1.3 Development of isogenic, patient derived lines for cardiovascular disease modeling. Induced pluripotent stem cells (iPSC) can be readily derived from patients harboring genetic mutations linked to specific diseases. A stable iPSC line will be generated from a noninvasively derived cell source (i.e., blood derived, circulating lymphocytes) through induction of Yamanaka factors. Gene editing corrections can be performed on stable cell lines to generate a gene corrected isogenic line from each patient, using TALEN and CRISPR/Cas9 technology. From here, engineered tissues can be developed from diseased cardiovascular cells and compared to tissues derived from isogenic control lines

Dilated cardiomyopathy is a relatively common (up to 1 in 250 people) but severe disease of the myocardium that manifests as reduced left ventricular ejection fraction and increased ventricular chamber size with simultaneous wall thinning [32]. Approximately 50% of DCM cases may have a genetic origin, usually inherited in an autosomal recessive pattern with the genetic defect present in a gene of the cardiac sarcomere; however, many cases are idiopathic and highly heterogeneous in disease penetrance and phenotypic expression [6, 32]. Since titin truncating mutations (TTNtv) have been found as one among the major causes (up to 20%) of genetic DCM, Hinson et al. designed a comprehensive study of TTNtv [33]. Utilizing a series of genetically edited isogenic and patient-derived iPSC lines to explore the influence of TTNtv in the A band and I band that were correlated with clinical disease severity, the investigators determined that contractile performance was decreased when cardiac microtissues [34] were made using hydrogels cast around mildly flexible cantilever beams; the auxotonic displacement of these cantilevers were optically measured and used to calculate the force produced by these engineered heart tissues with and without TTNtv. While alternative exon splicing attenuated the effects of the I band TTNtv to some extent, the A band TTNtv generally resulted in decreased incorporation of titin into the sarcomere, via mRNA and protein instability and degradation, limiting sarcomerogenesis and impairing the typical response to mechanical and adrenergic stimulus [33]. Using a different tissue engineering approach which fabricated circular engineered heart muscle rings [35], Streckfuss-Bomke et al. explored the effect of RMB20 mutation S635A in patient-derived iPSC cardiomyocytes, which results in aberrant TTN splicing [36].

Isometric measurements of engineered heart muscles demonstrated both decreased systolic and diastolic force production, correlated with reduced TTN N2B isoform expression at the protein and transcript level [36]. While both of these studies described above explore only a limited aspect of DCM pathophysiology given the diversity of primary genetic changes, the underlying defect of early impaired sarcomerogenesis identified in the iPSC-CMs may be one of the common mechanisms of genetic DCM and potentially be a fruitful target for therapy, an area open for much future investigation. Approaches to further elucidate key clinical features of DCM such as arrhythmogenesis and heterogeneous expression and penetrance may also be warranted to fully capture the underlying drivers and subsequent sequelae of genetic DCM.

Familial hypertrophic cardiomyopathy (HCM) is an inherited autosomal dominant disorder occurring in about 1 in 500 people which manifests as abnormal thickening of the heart wall, cardiomyocyte remodeling, diastolic dysfunction, fiber disarray, and interstitial fibrosis [37]. Over 90% of all genetic variants linked to HCM occur in the cardiac sarcomere, though many HCM cases have not yet been linked to a specific genetic change [37]. Mosqueria et al. used a series of isogenic lines to study the R453C variant in MYH7, one of the most common sarcomeric genes mutated in HCM, often leading to functional changes in the myosin muscle protein itself [37]. Using engineered heart tissues created from fibrin hydrogels attached to silicone posts, auxotonic contractions in the mutation-carrying EHTs had reduced force and prolonged time to maximal activation compared to control EHTs [38]. Attempted treatment of these hypocontractile mutant EHTs using the crossbridge activating agent omecamtiv mecarbil did not alleviate the behavior but led to further contractile deficits; studies of mitochondrial dynamics suggested that depletion of energetic substrates in the mutant iPSC-CMs and alterations in MYH7:MYH6 isoform ratio found in transcriptomic studies could underlie some aspects of the hypocontractile phenotype [38]. Utilizing similar approaches, recent work published from the same group by Smith et al. considered the phenotype of the E99K mutation to alpha-cardiac actin (ACTC1), using both isogenic and patient-derived iPSC lines [39]. Surprisingly, though previous nonhuman models had shown some calcium-dependent hypercontractility with this variant, not all cell lines revealed consistent contractile abnormalities, though there was evidence of prolonged contractions as well as a predominant phenotype of calcium-triggered arrhythmogenic events, suggesting that targeting calcium cycling through drugs such as ranolazine and dantrolene could be beneficial [39]. Importantly, this study underscores that complex clinical entities like HCM may not depend solely on the Mendelian inheritance of single rare variants such as ACTC1 E99K but also on the particular patients' genetic backgrounds potentially containing various genetic modifier of disease risk [40]. While not in the sarcomere itself, mutations to the regulatory subunit of AMPK, PRKAG2, have been noted to cause a HCM-like phenotype though notably without presence of significant fibrosis [41]. Hinson et al. utilized their cardiac microtissue platform to study the phenotype of PRKAG2 N488I iPSCs derived from both patients and from lines edited with TALEN; they found that the mutant EHTs produced greater twitch force as a result of increased

viability, which correlated with transcriptomic analysis revealing upregulation of metabolic and hypertrophic pathways [41]. Though it remains unclear whether the phenotype of HCM may depend specifically on gene involved and other genetic and epigenetic factors, tissue-engineered iPSC-CM models have already revealed novel interactions and events early in the pathogenesis of HCM, a condition which typically takes decades to develop in vivo. Much remains to be explored as only a few studies have been published at this time but engineered heart tissues should prove a valuable tool in integrated functional, structural, and biochemical analyses of disease pathophysiology. Going forward, these engineered heart tissue technologies offer a powerful new tool to produce more physiologically relevant information on development of cardiac diseases.

Vascular Disease Models

Discussion of Vascular Differentiation Protocols

Blood vessels are developed as the circulatory channels for blood supply between the beating heart and the peripheral tissues. Damaging of blood vessels, especially the vascular endothelial cells (ECs), is a major driving feature of ischemia related cardiovascular diseases. As such, a thorough understanding of these events is crucial for the development of more efficacious treatments down the line. Blood vessel diseases, especially those for arteries, are rampant worldwide. As such the most essential cellular components of the blood vessels, endothelial cells (ECs) and vascular smooth muscle cells (VSMCs) are intensively studied. To date, a growing body of reports have described the derivation of ECs and VSMCs from human induced pluripotent stem cells (hiPSCs) as the model, models of cultured cells or engineered tissues, for studies on vascular disease mechanisms in sophisticated 3D engineered culture systems.

Derivation of Endothelial Cells (ECs) from hiPSCs

As noted in the previous section on cardiac differentiation, protocols for development of robust vascular cells have also been derived from signaling cascades and genetic programs present in the natural development. During early embryogenesis, vascular cell precursors undergo mesodermal lineage commitment that is driven by bone morphogenetic protein 4 (BMP4) and fibroblast growth factor 2 (FGF2) signaling. From these mesodermal cells, a population of endothelial progenitor cells is progressively established [42]. This process is regulated by visceral endoderm-secreted vascular endothelial growth factors (VEGF), especially VEGF-A. From here, these EC precursors are committed to the endothelial lineages and participate in vasculogenesis [42]. Primordial endothelial cells can subsequently be specified into arterial, venous, and lymphatic ECs based on a variety of mechanical and biochemical cues [42–44]. The differentiated ECs are majorly characterized by a

cobblestone-like morphology in monolayer culture and their specific marker expression profile which includes KDR, VE-cadherin, CD31, and NOS3 at both mRNA and protein levels [42, 45]. The vessel forming capability is considered as an important functionality of the ECs, both in vitro and in vivo [46]. The production of nitric oxide is also assessed as one of the most authentic hallmark of the EC function [46].

One robust method for pluripotent cell differentiation of ECs uses a treatment of human iPSC (hiPSC) monolayers with growth factors and small molecules. Generally, the monolayer of undifferentiated hiPSCs are specifically induced into mesodermal progenitor cells by BMP4, FGF2, or GSK3 inhibitors to activate the activin/Nodal and Wnt pathways. Through this, cells are primed to become vascular EC progenitors [46]. Subsequently, the CD31+ or VECAD+ cell population are selected by magnetic-activated cell sorting (MACS) or fluorescence activated cell sorting (FACS) and further expanded in the EC growth medium. For example, Lian et al. reported that the Wnt agonist CHIR99021 could specifically induce the hiPSCs into mesodermal progenitor cells containing the population of CD31+ EC progenitor cells [47]. The EC progenitors, which were composed of over 50% differentiated cells, could be isolated by MACS, further differentiated into functional ECs and expanded in endothelial growth medium. Recently, Patsch et al. reported an alternative, but highly robust, method to derive ECs from hiPSCs [48]. Similarly, to previously mentioned protocols, GSK3 inhibition and BMP4 treatment effectively committed hiPSCs into mesodermal progenitors, and the following exposure to VEGF immediately pushed these cells into EC lineage. The authors claimed that this protocol can produce ECs from hiPSCs with efficiency over 80% within 6 days of differentiation. Moreover, 99% of these hiPSC-ECs present EC-specific markers, gene expression profiles, and functionality in vitro and in vivo. In addition, Prasain et al. reported the derivation of endothelial colony-forming cells (ECFCs) from human embryonic stem cells (hESCs) [49]. Treated by VEGF, BMP4, and FGF2, the hESCs were committed to mesodermal cells with endothelial potential, then the cells were further differentiated into the highly proliferative ECFCs, which could be expanded to 15–18 passages. Besides, these hESC-derived ECFCs displayed typical and stable EC phenotype in forming human vessels in mice and repairing the ischemic mouse tissue. Considering the high similarity between hESCs and hiPSCs, this method could be potentially applied to hiPSCs for EC derivation.

Derivation of Vascular Smooth Muscle Cells (VSMCs) from hiPSCs

Vascular smooth muscle cells (VSMCs) are the major cellular components of the vessel wall. VSMCs primarily contribute to the mechanical strength and extensibility of the vessel wall, and regulate the dilation and contraction of vessel lumen, in order to regulate local blood pressure in various tissues. Additionally, VSMCs play a major role in the maintenance of vascular extracellular matrix mechanics, which allow the vessel to withstand the pulsatile pressure from blood flow. Abnormality of VSMC's function and phenotype may fundamentally alter the vascular functions and plays crucial roles in various diseases including atherosclerosis, hypertension,

stenosis, and aneurysm [50]. In embryonic development, progenitors of VSMCs are established in multiple germ layers, and these VSMC populations with distinct embryonic origins are found in different vessels, or even adjacent segments of the same vascular conduit [51]. For instance, the thoracic segment of the aorta, including the ascending aorta, aortic arch, and descending aorta, is composed of VSMCs from three embryonic layers (neural crest, lateral plate mesoderm, and paraxial mesoderm, respectively) [52]. VSMCs with different embryonic lineages may present distinct phenotypes such as the resistance to thrombogenesis [51]. Despite the heterogeneity of embryonic origins, VSMCs are sharing similar regulatory pathways to fulfill the lineage commitment. Various signaling pathways and molecules are involved in the maturation of VSMC phenotype, such as MYOCD and serum reactive factor (SRF) complex, TGF family, PDGF, retinoid receptor, and others, and play major roles in VSMC development [53]. The phenotype of VSMCs transit from proliferative, extracellular matrix-synthesizing status to the quiescent and contractile status as the maturation of VSMCs proceed [54]. The mature VSMCs exhibit a series of protein components of cell contraction machinery such as alpha smooth muscle actin (α -SMA), calponin-1 (CNN1), transgelin (SM22 α), smooth muscle specific myosin heavy chain (SM-MHC) and smoothelin [54]. The VSMCs also contribute to the secretion and deposition of extracellular matrix including collagen and elastin [54]. Function-wise, contractile VSMCs exhibit contractility in the presence of vasoconstrictors such as carbachol or potassium chloride [53].

VSMCs can be derived from hiPSCs via embryoid body (EB)-driven method. As reported by Xie. et al., the dissociated hiPSC clusters can form EBs in suspension culture [55]. As the formation of three-dimensional structure and the withdrawal of pluripotency-supporting growth factors trigger the spontaneous differentiation of pluripotent stem cells, EBs mimic the processes of early embryonic development and form all three germ-layers. The differentiated cells from EBs are further cultured in attachment with VSMC-promoting medium to complete VSMC lineage commitment in order to derive the hiPSC-VSMCs in proliferation status. To further induced the contractile phenotype, these cells can be further maintained under the serum-starvation. The VSMCs generated from EB-based protocol displayed spindle-shaped morphology and expressed α -SMA, SM-MHC, and CNN1. FACS analysis indicated that the efficiency of VSMC differentiation was of 55.26% for SM-MHC expression and 96.81% for α -SMA expression. In addition, these hiPSC-VSMCs showed the contractility in response to vasoconstrictor treatment, indicating the contractility of these hiPSC-VSMCs. Besides the EB-driven approach, hiPSC-VSMCs can also be differentiated through monolayer culture model. By forming a monolayer in culture dish, individual hiPSCs are equally exposed to the culture condition favoring differentiation and promoted to desired somatic lineages. Multiple monolayer-based VSMC differentiation approaches have been reported. Wanjare et al. reported that both collagen synthesizing and contractile hiPSC-VSMCs could be derived from hiPSCs [56, 57]. Briefly, a monolayer of hiPSCs are subjected to differentiation toward VSMC-like cells, and these cells are further promoted to synthetic or contractile VSMC phenotypes, respectively, by using medium containing 10% serum with TGF β 1 and 0.5% serum with TGF β 1. The authors

further discovered that biomechanical stretching could dramatically enhance the ECM production of these contractile hiPSC-VSMCs including collagen and elastin [58]. These contractile hiPSC-VSMCs could be even derived when cultured on a PEGdma/PLA scaffold under the condition with pulsatile medium flow [59]. These contractile hiPSC-VSMCs developed along with the exposure to the biomechanical stimuli also presented largely improved elastin deposition. Notably, it was reported by Cheung et al. that the monolayer approach allowed the derivation of the lineage-specific VSMCs derived from hiPSCs [52]: hiPSCs cultured in monolayer are initiated to differentiation toward the progenitors of neuroectoderm, lateral plate mesoderm, or paraxial mesoderm, and these progenitors are initiated toward highly enriched, mature VSMCs with contractile phenotype with the treatment of TGF β 1 and PDGF-BB.

Tissue-Engineered Models for Vascular Diseases

The progress of tissue engineering technology has allowed the application of vascular cells, including the hiPSC-derived ECs and VSMCs, to fabricate bioengineered vessels as vascular disease models. Tissue-engineered blood vessels (TEBVs) can be produced by seeding the VSMCs onto the malleable, fibrous or porous, biodegradable scaffold and subsequently cultured in bioreactor with pulsatile, radial stress in the lumen [60]. The lumen of the TEBV is eventually coated with vascular ECs and maintained in the presence of luminal shear stress for a short period of time. Beside the biodegradable-based approaches, TEBVs can also be fabricated by mixing VSMCs with biodegradable hydrogel, such as fibrin gel or collagen gel, and then casting the mixture into polymerized tissue in tubule shape [61, 62]. The molded hydrogel-VSMCs mixture will be coated with a luminal layer of ECs and mounted onto the bioreactor and cultured in the presence of cyclic stretching or shear stress. To date, it was reported by Gui et al. that the implantable TEVGs have been produced by seeding hiPSC-VSMCs onto the biodegradable polyglycolic acid scaffold followed by 8 weeks of static culture [63]. Moreover, Fernandez et al. reported that collagen-gel-based small-caliber TEBVs using hiPSC-VSMCs with luminal endothelium layer were generated and cultured with constant luminal flow for drug screening purpose [64]. Subsequently, Atchison et al. reported that these hiPSC-based engineered vascular tissues have allowed the modeling of vascular diseases and studies on elucidating the pathological mechanism underneath [62]. Hutchison-Gilford Progeria Syndrome (HGPS) is an accelerated aging disorder caused by nuclear accumulation of progerin, and the primary cause of death is cardiovascular diseases such as stroke and coronary artery at 14 years old. Dysfunctional VSMCs are observed in HGPS patients and may cause defects associated with HGPS. Recently, Atchison et al. created TEBV using VSMCs derived from HGPS patient-specific iPSCs. As mentioned above, HGPS hiPSC-VSMCs were mixed with collagen gel and casted into the tubule shape to form the TEBVs. The TEBVs were further maintained in the presence of luminal constant flow. As a result, TEBVs fabricated from HGPS hiPSC-derived vascular cells showed the key features of

defect vessels from HGPS patients, including the reduced vasoactivity, increased medial wall thickness, increased calcification, and apoptosis of hiPSC-VSMCs. Additionally, treatment of HGPS patient's hiPSC-based TEBVs with proposed therapeutic Everolimus enhanced the vasoactivity of these TEBVs and preserved the hiPSC-VSMC properties.

Besides generating the tubule vessel-like tissue, the modulus vascular rings can be another option to model the vascular diseases. VSMCs can be seeded into an agarose-based mold to cast a ring-shape tissue via self-aggregation of the seed cells [65]. The dimension of the tissue rings such as the lumen diameter can be adjusted by changing the size of the agarose mold. The self-aggregated cells can be further cultured in the mold for 10–14 days to form vascular tissue rings before being subjected for analysis. These vascular tissue rings can serve as the modulus unit of a segment of blood vessels. Dash et al. have applied the hiPSC-VSMCs derived from supra-aortic stenosis (SVAS) patients to generate the vascular tissue rings [66]. SVAS is characterized by hyperproliferation and decrease contractility of VSMCs leading to blockage of the ascending aorta and other arterial vessels, which is attributed to the loss-of-function mutations in elastin gene (ELN). The SVAS hiPSC-based vascular tissue rings preserved the core phenotypes of SVAS such as the reduced tissue contractility when exposed to carbachol, as well as the dramatically high proliferation rate of the hiPSC-VSMCs within the rings.

Summary

With the advent of tissue engineering, more sophisticated models of human disease can be produced in a laboratory setting. This has become possible through the development of stable pluripotent cell sources and robust differentiation protocols for the development of cardiovascular cells. These initial differentiation strategies were derived from biomimetic approaches of recapitulating key aspects of the developmental environment for cardiovascular cells, an approach that has worked elegantly though with room for further improvement. Modulation of the Wnt/B-catenin signaling cascade is a major factor for production of cells of cardiovascular lineages. Similarly, questions surrounding phenotypic maturity of these cells, and by extension, these engineered models, are being addressed in the same fashion. The application of mechanical and electrical stimuli to these engineered tissues as well as more physiological media formulations has shown great promise in improving their maturity for the development of further refined and relevant disease models. Engineered tissue models holds promise for modeling disease progression due to cell intrinsic factors such as genetic mutations and extrinsic factors such as high blood pressure, altered preload, and electrical dysfunction. The versatility and wide array of design strategies for these engineered models greatly empowers researchers to pick one of a variety of tissue designs that best allows them to answer their intended question. Through the production of these human engineered models which may lead to a more realistic understanding of various pathologies, the efficiency of developing novel, precise, and targeted therapies may be improved.

Funding Acknowledgments This work was supported by 1R01HL116705, 1R01HL131940, DOD 11959515, Connecticut's Regenerative Medicine Research Fund (CRMRF) (all to YQ), P.D. Soros Fellowship for New Americans and a NIH/NIGMS Medical Scientist Training Program Grant (T32GM007205) (both to LRS), NIH 1F31HL143928-01 (to CWA), and 1R01HL136590 (to SC).

Competing Interests L.E.N. is a founder and shareholder in Humacyte, Inc., which is a regenerative medicine company. Humacyte produces engineered blood vessels from allogeneic smooth muscle cells for vascular surgery. L.E.N.'s spouse has equity in Humacyte, and L.E.N. serves on Humacyte's Board of Directors. L.E.N. is an inventor on patents that are licensed to Humacyte and that produce royalties for L.E.N. L.E.N. has received an unrestricted research gift to support research in her laboratory at Yale. Humacyte did not fund this review, and Humacyte did not influence the writing of this review.

Works Cited

1. Thomson J, et al. Embryonic stem cell lines derived from human blastocysts. *Science*. 1998;282:1145–7.
2. Itskovitz-Eldor J, et al. Differentiation of human embryonic stem cells into embryoid bodies compromising the three embryonic germ layers. *Mol Med*. 2000;6:88–95.
3. McLaren A. Ethical and social considerations of stem cell research. *Nature*. 2001;414:129–31.
4. Takahashi K, et al. Induction of pluripotent stem cells from adult human fibroblasts by defined factors. *Cell*. 2007;131:861–72. <https://doi.org/10.1016/j.cell.2007.11.019>.
5. Später D, Hansson EM, Zangi L, Chien KR. How to make a cardiomyocyte. *Development*. 2014;141:4418–31.
6. Lee TM, et al. Pediatric cardiomyopathies. *Circ Res*. 2017;121:855–73.
7. Hansen A, et al. Development of a drug screening platform based on engineered heart tissue. *Circ Res*. 2010;107:35–44.
8. Schwan J, et al. Anisotropic engineered heart tissue made from laser-cut decellularized myocardium. *Sci Rep*. 2016;6:32068.
9. Haraguchi Y, et al. Fabrication of functional three-dimensional tissues by stacking cell sheets in vitro. *Nat Protoc*. 2012;7:850–8.
10. Jackman CP, Carlson AL, Bursac N. Dynamic culture yields engineered myocardium with near-adult functional output. *Biomaterials*. 2016;111:66–79.
11. Bian W, Badie N, Himel HD, Bursac N. Robust T-tubulation and maturation of cardiomyocytes using tissue-engineered epicardial mimetics. *Biomaterials*. 2014;35:3819–28.
12. Tiburcy M, et al. Defined engineered human myocardium with advanced maturation for applications in heart failure modelling and repair. *Circulation*. 2017;116:024145. <https://doi.org/10.1161/CIRCULATIONAHA.116.024145>.
13. MacQueen LA, et al. A tissue-engineered scale model of the heart ventricle. *Nat Biomed Eng*. 2018;2:930.
14. Wu B, et al. Developmental mechanisms of aortic valve malformation and disease. *Annu Rev Physiol*. 2017;79:21–41.
15. Arevalos CA, et al. Valve interstitial cells act in a Pericyte manner promoting angiogenesis and invasion by valve endothelial cells. *Ann Biomed Eng*. 2016;44:1–17.
16. Varzideh F, et al. Human cardiomyocytes undergo enhanced maturation in embryonic stem cell-derived organoid transplants. *Biomaterials*. 2018;192:537–50.
17. Voges HK, et al. Development of a human cardiac organoid injury model reveals innate regenerative potential. *Development*. 2017;144:1118–27.
18. Mills RJ, et al. Functional screening in human cardiac organoids reveals a metabolic mechanism for cardiomyocyte cell cycle arrest. *Proc Natl Acad Sci*. 2017;114:E8372. <https://doi.org/10.1073/pnas.1707316114>.
19. Feric NT, Radisic M. Maturing human pluripotent stem cell-derived cardiomyocytes in human engineered cardiac tissues. *Adv Drug Deliv Rev*. 2016;96:110–34.

20. Robertson C, Tran D, George S. Concise review: maturation phases of human pluripotent stem cell-derived cardiomyocytes. *Stem Cells*. 2013;31:1–17.
21. French A, et al. Enabling consistency in pluripotent stem cell-derived products for research and development and clinical applications through material standards. *Stem Cells Transl Med*. 2015;4:217–23.
22. McMullen JR, Jennings GL. Differences between pathological and physiological cardiac hypertrophy: novel therapeutic strategies to treat heart failure. *Clin Exp Pharmacol Physiol*. 2007;34:255–62.
23. Feinberg AW, et al. Controlling the contractile strength of engineered cardiac muscle by hierarchical tissue architecture. *Biomaterials*. 2012;33:5732–41.
24. Ruan J-L, et al. Mechanical stress conditioning and electrical stimulation promote contractility and force maturation of induced pluripotent stem cell-derived human cardiac tissue clinical perspective. *Circulation*. 2016;134:1557–67.
25. Schwan J, Campbell SG. Prospects for in vitro myofilament maturation in stem cell-derived cardiac myocytes. *Biomark Insights*. 2015;2015:91–103.
26. Chong JJH, et al. Human embryonic-stem-cell-derived cardiomyocytes regenerate non-human primate hearts. *Nature*. 2014;510:273–7.
27. Hirt MN, et al. Functional improvement and maturation of rat and human engineered heart tissue by chronic electrical stimulation. *J Mol Cell Cardiol*. 2014;74:151–61.
28. Mihic A, et al. The effect of cyclic stretch on maturation and 3D tissue formation of human embryonic stem cell-derived cardiomyocytes. *Biomaterials*. 2014;35:2798–808.
29. Ronaldson-Bouchard K, et al. Advanced maturation of human cardiac tissue grown from pluripotent stem cells. *Nature*. 2018;556:239–43.
30. van Mil A, et al. Modelling inherited cardiac disease using human induced pluripotent stem cell-derived cardiomyocytes: progress, pitfalls, and potential. *Cardiovasc Res*. 2018;114(14):1828–42. <https://doi.org/10.1093/cvr/cvy208>.
31. Eschenhagen T, Carrier L. Cardiomyopathy phenotypes in human-induced pluripotent stem cell-derived cardiomyocytes—a systematic review. *Pflugers Arch*. 2018; <https://doi.org/10.1093/cvr/cvy208>.
32. Mestroni L, Brun F, Spezzacatene A, Sinagra G, MRG T. Genetic causes of dilated cardiomyopathy. *Prog Pediatr Cardiol*. 2015;37:13–8.
33. Hinson JT, et al. Titin mutations in iPSC cells define sarcomere insufficiency as a cause of dilated cardiomyopathy. *Science*. 2015;349:982–6.
34. Boudou T, et al. A microfabricated platform to measure and manipulate the mechanics of engineered cardiac microtissues. *Tissue Eng Part A*. 2012;18:910–9.
35. Tiburcy M, Meyer T, Soong PL, Zimmermann W-H. Collagen-based engineered heart muscle. *Methods Mol Biol*. 2014;1181:167–76.
36. Streckfuss-Bömeke K, et al. Severe DCM phenotype of patient harboring RBM20 mutation S635A can be modeled by patient-specific induced pluripotent stem cell-derived cardiomyocytes. *J Mol Cell Cardiol*. 2017;113:9–21.
37. Marian AJ, Braunwald E. Hypertrophic cardiomyopathy: genetics, pathogenesis, clinical manifestations, diagnosis, and therapy. *Circ Res*. 2017;121:749–70.
38. Mosqueira D, et al. CRISPR/Cas9 editing in human pluripotent stem cell-cardiomyocytes highlights arrhythmias, hypocontractility, and energy depletion as potential therapeutic targets for hypertrophic cardiomyopathy. *Eur Heart J*. 2018;39:3879–92.
39. Smith JGW, et al. Isogenic pairs of hiPSC-CMs with hypertrophic cardiomyopathy/LVNC-associated ACTC1 E99K mutation unveil differential functional deficits. *Stem Cell Reports*. 2018;11:1226–43.
40. Daw EW, et al. Genome-wide mapping of modifier chromosomal loci for human hypertrophic cardiomyopathy. *Hum Mol Genet*. 2007;16:2463–71.
41. Hinson JT, et al. Integrative analysis of PRKAG2 cardiomyopathy iPSC and microtissue models identifies AMPK as a regulator of metabolism, survival, and fibrosis. *Cell Rep*. 2016;17:3292–304.
42. Marcelo KL, Goldie LC, Hirschi KK. Regulation of endothelial cell differentiation and specification. *Circ Res*. 2013;112:1272–87.

43. Masumura T, Yamamoto K, Shimizu N, Obi S, Ando J. Shear stress increases expression of the arterial endothelial marker ephrinB2 in murine ES cells via the VEGF-notch signaling pathways. *Arterioscler Thromb Vasc Biol.* 2009;29:2125–31.
44. Sivarapatna A, et al. Arterial specification of endothelial cells derived from human induced pluripotent stem cells in a biomimetic flow bioreactor. *Biomaterials.* 2015;53:621–33.
45. Yoder MC. Endothelial stem and progenitor cells (stem cells): (2017 Grover Conference Series). *Pulm Circ.* 2018;8 <https://doi.org/10.1177/2045893217743950>.
46. Lee SJ, Kim KH, Yoon YS. Generation of human pluripotent stem cell-derived endothelial cells and their therapeutic utility. *Curr Cardiol Rep.* 2018;20(45):45.
47. Lian X, et al. Efficient differentiation of human pluripotent stem cells to endothelial progenitors via small-molecule activation of WNT signaling. *Stem Cell Reports.* 2014;3:804–16.
48. Patsch C, et al. Generation of vascular endothelial and smooth muscle cells from human pluripotent stem cells. *Nat Cell Biol.* 2015;17:994–1003.
49. Prasain N, et al. Differentiation of human pluripotent stem cells to cells similar to cord-blood endothelial colony-forming cells. *Nat Biotechnol.* 2014;32:1151–7.
50. Ellis MW, Luo J, Qyang Y. Modeling elastin-associated vasculopathy with patient induced pluripotent stem cells and tissue engineering. *Cell Mol Life Sci.* 2018. <https://doi.org/10.1007/s00018-018-2969-7> [pii].
51. Majesky MW, Mummery CL. Smooth muscle diversity from human pluripotent cells. *Nat Biotechnol.* 2012;30:152–4.
52. Cheung C, Bernardo AS, Trotter MW, Pedersen RA, Sinha S. Generation of human vascular smooth muscle subtypes provides insight into embryological origin-dependent disease susceptibility. *Nat Biotechnol.* 2012;30:165–73.
53. Xie C, Ritchie RP, Huang H, Zhang J, Chen YE. Smooth muscle cell differentiation in vitro: models and underlying molecular mechanisms. *Arterioscler Thromb Vasc Biol.* 2011;31:1485–94.
54. Renssen SS, Doevendans PA, van Eys GJ. Regulation and characteristics of vascular smooth muscle cell phenotypic diversity. *Neth Hear J.* 2007;15:100–8.
55. Xie CQ, et al. A highly efficient method to differentiate smooth muscle cells from human embryonic stem cells. *Arterioscler Thromb Vasc Biol.* 2007;27:e311–2.
56. Wanjare M, Kuo F, Gerecht S. Derivation and maturation of synthetic and contractile vascular smooth muscle cells from human pluripotent stem cells. *Cardiovasc Res.* 2013;97:321–30.
57. Wanjare M, Kusuma S, Gerecht S. Defining differences among perivascular cells derived from human pluripotent stem cells. *Stem Cell Reports.* 2014;2:746.
58. Wanjare M, Agarwal N, Gerecht S. Biomechanical strain induces elastin and collagen production in human pluripotent stem cell-derived vascular smooth muscle cells. *Am J Physiol Cell Physiol.* 2015;309:C271–81.
59. Eoh JH, et al. Enhanced elastin synthesis and maturation in human vascular smooth muscle tissue derived from induced-pluripotent stem cells. *Acta Biomater.* 2017;52:49–59.
60. Niklason LE, et al. Functional arteries grown in vitro. *Science.* 1999;284:489–93.
61. Syedain ZH, et al. A completely biological ‘off-the-shelf’ arteriovenous graft that recellularizes in baboons. *Sci Transl Med.* 2017;9:pii: eaan4209.
62. Atchison L, Zhang H, Cao K, Truskey GA. A tissue engineered blood vessel model of Hutchinson-Gilford Progeria Syndrome using human iPSC-derived smooth muscle cells. *Sci Rep.* 2017;7(8168):8168.
63. Gui L, et al. Implantable tissue-engineered blood vessels from human induced pluripotent stem cells. *Biomaterials.* 2016;102:120–9.
64. Fernandez CE, et al. Human vascular microphysiological system for in vitro drug screening. *Sci Rep.* 2016;6:21579.
65. Strobel HA, Calamari EL, Alphonse B, Hookway TA, Rolle MW. Fabrication of custom agarose wells for cell seeding and tissue ring self-assembly using 3D-printed molds. *J Vis Exp.* 2018; <https://doi.org/10.3791/56618>.
66. Dash BC, et al. Tissue-engineered vascular rings from human iPSC-derived smooth muscle cells. *Stem Cell Reports.* 2016;7:19–28.

67. Ren Y, et al. Small molecule Wnt inhibitors enhance the efficiency of BMP-4-directed cardiac differentiation of human pluripotent stem cells. *J Mol Cell Cardiol.* 2011;51:280–7.
68. Gui L, et al. Biomaterials implantable tissue-engineered blood vessels from human induced pluripotent stem cells. *Biomaterials.* 2016;102:120–9.
69. Zhang D, et al. Tissue-engineered cardiac patch for advanced functional maturation of human ESC-derived cardiomyocytes. *Biomaterials.* 2013;34:5813–20.
70. Abilez OJ, et al. Passive stretch induces structural and functional maturation of engineered heart muscle as predicted by computational modeling. *Stem Cells.* 2018;36:265–77.
71. Khan M, et al. Evaluation of changes in morphology and function of human induced pluripotent stem cell derived cardiomyocytes (hiPSC-CMs) cultured on an aligned-nanofiber cardiac patch. *PLoS One.* 2015;10:1–19.



Phenotypic Screening of iPSC-Derived Cardiomyocytes for Cardiotoxicity Testing and Therapeutic Target Discovery

2

Arne A. N. Bruyneel, Tyler Muser, Vaidya Parthasarathy, Dries Feyen, and Mark Mercola

Introduction

The overall probability of success for drug development from phase 1 studies to regulatory approval is 13.8%, with insufficient efficacy and inappropriate safety profiles accounting for 52% and 24% of failures, respectively [1, 2]. Discovering new drugs for heart failure (HF) has been particularly challenging. The contradiction of encouraging results from preclinical and early phase clinical data with disappointing outcomes in larger registration trials have increased the uncertainty of HF drug development programs, together contributing to the increased cost and time investment needed to create new HF medicines [3]. Cardiovascular toxicity, including cardiomyopathy, QT prolongation, ventricular tachycardia, and the fatal polymorphic ventricular tachycardia Torsade de Pointes (TdP), is the most common safety issue and remains difficult to predict, also contributing to increased cost and uncertainty [4, 5]. The significant commercial and societal ramifications of these issues underscore the need for new approaches for identifying and evaluating therapeutic targets and drug candidates that would optimize the development process.

The advent of induced pluripotent stem cell (iPSC) technology has revolutionized our ability to study human disease [6]. iPSCs are reprogrammed from somatic

A. A. N. Bruyneel · T. Muser · V. Parthasarathy · D. Feyen · M. Mercola (✉)
Cardiovascular Institute and the Department of Medicine, Stanford University,
Stanford, CA, USA
e-mail: abruynee@stanford.edu; tyler.a.muser@biola.edu; dfeyen@stanford.edu;
mmercola@stanford.edu

cells, typically from blood or skin biopsies, and can be modified by genome editing to introduce or correct disease-causing mutations [7, 8]. As such, they provide a potentially unlimited source of disease-specific or patient-specific cardiomyocytes and other cells, and their isogenic controls, without the limitations of donor biopsies. The modern drug discovery paradigm commonly uses biochemical or reductionist cell culture models for initial drug screening, and *in vivo* animal models later in the process. The human context is typically incorporated later in the process once lead compounds have emerged. Similarly, the identification of a therapeutic target typically proceeds from studies of disease mechanisms that focus on one or relatively few hypotheses rather than from large-scale unbiased testing, although the implementation of human genomics is rapidly changing target identification. Therefore, from the perspective of discovering drugs for heart disease or predicting cardiotoxic effects of drugs, iPSC technology coupled with advances in high throughput (HT) instrumentation offers an exciting path to introduce the human context into the early discovery and hit to lead phases of the drug discovery pipeline (Fig. 2.1) [9, 10].

Despite their advantages, iPSC-derived cardiomyocytes suffer from immature structural, electrophysiological, metabolic, and mechanical features that currently limit their faithful recapitulation of disease phenotypes and hence also their utility for drug discovery and safety testing [11, 12]. Not only are they young in terms of time from initiation of differentiation relative to their adult counterparts (few weeks compared to many years), a major and partially remediable problem might be that the simple culture conditions that do not recapitulate the anatomical and hemodynamic influences of the fetal heart. Consequently, iPSC-derived cardiomyocytes in simple monolayer culture are typically small and polygonal-shaped and are proliferative, in contrast to their adult counterparts that are larger, non-proliferative, and rod-shaped with well-organized sarcomeric structures. Even though iPSC-derived cardiomyocytes express most cardiac ion channels, sarcoplasmic reticulum components and the structural machinery resembling adult cardiomyocytes, there are important differences that impact force generation, metabolism, neurohormonal responsiveness, and electrophysiology [13]. For example, the lack of T-tubule network and poorly organized SR results in poor co-localization of calcium channels and ryanodine receptors, non-uniform distribution of calcium release, and slower release and reuptake kinetics compared to adult cardiomyocytes [14]. In addition, iPSC-cardiomyocytes rely mainly on glycolysis whereas the adult heart relies predominantly on fat oxidation while retaining the capability to metabolize multiple carbon sources [15, 16].

This chapter summarizes state-of-the-art large-scale applications of iPSC-cardiomyocytes to identify therapeutic targets for heart disease and assess the cardiotoxic risk of drugs, with emphasis on emerging technologies to address current limitations. Although delineating disease mechanisms, therapeutic target discovery and assessing cardiotoxic risk differ in experimental design, our philosophy is that advancing iPSC-cardiomyocyte models that recapitulate disease and have the throughput to enable large-scale chemical or functional genomics screening will enable all three applications.

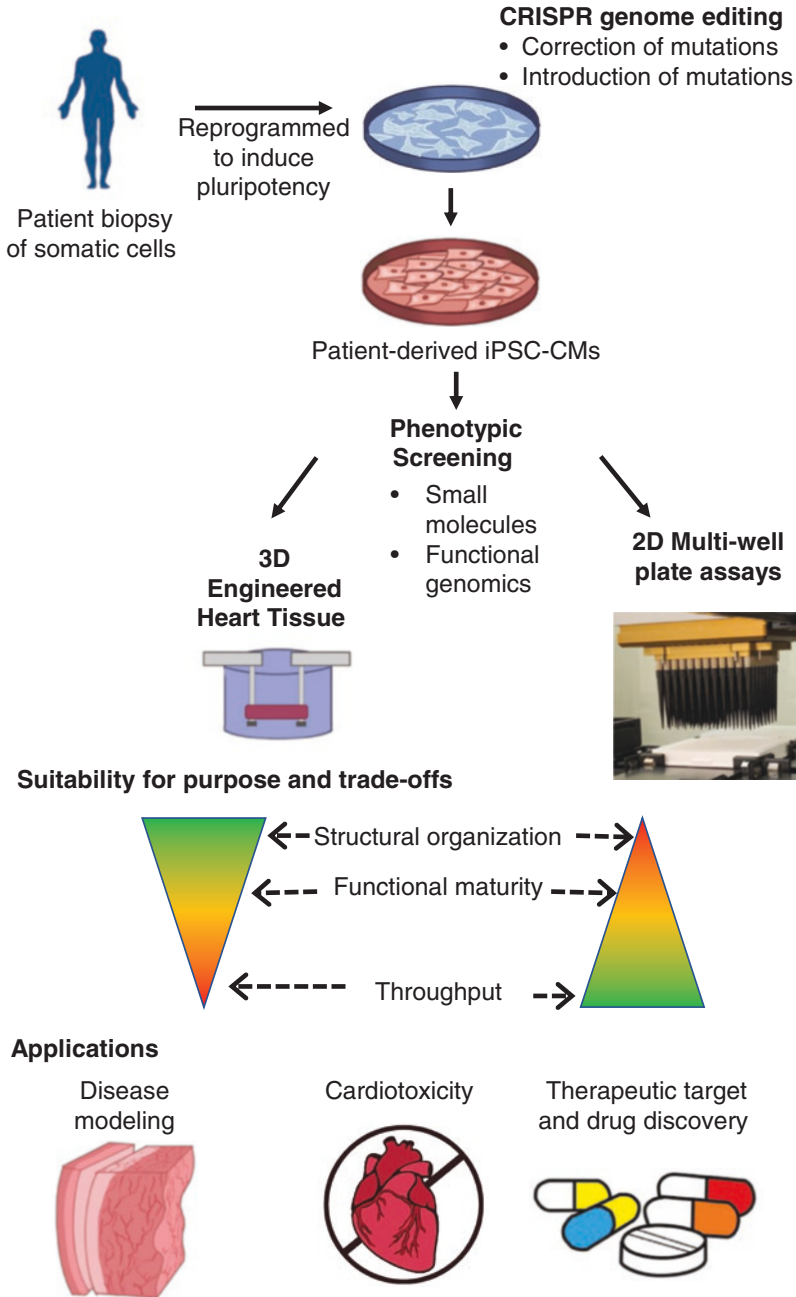


Fig. 2.1 Patient-derived cardiomyocytes as an in vitro disease model. Somatic cells derived from a patient biopsy are reprogrammed to induce pluripotency, and the expanded iPSCs are directed to differentiate into 2D or 3D cultures of iPSC-cardiomyocytes, capable of functioning as a disease model for drug discovery research and cardiotoxicity screening

Addressing Immaturity: How Mature Is Mature Enough?

There are important differences in the electrophysiology of adult cardiomyocytes and iPSC cardiomyocytes, as summarized in [17–19]. The iPSC-cardiomyocytes, produced by various protocols, contain most of the cardiac ion currents present in adult cardiomyocytes but nonetheless are immature and reflect their early fetal rather than adult counterparts. Important distinctions are that they are deficient in I_{K1} , which is important for the normally low resting potential of mature cardiomyocytes and a pronounced slow depolarizing I_f current that contributes to automaticity increasing the cell's membrane potential to the threshold for action potential firing. I_{K1} deficiency contributes to the relatively depolarized resting potential of -30 mV to -60 mV typical of early iPSC-derived or ESC-derived cardiomyocytes. Prolonged culture periods, especially in three dimensional systems, can decrease the resting potential to about -70 mV although not quite reaching the -80 mV typical of adult cardiomyocytes [20–24]. A consequence of the lack of a polarized resting potential is that functional Na^+ channel density is relatively low compared to more mature cells; consequently, the dependence of the action potential on Na^+ current has been inconsistent across iPSC-cardiomyocyte preparations and accounts for the slow velocities (V_{max}) of depolarization (about 2–100 V/s compared to about 300 V/s for adult ventricular cardiomyocytes [20, 21, 24]).

Ca^{2+} handling also differs between iPSC-derived and adult cardiomyocytes. Most notably, iPSC-cardiomyocytes have largely undeveloped transverse tubule (T-tubule) networks. In adult cardiomyocytes, T-tubules align with the sarcoplasmic reticulum (SR) [25]. Action potential depolarization causes voltage-gated L-type Ca^{2+} channels in the T-tubule sarcolamellae to open, triggering an influx of Ca^{2+} in close proximity to the SR. The influx of extracellular Ca^{2+} triggers the rapid release of Ca^{2+} from the SR through Ryanodine receptors (RyR) in a mechanism known as calcium-induced calcium release (CICR) that coordinates contraction with the action potential. In simple two-dimensional (2D) cultures of iPSC-cardiomyocytes, the underdeveloped T-tubule and SR networks means that intracellular Ca^{2+} for contraction comes primarily from entry of extracellular Ca^{2+} across the sarcolamella. The relatively slower extracellular Ca^{2+} influx (relative to release from SR stores) accounts for the negative force-frequency relationship in iPSC-derived cardiomyocytes when paced, whereas adult cardiomyocytes show a positive force-frequency relationship [26, 27].

Healthy adult cardiomyocytes rely on adrenergic signaling to regulate Ca^{2+} handling and contraction through phosphorylation of multiple proteins, including CAMKII, phospholamban (to regulate SERCA2 mediated Ca^{2+} reuptake into the SR) and cardiac Troponin-T, mediated by localized activity of β_2 adrenergic receptors (β_2 -ARs) and cAMP-hydrolyzing phosphodiesterases (PDEs) to caveolae/T tubules [28, 29]. In contrast to healthy adult cardiomyocytes, immature iPSC-cardiomyocytes have dysregulated catecholamine-dependent phosphorylation of Ca^{2+} handling and contractile proteins [30]. Interestingly, the immature adrenergic regulation of the SR/ Ca^{2+} machinery is reminiscent of failing cardiomyocytes. Failing adult myocytes lose T-tubule structure [31] and switch from

compartmentalized function of the β_2 AR to a dysregulated β_2 -AR and upregulated expression of β_1 -ARs [32, 33], which are less responsive to catecholamine-induced downregulation than are β_2 -ARs [34, 35].

Recent studies have succeeded in partially maturing the electrophysiological and mechanical properties of iPSC-derived cardiomyocytes. In the fetal and adult heart, hemodynamic load and alterations in metabolism lead to a coordinated metabolic, structural and mechanical (patho)physiological response. Not surprisingly, therefore, the manipulation of metabolism and load have had a positive influence on myocyte electrical, structural and mechanical maturation. Supplementation of culture media with T3 and dexamethasone, or promoting oxidative metabolism, can drive the cells to a more mature electrophysiological and structural state [36–38]. The influence of an elongated shape, constrained by culturing cells on a micropatterned surface in an optimized 7:1 ratio, had a positive influence on sarcomeric and mitochondrial organization, response to adrenergic stimulation and force generation, with evidence of a nascent T-tubule network [39, 40]. Recently, several vendors have introduced multiwell plates with micropatterned grooved surfaces that induce alignment of cardiomyocytes and are expected to improve their maturational properties.

Many studies have shown that engineering substrate stiffness influences the differentiation, myofibril organization and alignment of immature cardiomyocytes through signaling cascades that differentially respond to substratum elasticity, e.g. [41–44]. For example, Young et al. [45] have shown that mechanosensing at focal adhesions regulates the expression and phosphorylation of protein kinases known to control differentiation. Interestingly, they also found that cells matured best (judged by achieving z-disc spacing $<1.8 \mu\text{m}$) when the hydrogel substrata stiffened over time after cardiomyocyte plating, reaching about 8kPa in 11 days, approximating the stiffness of fetal myocardium (~ 10 kPa).

Three-dimensional (3D) engineered heart tissues (EHTs) improve upon 2D systems since they provide the possibility of imposing stiffness and load in the correct physiological ranges, which aligns cells and induces anisotropy, and also permit the inclusion of non-cardiomyocytes that can provide maturational cues. EHTs have been reported to develop positive a force-to-frequency relationship, T-tubule involvement in excitation-contraction coupling, increased oxidative metabolism, well-organized ultrastructure, and native sarcomere length and increased mitochondrial volumes [46–50]. Several studies have explored physical conditioning regimens, such as mechanical or electrical stimulation, to promote physiological maturation, e.g. [48, 51, 52]. Care must be exercised using these approaches because sustained afterload can induce pathological cardiac remodeling with reduced contractile function similar to chronic endothelin-1 or phenylephrine stimulation [53]. Addition of non-cardiomyocyte cell types, in particular fibroblasts, play crucial roles in developing optimal functional and structural properties of the EHT in part by regulating secretion of extracellular matrix proteins [54, 55]. Endothelial cells also enhance cardiomyocyte proliferation and maturation in 3D tissues [56, 57]. Most recently, atrial EHTs were generated [58]. EHTs face several hurdles for implementation with HTS platforms. For instance, creation of the constructs, and

certain readouts, such as measurement of force generation typically accomplished by optically or magnetically quantifying deflection of the posts that support the EHTs [59, 60] is more complicated in 3D than in 2D. The selection of 2D versus 3D systems depends on nature of the physiological response being probed, and the particular requirements for the extent of physiological maturation and degree that the assay model resembles native cardiac tissue. For instance, an interesting application of monoaxial EHTs is the reproduction of re-entry arrhythmia and the demonstration of restoration of rhythmic contraction and Ca^{2+} wave propagation by electrical shocking mimicking resynchronization therapy [61].

iPSC-Derived Cardiomyocytes for Disease Modeling and Drug Discovery

iPSC-derived cardiomyocytes have been used to model an increasing number of genetic heart diseases. Given the simplicity and relative immaturity of the iPSC-cardiomyocyte models, they have been used successfully to recapitulate a wide range of congenital diseases caused by early onset monogenic disorders for which the affected genes are expressed autonomously in cardiomyocytes [19].

Not surprisingly, familial arrhythmogenic disorders were among the first to be modeled, and examples include Long QT Syndrome [62], catecholaminergic polymorphic ventricular tachycardia [63], and Brugada Syndrome [64]. In addition, iPSC-derived cardiomyocytes have also been used to study familial cardiomyopathies [65], including multiple genetic mutations leading to hypertrophic cardiomyopathy (HCM) [66–68] or dilated cardiomyopathy (DCM) [69–71], and arrhythmogenic right ventricular cardiomyopathy (ARVD/C) [72–74]. EHTs have contributed to the study of a range of inherited cardiac diseases, including *Mybpc3* [75, 76], *Titin* DCM [77], *BRAF* HCM [78], *PLN-R14del* [79], and *PRKAG2* HCM [80].

Metabolic diseases have also been successfully modeled. The significant societal and economic impact of metabolic syndrome, obesity and type 2 diabetes, and the challenges inherent in studying multifactorial disease etiologies in animal models makes iPSC-based models an important contribution. Cardiometabolic diseases due to monogenic enzyme deficiencies can have cell autonomous pathologies amenable to iPSC modeling—on the other hand, however, many are polygenic for which current culture systems consisting of single or few cell types cannot be expected to recapitulate the range of pathologies [81]. One example of successful modeling neutral lipid storage disease (NLS), which is a rare disorder characterized by excessive accumulation of neutral lipids in a variety of cell types in the body, including cardiomyocytes. A deficiency in the patatin-like phospholipase domain-containing protein 2 (*PNPLA2*) gene encoding adipose triglyceride lipase (ATGL) causes NLS with myopathy (NLS-M), and the consistent pathological phenotype of increased lipid accumulation in cardiomyocytes can be observed Nile red staining of lipid droplets [82]. Another example is Barth syndrome, which is caused by mutations in the *Tafazzin*, a multifunctional protein that catalyzes the

modification of cardiolipin into its mature form that is essential for its roles in maintaining mitochondrial shape and energy production and is also a transcriptional co-activator with YAP in the Hippo pathway that regulates cell size and proliferation [83]. An example of acquired disease modeling is Drawnel et al. [84], who created environmental and patient-specific iPSC-CM models of diabetic cardiomyopathy and used them in conjunction with a library of 480 well-characterized bioactive compounds in a chemical biology exploration of possible therapeutic pathways. Several of the hits pointed to deranged calcium cycling and signaling as causative for the myopathic phenotype.

Modern drug discovery typically follows one or both of two approaches: (1) phenotypic screening and (2) target-based screening. Phenotypic screening, which identifies screen hits based on modulation of pathology or behavior, dominated historically but was overshadowed by target centric approaches following advances in the mechanistic understanding of disease and physiology during the twentieth century [85]. Unlike conventional target-centric drug discovery, phenotypic drug discovery is agnostic with regard to target and molecular mechanism of action and has enjoyed a revival in the past couple decades, contributing to about twice as many first-in-class small molecule drugs as solely target-centric approaches [79, 80]. Linking initial screening to disease phenotypes might address failures during drug development [86, 87] due to irreproducible targets [88–90] or overestimation of the role of a target in a disease process [91, 92] and underestimation of the molecular action of drugs (including potentially multiple targets) [93]. However, the approach has inherent weakness of providing little or no target information hindering risk assessment and hit advancement [78]. Nonetheless, it is our view that iPSC-based disease models have the potential of bringing the human disease context into the earliest stages of the drug discovery process, and embody criteria described by Vincent et al. [81] for predictive phenotypic assays: (1) disease relevance of the assay system, (2) disease relevance of the mechanism that evokes the phenotype, and (3) assay readout proximity to the clinical endpoint.

iPSC-Derived Cardiomyocytes to Assess Cardiotoxicity

Several drugs have been recalled or their use restricted due to cardiac safety concerns. A notable example is the 1992 US FDA black box warning for terfenadine, a non-sedating antihistamine used to treat allergic rhinitis. Ultimately, terfenadine was removed from the market in 1997. Other important examples include cisapride, a serotonin agonist associated with 125 deaths, Sibutramine, a weight loss drug, and propoxyphene, an opioid pain reliever. In addition to the patient harm, withdrawals and failures during development contribute the high cost to develop new medicines, now upwards of \$2 billion [5, 94].

Drug-induced tachyarrhythmias are commonly caused by off-target inhibition of the human Ether-à-go-go Related Gene (hERG/KCNH2) channel that mediates the delayed rectifier potassium current (I_{Kr}) that is important for action potential repolarization [95, 96]. Following documentation of hERG block and arrhythmogenicity

of proarrhythmic drugs, regulatory agencies mandated universal testing for hERG inhibition and clinical studies to assess proarrhythmic potential for investigational drugs that have now become industry standards [97]. Although hERG testing has prevented high risk drugs from entering the market, hERG binding per se is not entirely predictive of arrhythmia or QT prolongation [98, 99]. As a result, the reductionist hERG assays which are used for detecting cardiotoxicity may cause the unwarranted attrition of novel drug candidates [100]. Moreover, drugs can cause structural [101] and contractile dysfunction, but no single cellular mechanism is recognized as affecting cardiac contractile performance and has hence been difficult to predict in vitro. Hence, iPSC-derived cardiomyocytes have been proposed as an in vitro model system to predict both arrhythmic and contractile safety liabilities of drug candidates [100, 102, 103].

iPSC-derived cardiomyocytes are currently being evaluated as a model system for arrhythmic risk under the Comprehensive in vitro Proarrhythmia Assay (CiPA) initiative. Recently, a blinded, multisite validation study by Millard et al. [104] demonstrated high sensitivity of iPSC-derived cardiomyocytes for prominent depolarizing currents at 10 out of 18 studies; in qualifying studies, single and multichannel blocking compounds were observed to alter field potential duration (FPD) in concordance with known pharmacological behavior. Moreover, a second blinded, multisite validation study by Blinova et al. [105] amalgamated data from ten independent locations and reported overall predictability, consistent with data from single site studies, with minimal site-to-site variability. Although recent efforts have favored multielectrode array (MEA) for measuring field potential, alternatives are being explored. Pfeiffer et al. [102] utilized HT calcium imaging of iPSC-derived cardiomyocytes to identify arrhythmogenic drugs, reporting degrees of sensitivity and specificity that outperform hERG channel screens and match the upper bound of laborious non-rodent mammalian models. Taken together, these experiments indicate the utility of iPSC-derived cardiomyocyte models for detecting cardiotoxicity and represent a growing collection of studies that support iPSC-derived cardiomyocyte in vitro models [104–115]. Table 2.1 summarizes examples of published cardiotoxicity screens using iPSC-derived cardiomyocytes, typically in 2D.

Limitations of the above studies include the use of relatively few iPSC lines (the commercial lines were used across studies; typically, 1–2 lines/study). Therefore, the studies were incapable of assessing how patient variation might confer susceptibility to clinical cardiotoxicity and late-stage drug failure. Given the increasing availability of patient-specific and genome-edited lines, effort should be focused on understanding the influence of human genetic variation on drug-induced cardiomyopathic or proarrhythmic risk. Secondly, physiological properties of the iPSC-cardiomyocyte models (e.g., immaturity, homogeneity, 2D architecture), especially in MEA recordings, probably account for limited success in discriminating risk of certain compounds. For instance, drugs requiring metabolism to a cardiotoxic form or drugs that require a multicellular arrhythmia substrate would under-estimate clinical risk, whereas the increased sensitivity of iPSC-derived cardiomyocyte cultures to proarrhythmic effects of hERG blockade probably over-estimates the risk of hERG inhibitors with lesser clinical risk. To address cell type dependency,

Table 2.1 Overview of use of iPSC-derived cardiomyocytes for drug testing in 2D or 3D cultures

Culture modality	Measurement technology	Cell lines (source)	Cell line Genetic Background	# compounds evaluated	Compound Type	Reference
2D	Calcium (Fluo4)	1 (iCell)	WT	125	Various arrhythmia-related	[102]
2D	MEA/VSP	2 (iCell, Cor.4 U)	WT	26–28	CiPA	[105, 108]
2D	MEA	1 (iCell)	WT	10	Various arrhythmia-related	[107]
2D	MEA	1 (iCell)	WT	7	Various arrhythmia-related	[106]
2D	MEA	4 (iCell, Cor.4 U, GE, Stanford CVD)	WT	8	Various arrhythmia-related	[104]
2D	MEA	1 (iCell)	WT	60	Various arrhythmia-related	[109]
2D	MEA	1 (Cor.4 U)	WT	28	Various arrhythmia-related	[110]
2D	MEA	1 (iCell)	WT	15	Various arrhythmia-related	[111]
2D	MEA	1 (iCell)	WT	7–31	CSHAi, Various	[112–115]
2D	VSP (FluoVolt)	2 (iCell, in house)	WT	4–14	Various arrhythmia-related	[9]
2D	Contractility	5 (iCell, 4 in house)	WT	3–21	Kinase inhibitors	[124]
2D	Impedance contractility	1 (iCell)	WT	65	Kinase inhibitors	[125]
3D	Contractility	1 (in house)	WT	2	Isoproterenol, Verapamil	[132]
3D	Contractility	1 (iCell)	WT	10	Inotropes	[133]
3D	Contractility	1 (in house)	WT	8	Various	[131]
3D	Motion, VSP(FluoVolt)	2 (MiraCell, in house)	WT	1–3	Various arrhythmia-related	[128]
3D	Calcium and contractility	1 (in house)	WT	3	Various	[129]
3D	Beat rate	1 (in house)	WT	1	Doxorubicin	[130]

Abbreviations: MEA multielectrode array, VSP voltage-sensitive probe

multiplexed assays incorporating iPSC-derived hepatocytes [116] or neural cells [117] have been proposed. Finally, a greater understanding of how cellular phenotypes reflect clinical arrhythmia should increase predictiveness. Artificial intelligence is being used currently to classify ECG features to discriminate different cardiac conditions [118–120], and similar approaches might help to classify predictive features of iPSC-cardiomyocyte arrhythmia phenotypes.

Oncology drugs as a class exhibit cardiomyopathic and proarrhythmic effects. As many as 30% of patients experience heart disease during or after treatment, in some cases decades after their cancer treatment is completed [121, 122]. Not only older chemotherapeutics, such as anthracyclines, but also modern molecularly targeted therapeutics such as kinase inhibitors (KIs) have considerable adverse effects on the heart [121–123]. iPSC-cardiomyocytes have been used to detect cardiotoxicity that stems from KIs. Sharma et al. [124] screened 21 KIs and devised a cardiac safety index extracted from data on viability, contractility, calcium handling, and cellular electrophysiology. Low safety index values correlated with arrhythmogenic compounds, substantiating potential clinical utility. In addition, pathways conferring protection to toxicity of anticancer drugs were also explored. Further, Lamore et al. [125] screened 65 kinase inhibitors using a impedance contractility assay in an attempt to identify the kinases responsible for kinase inhibitor induced toxicity. In addition, Talbert et al. [126] explored the toxicity mechanism of ponatinib using a multi-parameter toxicity screen. Ponatinib is approved as the only KI used to treat chronic myelogenous leukemias with mutated BCR/ABL kinase, including the common “gatekeeper” T315I mutation, and is associated with a high incidence of cardiovascular toxicity [127]. Talbert et al. reported that ponatinib disrupts key signaling pathways, inflicts of structural toxicity, and perturbs beat rate of iPSC-derived cardiomyocyte models [126].

3D tissues have also been utilized to model drug-induced cardiotoxicity (Table 2.1). Recent efforts by Kawatou et al. [128] reported visualization of drug-induced TdP in 3D cardiac sheets. Likewise, Takeda et al. [129] studied the effect of doxorubicin in 3D cardiac tissues and observed toxicity at levels comparable to what has been observed in monolayer cultures. In contrast, Amano et al. [130] observed that 3D tissues were less susceptible to doxorubicin and noted reduced vascularization in 3D tissues with embedded microvasculature exposed to doxorubicin. Lu et al. [131] studied the cardiotoxic effects of a panel of drugs in stem cell derived cardiac tissues.

Conclusions and Future Perspectives

The advent of iPSC technologies—encompassing advances in cardiac cell type production, patient and disease specific genetics, high-throughput physiological recording, and tissue engineering—is promising for the study of cardiac disease mechanisms in vitro, drug discovery, and safety pharmacology. Major limitations are the physiological immaturity of the derived cardiomyocytes, and the homogeneity and simple architecture of the cultures. Research to address these issues by

culture media optimization and the fabrication of 3D micro tissues should have near-term improvements in predictiveness of the system. Furthermore, machine learning approaches will likely improve predictiveness of the in vitro models for clinical disease.

Acknowledgments We gratefully acknowledge support from the National Institutes of Health (NIH) (R01HL130840, R01HL128072 and R21HL141019 to MM). TM acknowledges support from AHA (Undergraduate Summer Research Program). DAMF is funded by the European Union's Horizon 2020 research and innovation programme under the Marie Skłodowska-Curie grant agreement No 708459.

Conflict of Interest Statement The authors have no conflicting interests.

References

1. Harrison RK. Phase II and phase III failures: 2013-2015. *Nat Rev Drug Discov.* 2016;15(12):817–8.
2. Wong CH, et al. Estimation of clinical trial success rates and related parameters. *Biostatistics.* 2018; <https://doi.org/10.1093/biostatistics/kxx069>.
3. Fordyce CB, et al. Cardiovascular drug development: is it dead or just hibernating? *J Am Coll Cardiol.* 2015;65(15):1567–82.
4. MacDonald JS, et al. Toxicity testing in the 21st century: a view from the pharmaceutical industry. *Toxicol Sci.* 2009;110(1):40–6.
5. Waring MJ, et al. An analysis of the attrition of drug candidates from four major pharmaceutical companies. *Nat Rev Drug Discov.* 2015;14(7):475–86.
6. Takahashi K, et al. Induction of pluripotent stem cells from mouse embryonic and adult fibroblast cultures by defined factors. *Cell.* 2006;126(4):663–76.
7. Lian X, et al. Directed cardiomyocyte differentiation from human pluripotent stem cells by modulating Wnt/ β -catenin signaling under fully defined conditions. *Nat Protoc.* 2013;8(1):162–75.
8. Burridge PW, et al. Chemically defined generation of human cardiomyocytes. *Nat Methods.* 2014;11(8):855–60.
9. McKeithan WL, et al. An automated platform for assessment of congenital and drug-induced arrhythmia with hiPSC-derived cardiomyocytes. *Front Physiol.* 2017;8:766.
10. Bedut S, et al. High-throughput drug profiling with voltage- and calcium-sensitive fluorescent probes in human iPSC-derived cardiomyocytes. *Am J Physiol Heart Circ Physiol.* 2016;311(1):H44–53.
11. Kolanowski TJ, et al. Making human cardiomyocytes up to date: Derivation, maturation state and perspectives. *Int J Cardiol.* 2017;241:379–86.
12. Yang X, et al. Engineering adolescence: maturation of human pluripotent stem cell-derived cardiomyocytes. *Circ Res.* 2014;114(3):511–23.
13. Koivumäki JT, et al. Structural immaturity of human iPSC-derived cardiomyocytes. *Front Physiol.* 2018;9:80.
14. Kane C, et al. Excitation-contraction coupling of human induced pluripotent stem cell-derived cardiomyocytes. *Front Cell Dev Biol.* 2015;3:59.
15. Dai DF, et al. Mitochondrial maturation in human pluripotent stem cell derived cardiomyocytes. *Stem Cells Int.* 2017;2017:5153625.
16. Malandraki-Miller S, et al. Changing metabolism in differentiating cardiac progenitor cells-can stem cells become metabolically flexible cardiomyocytes? *Front Cardiovasc Med.* 2018;5:119.
17. Knollmann BC. Induced pluripotent stem cell-derived cardiomyocytes: boutique science or valuable arrhythmia model? *Circ Res.* 2013;112(6):969–76. discussion 976

18. Keung W, et al. Developmental cues for the maturation of metabolic, electrophysiological and calcium handling properties of human pluripotent stem cell-derived cardiomyocytes. *Stem Cell Res Ther.* 2014;5(1):17.
19. Del Alamo JC, et al. High throughput physiological screening of iPSC-derived cardiomyocytes for drug development. *Biochim Biophys Acta.* 2016;1863(7 Pt B):1717–27.
20. Kim C, et al. Non-cardiomyocytes influence the electrophysiological maturation of human embryonic stem cell-derived cardiomyocytes during differentiation. *Stem Cells Dev.* 2010;19(6):783–95.
21. Ma J, et al. High purity human-induced pluripotent stem cell-derived cardiomyocytes: electrophysiological properties of action potentials and ionic currents. *Am J Physiol Heart Circ Physiol.* 2011;301(5):H2006–17.
22. Pekkanen-Mattila M, et al. The effect of human and mouse fibroblast feeder cells on cardiac differentiation of human pluripotent stem cells. *Stem Cells Int.* 2012;2012:875059.
23. Zhang Q, et al. Direct differentiation of atrial and ventricular myocytes from human embryonic stem cells by alternating retinoid signals. *Cell Res.* 2011;21(4):579–87.
24. Lundy SD, et al. Structural and functional maturation of cardiomyocytes derived from human pluripotent stem cells. *Stem Cells Dev.* 2013;22(14):1991–2002.
25. Ibrahim M, et al. The structure and function of cardiac t-tubules in health and disease. *Proc Biol Sci.* 2011;278(1719):2714–23.
26. Dolnikov K, et al. Functional properties of human embryonic stem cell-derived cardiomyocytes: intracellular Ca²⁺ handling and the role of sarcoplasmic reticulum in the contraction. *Stem Cells.* 2006;24(2):236–45.
27. Poon E, et al. Human pluripotent stem cell-based approaches for myocardial repair: from the electrophysiological perspective. *Mol Pharm.* 2011;8(5):1495–504.
28. Nikolaev VO, et al. Cyclic AMP imaging in adult cardiac myocytes reveals far-reaching beta1-adrenergic but locally confined beta2-adrenergic receptor-mediated signaling. *Circ Res.* 2006;99(10):1084–91.
29. Perry SJ, et al. Targeting of cyclic AMP degradation to beta 2-adrenergic receptors by beta-arrestins. *Science.* 2002;298(5594):834–6.
30. Jung G, et al. Time-dependent evolution of functional vs. remodeling signaling in iPSC-derived cardiomyocytes and induced maturation with biomechanical stimulation. *FASEB J.* 2016;30(4):1464–79.
31. Lyon AR, et al. Loss of T-tubules and other changes to surface topography in ventricular myocytes from failing human and rat heart. *Proc Natl Acad Sci U S A.* 2009;106(16):6854–9.
32. Nikolaev VO, et al. Beta2-adrenergic receptor redistribution in heart failure changes cAMP compartmentation. *Science.* 2010;327(5973):1653–7.
33. Kaumann A, et al. Activation of beta2-adrenergic receptors hastens relaxation and mediates phosphorylation of phospholamban, troponin I, and C-protein in ventricular myocardium from patients with terminal heart failure. *Circulation.* 1999;99(1):65–72.
34. Lefkowitz RJ. G protein-coupled receptors. III. New roles for receptor kinases and beta-arrestins in receptor signaling and desensitization. *J Biol Chem.* 1998;273(30):18677–80.
35. Rapacciuolo A, et al. Protein kinase A and G protein-coupled receptor kinase phosphorylation mediates beta-1 adrenergic receptor endocytosis through different pathways. *J Biol Chem.* 2003;278(37):35403–11.
36. Yang X, et al. Tri-iodo-L-thyronine promotes the maturation of human cardiomyocytes-derived from induced pluripotent stem cells. *J Mol Cell Cardiol.* 2014;72:296–304.
37. Parikh SS, et al. Thyroid and glucocorticoid hormones promote functional T-tubule development in human-induced pluripotent stem cell-derived cardiomyocytes. *Circ Res.* 2017;121(12):1323–30.
38. Hu D, et al. Metabolic maturation of human pluripotent stem cell-derived cardiomyocytes by inhibition of HIF1 α and LDHA. *Circ Res.* 2018;123(9):1066–79.
39. Ribeiro AJ, et al. Contractility of single cardiomyocytes differentiated from pluripotent stem cells depends on physiological shape and substrate stiffness. *Proc Natl Acad Sci U S A.* 2015;112(41):12705–10.

40. Jung G, et al. Time-dependent evolution of functional vs. remodeling signaling in induced pluripotent stem cell-derived cardiomyocytes and induced maturation with biomechanical stimulation. *FASEB J*. 2016;30(4):1464–79.
41. McBeath R, et al. Cell shape, cytoskeletal tension, and RhoA regulate stem cell lineage commitment. *Dev Cell*. 2004;6(4):483–95.
42. Lutolf MP, et al. Synthetic biomaterials as instructive extracellular microenvironments for morphogenesis in tissue engineering. *Nat Biotechnol*. 2005;23(1):47–55.
43. Young JL, et al. Hydrogels with time-dependent material properties enhance cardiomyocyte differentiation in vitro. *Biomaterials*. 2011;32(4):1002–9.
44. Jacot JG, et al. Mechanobiology of cardiomyocyte development. *J Biomech*. 2010;43(1):93–8.
45. Young JL, et al. Mechanosensitive kinases regulate stiffness-induced cardiomyocyte maturation. *Sci Rep*. 2014;4:6425.
46. Ravi M, et al. 3D cell culture systems: advantages and applications. *J Cell Physiol*. 2015;230(1):16–26.
47. Lemoine MD, et al. Human iPSC-derived cardiomyocytes cultured in 3D engineered heart tissue show physiological upstroke velocity and sodium current density. *Sci Rep*. 2017;7(1):5464.
48. Fink C, et al. Chronic stretch of engineered heart tissue induces hypertrophy and functional improvement. *FASEB J*. 2000;14(5):669–79.
49. Mathur A, et al. Human iPSC-based cardiac microphysiological system for drug screening applications. *Sci Rep*. 2015;5:8883.
50. Langhans SA. Three-dimensional in vitro cell culture models in drug discovery and drug repositioning. *Front Pharmacol*. 2018;9:6.
51. Ulmer BM, et al. Contractile work contributes to maturation of energy metabolism in hiPSC-derived cardiomyocytes. *Stem Cell Reports*. 2018;10(3):834–47.
52. Ronaldson-Bouchard K, et al. Advanced maturation of human cardiac tissue grown from pluripotent stem cells. *Nature*. 2018;556(7700):239–43.
53. Hirt MN, et al. Increased afterload induces pathological cardiac hypertrophy: a new in vitro model. *Basic Res Cardiol*. 2012;107(6):307.
54. Stevens KR, et al. Physiological function and transplantation of scaffold-free and vascularized human cardiac muscle tissue. *Proc Natl Acad Sci U S A*. 2009;106(39):16568–73.
55. Naito H, et al. Optimizing engineered heart tissue for therapeutic applications as surrogate heart muscle. *Circulation*. 2006;114(1 Suppl):I72–8.
56. Tulloch NL, et al. Growth of engineered human myocardium with mechanical loading and vascular coculture. *Circ Res*. 2011;109(1):47–59.
57. Giacomelli E, et al. Three-dimensional cardiac microtissues composed of cardiomyocytes and endothelial cells co-differentiated from human pluripotent stem cells. *Development*. 2017;144(6):1008–17.
58. Lemme M, et al. Atrial-like engineered heart tissue: an in vitro model of the human atrium. *Stem Cell Reports*. 2018;11:1378.
59. Mannhardt I, et al. Human engineered heart tissue: analysis of contractile force. *Stem Cell Reports*. 2016;7(1):29–42.
60. Bielawski KS, et al. Real-time force and frequency analysis of engineered human heart tissue derived from induced pluripotent stem cells using magnetic sensing. *Tissue Eng Part C Methods*. 2016;22(10):932–40.
61. Thavandiran N, et al. Design and formulation of functional pluripotent stem cell-derived cardiac microtissues. *Proc Natl Acad Sci U S A*. 2013;110(49):E4698–707.
62. Moretti A, et al. Patient-specific induced pluripotent stem-cell models for long-QT syndrome. *N Engl J Med*. 2010;363(15):1397–409.
63. Itzhaki I, et al. Modeling of catecholaminergic polymorphic ventricular tachycardia with patient-specific human-induced pluripotent stem cells. *J Am Coll Cardiol*. 2012;60(11):990–1000.
64. Liang P, et al. Patient-specific and genome-edited induced pluripotent stem cell-derived cardiomyocytes elucidate single-cell phenotype of Brugada syndrome. *J Am Coll Cardiol*. 2016;68(19):2086–96.
65. Karakikes I, et al. Human-induced pluripotent stem cell models of inherited cardiomyopathies. *Curr Opin Cardiol*. 2014;29(3):214–9.

66. Birket MJ, et al. Contractile defect caused by mutation in MYBPC3 revealed under conditions optimized for human PSC-cardiomyocyte function. *Cell Rep.* 2015;13(4):733–45.
67. Lan F, et al. Abnormal calcium handling properties underlie familial hypertrophic cardiomyopathy pathology in patient-specific induced pluripotent stem cells. *Cell Stem Cell.* 2013;12(1):101–13.
68. Han L, et al. Study familial hypertrophic cardiomyopathy using patient-specific induced pluripotent stem cells. *Cardiovasc Res.* 2014;104(2):258–69.
69. Sun N, et al. Patient-specific induced pluripotent stem cells as a model for familial dilated cardiomyopathy. *Sci Transl Med.* 2012;4(130):130ra47.
70. Streckfuss-Bömeke K, et al. Severe DCM phenotype of patient harboring RBM20 mutation S635A can be modeled by patient-specific induced pluripotent stem cell-derived cardiomyocytes. *J Mol Cell Cardiol.* 2017;113:9–21.
71. Wyles SP, et al. Pharmacological modulation of calcium homeostasis in familial dilated cardiomyopathy: an in vitro analysis from an RBM20 patient-derived iPSC model. *Clin Transl Sci.* 2016;9(3):158–67.
72. Ma D, et al. Generation of patient-specific induced pluripotent stem cell-derived cardiomyocytes as a cellular model of arrhythmogenic right ventricular cardiomyopathy. *Eur Heart J.* 2013;34(15):1122–33.
73. Caspi O, et al. Modeling of arrhythmogenic right ventricular cardiomyopathy with human induced pluripotent stem cells. *Circ Cardiovasc Genet.* 2013;6(6):557–68.
74. Kim C, et al. Studying arrhythmogenic right ventricular dysplasia with patient-specific iPSCs. *Nature.* 2013;494(7435):105–10.
75. Seeger T, et al. A premature termination codon mutation of MYBPC3 causes hypertrophic cardiomyopathy via chronic activation of nonsense-mediated decay. *Circulation.* 2019;139:799–811.
76. Stöhr A, et al. Contractile abnormalities and altered drug response in engineered heart tissue from Mybpc3-targeted knock-in mice. *J Mol Cell Cardiol.* 2013;63:189–98.
77. Hinson JT, et al. HEART DISEASE. Titin mutations in iPSC cells define sarcomere insufficiency as a cause of dilated cardiomyopathy. *Science.* 2015;349(6251):982–6.
78. Cashman TJ, et al. Human engineered cardiac tissues created using induced pluripotent stem cells reveal functional characteristics of BRAF-mediated hypertrophic cardiomyopathy. *PLoS One.* 2016;11(1):e0146697.
79. Stillitano F, et al. Genomic correction of familial cardiomyopathy in human engineered cardiac tissues. *Eur Heart J.* 2016;37(43):3282–4.
80. Hinson JT, et al. Integrative analysis of PRKAG2 cardiomyopathy iPSC and microtissue models identifies AMPK as a regulator of metabolism, survival, and fibrosis. *Cell Rep.* 2017;19(11):2410.
81. Nakamura K, et al. iPSC cell modeling of cardiometabolic diseases. *J Cardiovasc Transl Res.* 2013;6(1):46–53.
82. Tavian D, et al. Generation of induced Pluripotent Stem Cells as disease modelling of NLSDM. *Mol Genet Metab.* 2017;121(1):28–34.
83. Wang G, et al. Modeling the mitochondrial cardiomyopathy of Barth syndrome with induced pluripotent stem cell and heart-on-chip technologies. *Nat Med.* 2014;20(6):616–23.
84. Drawnel FM, et al. Disease modeling and phenotypic drug screening for diabetic cardiomyopathy using human induced pluripotent stem cells. *Cell Rep.* 2014;9(3):810–21.
85. Prathipati P, et al. Systems biology approaches to a rational drug discovery paradigm. *Curr Top Med Chem.* 2016;16(9):1009–25.
86. Moffat JG, et al. Opportunities and challenges in phenotypic drug discovery: an industry perspective. *Nat Rev Drug Discov.* 2017;16(8):531–43.
87. Vincent F, et al. Developing predictive assays: the phenotypic screening “rule of 3”. *Sci Transl Med.* 2015;7(293):293ps15.
88. Ioannidis JP. Why most published research findings are false. *PLoS Med.* 2005;2(8):e124.
89. Osherovich L. Hedging against academic risk. *Science-Business eXchange.* 2011;4(15):416.
90. Prinz F, et al. Believe it or not: how much can we rely on published data on potential drug targets? *Nat Rev Drug Discov.* 2011;10:712.

91. Scannell JW, et al. When quality beats quantity: decision theory, drug discovery, and the reproducibility crisis. *PLoS One*. 2016;11(2):e0147215.
92. Nelson MR, et al. The support of human genetic evidence for approved drug indications. *Nat Genet*. 2015;47(8):856–60.
93. Reddy AS, et al. Polypharmacology: drug discovery for the future. *Expert Rev Clin Pharmacol*. 2013;6(1):41–7.
94. Mullard A. New drugs cost US\$2.6 billion to develop. *Nat Rev Drug Discov*. 2014;13:877.
95. Hoffmann P, et al. Are hERG channel inhibition and QT interval prolongation all there is in drug-induced torsadogenesis? A review of emerging trends. *J Pharmacol Toxicol Methods*. 2006;53(2):87–105.
96. Redfern WS, et al. Relationships between preclinical cardiac electrophysiology, clinical QT interval prolongation and torsade de pointes for a broad range of drugs: evidence for a provisional safety margin in drug development. *Cardiovasc Res*. 2003;58(1):32–45.
97. Sager PT, et al. Rechanneling the cardiac proarrhythmia safety paradigm: a meeting report from the Cardiac Safety Research Consortium. *Am Heart J*. 2014;167(3):292–300.
98. Lawrence CL, et al. Nonclinical proarrhythmia models: predicting Torsades de Pointes. *J Pharmacol Toxicol Methods*. 2005;52(1):46–59.
99. Kannankeril P, et al. Drug-induced long QT syndrome. *Pharmacol Rev*. 2010;62(4):760–81.
100. Gintant G, et al. Evolution of strategies to improve preclinical cardiac safety testing. *Nat Rev Drug Discov*. 2016;15(7):457–71.
101. Andrejak M, et al. Drug-induced valvular heart disease: an update. *Arch Cardiovasc Dis*. 2013;106(5):333–9.
102. Pfeiffer ER, et al. Specific prediction of clinical QT prolongation by kinetic image cytometry in human stem cell derived cardiomyocytes. *J Pharmacol Toxicol Methods*. 2016;81:263–73.
103. Watanabe H, et al. Usefulness of cardiotoxicity assessment using calcium transient in human induced pluripotent stem cell-derived cardiomyocytes. *J Toxicol Sci*. 2017;42(4):519–27.
104. Millard D, et al. Cross-site reliability of human induced pluripotent stem cell-derived cardiomyocyte based safety assays using microelectrode arrays: results from a blinded CiPA Pilot Study. *Toxicol Sci*. 2018;164(2):550–62.
105. Blinova K, et al. International multisite study of human-induced pluripotent stem cell-derived cardiomyocytes for drug proarrhythmic potential assessment. *Cell Rep*. 2018;24(13):3582–92.
106. Gilchrist KH, et al. High-throughput cardiac safety evaluation and multi-parameter arrhythmia profiling of cardiomyocytes using microelectrode arrays. *Toxicol Appl Pharmacol*. 2015;288(2):249–57.
107. Harris K, et al. Comparison of electrophysiological data from human-induced pluripotent stem cell-derived cardiomyocytes to functional preclinical safety assays. *Toxicol Sci*. 2013;134(2):412–26.
108. Blinova K, et al. Comprehensive translational assessment of human-induced pluripotent stem cell derived cardiomyocytes for evaluating drug-induced arrhythmias. *Toxicol Sci*. 2017;155(1):234–47.
109. Ando H, et al. A new paradigm for drug-induced torsadogenic risk assessment using human iPSC cell-derived cardiomyocytes. *J Pharmacol Toxicol Methods*. 2017;84:111–27.
110. Yamazaki D, et al. Proarrhythmia risk prediction using human induced pluripotent stem cell-derived cardiomyocytes. *J Pharmacol Sci*. 2018;136(4):249–56.
111. Qu Y, et al. Proarrhythmia risk assessment in human induced pluripotent stem cell-derived cardiomyocytes using the Maestro MEA Platform. *Toxicol Sci*. 2015;147(1):286–95.
112. Kitaguchi T, et al. CSAHi study: Evaluation of multi-electrode array in combination with human iPSC cell-derived cardiomyocytes to predict drug-induced QT prolongation and arrhythmia – effects of 7 reference compounds at 10 facilities. *J Pharmacol Toxicol Methods*. 2016;78:93–102.
113. Kitaguchi T, et al. CSAHi study: detection of drug-induced ion channel/receptor responses, QT prolongation, and arrhythmia using multi-electrode arrays in combination with human induced pluripotent stem cell-derived cardiomyocytes. *J Pharmacol Toxicol Methods*. 2017;85:73–81.

114. Nozaki Y, et al. CSAHi study: validation of multi-electrode array systems (MEA60/2100) for prediction of drug-induced proarrhythmia using human iPS cell-derived cardiomyocytes – assessment of inter-facility and cells lot-to-lot-variability. *Regul Toxicol Pharmacol.* 2016;77:75–86.
115. Nozaki Y, et al. CSAHi study-2: Validation of multi-electrode array systems (MEA60/2100) for prediction of drug-induced proarrhythmia using human iPS cell-derived cardiomyocytes: assessment of reference compounds and comparison with non-clinical studies and clinical information. *Regul Toxicol Pharmacol.* 2017;88:238–51.
116. Grimm FA, et al. High-content assay multiplexing for toxicity screening in induced pluripotent stem cell-derived cardiomyocytes and hepatocytes. *Assay Drug Dev Technol.* 2015;13(9):529–46.
117. Csöbönyeiová M, et al. Toxicity testing and drug screening using iPSC-derived hepatocytes, cardiomyocytes, and neural cells. *Can J Physiol Pharmacol.* 2016;94(7):687–94.
118. Savalia S, et al. Cardiac arrhythmia classification by multi-layer perceptron and convolution neural networks. *Bioengineering (Basel).* 2018;5(2):35.
119. Andreotti F, et al. Comparing feature-based classifiers and convolutional neural networks to detect arrhythmia from short segments of ECG. *Comput Cardiol.* 2017;44:1–4.
120. Rajpurkar P, et al. Cardiologist-level arrhythmia detection with convolutional neural networks. *arXiv170701836.* 2017. 2017.
121. Yeh ET, et al. Cardiovascular complications of cancer therapy: incidence, pathogenesis, diagnosis, and management. *J Am Coll Cardiol.* 2009;53(24):2231–47.
122. Aleman BM, et al. Cardiovascular disease after cancer therapy. *EJC Suppl.* 2014;12(1):18–28.
123. Moslehi J, et al. Grounding cardio-oncology in basic and clinical science. *Circulation.* 2017;136(1):3–5.
124. Sharma A, et al. High-throughput screening of tyrosine kinase inhibitor cardiotoxicity with human induced pluripotent stem cells. *Sci Transl Med.* 2017;9(377):eaaf2584.
125. Lamore SD, et al. Deconvoluting kinase inhibitor induced cardiotoxicity. *Toxicol Sci.* 2017;158(1):213–26.
126. Talbert DR, et al. A multi-parameter in vitro screen in human stem cell-derived cardiomyocytes identifies ponatinib-induced structural and functional cardiac toxicity. *Toxicol Sci.* 2015;143(1):147–55.
127. Moslehi JJ, et al. Tyrosine kinase inhibitor-associated cardiovascular toxicity in chronic myeloid leukemia. *J Clin Oncol.* 2015;33(35):4210–8.
128. Kawatou M, et al. Modelling Torsade de Pointes arrhythmias in vitro in 3D human iPS cell-engineered heart tissue. *Nat Commun.* 2017;8(1):1078.
129. Takeda M, et al. Development of in vitro drug-induced cardiotoxicity assay by using three-dimensional cardiac tissues derived from human induced pluripotent stem cells. *Tissue Eng Part C Methods.* 2018;24(1):56–67.
130. Amano Y, et al. Development of vascularized iPSC derived 3D-cardiomyocyte tissues by filtration Layer-by-Layer technique and their application for pharmaceutical assays. *Acta Biomater.* 2016;33:110–21.
131. Lu HF, et al. Engineering a functional three-dimensional human cardiac tissue model for drug toxicity screening. *Biofabrication.* 2017;9(2):025011.
132. Huebsch N, et al. Miniaturized iPS-cell-derived cardiac muscles for physiologically relevant drug response analyses. *Sci Rep.* 2016;6:24726.
133. Mannhardt I, et al. Blinded contractility analysis in hiPSC-cardiomyocytes in engineered heart tissue format: comparison with human atrial trabeculae. *Toxicol Sci.* 2017;158(1):164–75.



Decellularized Extracellular Matrix-Based Cardiovascular Tissue Engineering

3

Kristin M. French and Michael E. Davis

Introduction

Cardiovascular disease remains an extremely deadly and costly burden across the globe. Since the myocardium has a limited regenerative capacity, current therapies are restricted to pharmaceuticals, mechanical and electrical support devices, and synthetic materials. Decellularized extracellular matrices have strong potential to provide support to failing myocardium. Their native composition offers complex biochemical cues beyond what can be synthesized in the laboratory. Their physical versatility affords multiple application routes as entire recellularized organs, acellular or recellularized patches, or injectable materials that conform to the dimensions of the injury. Manipulating the materials allows for engineering their mechanical properties, such as stiffness and degradation kinetics, through crosslinking or building hybrid scaffolds. Decellularized matrices can also serve as delivery vehicles by harnessing native conjugation sites for bioactive molecules. When delivered with cells, the decellularized matrix improves cell retention, protects these cells from the harsh microenvironment of the injured tissue, and directs their behavior. Importantly, the materials mimic the native extracellular matrix and can be remodeled, adapting and growing with the repaired tissue.

The field for decellularization of extracellular matrices has grown tremendously in the last decade and a half. To date, research has focused on the best material

K. M. French

Internal Medicine, Cardiology, University of Texas Southwestern Medical Center,
Dallas, TX, USA

e-mail: Kristin.french@utsouthwestern.edu

M. E. Davis (✉)

Wallace H. Coulter Department of Biomedical Engineering, Emory University,
Atlanta, GA, USA

Division of Cardiology, Emory University School of Medicine, Atlanta, GA, USA

e-mail: michael.davis@bme.gatech.edu

sourcing and decellularization process. Ultimately, the goal of decellularization is complete removal of cellular material, including immunogenic antigens, and preservation of the underlying matrix structure and composition. Methods for this include ionic and nonionic detergents, hypotonic and hypertonic solution, acidic and basic solutions, physical disruption with pressure or temperature alterations, enzymatic degradation, chelating agents, or a combination of the above. For therapeutic applications, material-specific properties, nontoxicity, and sterility must also be achieved. The versatility and adaptability of decellularized extracellular matrices makes them strong tools in cardiovascular tissue engineering.

The cardiovascular network is a complex system composed of conduits (blood vessels), valves, and contractile muscle (the myocardium). Within each of these components is further heterogeneity. For example, healthy myocardium ranges in localized mechanical stiffness due to variations in matrix protein composition and organization [1]. Dynamic alterations with aging also result in the increased deposition and changing composition of structural extracellular matrix proteins [2–4]. This is paralleled by an increase in mechanical stiffness with development as well [4]. Heart disease, such as that induced by pressure overload, volume overload, and myocardial infarction, results in remodeling of myocardium [5, 6]. Typically, an increase in structural matrix protein deposition is observed [7–11]. This, in combination with increased crosslinking of the extracellular matrix leads to progressive passive stiffening of the myocardium [7, 11]. This is underscored by remodeling of nonstructural extracellular matrix components that regulate cell behavior [10, 12]. This description is specific to overall changes in the myocardium with ageing and disease, but similarly, increased stiffness and mineralization is observed in blood vessels and cardiac valves as well. Cardiac remodeling drives a need for tissue engineering strategies and also dictates the sources of choice materials for such strategies.

Methods for Decellularization

Decellularization and Characterization of Myocardium and Pericardium

To date, the most common method of decellularization of the myocardium is detergent based. Protocols vary in format of the native material (whole heart, slices, pieces, etc.), which dictates timing of the decellularization and the final application. These protocols are summarized in Table 3.1. To summarize, ventricular tissue is cut into small (millimeter or centimeter cubed) size pieces. Decellularization is then carried out by immersion and stirring in 1% sodium dodecyl sulfate (SDS) for several days [16, 17]. This process may be followed by a shorter 30-min incubation in 1% Triton X-100. The decellularized material (cECM) is then washed in water for several hours to remove any remaining detergent. In comparison, the pericardium can be

Table 3.1 A comparison of various reported protocols for decellularization of myocardial tissues. Note that the tissue type and source dictate the success of a given method.

Tissue	Source	Structure	Method	Sterilization	Citation
Pericardium	Human	Pieces; later milled and pepsin digested	Water, 1% SDS in PBS for 60–65 h	Not reported	[13]
Pericardium	Human	Intact	Hypotonic buffer (10 mM Tris–HCl, pH 8) for 16 h at 4 °C, 0.1% SDS for 24 h, DNase and RNase for 3 h at 37 °C	Not reported	[14]
Pericardium	Bovine	Intact	(1) 1% SDS, (2) 1% SDS + 0.5% sodium deoxycholate (3) 1% Triton X-100 (4) 1% Triton X-100 + 0.5% sodium deoxycholate (5) Freeze–thaw cycles + 1% SDS + 0.5% sodium deoxycholate (6) Freeze–thaw cycles + 1% Triton X-100 + 0.5% sodium deoxycholate	Not reported	[15]
Myocardium	Porcine	Pieces; later milled and pepsin digested	1% SDS for 4–5 days, 1% Triton X-100 30 min	Not reported	[16, 17]
Myocardium	Human	300 μm sections	10 mM Tris, 0.15 EDTA, pH 7.4 for 2 h, 0.5% SDS for 6 h	Penicillin, streptomycin, nystatin	[18]
Myocardium	Porcine	2 mm sheets	(1) 1% Triton X-100 (2) 1% SDS (3) 0.5% trypsin for 3 days at 4 °C	Cefazolin, gentamicin, amphotericin B, metronidazole	[19]
Myocardium	Human	300 μm sections	(1) 0.5% SDS for 9 h (2) 5% Triton X-100 for 48 h (3) 4% sodium deoxycholate for 40 h (4) Alternating hypo/hypertonic treatment for 3 days, (5) 3-step protocol: 10 mM Tris for 2 h, 0.5% SDS for 6 h and FBS for 3 h at 37 °C	Penicillin, streptomycin, nystatin	[20]

(continued)

Table 3.1 (continued)

Tissue	Source	Structure	Method	Sterilization	Citation
Epicardium, myocardium, endocardium	Porcine	Sheets	(1) 1% SDS for 72 h, 1% Triton X-100 for 48 h, DNase for 72 h (2) Alternating 1.1% NaCl and hypotonic 0.7% NaCl for 8 h, 0.05% trypsin for 48 h at 37 °C, 1% triton X-100 plus 1% ammonium hydroxide for 96 h	UV	[21]
Myocardium and skeletal muscle	Porcine	Pieces; later milled and pepsin digested	1% SDS for 3–4 days; skeletal muscle also treated with isopropanol (12–24 h) to remove lipids	Penicillin, streptomycin	[22]
Myocardium	Human, porcine	Pieces; later milled and pepsin digested	Porcine: 1% SDS solution 3–5 days Human: 1% SDS solution 6–8 days, isopropanol 12–24 h, DNase/RNase 24 h, 1% SDS 24 h, 0.001% triton X-100 30 min	Penicillin, streptomycin	[23]
Myocardium	Rat	Pieces	Submerged in ethanol in a high-pressure reactor; supercritical CO ₂ added at 37 °C and 350 bar for 6 h, DNase	Penicillin	[24]
Myocardium	Rat (fetal, neonatal, and adult)	Intact or pieces	0.05% fetal (immersion), 0.5% neonatal (immersion), 1% adult (perfusion or minced before immersion) SDS, then Triton X-100 for several hours; Pepsin digestion: 1 h for fetal, 2–4 h for neonatal, 24–48 h for adult	Not reported	[3]
Myocardium	Rat (fetal, neonatal, and adult)	Intact or pieces	Hypotonic buffer for 18 h, 0.2% SDS for 24 h, hypotonic buffer 1 h, DNase 3 h at 37 °C	Penicillin, streptomycin, fungizone	[25]
Whole heart	Rat	Intact	Heparinized PBS with adenosine at pressure of 77.4 mmHg for 15 min, 1% SDS for 12 h, 1% Triton-X100 for 30 min	Penicillin, streptomycin, amphotericin B	[26]

Table 3.1 (continued)

Tissue	Source	Structure	Method	Sterilization	Citation
Whole heart	Porcine	Intact	Freeze–thaw, hypotonic wash, 0.02% trypsin at 37 °C for 2 h, 3% Triton X-100 perfusion for 2 h, 4% deoxycholic acid solution for 2 h	Peracetic acid, ethanol	[27]

decellularized by gentler conditions, such as hypotonic buffer and 0.1–1% SDS in just 1–2 days [13, 14]. If the myocardium is instead sectioned into thin sheets (hundreds of microns thick), it can also be decellularized under gentler conditions. One such example is a three-step immersion protocol, that is, a few hours each in hypotonic Tris buffer and 0.5% SDS, followed by overnight sterilization in antibiotics [18].

In an effort to determine the optimal procedure several studies have performed head-to-head comparison of decellularization methods. SDS also better removed cellular material and preserved fiber structure when compared to 1% Triton X-100 concentrations or enzymatic degradation by 0.5% trypsin [19]. While SDS is the strongest decellularization tested, its use can also result in lost elastic fibers, glycosaminoglycans, and even collagen matrix proteins. Combination methods that allow for lower concentration of SDS with the addition of cell bursting (freezing or hypotonic solution) and Triton X-100 incubation improve preservation of cECM composition and biomechanics, without sacrificing removal of cellular material [15, 20]. A comparison of 0.5% SDS, 5% Triton X-100, 4% sodium deoxycholate, alternating hypo- and hypertonic solutions or a combination as described in the three-step protocol above demonstrated that the combination method outperformed the others. Triton X-100, sodium deoxycholate, and hypo/hypertonic treatment damaged the matrix structure of the myocardium and did not completely remove cellular material [20]. Interestingly, the authors also demonstrated that cECM derived from infarcted tissue had a denser fibrotic network.

A drawback to these methods is that detergent-based decellularization can be overly harsh and may result in alteration of biomechanical properties or composition. To overcome this, Seo et al. submerged freeze-dried rat myocardium in ethanol in a high-pressure reactor. The tissue was then decellularized with supercritical carbon dioxide at 37 °C and 350 bar in 6 h [24]. Supercritical carbon better preserved glycosaminoglycans, extracellular matrix proteins, and angiogenic cytokines than an SDS and Triton X-100 protocol; however, the fibrous structure was more fragmented and required mixture with collagen before gelation. After bulk decellularization, cECM can also be treated with deoxyribonuclease I and ribonuclease A or serum to further reduce DNA content. Finally, if the final desired application of the material is a culture coating or injectable hydrogel, then the cECM should be lyophilized, milled into a powder, and solubilized in pepsin under acidic conditions for 48 h [13, 16, 18, 24].

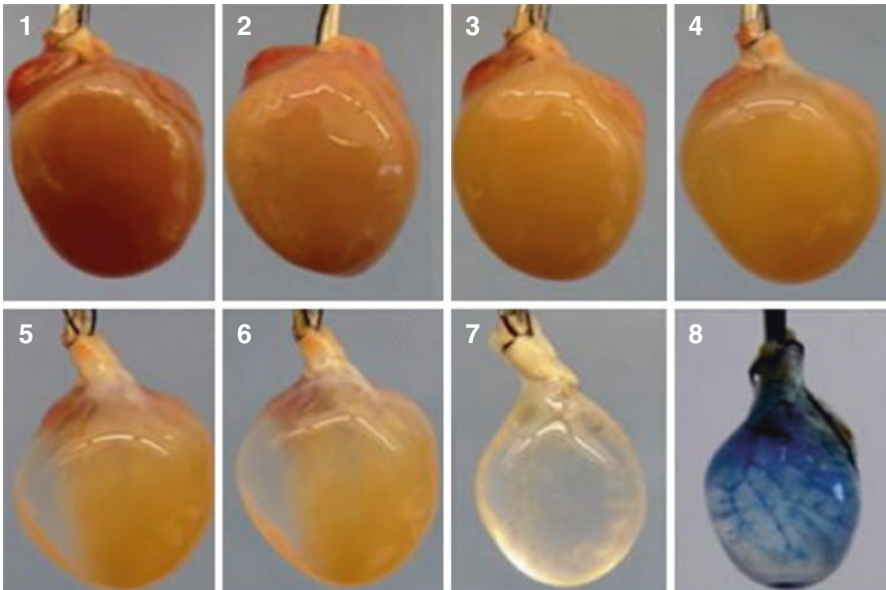


Fig. 3.1 Photographs showing each step of decellularization process: before decellularization (1); after deionized water perfusion (2); after PBS perfusion (3); after enzymatic perfusion (4); after 1% SDS solution perfusion (5); after 3% Triton X-100 solution perfusion (6); after acidic perfusion (7); perfusion of DC-ECMs with trypan blue solution to visualize the intact coronary vasculature (8). (Adapted from Lu [28])

The above methods focused on decellularizing pieces of myocardial or pericardial tissue. A landmark study in 2008 demonstrated that retrograde perfusion of an intact rat heart was possible, allowing the geometry of the heart to be preserved in its entirety [26]. With the vascular tree intact, decellularized hearts can be repopulated and conditioned in a bioreactor. Since this initial study, intact mouse (Fig. 3.1) and porcine hearts have been decellularized. Decellularization of a porcine heart, the most studied for its physiological similarities to the human heart, was performed in a matter of hours through retrograde perfusion [29]. Perfusion solutions contained both enzymatic (trypsin) and detergent (Triton X-100) components. Maintaining a high flow rate improves decellularization by removing waste components. Once decellularized, the hearts can be frozen and lyophilized and then used for recellularization or cut for cardiac patches. Lee et al. improved upon this method by inverting the heart during retrograde perfusion [30]. They used hypertonic and hypotonic solutions followed by SDS perfusion and showed that inverting the heart required lower flow rates, which reduced the amount of damage done to the aortic valve. This method addresses the varying thickness of the myocardium and best maintains the structure stiffness and collagen and elastin content, while leaving the least amount of residual DNA and SDS.

The source of tissue used for decellularization should be considered for each desired application. Decellularization of cECM from different developmental ages

requires tuning the decellularization method, but results in materials with distinct protein compositions [3]. Younger hearts were decellularized with lower detergent concentrations and required less time to solubilize. The cECM contained collagen I and IV–VI, fibrillin-1, fibronectin, periostin, and emilin-1. Laminin was observed to increase with age, while perlecan decreased. The most studied developmental age, adult cECM, exhibited larger diameter fibers and exclusively contained collagen III and lacked fibrillin-2. Similar results were observed from three-dimensional constructs, with smaller fiber diameter in fetal than adult scaffolds [25]. In these scaffolds, fetal cECM had less collagen I and more fibronectin than adult scaffolds. In both cases, fetal scaffolds better supported cardiomyocytes [3, 25]. In adult tissue, decellularization of distinct cardiac layers yielded materials with similar ultrastructure, protein content, and mechanical stiffness [21]. Interestingly, culture of adipose-derived progenitors on these decellularized sheets resulted in higher cell density and cardiac marker expression after the detergent-based decellularization. However, no effect of the cardiac layer was observed, suggesting decellularization of the entire myocardium is sufficient.

A head-to-head comparison of the decellularization of human and porcine myocardium revealed that human myocardium required more processing, likely due to increased fibrosis, crosslinking and adipose tissue deposition from aging [23]. Further the human material did not always form a gel and yielded softer gels when it did. Although the protein composition of the porcine and human myocardium is distinct, porcine myocardium remains a more attractive option given the difficulties of decellularization, limited availability, and patient-to-patient variability of human tissue. In order to maximize the amount of decellularized material from a single animal, skeletal muscle has also been considered for cardiac therapies. Decellularization of cardiac and skeletal muscle can be achieved with SDS, although lipid removal from skeletal muscle requires an additional treatment with isopropanol [22]. Pepsin digestion of material from either source generates a sheer thinning, injectable material that forms a porous nanofiber structure upon gelation.

Decellularization of Cardiac Valves

Mechanical valves have been very successful in the clinic, but require lifelong anti-coagulation therapy and in pediatric patients, are not capable of growth. Biologic valves on the other hand, deteriorate and calcify in patients. Decellularized heart valves may address these limitations as they can remodel with the patient and should not elicit an immune response. Detergent and basic conditions have been evaluated by multiple groups for the decellularization of heart valves.

Recent studies have examined the question of the ideal buffer for valve decellularization. In a direct comparison, SDS-based methods better removed DNA and cytosolic proteins and induced a weaker inflammatory response than Triton-based methods in decellularizing a porcine aortic valve [31]. Both detergents removed xenogeneic antigens, while also unfortunately reducing collagen and elastin content. In a porcine pulmonary valve, detergent-based (SDS and Triton combination)

methods outperformed enzymatic decellularization methods with either trypsin or commercially available Accutase [32]. Enzymatic-based methods either loosened and thinned the pulmonary valves or enlarged the leaflets. These methods also created rough, partially degraded, disorderly microstructures. In a separate study, sodium hydroxide and hydrogen peroxide better preserved glycosaminoglycan and elastin content compared to SDS-based decellularization of a porcine pulmonary valve [33]. Both methods maintained the mechanical integrity of the valves. Three months after implantation, the valve leaflets were intact, flexible, and partially repopulated with cells, and only minor calcification was observed.

The heterogeneity of the heart valve root and leaflets adds a challenge to decellularization. Immersion in a basic solution containing the detergents SDS and Triton X-100 for 16 days was insufficient to decellularize the wall of a porcine aorta. However, a perfusion system that generated internal pressure within the aortic root, forcing the decellularization solution through the wall without applying pressure to the leaflets, was successful for DNA removal [34]. Further this method maintained the collagen and elastin fibers.

Decellularization of Blood Vessels

As with any tissue, to determine the best decellularization method, multiple protocols should be considered in parallel. Increasing doses of SDS for increasing incubation times were compared for the decellularization of human umbilical arteries that were either fresh or frozen [35]. The most effective decellularization was realized by the highest dose of SDS (1%) for the longest duration (48 h) in fresh tissues. This procedure also reduced the collagen content of the material. Freezing should be avoided as it reduces material compliance and glycosaminoglycan content. Slicing of human aortic tissue into micrometer scale pieces reduced the dose and treatment duration of SDS [36]. However, this also destroys the structure of the blood vessel, potentially limiting its therapeutic use. Triton-X 100 is an alternative detergent for vessel decellularization. While Triton-X 100 and SDS produce decellularized vessels with similar mechanical properties, Triton-X 100 better preserves the glycosaminoglycan content of the matrix [37]. As an additional modification heparin was covalently incorporated into these vessels after decellularization to reduce thrombogenicity upon implantation. In addition to the characterization performed in decellularized myocardium, decellularized vessels should be assessed for preservation of their elastic fibers, burst strength, and calcification after implantation.

While efficient decellularization agents, detergents may destroy components of the extracellular matrix and lead to cytotoxicity. In order to avoid the use of detergents, decellularization methods using high hydrostatic pressure, activated serum, and enzymatic methods have also been evaluated for blood vessels. Decellularization by hydrostatic pressure is rapid and requires just 10 min at 980 MPa to clear a porcine radial artery of cellular material; however, this is followed by a week-long exposure to DNase [38]. This method maintains both the internal elastic lamina and

inner surface collagen layer of the artery. Ishino et al. used the inherent complement system and DNase activity of human or rat serum to decellularize a porcine carotid artery within 5 days [39]. While serum-based decellularization better retained the native fiber structure and resulted in more stable graft material, it was less efficient in removing nuclei and DNA from the scaffolds (leaving 80 ng/mg tissue) and would require further optimization before clinical use (Fig. 3.2). Decellularization of a blood vessel, in this case a porcine coronary artery, can also be achieved by alternating hypotonic and hypertonic solutions to burst the cells followed by enzymatic degradation with trypsin [40]. Optimization of this method is also required as it quickly reduces collagen and glycosaminoglycan content without fully removing DNA from the matrix.

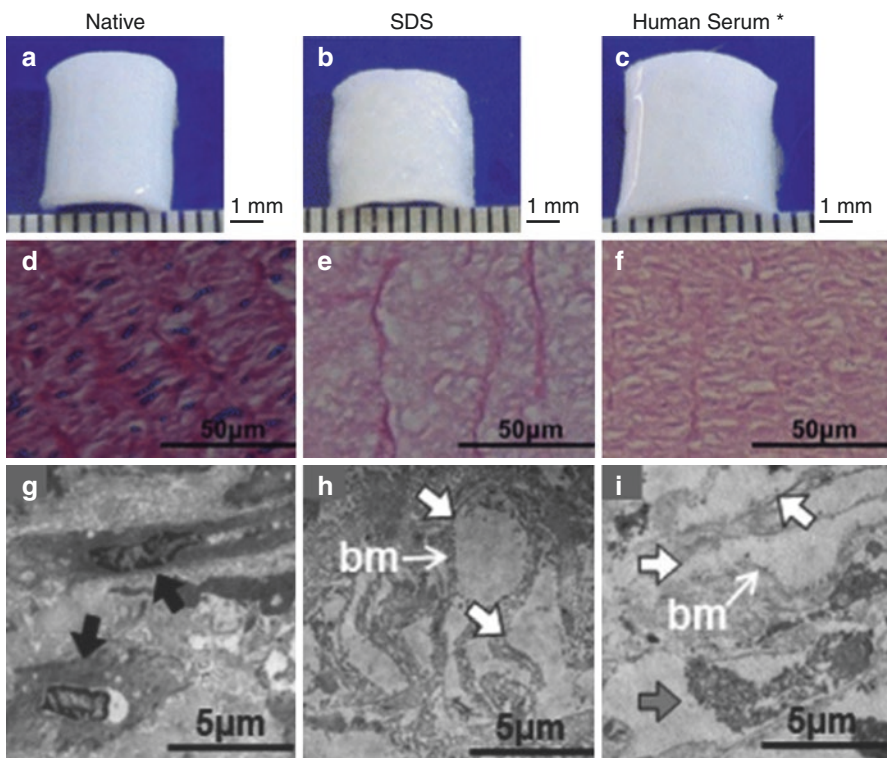
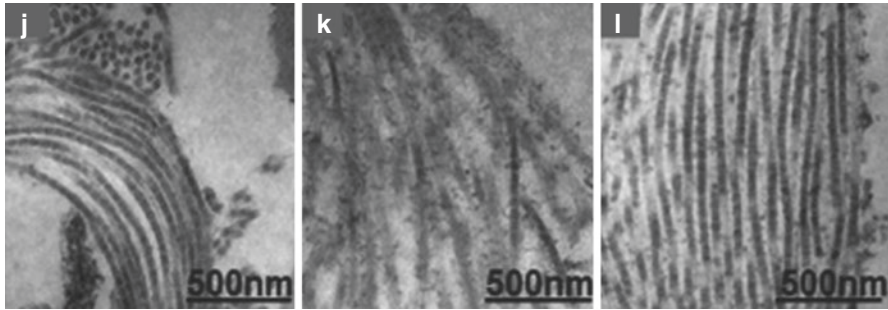


Fig. 3.2 Pictures of native and SDS- or human-serum-treated porcine carotid (a–c) and H&E-stained images (d–f). The surface of the vessel after SDS treatment seems to turn coarse (b), but it does not change much after serum treatment (c). In the H&E-stained images, many nuclei in native tissues are stained (d). Smooth muscle cells (black arrows) observed in native tissue (g). Cellular components removed (white arrows) after SDS treatment (h) and 5 days of serum treatment (i). Some components remain in serum-treated samples (gray arrow). Striation patterns of collagen fibers observed in native and serum-treated samples (j, l). Collagen fibers in the SDS-treated sample are destroyed (k). bm, basement membrane. (Adapted from Ishino [39])



* 20% CO₂ and 20 mM Mg²⁺ addition, 5 days treated.

Fig. 3.2 (continued)

Other Decellularization Strategies

Given the promise of decellularized matrices, simple cost-effective strategies for generating reproducible matrices will be important to clinical applications. Searches for such a process have led beyond the mammalian heart and include decellularized plant tissue and ex vivo cell-derived matrices. These isolation schemes also reduce the risk of disease transfer and inflammation induced by xenogeneic epitopes.

Plant tissues are porous and vascularized and exhibit a range of mechanical properties. Decellularization of plant tissue is carried out with detergent or ionic solutions similar to mammalian tissues [41]. Once lyophilized, it can be stored at RT under low humidity. One potential drawback of decellularized plant tissues is that they require the addition of adhesion sequences in order to support cell attachment and spreading. Given the negligible degradation of cellulose by mammalian cells, decellularized plant material is appropriate for long-lived applications.

Cell-derived matrices can be manufactured in a dish, allowing for controlled deposition, and better recapitulate the mammalian microenvironment than plant tissues. Human cardiac fibroblasts are commercially available and easily expanded in culture, reducing the xenogeneic burden. This simple technique is highly scalable and has the potential for off-the-shelf therapies. Alternatively, given a longer production time, a patient's own fibroblasts could be used as an autologous therapy.

Two weeks of culture is sufficient to produce scaffolds 20 mm in diameter and in controlled shapes and sizes [42]. The produced matrix can be decellularized by detergent or acidic conditions [42, 43]. Processing conditions of cell-derived matrices are typically milder than that required for decellularization of tissue pieces. This may help to preserve bioactive molecules in the extracellular matrix such as growth factors or glycosaminoglycans. Schmuck et al. found that cardiac fibroblasts produced an extracellular matrix that was composed primarily of fibronectin (>80%), followed by collagen I and III and elastin [42]. These matrices can be repopulated and remodeled by host cells, and also serve as a suitable scaffold for the delivery of cells into the epicardium (Fig. 3.3).

A further benefit of manufacturing cell-derived ECM is that it can be cultivated in many formats, including monolayers, inside tubes, on porous scaffolds, or within

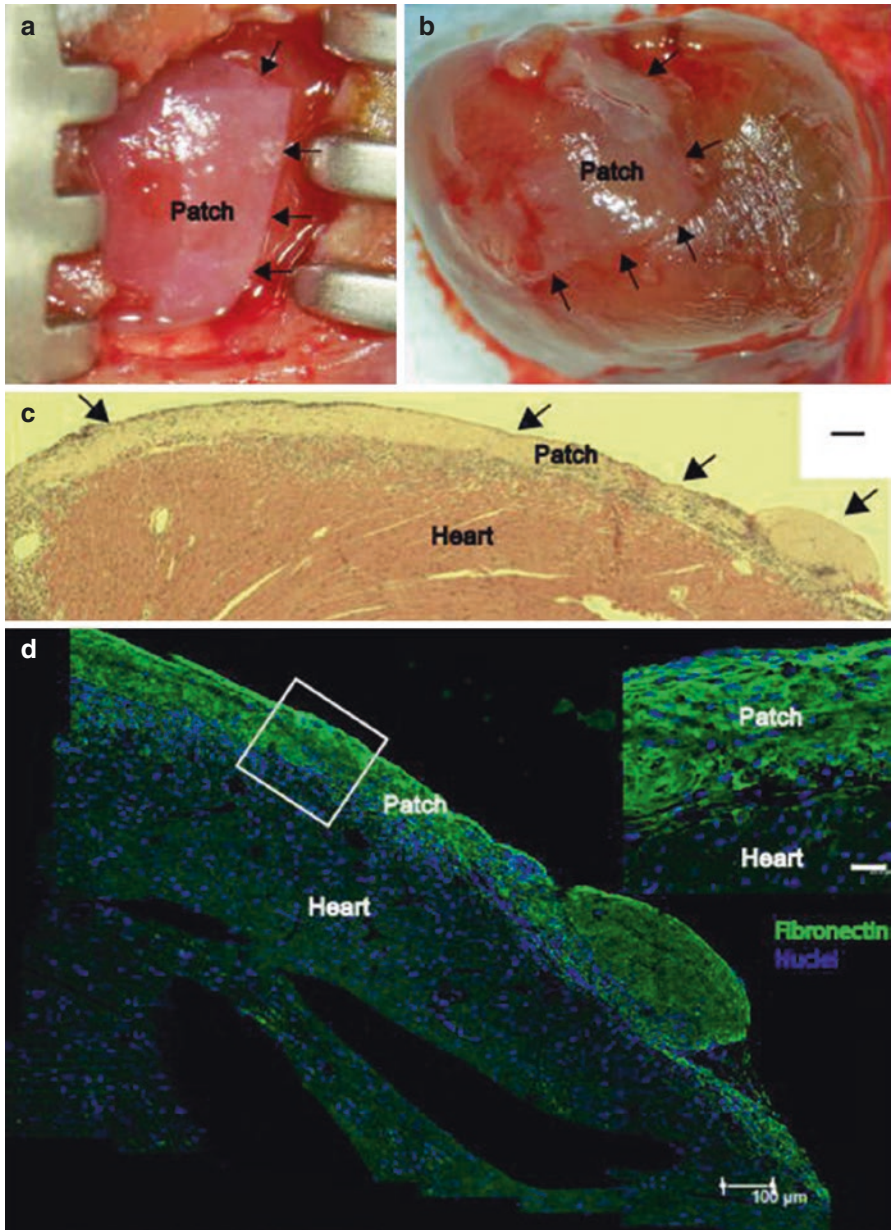


Fig. 3.3 Cardiac fibroblast derived ECM at time of placement on the mouse heart (0 h), arrows denote the edge of the scaffold (a). Attached scaffold after 48 h the beating mouse heart, arrows denote the edge of the scaffold (b). Hematoxylin and eosin stain of a cross-section of the epicardial surface, arrows denote the scaffold (c). Note the absence of gaps between the scaffold and epicardial surface (scale bar = 100 μ m) confirming adherence. Immunofluorescent micrograph of an attached scaffold after 48 h on the beating mouse heart (d; scale bar = 100 μ m). Inset image denotes the tight attachment between CF-ECM scaffold and the epicardial surface. Fibronectin (green), DAPI (blue) (scale bar = 25 μ m). (Reused with permission Schmuck [42])

a degradable carrier [43, 44]. These forms allow for appropriate mechanical preconditioning to strengthen the matrix and are maintained after decellularization for relevant applications. They can be stored for several months under refrigeration, allowing for off-the-shelf therapies. In the future, in addition to tailoring the physical shape of these constructs, genetic engineering or small molecule delivery will allow the deposition of specific biochemical components to be controlled [44].

Characterization of Decellularized Extracellular Matrix

Finally, after decellularization, careful characterization of the material is required to ensure adequate removal of cellular material and maintenance of material composition and structure. At minimum, the DNA content must be determined and should be lower than 50 ng/mg of ECM (dry weight). Given the sample preparation, this concentration is at the low end of the detectable range of DNA measure by Nanodrop 2000 spectrophotometers. More sensitive quantification should be performed with a Picogreen assay. Additionally, an agarose gel can be employed to ensure that any remaining DNA fragments are less than 200 bp in length. While Hoechst or DAPI staining can confirm any remaining nuclei, they are not quantitative or sensitive enough for free DNA. If detergents or crosslinking reagents were used in producing the material, then residual content needs to be assessed. A recommended maximum threshold for SDS is 200 μM [45]. Also necessary are tests for biocompatibility and cytotoxicity. Currently, these are less quantitative assays, but include *in vitro* culture methods or *in vivo* transplant.

Further characterization provides great insight into the material properties. Scanning electron microscopy (known as SEM) is extremely common and useful to determine qualitative ultrastructure, fiber diameter, and pore size (Fig. 3.4). Histology is also frequently employed to demonstrate cell removal and intact fibrous structure. The most common method is hematoxylin and eosin (H&E) to reveal tissue structure. Masson's trichrome can also be used to stain collagen fibers and confirm the lack of intact cells. Elastic fibers can be visualized by Verhoeff–Van Gieson staining. In addition to the methods discussed below, individual matrix components can be determined by Alcain blue staining (glycosaminoglycans) or immunohistochemistry for specific proteins (i.e., collagen I, laminin, and fibronectin). Finally, immunohistochemistry can be used to identify potential xenogeneic antigens such as alpha-Gal, T-antigen, and major histocompatibility complexes I and II.

Although not sensitive enough to reveal individual proteins, gross comparisons of the protein composition of decellularized matrices can be made by SDS-polyacrylamide gel electrophoresis analysis. Liquid chromatography with tandem mass spectrometry, on the other hand, provides an unbiased and quantitative assessment of protein composition, but is more expensive and less readily available. Quantification of individual matrix proteins can also be determined by modified enzyme-linked immunosorbent assays or biochemical assays. Glycosaminoglycan content is also commonly assessed as these molecules are bioactive and alter

mechanical properties of the extracellular matrix. Quantification is carried out by absorbance reading after binding with 1,9-dimethylmethylene blue, also known commercially as the Blyscan assay.

In addition to composition, application-specific characterization of mechanical properties can, and in the case of blood vessel burst strength should, be performed. For hydrogels this includes rheometry for storage and loss modulus and gelation

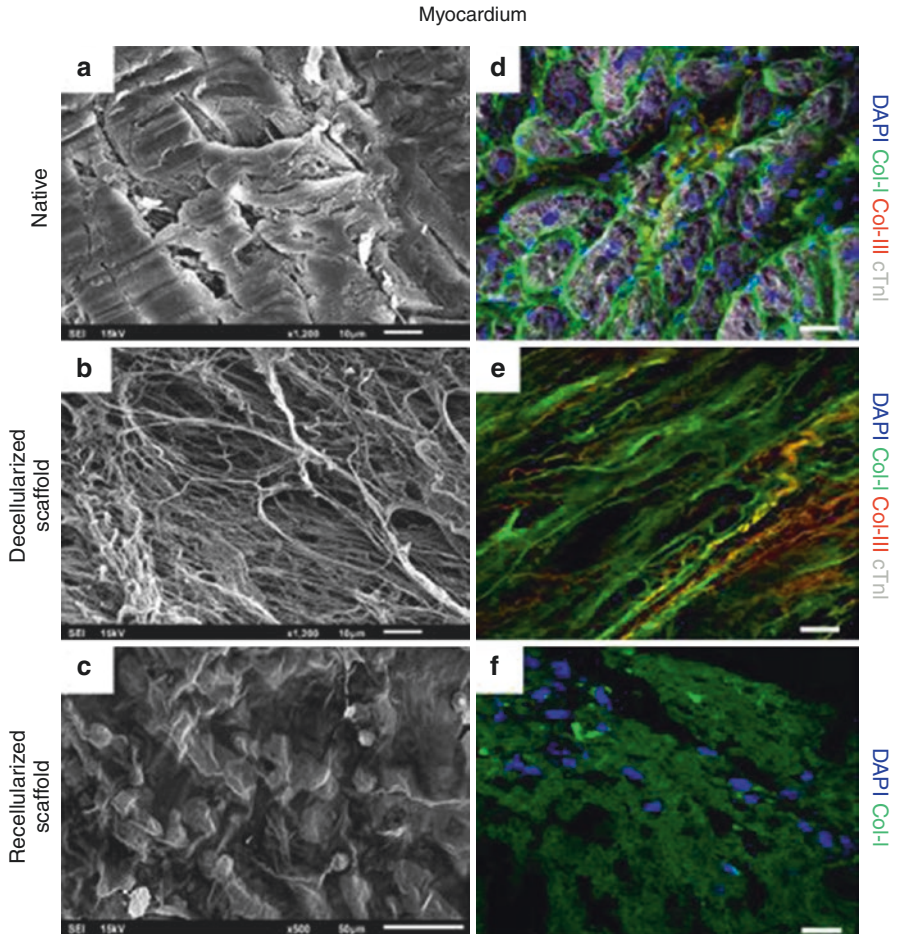


Fig. 3.4 Internal structure and protein composition of the cardiac scaffolds. Ultrastructure determined by SEM of the native myocardium (a) and acellular myocardial scaffolds (b); or native pericardium (g) and acellular pericardial scaffolds (h). Representative images for the native myocardium and decellularized myocardial scaffolds (d, e), respectively; and native pericardium and decellularized pericardial scaffolds (j, k) showing immunostaining for col-I (green), col-III (red), and cTnI (white). SEM images for recellularized myocardial (c) and pericardial scaffolds (i). Photographs displaying immunostaining for col-I (green) for recellularized myocardial and pericardial scaffolds (f, l). Nuclei were counterstained with DAPI (blue). Scale bars = 50 μ m. (Reused with permission Perea-Gil [21])

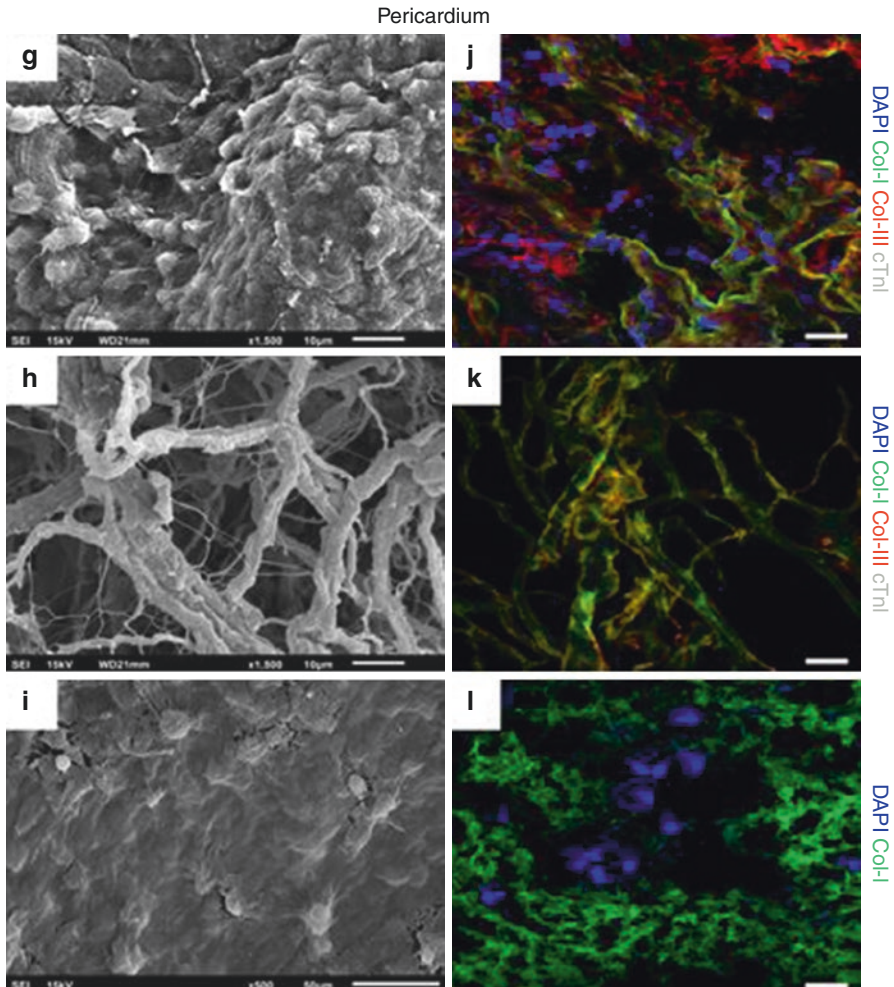


Fig. 3.4 (continued)

kinetics if injecting. For intact structures biomechanical assays for tensile strength and stiffness are commonly assessed. Biodegradability, which will affect not only the mechanical properties but also biocompatibility potentially, can be assessed *in vitro* by controlled enzymatic degradation. Ultimately, safety is the primary goal of any potential therapeutic and appropriate testing should be performed to minimize patient risk. Additional testing can be performed to help improve efficacy of the treatment.

Crosslinking and Sterilization of Decellularized Extracellular Matrix

Ideally, complete removal of cellular material from the extracellular matrix would prevent the stimulation of an inflammatory response upon implantation. However,

this is also influenced by the chemicals used in the decellularization process and for crosslinking. Detoxification of glutaraldehyde crosslinked materials can be achieved with citric acid or a combination of citric acid and ethanol to reduce free aldehydes present in the material [47]. A comparison of the macrophage-like cell response to crosslinking reagents glutaraldehyde and 1-ethyl-3-(3-dimethyl-aminopropyl)-carbodiimide in vitro demonstrated cytotoxicity of glutaraldehyde [48]. Fewer cells attached and survived on glutaraldehyde crosslinked matrices; the cells present had disrupted membranes and released more proinflammatory cytokines. Interestingly, the authors concluded that this response was due to the surface characteristics of the crosslinked material.

Residual detergents, such as SDS, also reduce cell viability, with the half-maximal cell viability occurring around 200 μM SDS [45]. This is a relevant concentration of detergent found after washing alone of a decellularized matrix. Higher concentrations of the detergent induced fibroblast activation, while detergent precipitation out of the material with calcium chloride beneficially induced more reparative-like macrophages. When implanted in vivo, high SDS concentrations reduced cell infiltration, induced expression of inflammatory cytokines, limited vascularization, increased myofibroblast presence, and resulted in fibrotic encapsulation.

Finally, sterility is also an important concern for decellularized matrices, especially for implantation. If performed under aseptic conditions, decellularization with detergents or acidic or basic conditions will largely sterilize matrices. However, out of an abundance of caution, sterility should be confirmed. Antibiotic and antimetabolic treatments alone are insufficient to guarantee sterilization, but the addition of low dose (<0.1%) peracetic acid effectively disinfects matrices [49]. This avoids harsh sterilization techniques which may damage the matrix structure or biochemistry.

Decellularized Extracellular Matrix Formats

Culture Coating

Rigid tissue culture plastic hardly mimics the native microenvironment of the myocardium. Solubilized cECM can be applied as a culture coating to study cell behavior by providing at least tissue-specific biochemical cues. The naturally derived cECM improved cell viability, proliferation, cardiomyogenic differentiation, and growth factor secretion in cardiac progenitor cells compared to collagen controls [50]. Age-dependent effects of cECM on cultured neonatal rat ventricular myocytes were also observed, with fetal-derived cECM supporting the adhesion and proliferation of cardiomyocytes better than neonatal or adult cECM [3].

In addition to simple culture coatings, more advanced culture conditions, including engineered heart tissues, will be useful for pharmaceutical drug testing. By cryosectioning porcine myocardium, Schwan et al. was able to maintain the anisotropy and microstructure of the native material [51]. After laser cutting the sheets to the desired shapes, they were decellularized. Laser cut shapes allow for simplified and uniform mechanical testing. Seeding of these constructs with neonatal rat ventricular myocytes led to cell alignment and force generation parallel to the underlying fiber orientation.

Injectable Materials

Injectable extracellular matrices are attractive because they require only minimally invasive delivery either through direct injection or catheter delivery into the myocardium [52]. They assemble into hydrogels within the tissue and provide biochemical and biomechanical cues to native infiltrating cells. Additionally, they can be used as delivery scaffold for cells or other bioactive molecules (e.g., growth factors, cytokines, DNA, or siRNA).

Early work with tissue-specific decellularized matrices demonstrated that cECM injected into the myocardium gelled within 30 min of exposure to body temperature and mimics the microscopic structure and porosity of native myocardium [16]. The same group later showed that both human- and porcine-derived cECM gelled in the rat myocardium [13]. Further, arteriole-sized vessels were observed within the hydrogel 2 weeks after injection.

In a similar approach, a decellularized rat liver was milled into a powder and then glued to the infarct in a rat model of myocardial infarction by mixing with fibrin glue [53]. The powder induced neovascularization of the infarct area. As an alternative, the solubilized form of this decellularized liver powder could be injected directly into the myocardium for a more spatially relevant treatment. The potential drawback to injected materials is that their delivery may require special training, material delivery into the tissue is not well controlled, and crosslinking strategies are limited by the required slow gelling kinetics [52].

Patch

Patches for tissue engineering are advantageous because they allow for development and maturation in culture or a bioreactor prior to implantation. They are also strong enough to be manipulated and may provide mechanical support when applied to a tissue. As a drawback, they require invasive delivery and still only contact the surface of a tissue, limiting their restorative capabilities. Unless vascularized, patches are also limited in thickness by the diffusion of nutrients.

For example, 2-mm slides of porcine myocardium can be decellularized without disrupting the interstitial fibers or vascular structure [54]. However, when repopulated, cell death inside the construct was still apparent. Alternatively, an intact rat heart can be decellularized and then cut into pieces of the desired shape [55]. These slices can then be repopulated. Sheets of cECM increase cardiac gene marker expression in human-induced pluripotent stem cell-derived cardiomyocytes compared to cell aggregates alone. The sheets also demonstrated spontaneous contractions and can be applied as patches to an infarcted myocardium.

Jakus et al. took a modified approach to creating patches, which they termed tissue paper, from decellularized, lyophilized, and milled extracellular matrix [56]. Tissue papers can be rapidly produced in any castable geometric shape at room temperature, making fabrication highly scalable. Poly(lactic-co-glycolic)

acid can be incorporated for mechanical support. The tissue papers are flexible enough to be rolled, folded, cut, and sutured and have a long shelf-life. They are also highly porous, maintain their shape, and support cell adhesion, proliferation, and migration. The main drawback to their fabrication is the use of organic solvents, which limits cell incorporation. However, sheets of repopulated tissue paper can be stacked to create thicker patches.

Whole Organ Decellularization

While decellularization of myocardial sheets preserves the microstructure of the tissue, it does not maintain the complexity of the intact heart as an organ. Ideally, decellularization of an intact organ preserves vascular structure in addition to organ structure. This vasculature can be harnessed for perfusion-based decellularization in order to remove cellular material from the full thickness of the tissue [57]. In the heart this can be done through retrograde or antegrade perfusion. Successful decellularization of an intact heart, and its subsequent repopulation, would open the door to functional, transplantable organs, although the ideal source of donor material would have to be established.

Perfusion decellularization has been achieved in whole hearts in small and large animal models [26, 27, 58]. This is achieved by freezing and serial perfusion of an enzymatic, nonionic detergent, ionic detergent, and acid solution with hypotonic and hypertonic rinses [27]. The decellularized matrix maintains its composition and can support cardiomyocytes *in vitro*. Weymann et al. describe a compact, easy to handle, sterilizable, and low-cost system for decellularization [58]. Antegrade perfusion of detergents for the decellularization of whole organs has been outlined in a detailed protocol that can be adapted for small to large animal models [59].

More recent studies have aimed repopulation of decellularized intact hearts. Human-induced pluripotent stem cell-derived cardiac progenitor cells were used to repopulate an intact decellularized mouse heart [28]. Using a multipotent progenitor cell allows for the generation of multiple required cell types. Repopulated hearts were perfused with growth factors to promote *in situ* differentiation of the progenitor cells. Cardiac and smooth muscle markers were later detected in the repopulated hearts, along with vessel-like structures. While some spontaneous contractions were also observed, distinct tissue regions were largely uncoupled.

Given the variety of cell populations and large number of cells required to repopulate an entire heart, complete repopulation of organized functional cells remains a challenge. To address this, Taylor et al. transplanted an intact decellularized porcine heart in line with the recipient animal's circulation to allow for endogenous repopulation [60]. Within 6 h, endothelial cells were observed in the donor heart vessels. By 60 days, more mature vessels and evidence of muscle tissue had formed. While promising, this technique is not capable of subjecting the heart to the mechanical or electrical loads that may be required for tissue maturation. Further, it is limited by the risk of coagulation and thrombosis.

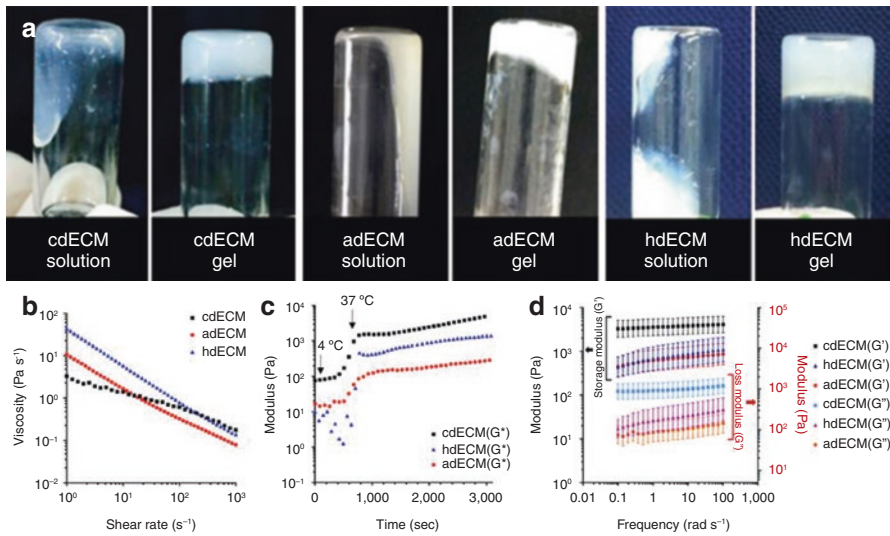


Fig. 3.5 Rheological behavior of the dECM pregels. Solution to gel transition (a) of the dECM pregels prepared from cartilage dECM (cdECM), heart dECM (hdECM), and adipose dECM (adECM). Rheological properties of the dECM pregels: viscosity at 15 °C (b), gelation kinetics from 4 to 37 °C (c) (initial temperature: 4 °C, increment of 5 °C/min with holding at 15 °C for 5 min, reaching to 37 °C, and maintaining 37 °C for 40 min), and dynamic modulus at varying frequency at 37 °C (d). All experiments were performed in triplicate. Error bars represent standard deviation. (Reused with permission Pati [46])

Bioink

The increasing popularity of three-dimensional printing tissue-engineered constructs has realized the potential of decellularized matrices to be used as bioinks. In addition to the typical characterization of decellularized materials that must be performed, bioinks should also be assessed for their viscoelasticity and shear thinning [61]. In extrusion-based bioprinting, the nozzle diameter and printing speed should also be considered. Similar to other forms of cECM, bioinks provide tissue-specific biochemical cues and mechanical support, although they may require crosslinking or composites to be mechanically strong.

Bioinks can be generated from a number of tissues, including the myocardium [46]. They provide a complex fibrous matrix that self-assembles at body temperature without the immediate need for crosslinking agents (Fig. 3.5). Materials should be kept cool during the printing process. Cell-laden cECM can be printed and gelled without loss to cell viability. Compared to collagen controls, cECM enhanced cardiac marker gene expression in myoblasts of printed constructs. Using multiple printing heads, naturally derived bioinks can be printed in patterns with synthetic materials such as polycaprolactone to create desired structures [62]. Further, each material can contain a distinct cell population. This improves vascularization after

implantation. Additionally, to enhance cell maturation or recruitment, growth factors can be incorporated into the bioink before printing.

Cardiac Applications

Myocardial Application of Cardiac-Derived Matrices

Pepsin digestion of decellularized porcine ventricular matrix allows for catheter delivery of the material, a promising minimally invasive approach. Crosslinking of cECM with glutaraldehyde to improve mechanical properties does not interfere with its delivery [63]. In a rat model of ischemia reperfusion, cECM was injected 2-weeks after the surgery to mimic a clinical setting. After injection no increase in risk for arrhythmia was observed and the cECM prevented the decline in cardiac function observed with saline control [64]. Similarly, the group demonstrated trans-endocardial delivery of the solubilized cECM into post-infarcted pigs preserved cardiac function and reduced ventricular dilation. A visible band of muscle tissue, representing enhanced survival or tissue repair, was observed near the injected material [65]. A lack of thrombogenicity also makes these preclinical studies promising.

Chen et al. followed an interesting premise that since zebrafish have more cardiac regenerative potential than mammals, the extracellular matrix comprising their myocardium may elicit a stronger regenerative response [66]. Additionally, since zebrafish myocardium is thinner, it can be decellularized under gentler conditions, potentially retaining more bioactive molecules. In a head-to-head comparison, zebrafish cECM better preserved cardiac function and decreased infarct size compared to murine cECM in a murine model of myocardial infarction. Interestingly, zebrafish cECM that was harvested after an apical resection (deemed “healing”) had an even stronger effect on preserving the cardiac ejection fraction. The zebrafish cECM induced more proliferation, possibly due to higher elastin and glycosaminoglycan content. Given the inexpensiveness and ease of breeding zebrafish, this may prove to be an attractive material in the future.

Decellularized scaffolds can be applied as patches either alone or in combination with cells. A decellularized rat cECM increased the gene expression of cardiac markers in human-induced pluripotent stem cell-derived cardiomyocytes when seeded on the matrix in combination with fibroblasts [55]. These patches showed good cell viability and no observable segregation from native tissue in a rat model of myocardial infarction. In fact, when patched over the infarct zone, the construct improved cardiac function, increased peri-infarct vascularization, and decreased infarct size. Inclusion of cells in extracellular matrix patches may outperform acellular patches alone [67].

In order to bring additional benefit to patch constructs, Jang et al. created a pre-vascularized patch, patterning stem cells and endothelial cells in bioink containing decellularized rat myocardium [62]. Through this technique, they were able to create fairly stiff (16 kPa), millimeter scale patches. These patches were able to improve cardiac function and reduce left ventricle dilation and fibrosis after

myocardial infarction in rats. Interestingly, these patches had a positive outcome on cardiac function even when implanted without cells.

In a clinical setting, the application of a patch in a patient is not realistic until the patient has been stabilized. At this point, fibrotic remodeling is already underway. In most animal models of myocardial infarction, biomaterial-based therapies are applied shortly after injury and may not mimic the clinical setting. However, in a rat model of myocardial infarction, when porcine cECM patches were placed on the infarct as late as 30 days post-injury they were still successful [68]. The patches were vascularized, infiltrated by immature myocytes, induced a more reparative macrophage phenotype. Ultimately, this led to improved cardiac function and reduced infarct size. Similarly, an injected porcine cECM-hybrid hydrogel also improved cardiac function when applied 4 weeks after injury in a rat model of myocardial infarction [69].

Myocardial Application of Noncardiac-Derived Matrices

While they do not provide tissue-specific microenvironments, decellularized matrices derived from other tissue have shown promise in cardiac applications. These matrices are capable of attracting native cells and do not risk mineralization, fibrosis, and infection like some synthetic matrices. For example, both porcine small intestinal submucosa and urinary bladder submucosa were used to successfully repair right ventricle wall defects in a porcine model [70]. No scar tissue or thrombi were observed in or around the implanted material. Instead, a mixture of muscle and connective tissue was observed to be created and well vascularized. In fact, the implanted extracellular matrices were degraded and replaced. The regenerated tissue exhibited spontaneous contractions at approximately 70% of the force of the native myocardium.

Interestingly, the human heart valve has also been shown to be a viable source for myocardial repair [71]. After sectioning into sheets, the valve tissue was decellularized and then repopulated with murine bone marrow-derived cells. Implantation in a mouse model of myocardial infarction demonstrated that the patch alone and the cell-laden patch could both improve cardiac function and decrease infarct size.

Myocardial Application of Hybrid Scaffolds

While decellularized myocardial scaffolds maintain the fibrous structure and biochemical composition of the native myocardium, they often lack adequate mechanical strength. Further, instructive materials can be designed to influence the regenerative process. The addition of crosslinking agents, biological factors, or synthetic materials restores function of the matrix lost during the decellularization process and pushes beyond the restorative capabilities of the native microenvironment.

In an effort to increase the stiffness of cECM, Grover et al. used two methods of crosslinking polyethylene glycol to the decellularize scaffolds [72]. Based on the

crosslinking method and polyethylene glycol molecular weight, hybrid scaffolds were generated with storage moduli ranging from that of gelled cECM (5 Pa) to 700 Pa, beyond that which is achieved by glutaraldehyde crosslinking (140 Pa). These methods achieve increased stiffness while maintaining a nanofibrous network and cell adhesion and migration. Given the distinct crosslinking kinetics of the two methods, each approach might be better suited for *in vitro* cell culturing or *in vivo* injection.

A similar approach harnessed the naturally occurring biomaterial silk to create hybrid hydrogels with tunable mechanical properties and controllable stiffening kinetics [73]. Incorporation of lower molecular weight silk led to faster gelling kinetics, while using a higher weight percent of silk increased the elastic modulus. Tuning the composition of these gels altered cardiac myofibroblast activation *in vitro* as well as cell infiltration and vascularization in a subcutaneous model.

Chitosan, another biocompatible, naturally occurring material, has been used to provide mechanical support to cECM. Incorporating 3% (w/v) chitosan in 0.5% (w/v) cECM yields hydrogels with storage moduli on the order of 15,000 Pa after glutaraldehyde crosslinking [74]. In order to avoid the cytotoxicity of glutaraldehyde, hydrogels can be crosslinked with the natural crosslinker genipin [69]. In either case, chitosan incorporation leads to the formation of denser hydrogels that are capable of supporting cell viability.

In addition to tuning mechanical properties of cECM hydrogels, the biochemical properties can be tuned by incorporating bioactive molecules such as growth factors or adhesion peptides. To improve cell adhesion and survival, RAD16-I was incorporated into decellularized porcine myocardium and pericardium [21]. The two scaffolds shared only 40% of their proteins, but after reseeding with adipose-derived mesenchymal stem cells, both decreased infarct size and improved ejection fraction in swine subjected to coronary ligation.

Through carbodiimide crosslinking, basic fibroblast growth factor can be tethered to cECM, even in an intact decellularized whole heart [75]. This incorporation leads to a higher cell density, more synchronous contractions, and upregulation of cardiac markers after reseeding of the scaffold with human embryonic stem cell-derived cardiac progenitor cells. A more efficient reseeding will reduce the total number of cells required. Namiri et al. applied a similar method to tether either stromal cell-derived factor-1a or basic fibroblast growth factor to decellularized heart valves [76]. Culture of the hybrid scaffolds with umbilical cord blood-derived mononuclear cells leads to higher cell adhesion and migration on stromal cell-derived factor-1a scaffolds, while these scaffolds elicited lower platelet adhesion *in vitro*. After subcutaneous implantation stromal cell-derived factor 1a decreased calcification of the scaffolds, especially compared to the increase noted in basic fibroblast growth factor scaffolds. This suggests that incorporation of the most advantageous bioactive molecules is application specific.

Recent work has demonstrated the incorporation of gold nanoparticles into a decellularized scaffold in order to create a conductive material [77]. A more conductive material was generated by incorporating larger nanoparticles. Compared to pristine scaffolds, when seeded with neonatal rat ventricular myocytes, the cells

exhibited more organized connexin43, a gap junction protein. The nanoparticle-containing matrices also demonstrated increased contraction amplitude, with a lower excitation threshold and faster calcium transients. In this study the authors used a decellularized matrix derived from the omentum, suggesting that given the right engineered cues, noncardiac substrates can provide successful therapeutics. In the future, incorporation of carbon nanotubes into decellularized matrices may also provide cardiomyocytes with the requisite environment for electrical stimulation and signal transduction [78]. While extremely promising, materials with altered conductive properties will have to be evaluated for risk of arrhythmia in vivo.

Repair of Cardiac Valves and Blood Vessels

Decellularized cardiac valves have received the most attention in a clinical setting and will be discussed in the next section. While engineered blood vessels have also advanced to preclinical testing, much work is still being performed in animal models. The need for small diameter vascular grafts is not well met by synthetic materials which are not only limited in availability but also plagued by acute thrombogenicity, anastomotic intimal hyperplasia, and minimal spontaneous reendothelialization. Toward this end, Schneider et al. decellularized human placenta chorion vessels with diameters less than 3 mm [37]. After implantation into the rat infrarenal aorta, the matrices were infiltrated by endothelial and smooth muscle cells. The grafts functioned properly, without a severe immune response, clotting, luminal narrowing, or dilatation noted after 1 month. Further, the grafts were capable of vasoconstriction.

Small diameter vessels (500–1500 μm) have also been generated by three-dimensional printing. The inner diameter of the vessel and the wall thickness can be tuned by adjusting coaxial needle size when printing. Gao et al. used this technique to print alginate-based hydrogels, loaded with decellularized aortic tissue, endothelial progenitor cells, and drug carrying microspheres, around a dissolvable core [36]. When implanted in a model of hind limb ischemia, the hybrid constructs improved the survival and differentiation of the endothelial progenitor cells, while also increasing local neovascularization and blood flow. Unfortunately, these vessels lack mechanical strength.

Decellularized Extracellular Matrix in Preclinical and Clinical Trials

As discussed, decellularized materials come in a variety of formats, appropriate to different applications. The ideal material would be available off the shelf and would be capable of remodeling to match host tissue. Before advancing decellularized matrix technologies to a clinical setting, rigorous testing is performed in large animal models. Cardiac valves and blood vessels reached preclinical and clinical testing first, in part due to the already occurring transplant of biological equivalents. Myocardial patches have also advanced to this stage and are of particular

interest for therapeutic application in congenital heart defects. Guidelines will need to be developed to ensure sufficient removal of cellular material, xenogenic epitopes, and detergents [79]. Thorough decellularization should also be shown to not compromise function. Swine are appropriate models for cardiac therapies as they share similar cardiac anatomy and physiology with humans. Care should be taken in considering data from ovine models as they have a lower risk of thrombosis and demonstrate more spontaneous reendothelialization of valves and vessels that are not observed in humans. Of significance, anticoagulants, antibiotics, and/or anti-inflammatory drug regimens are used in many of these studies.

Success has been demonstrated in decellularized valve replacement. Gallo et al. used a decellularized porcine aortic valve in place of a porcine pulmonary valve [80]. The valves remained functional for 15 months with no signs of thrombi formation, calcification, or deterioration. Decellularized valves had higher flow velocity and pressure gradients compared to autologous pulmonary valve transplants, but performed well. There was no noted infection or signs of inflammation post-transplantation. Of concern is that only 11 of 17 surgeries were free of complications. Strategies to increase remodeling of implanted heart valves include the addition of protein coatings or reendothelialization *in vitro* before implantation. Decellularized sheep pulmonary valve allografts subjected to these methods showed more repopulated valves and stronger von Willebrand Factor staining [81]. Despite the additional remodeling, all valve groups performed similarly.

Despite the ongoing work in animal models, decellularized valves have been implanted in patients for more than a decade. With great tragedy, the first implantations resulted in rapid failure due to a heightened inflammatory response [82]. Continued work with a similar tissue-engineered construct fared better but still required reparative surgery in a third of the patients [83]. Advances in decellularized allograft preservation, however, led to enhanced successful pulmonary valve replacement in the Ross procedure out to 5 years [84]. In a case study from Japan, a 6-month old infant with doubly committed ventricular septal defect and right ventricle outflow tract (RVOT) stenosis received a decellularized donor pulmonary valve allograft [85]. The graft was transplanted within 4 months of preparation and did not require cryopreservation. Even though the donor valve was twice the diameter of the patient valve, the surgery was successful with normal pressure gradients across the valve a year later. Decellularized xenografts on the other hand require further improvement as inflammation and fibrosis lead to failure of half of the grafts [86].

In an effort to manufacture off-the-shelf, nonxenogeneic valve scaffold, Weber et al. seeded human fibroblasts on polyglycolic-acid meshes, cultured the constructs under dynamic conditions for 4 weeks, and then decellularized the scaffolds [87]. After implantation in a baboon model, these constructs showed greater cell repopulation than decellularized valves, maintained mobile and pliable leaflets, and showed no sign of thrombi. However, functionally, these constructs require improvement because they demonstrated reduced coaptation, increased transvalvular pressure, regurgitation, and surgical detachment. If successful, a significant benefit of this engineered valve is its incorporation into a stent, making minimally invasive delivery possible.

Similar to the construct manufacturing described above, Syedain et al. engineered a decellularized vascular graft from ovine dermal fibroblasts cultured on a fibrin scaffold in a tubular mold under pulsatile flow [88]. The decellularized grafts matched the thickness, ultimate tensile strength, stiffness, anisotropy, collagen content, and cellular content of a native femoral artery 6 months after implantation in an ovine model, with no sign of aneurysm or mineralization. In order to repair higher pressure vessels, Dohmen et al. derived a patch from equine pericardium [89]. Equine pericardium is stronger than porcine pericardium. Four months after implantation in the descending aorta of sheep, the patches were pliable, with minimal adhesion, no hematomas, vegetations, thrombi, or calcification. No adverse events were observed.

Future Outlook

Decellularization of cardiac structures began two decades ago with heart valves and quickly led the way for the decellularization of vessels, pericardium, myocardium, and other tissues with cardiac applications. The field has reached a stage of optimization in decellularization strategies and is beginning to explore new methods of fabrication like 3D-printing and cell-based manufacturing. These will be exciting resources that allow for better control of materials of design properties. Meanwhile, we eagerly await the results of early clinical trials utilizing decellularized myocardium.

As the field expands its successes, we will also see this material translated to nonischemic cardiac diseases. Congenital heart defects are often cited as motivation for tissue-engineered therapies; however, these studies are largely underrepresented in animal studies. This may in part be due to a lack of appropriate animal models or risk of congenital heart repair, but the clinical need persists. Other forms of adult cardiac disease do not generate large scar regions the way ischemic disease (i.e., myocardial infarction) does but still lead to heart failure that is just as deadly. Decellularized matrices may prove useful as localized therapeutic delivery vehicles in nonischemic diseases.

References

1. Andreu I, et al. Heterogeneous micromechanical properties of the extracellular matrix in healthy and infarcted hearts. *Acta Biomater.* 2014;10(7):3235–42.
2. Burgess ML, McCrea JC, Hedrick HL. Age-associated changes in cardiac matrix and integrins. *Mech Ageing Dev.* 2001;122(15):1739–56.
3. Williams C, et al. Young developmental age cardiac extracellular matrix promotes the expansion of neonatal cardiomyocytes in vitro. *Acta Biomater.* 2014;10(1):194–204.
4. Gershlag JR, et al. Mesenchymal stem cells ability to generate traction stress in response to substrate stiffness is modulated by the changing extracellular matrix composition of the heart during development. *Biochem Biophys Res Commun.* 2013;439(2):161–6.
5. Li AH, et al. Dynamic changes in myocardial matrix and relevance to disease: translational perspectives. *Circ Res.* 2014;114(5):916–27.

6. Swynghedauw B. Molecular mechanisms of myocardial remodeling. *Physiol Rev.* 1999;79(1):215–62.
7. Jalil JE, et al. Fibrillar collagen and myocardial stiffness in the intact hypertrophied rat left ventricle. *Circ Res.* 1989;64(6):1041–50.
8. Bishop JE, Laurent GJ. Collagen turnover and its regulation in the normal and hypertrophying heart. *Eur Heart J.* 1995;16(Suppl C):38–44.
9. Lui K, et al. Modification of the extracellular matrix following myocardial infarction monitored by FTIR spectroscopy. *Biochim Biophys Acta.* 1996;1315(2):73–7.
10. Barallobre-Barreiro J, et al. Proteomics analysis of cardiac extracellular matrix remodeling in a porcine model of ischemia/reperfusion injury. *Circulation.* 2012;125(6):789–802.
11. Cleutjens JP, Creemers EE. Integration of concepts: cardiac extracellular matrix remodeling after myocardial infarction. *J Card Fail.* 2002;8(6 Suppl):S344–8.
12. Rienks M, et al. Myocardial extracellular matrix: an ever-changing and diverse entity. *Circ Res.* 2014;114(5):872–88.
13. Seif-Naraghi SB, et al. Design and characterization of an injectable pericardial matrix gel: a potentially autologous scaffold for cardiac tissue engineering. *Tissue Eng Part A.* 2010;16(6):2017–27.
14. Vinci MC, et al. Mechanical compliance and immunological compatibility of fixative-free decellularized/cryopreserved human pericardium. *PLoS One.* 2013;8(5):e64769.
15. Li N, et al. Efficient decellularization for bovine pericardium with extracellular matrix preservation and good biocompatibility. *Interact Cardiovasc Thorac Surg.* 2018;26(5):768–76.
16. Singelyn JM, et al. Naturally derived myocardial matrix as an injectable scaffold for cardiac tissue engineering. *Biomaterials.* 2009;30(29):5409–16.
17. DeQuach JA, et al. Simple and high yielding method for preparing tissue specific extracellular matrix coatings for cell culture. *PLoS One.* 2010;5(9):e13039.
18. Becker M, et al. Processing of human cardiac tissue toward extracellular matrix self-assembling hydrogel for in vitro and in vivo applications. *J Vis Exp.* 2017;(130):e56419.
19. Ye X, et al. Impact of decellularization on porcine myocardium as scaffold for tissue engineered heart tissue. *J Mater Sci Mater Med.* 2016;27(4):70.
20. Oberwallner B, et al. Preparation of cardiac extracellular matrix scaffolds by decellularization of human myocardium. *J Biomed Mater Res A.* 2014;102(9):3263–72.
21. Perea-Gil I, et al. In vitro comparative study of two decellularization protocols in search of an optimal myocardial scaffold for recellularization. *Am J Transl Res.* 2015;7(3):558–73.
22. Ungerleider JL, et al. Fabrication and characterization of injectable hydrogels derived from decellularized skeletal and cardiac muscle. *Methods.* 2015;84:53–9.
23. Johnson TD, et al. Human versus porcine tissue sourcing for an injectable myocardial matrix hydrogel. *Biomater Sci.* 2014;2014:60283D.
24. Seo Y, Jung Y, Kim SH. Decellularized heart ECM hydrogel using supercritical carbon dioxide for improved angiogenesis. *Acta Biomater.* 2018;67:270–81.
25. Silva AC, et al. Three-dimensional scaffolds of fetal decellularized hearts exhibit enhanced potential to support cardiac cells in comparison to the adult. *Biomaterials.* 2016;104:52–64.
26. Ott HC, et al. Perfusion-decellularized matrix: using nature’s platform to engineer a bioartificial heart. *Nat Med.* 2008;14(2):213–21.
27. Wainwright JM, et al. Preparation of cardiac extracellular matrix from an intact porcine heart. *Tissue Eng Part C Methods.* 2010;16(3):525–32.
28. Lu TY, et al. Repopulation of decellularized mouse heart with human induced pluripotent stem cell-derived cardiovascular progenitor cells. *Nat Commun.* 2013;4:2307.
29. Remlinger NT, Wearden PD, Gilbert TW. Procedure for decellularization of porcine heart by retrograde coronary perfusion. *J Vis Exp.* 2012;70:e50059.
30. Lee PF, et al. Inverted orientation improves decellularization of whole porcine hearts. *Acta Biomater.* 2017;49:181–91.
31. Liu X, et al. Comparison of detergent-based decellularization protocols for the removal of antigenic cellular components in porcine aortic valve. *Xenotransplantation.* 2018;25(2):e12380.

32. Haupt J, et al. Detergent-based decellularization strategy preserves macro- and microstructure of heart valves. *Interact Cardiovasc Thorac Surg*. 2018;26(2):230–6.
33. van Steenberghe M, et al. Porcine pulmonary valve decellularization with NaOH-based vs detergent process: preliminary in vitro and in vivo assessments. *J Cardiothorac Surg*. 2018;13(1):34.
34. Sierad LN, et al. Functional heart valve scaffolds obtained by complete decellularization of porcine aortic roots in a novel differential pressure gradient perfusion system. *Tissue Eng Part C Methods*. 2015;21(12):1284–96.
35. Tuan-Mu HY, Yu CH, Hu JJ. On the decellularization of fresh or frozen human umbilical arteries: implications for small-diameter tissue engineered vascular grafts. *Ann Biomed Eng*. 2014;42(6):1305–18.
36. Gao G, et al. Tissue engineered bio-blood-vessels constructed using a tissue-specific bioink and 3D coaxial cell printing technique: a novel therapy for ischemic disease. *Adv Funct Mater*. 2017;27(33):1700798.
37. Schneider KH, et al. Acellular vascular matrix grafts from human placenta chorion: impact of ECM preservation on graft characteristics, protein composition and in vivo performance. *Biomaterials*. 2018;177:14–26.
38. Negishi J, et al. Porcine radial artery decellularization by high hydrostatic pressure. *J Tissue Eng Regen Med*. 2015;9(11):E144–51.
39. Ishino N, Fujisato T. Decellularization of porcine carotid by the recipient's serum and evaluation of its biocompatibility using a rat autograft model. *J Artif Organs*. 2015;18(2):136–42.
40. Lin CH, et al. An investigation on the correlation between the mechanical property change and the alterations in composition and microstructure of a porcine vascular tissue underwent trypsin-based decellularization treatment. *J Mech Behav Biomed Mater*. 2018;86:199–207.
41. Adamski M, et al. Two methods for decellularization of plant tissues for tissue engineering applications. *J Vis Exp*. 2018;(135):e57586.
42. Schmuck EG, et al. Cardiac fibroblast-derived 3D extracellular matrix seeded with mesenchymal stem cells as a novel device to transfer cells to the ischemic myocardium. *Cardiovasc Eng Technol*. 2014;5(1):119–31.
43. Harris GM, Raitman I, Schwarzbauer JE. Cell-derived decellularized extracellular matrices. *Methods Cell Biol*. 2018;143:97–114.
44. Fitzpatrick LE, McDevitt TC. Cell-derived matrices for tissue engineering and regenerative medicine applications. *Biomater Sci*. 2015;3(1):12–24.
45. Friedrich EE, et al. Residual sodium dodecyl sulfate in decellularized muscle matrices leads to fibroblast activation in vitro and foreign body response in vivo. *J Tissue Eng Regen Med*. 2018;12(3):e1704–15.
46. Pati F, et al. Printing three-dimensional tissue analogues with decellularized extracellular matrix bioink. *Nat Commun*. 2014;5:3935.
47. Mathapati S, et al. Biomimetic acellular detoxified glutaraldehyde cross-linked bovine pericardium for tissue engineering. *Korean J Couns Psychother*. 2013;33(3):1561–72.
48. McDade JK, et al. Interactions of U937 macrophage-like cells with decellularized pericardial matrix materials: influence of crosslinking treatment. *Acta Biomater*. 2013;9(7):7191–9.
49. Fidalgo C, et al. A sterilization method for decellularized xenogeneic cardiovascular scaffolds. *Acta Biomater*. 2018;67:282–94.
50. French KM, et al. A naturally derived cardiac extracellular matrix enhances cardiac progenitor cell behavior in vitro. *Acta Biomater*. 2012;8(12):4357–64.
51. Schwan J, et al. Anisotropic engineered heart tissue made from laser-cut decellularized myocardium. *Sci Rep*. 2016;6:32068.
52. Johnson TD, Christman KL. Injectable hydrogel therapies and their delivery strategies for treating myocardial infarction. *Expert Opin Drug Deliv*. 2013;10(1):59–72.
53. Tabuchi M, et al. Effect of decellularized tissue powders on a rat model of acute myocardial infarction. *Korean J Couns Psychother*. 2015;56:494–500.
54. Wang B, et al. Fabrication of cardiac patch with decellularized porcine myocardial scaffold and bone marrow mononuclear cells. *J Biomed Mater Res A*. 2010;94(4):1100–10.

55. Wang Q, et al. Functional engineered human cardiac patches prepared from nature's platform improve heart function after acute myocardial infarction. *Biomaterials*. 2016;105:52–65.
56. Jakus AE, et al. "Tissue papers" from organ-specific decellularized extracellular matrices. *Adv Funct Mater*. 2017;27(3):1700992.
57. Arenas-Herrera JE, et al. Decellularization for whole organ bioengineering. *Biomed Mater*. 2013;8(1):014106.
58. Weymann A, et al. Development and evaluation of a perfusion decellularization porcine heart model – generation of 3-dimensional myocardial neoscaffolds. *Circ J*. 2011;75(4):852–60.
59. Guyette JP, et al. Perfusion decellularization of whole organs. *Nat Protoc*. 2014;9(6):1451–68.
60. Taylor DA, et al. Building a total bioartificial heart: harnessing nature to overcome the current hurdles. *Artif Organs*. 2018;42(10):970–82.
61. Choudhury D, et al. Organ-derived decellularized extracellular matrix: a game changer for bioink manufacturing? *Trends Biotechnol*. 2018;36(8):787–805.
62. Jang J, et al. 3D printed complex tissue construct using stem cell-laden decellularized extracellular matrix bioinks for cardiac repair. *Biomaterials*. 2017;112:264–74.
63. Singelyn JM, Christman KL. Modulation of material properties of a decellularized myocardial matrix scaffold. *Macromol Biosci*. 2011;11(6):731–8.
64. Singelyn JM, et al. Catheter-deliverable hydrogel derived from decellularized ventricular extracellular matrix increases endogenous cardiomyocytes and preserves cardiac function post-myocardial infarction. *J Am Coll Cardiol*. 2012;59(8):751–63.
65. Seif-Naraghi SB, et al. Safety and efficacy of an injectable extracellular matrix hydrogel for treating myocardial infarction. *Sci Transl Med*. 2013;5(173):173ra25.
66. Chen WC, et al. Decellularized zebrafish cardiac extracellular matrix induces mammalian heart regeneration. *Sci Adv*. 2016;2(11):e1600844.
67. Kajbafzadeh AM, et al. Evaluating the role of autologous mesenchymal stem cell seeded on decellularized pericardium in the treatment of myocardial infarction: an animal study. *Cell Tissue Bank*. 2017;18(4):527–38.
68. Sarig U, et al. Natural myocardial ECM patch drives cardiac progenitor based restoration even after scarring. *Acta Biomater*. 2016;44:209–20.
69. Efraim Y, et al. Biohybrid cardiac ECM-based hydrogels improve long term cardiac function post myocardial infarction. *Acta Biomater*. 2017;50:220–33.
70. Badylak S, et al. Extracellular matrix for myocardial repair. *Heart Surg Forum*. 2003;6(2):E20–6.
71. Wan L, et al. Human heart valve-derived scaffold improves cardiac repair in a murine model of myocardial infarction. *Sci Rep*. 2017;7:39988.
72. Grover GN, Rao N, Christman KL. Myocardial matrix-polyethylene glycol hybrid hydrogels for tissue engineering. *Nanotechnology*. 2014;25(1):014011.
73. Stoppel WL, et al. Elastic, silk-cardiac extracellular matrix hydrogels exhibit time-dependent stiffening that modulates cardiac fibroblast response. *J Biomed Mater Res A*. 2016;104(12):3058–72.
74. Esmaeili Pourfarhangi K, et al. Construction of scaffolds composed of acellular cardiac extracellular matrix for myocardial tissue engineering. *Biologicals*. 2018;53:10–8.
75. Rajabi S, et al. Human embryonic stem cell-derived cardiovascular progenitor cells efficiently colonize in bFGF-tethered natural matrix to construct contracting humanized rat hearts. *Biomaterials*. 2018;154:99–112.
76. Namiri M, et al. Improving the biological function of decellularized heart valves through integration of protein tethering and three-dimensional cell seeding in a bioreactor. *J Tissue Eng Regen Med*. 2018;12(4):e1865–79.
77. Shevach M, et al. Gold nanoparticle-decellularized matrix hybrids for cardiac tissue engineering. *Nano Lett*. 2014;14(10):5792–6.
78. Gorain B, et al. Carbon nanotube scaffolds as emerging nanoplatform for myocardial tissue regeneration: a review of recent developments and therapeutic implications. *Biomed Pharmacother*. 2018;104:496–508.
79. Naso F, et al. Are FDA and CE sacrificing safety for a faster commercialization of xenogeneic tissue devices? Unavoidable need for legislation in decellularized tissue manufacturing. *Tissue Antigens*. 2014;83(3):193–4.

80. Gallo M, et al. Physiological performance of a detergent decellularized heart valve implanted for 15 months in Vietnamese pigs: surgical procedure, follow-up, and explant inspection. *Artif Organs*. 2012;36(6):E138–50.
81. Theodoridis K, et al. Successful matrix guided tissue regeneration of decellularized pulmonary heart valve allografts in elderly sheep. *Biomaterials*. 2015;52:221–8.
82. Simon P, et al. Early failure of the tissue engineered porcine heart valve SYNERGRAFT in pediatric patients. *Eur J Cardiothorac Surg*. 2003;23(6):1002–6; discussion 1006
83. Konertz W, et al. Hemodynamic characteristics of the Matrix P decellularized xenograft for pulmonary valve replacement during the Ross operation. *J Heart Valve Dis*. 2005;14(1):78–81.
84. Brown JW, et al. Performance of the CryoValve SG human decellularized pulmonary valve in 342 patients relative to the conventional CryoValve at a mean follow-up of four years. *J Thorac Cardiovasc Surg*. 2010;139(2):339–48.
85. Ozawa H, et al. Application of decellularized allograft for primary repair of congenital heart disease in Japan. *Gen Thorac Cardiovasc Surg*. 2018. <https://doi.org/10.1007/s11748-018-0988-9>.
86. Voges I, et al. Adverse results of a decellularized tissue-engineered pulmonary valve in humans assessed with magnetic resonance imaging. *Eur J Cardiothorac Surg*. 2013;44(4):e272–9.
87. Weber B, et al. Off-the-shelf human decellularized tissue-engineered heart valves in a non-human primate model. *Biomaterials*. 2013;34(30):7269–80.
88. Syedain ZH, et al. Implantation of completely biological engineered grafts following decellularization into the sheep femoral artery. *Tissue Eng Part A*. 2014;20(11–12):1726–34.
89. Dohmen PM, et al. Successful implantation of a decellularized equine pericardial patch into the systemic circulation. *Med Sci Monit Basic Res*. 2014;20:1–8.



3D Bioprinting of Cardiovascular Tissue Constructs: Cardiac Bioinks

4

Martin L. Tomov, Andrea Theus, Rithvik Sarasani, Huyun Chen, and Vahid Serpooshan

Introduction

Cardiovascular tissue bioprinting occupies a critical crossroads position between the fields of biomaterials engineering, cardiovascular biology, three-dimensional (3D) design and modeling, and biomanufacturing [1–4]. This complex area of research requires expertise from all these disciplines to provide a multidisciplinary approach that enables fabrication of functional and living tissues and organs, whether for basic science or translational research applications [5]. A major challenge that hampers this field is the lack of systematic characterization of the physical and chemical properties of hydrogel-based bioinks that are applicable to organ and tissue bioprinting [6–8]. Tailoring bioink properties to mimic the complex native tissue extracellular matrix (ECM) is of great importance and a slight divergence could result in pathological or loss of function manifests [9, 10].

M. L. Tomov · A. Theus · H. Chen

Wallace H. Coulter Department of Biomedical Engineering, Emory University School of Medicine and Georgia Institute of Technology, Atlanta, GA, USA

e-mail: martin.lyubomirov@emory.edu; andrea.theus@emory.edu; chenhuyun@gatech.edu

R. Sarasani

Scheller College of Business, Georgia Institute of Technology, Atlanta, GA, USA

e-mail: rsarasani3@gatech.edu

V. Serpooshan (✉)

Department of Biomedical Engineering, Emory University School of Medicine and Georgia Institute of Technology, Atlanta, GA, USA

Department of Pediatrics, Emory University School of Medicine, Atlanta, GA, USA

Children's Healthcare of Atlanta, Atlanta, GA, USA

e-mail: vahid.serpooshan@bme.gatech.edu

© Springer Nature Switzerland AG 2019

V. Serpooshan, S. M. Wu (eds.), *Cardiovascular Regenerative Medicine*, https://doi.org/10.1007/978-3-030-20047-3_4

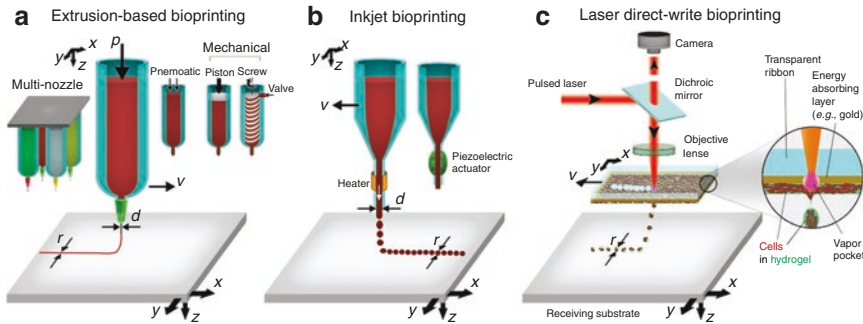


Fig. 4.1 Major methods that are available to bioprint tissue analogues. **(a)** Extrusion-based bioprinters use single- or multi-nozzle print heads, squeezing out the bioink using mechanical or pneumatic forces. **(b)** Droplet-based bioprinting uses thermal or piezoelectric forces to discharge droplets of bioinks. **(c)** Laser-based bioprinters use high-energy pulsed laser to eject bioink droplets from a donor layer onto the receiving substrate. (Adapted from [32])

Functional tissue bioprinting holds great promise to combine rationally designed biomaterials, functional cells, and macromolecules into 3D constructs that closely recapitulate the mechanical, structural, and functional microenvironment of native tissues [11]. With precise control over spatial arrangement of the cell-biomaterial architecture, 3D bioprinting can provide complex physiochemical and biological cues that are necessary for the maintenance and maturation of functional tissue analogues. To date, a range of bioprinting platforms have been used to create artificial tissue constructs, such as extrusion-based [12–15], droplet-based [16–18], and laser-based printing [19–21] (Fig. 4.1).

Recent advances in *in vitro* tissue development has made 3D bioprinting an attractive means for the next-generation regenerative medicine, specifically as a platform for tissue replacement to rescue failed organs in patient-specific therapies [6, 22–24]. Some of these applications include pancreatic tissue printing, to address loss of function in diabetes [25, 26], bioprinted kidney tissue analogues that can be used instead of, or in conjunction with, dialysis in kidney failure therapies [27, 28] and cardiac tissue constructs which can be bioprinted to repair the damaged heart tissue post injury (e.g., myocardial infarction), or in the case of congenital heart diseases [29–31].

This chapter explores the critical parameters of hydrogel-based bioinks that are necessary for their successful application in functional cardiovascular tissue engineering, as tissue analogues for disease modeling and drug screening *in vitro*, or as implantable tissue grafts to treat a range of congenital and acquired cardiovascular diseases. We will explore the biophysical, biochemical, and biological considerations for the candidate bioinks that enable 3D bioprinting of functional cardiovascular constructs.

Types of Bioinks

Bioink can be defined as a printable biomaterial, based on naturally occurring or synthetically derived polymers (hydrogels), that can recreate some aspects of native tissue ECM [6, 7, 14]. In addition to the hydrogel component, bioinks

typically consist of cells and/or small molecules (e.g., growth or angiogenic factors) to enhance their bioactivity. Successful bioinks maintain (or promote) encapsulated cell survival, adhesion, proliferation, and function in vitro and ultimately in vivo. Some of the desirable features of bioinks include the ability to form stable filaments during printing and gentle crosslinking mechanisms, which allow for spatial control of hydrogel deposition while maintaining cell viability [7, 8, 15, 33]. Currently available bioink formulations are often based on existing hydrogel biomaterials, such as alginate [34, 35], fibrin [36, 37], hyaluronic acids [38, 39], and gelatin [13, 40–42]. These bioinks can be divided into several broad categories based on the specific crosslinking/solidification characteristics of their parent hydrogel (Table 4.1). Critical for a successful bioink, it should be able to incorporate and protect bioactive compounds within the formed hydrogel. This could enhance the bioink functional mimicry to native tissues and enhance the function of encapsulated cells [43].

To achieve an optimal bioink formulation and successfully print functional tissues, the choice of specific bioprinting process and post-print tissue culture, maintenance, and maturation is critically important [6, 7, 14]. Further, hydrogel properties such as viscosity, crosslinking mechanism, stiffness, mass transfer properties (e.g., diffusion and permeability), and biodegradability must be taken into consideration, depending on the specific application [6, 8, 15, 19, 44]. To generate a biomimetic niche that can support tissue functionality and cell maturation, the chosen bioink would need to also allow for specific chemical modifications such as small molecule conjugation and ECM proteins immobilization within the 3D printed construct.

Cardiac Bioink Characteristics

Printability Printing resolution is dependent on the volume of deposited layer. To maintain a fine balance between thin prints (high resolution) and cell viability, the bioink should generate relatively low shear stress levels under modest pressures [33, 45, 46]. Shape fidelity at high-resolution prints is critical for building up functional tissue analogues, particularly for organs that are highly vascularized and have complex tissue organization such as the heart [8, 15, 40, 41]. To maintain fidelity, bioinks should have low reflow rate during the printing process and facile crosslinking steps and culture conditions (Fig. 4.2). This requires the ability of printed construct to be self-supporting at the macroscale, ideally with little to no supporting materials. While some support bioinks might be required to maintain complex/hollow shapes during printing, they would have to be either incorporated as a functional component of the tissue analogue or allow for full removal post-printing (i.e., sacrificial inks such as pluronic). This is particularly important in bioprinting of cardiovascular tissues, considering the remarkably high blood vessel density in the tissue (about 160 capillaries per mm² of myocardial tissue [47]). For cardiac tissue bioprinting, therefore, successful fabrication of self-standing and stable, hollow channels at diameters ranging from micrometers (capillaries) to centimeters (arteries) would be a major challenge. These perfusable vascular

Table 4.1 Classification of hydrogel bioinks based on crosslinking or solidification mechanism

Hydrogel formation	Ionic interactions	Temperature based	Time dependent	Photoinitiator based	Chemical initiator
Advantages	Physiological conditions Stability in vitro and in vivo	Wide stiffness range Physiological conditions	Gentle crosslinking Easily modifiable	Biodegradable Wide range of stiffness	Biodegradable Wide range of stiffness
Disadvantages	Gentle cell recovery	Great sacrificial hydrogel	Biodegradable	Easily modifiable	Well-established bioink formulations Not always xeno-free
	Not always xeno-free	Damage encapsulated cells	Not always xeno-free	Light-based cell damage	Not always xeno-free
	Limited modification ability	Printing resolution can be low	Not chemically defined	Chemically defined	Limited gas and nutrient diffusion
	Limited biodegradability	Can induce immune responses	Printing resolution can be low	Xeno-free	Endotoxin contamination
Bioink examples	Alginate; Dextran	Pluronic; PNIPAM*	Matrigel; HyStem	PEGDA ^{**} ; GELMA ^{***}	Gelatin based; silk-based

* PNIPAM - Poly(N-isopropylacrylamide)

** PEGDA - Poly(ethylene glycol) diacrylate

*** GelMA - Methacrylated gelatin

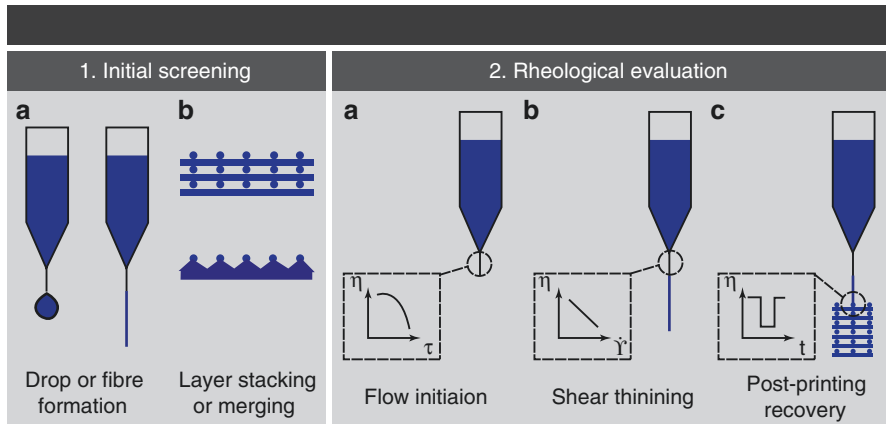


Fig. 4.2 Schematic demonstration of the typical approach to assess bioink printability. **1:** Initial screening of bioink formulations to (a) establish fiber versus droplet formation, and (b) successfully stack multiple layers without fusing between the layers. **2:** Rheological evaluations are performed to determine (a) the flow initiation and yield stress properties, (b) degree of shear thinning, and (c) recovery from shear thinning after printing. (Adapted from [14])

cardiac constructs can provide an invaluable platform for drug screening [27, 48, 49] and disease modeling studies [2, 27, 48, 50] *in vitro*, and a new generation of cardiac patch devices for *in vivo* regenerative therapies [38, 51, 52].

Post-print Processing Post-print processes are required to achieve the adequate print fidelity, as bioinks often require crosslinking [7, 53, 54]. Introducing crosslinking agents via an additional liquid phase may be detrimental to the shape fidelity. Therefore, employing a crosslinking step via long-wave ultraviolet (UV) radiation [53, 55] or visible light [40, 56] exposure at appropriate durations and intensities would be beneficial. Other types of post-print processes have often been used. For instance, promising results have been shown for salt-based post-processing after the constructs were printed [57–59]. Regardless of the chosen process, the structural and chemical stability of the initial print are critical to maintain reproducibility of engineered tissues. One challenge with light-based crosslinking is, however, the possible cell damage due to UV light irradiation [60]. This can be mitigated by combining or replacing UV with other more cytocompatible post-processing methods. Some alternative processes include aerosolized salt solution spray [61], incubation at elevated temperatures (>30 °C) [62], and enzymatic reactions [63] (Table 4.1). Additionally, less reliance upon ionic-based crosslinking may mitigate the precipitation or *salting-out* of adjunct proteins [64].

A successful cardiac bioprint will rely on a fast-acting crosslinking reagent with negligible cytotoxicity, while capable of retaining high printing fidelities. UV-crosslinked hydrogels, such as methacrylate modified gelatin (gelMA), have been extensively used for cardiac tissue printing as these hydrogels can generate

stable yet relatively soft matrices that mimic the biomechanical and biochemical properties of the native heart tissue [5, 65]. GelMA crosslinking via UV light occurs at relatively short times and moderate intensities (~2 minutes and between 1 and 20 mW/cm²), which could help to avoid excessive cell damage and death [16, 65].

Printed Tissue Stability and Controlled Degradation Swelling and contraction of hydrogels upon crosslinking and during tissue culture could be detrimental to the printed construct fidelity and cellular interactions/functions [66]. This can also alter the final mechanical properties of the bioink and skew its 3D arrangement [67, 68]. Controlled degradation and remodeling of bioprinted construct, along with secretion of ECM proteins by encapsulated cells, are critical for engineering a biomimetic tissue microenvironment [69]. However, printed tissue breakdown and remodeling, in an uncontrolled manner, can severely limit its translational applications, as they could cause implant detachment and failure in vivo [70, 71]. To alleviate these challenges, extensive research has focused on the development of new bioink formulations with tunable degradation profile, to enable cell-mediated tissue remodeling, while maintaining the construct integrity [72–79]. Particularly in the case of cardiac tissue constructs, a significant degree of matrix remodeling by bioprinted cells is necessary to achieve the intercellular connectivity and the remarkably high cell packing density of the native heart tissue [50, 80–83]. To that end, gelMA-based bioinks are specifically favorable as they are both biodegradable and chemically defined.

Mass Transfer Properties of Cardiac Bioinks Incorporating functional vascularization is a critical aspect of tissue bioprinting to generate and maintain large (clinically relevant) tissue constructs [84–93]. This is particularly important for bioengineered cardiac constructs, considering the remarkably high vascular density in the native myocardial tissue (approximately one capillary per cardiomyocyte) [94, 95]. With passive perfusion alone, the maximum thickness of a viable 3D tissue construct is usually around 100–250 μm [96, 97] before vascularization is required. This distance can potentially be extended to about 600 μm in bioprinted constructs that can be prevascularized prior to cell seeding. If the construct's pore size is large enough to allow for more effective passive diffusion, a similar effect can occur [98–100].

Tissue-Specific and Chemically Modifiable Bioinks The ability to incorporate tissue- and cell type-specific materials into the bioink is critically important for achieving in vivo-like functionality. Modification chemistry can provide the small molecules and ECM factors that are specific to the tissue/organ microenvironment [73, 78, 101]. For this purpose, covalent conjugation, or similar levels of immobilization, would be an effective approach to recapitulate the specific tissue cues for bioprinted cells and initiate self-directed environmental remodeling. Keeping the modification chemistry and bioink preparation steps simple would also be significantly beneficial by cutting down on preparation time and equipment and material expenses and by enhancing batch-to-batch consistency [6]. Furthermore, the hydrogel bioink should

be xeno-free or consist of entirely chemically defined components, to facilitate translational use in regenerative medicine and to enhance the reliability for use in *in vitro* assays, such as drug screening and disease modeling [3].

To generate a bioink that is supportive to cardiac cells and recapitulates the organ/tissue-specific niche, high-throughput analysis techniques, such as transcriptome analysis (RNA-Seq) and proteomics can be used to characterize the native cardiac tissue ECM. For instance, bone morphogenic proteins (BMP2/BMP4) and Wnt inhibitors (IWP2) are known to play key roles in generation of early cardiomyocytes *in vitro* [102–110]. Incorporating certain concentrations of these factors in the tissue generation pipeline (e.g., in cardiac bioink) may promote the regenerative capacity of printed constructs. Further, functionalizing the bioink with ECM proteins, such as cadherins, connexins, and collagen, can be used to promote cell attachment, migration, and remodeling [86, 111–116]. ECM proteins coupled with secreted small molecules such as tumor necrosis factor alpha (TNF α), interleukin (IL)-1, IL-6, transforming growth factor beta (TGF β), angiotensin II, and endothelin 1 can also help promote tissue maturation and vascularization in cardiac constructs (Fig. 4.3) [117, 118].

Tunable Mechanical Properties Altering biomechanical characteristics of the bioinks can be achieved via initial or secondary crosslinking processes. Such modifications can provide the specific mechanical cues to encapsulated cells and promote desired cellular functionalities [14, 119]. The ability to independently tune chemical and mechanical properties of these hydrogels is critically important. For example, crosslinking of hydrogel matrices can tune their stiffness [120–123], while conjugation of various ECM proteins and small molecules can independently provide biochemical cues to the cells [7, 124]. Mechanical properties play a major role in successful application of bioprinted cardiac constructs, as these tissues require strictly regulated stiffness values to exhibit proper functionality both *in vitro* and

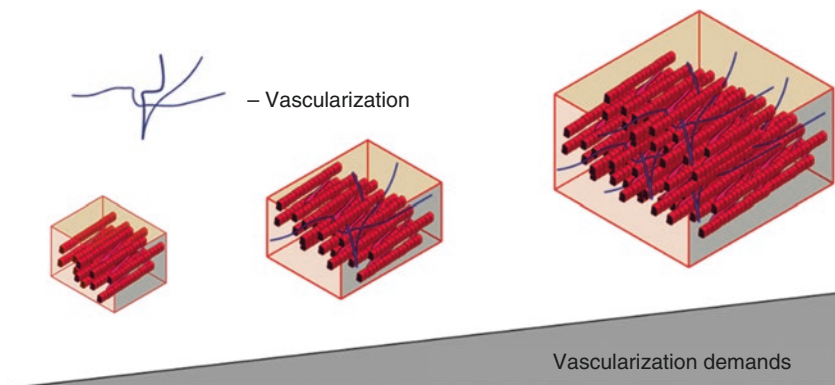


Fig. 4.3 The demand for effective vascularization *in vitro* increases with tissue construct size and complexity

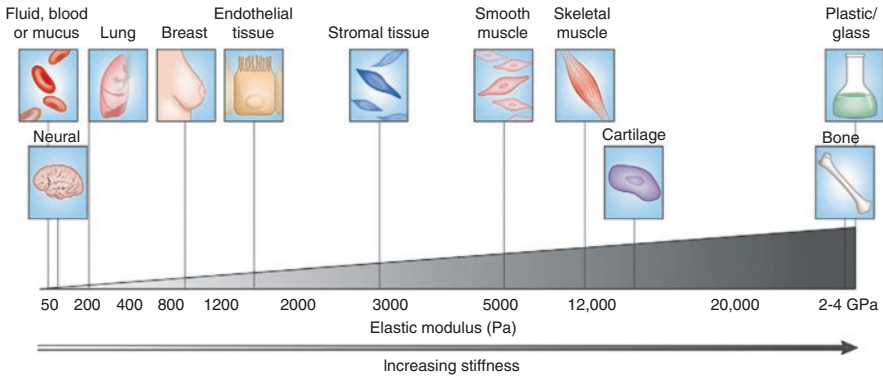


Fig. 4.4 Range of ECM stiffness required for proper organ development and functionality of various organs and tissues. (Adapted from [127])

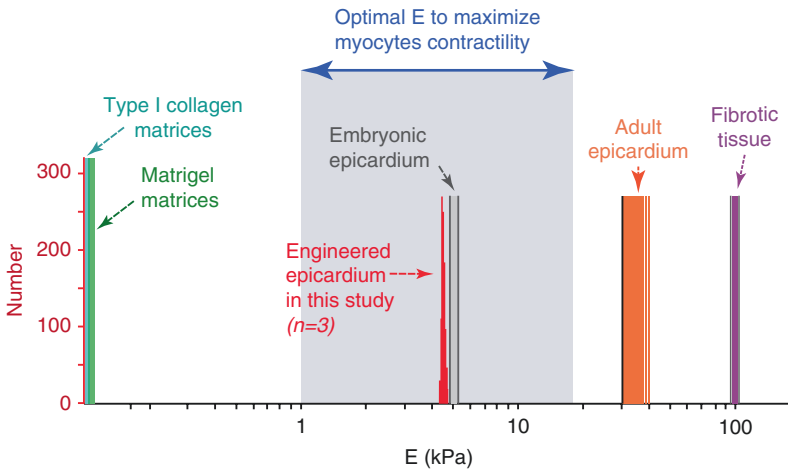


Fig. 4.5 Demonstration of varying range of stiffness for various cardiac tissues and tissue engineering hydrogels. Optimal range of stiffness, resulting in maximum contractile work of cardiac myocytes, is highlighted in blue. (Adapted from [126])

in vivo (Fig. 4.4) [32, 82, 123, 125, 126]. The post-print crosslinking mechanisms that are used for most hydrogel bioinks allow for generating tissues with a relatively broad range of stiffness. Therefore, bioprinting technology holds a great potential for manufacturing a wide variety of functional tissues.

It has been shown by different groups that cardiomyocytes exhibit maximal contractile function on matrix stiffnesses ranging from 1 to 16 kPa [51, 82, 115, 123, 126]. Thus, an optimal cardiac-specific bioink may be expected to show elastic modulus within this range (Fig. 4.5) [126]. Incorporating large numbers of nondividing cardiomyocytes in bioinks can compromise their mechanical properties and

printing fidelity (resolution and stability). To address this issue, cardiomyocytes can be combined with proliferative cardiac precursor/stem cells, cardiac, and vascular cells (endothelial and smooth muscle cells) and be encapsulated in the bioink at remarkably lower cell densities [29, 128–130]. Multiplication, differentiation, and maturation of these multilineage cardiac cell populations in bioprinted constructs, in association with controlled matrix degradation and remodeling, can lead to generation of myocardial mimetic tissue constructs at appropriate cell density and configuration. The use of stem cell sources for cardiac tissue printing may require additional examination and characterization to avoid incomplete or undesirable cell differentiation (e.g., tumor formation or reduced functionality of the engrafted tissue) that could impact the clinical application of the printed constructs [131–133].

Outlook and Conclusions

To maintain cell viability and functionality, hydrogel-based bioinks must fulfill several key biophysical and biochemical requirements, before, during, and post-printing processes. These parameters, together with the need for a functional vascular network in the construct, are critical for generating high fidelity cardiac tissue analogues. Initial and/or secondary crosslinking processes would allow for better control over the chemical and mechanical cues within the 3D constructs and therefore, enable reconstructing diverse tissue microenvironments. Preparing commercially available *cardiac bioink kits* that can be optimized for a specific tissue bioprinting would be a significant advancement in the field, especially if different chemical and mechanical properties of the hydrogels could be decoupled and independently tuned. A balance must be obtained between cardiac bioink crosslinking degree, stiffness, and biodegradation to allow for bioprinted cells to remodel their microenvironment. This is a critical step toward achieving enhanced cardiac cell connectivity, maturation, and function. Additionally, keeping bioink synthesis and modification chemistry robust and simple would be highly beneficial for wider appeal to researchers in the field.

In summary, cardiac bioprinting aims to generate clinically applicable, cardiac tissue analogues that can replace damaged/diseased tissue *in vivo* or be used as biomimetic platforms *in vitro* to model various diseases. Recent advances in bioprinting technologies have enabled fabrication of complex, patient-specific, tissue architectures at an organ-relevant spatial resolution, while supporting viability and function of multiple cell types. However, there remain some challenges for the clinical application of bioprinted cardiac constructs. Development of new cardiac-specific bioinks, using tailored biomaterials and precisely tuned selection of macromolecules, could be a great step forward toward clinical bioprinting. New methods are also needed to incorporate functional, multiscale vascular networks within printed constructs that can be perfused to maintain functionality of large-scale tissue constructs. Further, enhanced temporal and spatial resolutions in the new generation of bioprinters can help engineering more advanced cardiac tissue substitutes for regenerative medicine.

References

1. Murphy SV, Atala A. 3D bioprinting of tissues and organs. *Nat Biotechnol.* 2014;32(8):773–85.
2. Wang Z, et al. 3D bioprinted functional and contractile cardiac tissue constructs. *Acta Biomater.* 2018;70:48–56.
3. Ji S, Guvendiren M. Recent advances in bioink design for 3D bioprinting of tissues and organs. *Front Bioeng Biotechnol.* 2017;5:23.
4. Suntornnond R, et al. A mathematical model on the resolution of extrusion bioprinting for the development of new bioinks. *Materials (Basel).* 2016;9(9):756.
5. Jang J. 3D bioprinting and in vitro cardiovascular tissue modeling. *Bioengineering (Basel).* 2017;4(3):71.
6. Gopinathan J, Noh I. Recent trends in bioinks for 3D printing. *Biomater Res.* 2018;22:11.
7. Holzl K, et al. Bioink properties before, during and after 3D bioprinting. *Biofabrication.* 2016;8(3):032002.
8. Ouyang L, et al. Effect of bioink properties on printability and cell viability for 3D bioplotting of embryonic stem cells. *Biofabrication.* 2016;8(3):035020.
9. Smith L, Cho S, Discher DE. Mechanosensing of matrix by stem cells: From matrix heterogeneity, contractility, and the nucleus in pore-migration to cardiogenesis and muscle stem cells in vivo. *Semin Cell Dev Biol.* 2017;71:84–98.
10. Geckil H, et al. Engineering hydrogels as extracellular matrix mimics. *Nanomedicine.* 2010;5(3):469–84.
11. Mandrycky C, et al. 3D bioprinting for engineering complex tissues. *Biotechnol Adv.* 2016;34(4):422–34.
12. Chung JHY, et al. Bio-ink properties and printability for extrusion printing living cells. *Biomater Sci.* 2013;1(7):763–73.
13. Liu W, et al. Coaxial extrusion bioprinting of 3D microfibrinous constructs with cell-favorable gelatin methacryloyl microenvironments. *Biofabrication.* 2018;10(2):024102.
14. Paxton N, et al. Proposal to assess printability of bioinks for extrusion-based bioprinting and evaluation of rheological properties governing bioprintability. *Biofabrication.* 2017;9(4):044107.
15. Zhao Y, et al. The influence of printing parameters on cell survival rate and printability in microextrusion-based 3D cell printing technology. *Biofabrication.* 2015;7(4):045002.
16. Stratesteffen H, et al. GelMA-collagen blends enable drop-on-demand 3D printability and promote angiogenesis. *Biofabrication.* 2017;9(4):045002.
17. Graham AD, et al. High-resolution patterned cellular constructs by droplet-based 3D printing. *Sci Rep.* 2017;7(1):7004.
18. Gudapati H, Dey M, Ozbolat I. A comprehensive review on droplet-based bioprinting: past, present and future. *Biomaterials.* 2016;102:20–42.
19. Dababneh AB, Ozbolat IT. Bioprinting technology: a current state-of-the-art review. *J Manuf Sci Eng-Trans ASME.* 2014;136(6):061016.
20. Entsfellner K, et al. First 3D printed medical robot for ENT surgery – application specific manufacturing of laser sintered disposable manipulators. 2014 IEEE/RSJ international conference on Intelligent Robots and Systems (Iros 2014), 2014. p. 4278–83.
21. Zhang Z, et al. Effects of living cells on the bioink printability during laser printing. *Biomicrofluidics.* 2017;11(3):034120.
22. Leberfinger AN, et al. Concise review: bioprinting of stem cells for transplantable tissue fabrication. *Stem Cells Transl Med.* 2017;6(10):1940–8.
23. Malyala SK, Kumar YR, Rao CSP. Organ printing with life cells: a review. *Mater Today-Proc.* 2017;4(2):1074–83.
24. Datta P, Ayan B, Ozbolat IT. Bioprinting for vascular and vascularized tissue biofabrication. *Acta Biomater.* 2017;51:1–20.
25. Ravnicek DJ, Leberfinger AN, Ozbolat IT. Bioprinting and cellular therapies for type 1 diabetes. *Trends Biotechnol.* 2017;35(11):1025–34.

26. Woliner-van der Weg W, et al. A 3D-printed anatomical pancreas and kidney phantom for optimizing SPECT/CT reconstruction settings in beta cell imaging using (111)In-exendin. *EJNMMI Phys.* 2016;3(1):29.
27. Homan KA, et al. Bioprinting of 3D Convoluted Renal Proximal Tubules on Perfusable Chips. *Scientific Reports.* 2016;6:34845.
28. Zhang YS, et al. 3D bioprinting for tissue and organ fabrication. *Ann Biomed Eng.* 2017;45(1):148–63.
29. Ong CS, et al. Biomaterial-free three-dimensional bioprinting of cardiac tissue using human induced pluripotent stem cell derived cardiomyocytes. *Sci Rep.* 2017;7:4566.
30. Cheung DYC, Duan B, Butcher JT. Chapter 21 – Bioprinting of cardiac tissues. In: Atala A, Yoo JJ, editors. *Essentials of 3D biofabrication and translation.* Boston: Academic; 2015. p. 351–70.
31. Lee S, et al. 3D bioprinted functional and contractile cardiac tissue constructs. *Tissue Eng A.* 2017;23:S96.
32. Serpooshan V, et al. Bioengineering cardiac constructs using 3D printing. *J 3D Print Med.* 2017;1(2):123.
33. Nair K, et al. Characterization of cell viability during bioprinting processes. *Biotechnol J.* 2009;4(8):1168–77.
34. Axpe E, Oyen ML. Applications of alginate-based bioinks in 3D bioprinting. *Int J Mol Sci.* 2016;17(12):1976.
35. Duan B, et al. 3D Bioprinting of heterogeneous aortic valve conduits with alginate/gelatin hydrogels. *J Biomed Mater Res A.* 2013;101(5):1255–64.
36. Lee YB, et al. Bio-printing of collagen and VEGF-releasing fibrin gel scaffolds for neural stem cell culture. *Exp Neurol.* 2010;223(2):645–52.
37. Kolesky DB, et al. 3D bioprinting of vascularized, heterogeneous cell-laden tissue constructs. *Adv Mater.* 2014;26(19):3124–30.
38. Gaetani R, et al. Epicardial application of cardiac progenitor cells in a 3D-printed gelatin/hyaluronic acid patch preserves cardiac function after myocardial infarction. *Biomaterials.* 2015;61:339–48.
39. Luo Y, et al. Injectable hyaluronic acid-dextran hydrogels and effects of implantation in ferret vocal fold. *J Biomed Mater Res B Appl Biomater.* 2010;93b(2):386–93.
40. Lim KS, et al. New visible-light photoinitiating system for improved print fidelity in gelatin-based bioinks. *ACS Biomater Sci Eng.* 2016;2(10):1752–62.
41. Liu W, et al. Extrusion bioprinting of shear-thinning gelatin methacryloyl bioinks. *Adv Healthc Mater.* 2017;6(12). <https://doi.org/10.1002/adhm.201601451>.
42. Yin J, et al. 3D bioprinting of low-concentration cell-laden gelatin methacrylate (GelMA) bioinks with a two-step cross-linking strategy. *ACS Appl Mater Interfaces.* 2018;10(8):6849–57.
43. Levato R, et al. Biofabrication of tissue constructs by 3D bioprinting of cell-laden microcarriers. *Biofabrication.* 2014;6(3):035020.
44. Duan B. State-of-the-art review of 3D bioprinting for cardiovascular tissue engineering. *Ann Biomed Eng.* 2017;45(1):195–209.
45. Blaeser A, et al. Controlling shear stress in 3D bioprinting is a key factor to balance printing resolution and stem cell integrity. *Adv Healthc Mater.* 2016;5(3):326–33.
46. Forget A, et al. Mechanically tunable bioink for 3D bioprinting of human cells. *Adv Healthc Mater.* 2017;6(20). <https://doi.org/10.1002/adhm.201700255>.
47. Khazaei M, Salehi E. Myocardial capillary density in normal and diabetic male rats: effect of bezafibrate. *Res Pharm Sci.* 2013;8(2):119–23.
48. Vanderburgh J, Sterling JA, Guelcher SA. 3D printing of tissue engineered constructs for in vitro modeling of disease progression and drug screening. *Ann Biomed Eng.* 2017;45(1):164–79.
49. Zhang YS, et al. Bioprinting 3D microfibrillar scaffolds for engineering endothelialized myocardium and heart-on-a-chip. *Biomaterials.* 2016;110:45–59.
50. Serpooshan V, et al. Use of bio-mimetic three-dimensional technology in therapeutics for heart disease. *Bioengineered.* 2014;5(3):193–7.

51. Serpooshan V, Ruiz-Lozano P. Ultra-rapid manufacturing of engineered epicardial substitute to regenerate cardiac tissue following acute ischemic injury. *Methods Mol Biol.* 2014;1210:239–48.
52. Serpooshan V, Wu SM. Patching up broken hearts: cardiac cell therapy gets a bioengineered boost. *Cell Stem Cell.* 2014;15(6):671–3.
53. Bartnikowski M, et al. Tailoring hydrogel viscoelasticity with physical and chemical crosslinking. *Polymers.* 2015;7(12):2650–69.
54. Schoenmakers DC, Rowan AE, Kouwer PHJ. Crosslinking of fibrous hydrogels. *Nat Commun.* 2018;9:2172.
55. Jung J, Oh J. Influence of photo-initiator concentration on the viability of cells encapsulated in photo-crosslinked microgels fabricated by microfluidics. *Dig J Nanomater Biostruct.* 2014;9(2):503–9.
56. Zhou D, Ito Y. Visible light-curable polymers for biomedical applications. *Sci China-Chem.* 2014;57(4):510–21.
57. Akar E, Altinisik A, Seki Y. Preparation of pH- and ionic-strength responsive biodegradable fumaric acid crosslinked carboxymethyl cellulose. *Carbohydr Polym.* 2012;90(4):1634–41.
58. Fekete T, et al. Synthesis and characterization of superabsorbent hydrogels based on hydroxyethylcellulose and acrylic acid. *Carbohydr Polym.* 2017;166:300–8.
59. Segura T, Chung PH, Shea LD. DNA delivery from hyaluronic acid-collagen hydrogels via a substrate-mediated approach. *Biomaterials.* 2005;26(13):1575–84.
60. Boerma M, et al. Microarray analysis of gene expression profiles of cardiac myocytes and fibroblasts after mechanical stress, ionising or ultraviolet radiation. *BMC Genomics.* 2005;6:6.
61. Johnson DM, et al. Polymer spray deposition: a novel aerosol-based, electrostatic digital deposition system for additive manufacturing. *NIP Digit Fabric Conf.* 2016;2016(1):129–33.
62. Wu Z, et al. Bioprinting three-dimensional cell-laden tissue constructs with controllable degradation. *Sci Rep.* 2016;6:24474.
63. Irvine SA, et al. Printing cell-laden gelatin constructs by free-form fabrication and enzymatic protein crosslinking. *Biomed Microdevices.* 2015;17(1):16.
64. Najdanovic-Visak V, et al. Salting-out in aqueous solutions of ionic liquids and K(3)PO(4): aqueous biphasic systems and salt precipitation. *Int J Mol Sci.* 2007;8(8):736–48.
65. Wang X, et al. Gelatin-based hydrogels for organ 3D bioprinting. *Polymers (Basel).* 2017;9(9):401.
66. Ersumo N, Witherel CE, Spiller KL. Differences in time-dependent mechanical properties between extruded and molded hydrogels. *Biofabrication.* 2016;8(3):–035012.
67. Bueno VB, et al. Synthesis and swelling behavior of xanthan-based hydrogels. *Carbohydr Polym.* 2013;92(2):1091–9.
68. Rahali K, et al. Synthesis and characterization of nanofunctionalized gelatin methacrylate hydrogels. *Int J Mol Sci.* 2017;18(12):2675.
69. Swinehart IT, Badyalak SF. Extracellular matrix bioscaffolds in tissue remodeling and morphogenesis. *Dev Dyn.* 2016;245(3):351–60.
70. Tosun Z, Villegas-Montoya C, McFetridge PS. The influence of early-phase remodeling events on the biomechanical properties of engineered vascular tissues. *J Vasc Surg.* 2011;54(5):1451–60.
71. Velasco MA, Narvaez-Tovar CA, Garzon-Alvarado DA. Design, materials, and mechanobiology of biodegradable scaffolds for bone tissue engineering. *Biomed Res Int.* 2015;2015:729076.
72. Fenn SL, Oldinski RA. Visible light crosslinking of methacrylated hyaluronan hydrogels for injectable tissue repair. *J Biomed Mater Res B Appl Biomater.* 2016;104(6):1229–36.
73. Burkoth AK, Burdick J, Anseth KS. Surface and bulk modifications to photocrosslinked poly-anhydrides to control degradation behavior. *J Biomed Mater Res.* 2000;51(3):352–9.
74. Coletta DJ, et al. (*) Bone regeneration mediated by a bioactive and biodegradable extracellular matrix-like hydrogel based on elastin-like recombinamers. *Tissue Eng Part A.* 2017;23(23–24):1361–71.

75. Du JZ, et al. Synthesis and characterization of photo-cross-linked hydrogels based on biodegradable polyphosphoesters and poly(ethylene glycol) copolymers. *Biomacromolecules*. 2007;8(11):3375–81.
76. Jeon O, et al. The effect of oxidation on the degradation of photocrosslinkable alginate hydrogels. *Biomaterials*. 2012;33(13):3503–14.
77. Kocen R, et al. Viscoelastic behaviour of hydrogel-based composites for tissue engineering under mechanical load. *Biomed Mater*. 2017;12(2):025004.
78. Prestwich GD, et al. Controlled chemical modification of hyaluronic acid: synthesis, applications, and biodegradation of hydrazide derivatives. *J Control Release*. 1998;53(1–3):93–103.
79. Shin H, et al. In vivo bone and soft tissue response to injectable, biodegradable oligo(poly(ethylene glycol) fumarate) hydrogels. *Biomaterials*. 2003;24(19):3201–11.
80. Badylak SF, et al. The use of extracellular matrix as an inductive scaffold for the partial replacement of functional myocardium. *Cell Transplant*. 2006;15:S29–40.
81. Eitan Y, et al. Acellular cardiac extracellular matrix as a scaffold for tissue engineering: in vitro cell support, remodeling, and biocompatibility. *Tissue Eng Part C Methods*. 2010;16(4):671–83.
82. Serpooshan V, et al. The effect of bioengineered acellular collagen patch on cardiac remodeling and ventricular function post myocardial infarction. *Biomaterials*. 2013;34(36):9048–55.
83. Wang B, et al. Myocardial scaffold-based cardiac tissue engineering: application of coordinated mechanical and electrical stimulations. *Langmuir*. 2013;29(35):11109–17.
84. Dvir T, et al. Prevascularization of cardiac patch on the omentum improves its therapeutic outcome. *Proc Natl Acad Sci U S A*. 2009;106(35):14990–5.
85. Hirt MN, Hansen A, Eschenhagen T. Cardiac tissue engineering: state of the art. *Circ Res*. 2014;114(2):354–67.
86. Kreutziger KL, et al. Developing vasculature and stroma in engineered human myocardium. *Tissue Eng Part A*. 2011;17(9–10):1219–28.
87. Lux M, et al. In vitro maturation of large-scale cardiac patches based on a perfusable starter matrix by cyclic mechanical stimulation. *Acta Biomater*. 2016;30:177–87.
88. Mannhardt I, Marsano A, Teuschl A. Perfusion bioreactors for prevascularization strategies in cardiac tissue engineering. In: Holthoner W, et al., editors. *Vascularization for tissue engineering and regenerative medicine*. Cham: Springer International Publishing; 2017. p. 1–14.
89. Montgomery M, Zhang B, Radisic M. Cardiac tissue vascularization: from angiogenesis to microfluidic blood vessels. *J Cardiovasc Pharmacol Ther*. 2014;19(4):382–93.
90. Pagliari S, et al. A multistep procedure to prepare pre-vascularized cardiac tissue constructs using adult stem cells, dynamic cell cultures, and porous scaffolds. *Front Physiol*. 2014;5:210.
91. Sarig U, et al. Pushing the envelope in tissue engineering: ex vivo production of thick vascularized cardiac extracellular matrix constructs. *Tissue Eng Part A*. 2015;21(9–10):1507–19.
92. Schaefer JA, et al. A cardiac patch from aligned microvessel and cardiomyocyte patches. *J Tissue Eng Regen Med*. 2018;12(2):546–56.
93. Vunjak-Novakovic G, et al. Challenges in cardiac tissue engineering. *Tissue Eng B-Rev*. 2010;16(2):169–87.
94. Johansson B, et al. Myocardial capillary supply is limited in hypertrophic cardiomyopathy: a morphological analysis. *Int J Cardiol*. 2008;126(2):252–7.
95. Mohammed SF, et al. Coronary microvascular rarefaction and myocardial fibrosis in heart failure with preserved ejection fraction. *Circulation*. 2015;131(6):550–9.
96. Rouwkema J, et al. Supply of nutrients to cells in engineered tissues. *Biotechnol Genet Eng Rev*. 2010;26:163–78.
97. Liu J, et al. Monitoring nutrient transport in tissue-engineered grafts. *J Tissue Eng Regen Med*. 2015;9(8):952–60.
98. McMurtrey RJ. Analytic models of oxygen and nutrient diffusion, metabolism dynamics, and architecture optimization in three-dimensional tissue constructs with applications and insights in cerebral organoids. *Tissue Eng Part C Methods*. 2016;22(3):221–49.

99. Lovett M, et al. Vascularization strategies for tissue engineering. *Tissue Eng Part B Rev.* 2009;15(3):353–70.
100. Phelps EA, Garcia AJ. Engineering more than a cell: vascularization strategies in tissue engineering. *Curr Opin Biotechnol.* 2010;21(5):704–9.
101. Hoch E, et al. Chemical tailoring of gelatin to adjust its chemical and physical properties for functional bioprinting. *J Mater Chem B.* 2013;1(41):5675–85.
102. Chen WP, Wu SM. Small molecule regulators of postnatal Nkx2.5 cardiomyoblast proliferation and differentiation. *J Cell Mol Med.* 2012;16(5):961–5.
103. Lee K, Silva EA, Mooney DJ. Growth factor delivery-based tissue engineering: general approaches and a review of recent developments. *J R Soc Interface.* 2011;8(55):153–70.
104. Ghazizadeh Z, et al. Transient activation of reprogramming transcription factors using protein transduction facilitates conversion of human fibroblasts toward cardiomyocyte-like cells. *Mol Biotechnol.* 2017;59(6):207–20.
105. Braam SR, et al. Inhibition of ROCK improves survival of human embryonic stem cell-derived cardiomyocytes after dissociation. *Ann N Y Acad Sci.* 2010;1188:52–7.
106. Cagavi E, et al. Functional cardiomyocytes derived from Isl1 cardiac progenitors via Bmp4 stimulation. *PLoS One.* 2014;9(12):e110752.
107. Cai CL, et al. Isl1 identifies a cardiac progenitor population that proliferates prior to differentiation and contributes a majority of cells to the heart. *Dev Cell.* 2003;5(6):877–89.
108. Degeorge BR Jr, et al. BMP-2 and FGF-2 synergistically facilitate adoption of a cardiac phenotype in somatic bone marrow c-kit+/Sca-1+ stem cells. *Clin Transl Sci.* 2008;1(2):116–25.
109. Hao J, et al. Dorsomorphin, a selective small molecule inhibitor of BMP signaling, promotes cardiomyogenesis in embryonic stem cells. *PLoS One.* 2008;3(8):e2904.
110. Serpooshan V, et al. Nkx2.5+cardiomyoblasts contribute to cardiomyogenesis in the neonatal heart. *Sci Rep.* 2017;7(7):12590.
111. Bax NA, et al. Matrix production and remodeling capacity of cardiomyocyte progenitor cells during in vitro differentiation. *J Mol Cell Cardiol.* 2012;53(4):497–508.
112. Fan D, et al. Cardiac fibroblasts, fibrosis and extracellular matrix remodeling in heart disease. *Fibrogenesis Tissue Repair.* 2012;5(1):15.
113. Hanson KP, et al. Spatial and temporal analysis of extracellular matrix proteins in the developing murine heart: a blueprint for regeneration. *Tissue Eng Part A.* 2013;19(9–10):1132–43.
114. Lindsey ML, et al. A novel collagen matricryptin reduces left ventricular dilation post-myocardial infarction by promoting scar formation and angiogenesis. *J Am Coll Cardiol.* 2015;66(12):1364–74.
115. Suhaeri M, et al. Cardiomyoblast (h9c2) differentiation on tunable extracellular matrix microenvironment. *Tissue Eng Part A.* 2015;21(11–12):1940–51.
116. Ungerleider JL, et al. Fabrication and characterization of injectable hydrogels derived from decellularized skeletal and cardiac muscle. *Methods.* 2015;84:53–9.
117. Porter KE, Turner NA. Cardiac fibroblasts: at the heart of myocardial remodeling. *Pharmacol Ther.* 2009;123(2):255–78.
118. Nian M, et al. Inflammatory cytokines and postmyocardial infarction remodeling. *Circ Res.* 2004;94(12):1543–53.
119. Diamantides N, et al. Correlating rheological properties and printability of collagen bioinks: the effects of riboflavin photocrosslinking and pH. *Biofabrication.* 2017;9(3):034102.
120. Duong H, Wu B, Tawil B. Modulation of 3D fibrin matrix stiffness by intrinsic fibrinogen-thrombin compositions and by extrinsic cellular activity. *Tissue Eng Part A.* 2009;15(7):1865–76.
121. Kaiser NJ, Coulombe KLK. Physiologically inspired cardiac scaffolds for tailored in vivo function and heart regeneration. *Biomed Mater.* 2015;10(3):034003.
122. Thom Quinlan AM, et al. Combining dynamic stretch and tunable stiffness to probe cell mechanobiology in vitro. *PLoS One.* 2011;6(8):e23272.
123. Lee S, et al. Contractile force generation by 3D hiPSC-derived cardiac tissues is enhanced by rapid establishment of cellular interconnection in matrix with muscle-mimicking stiffness. *Biomaterials.* 2017;131:111–20.

124. Lee JP, et al. N-terminal specific conjugation of extracellular matrix proteins to 2-pyridinecarboxaldehyde functionalized polyacrylamide hydrogels. *Biomaterials*. 2016;102:268–76.
125. Serpooshan V, et al. Chapter 8 – 4D printing of actuating cardiac tissue. In: Al'Aref SJ, et al., editors. *3D printing applications in cardiovascular medicine*. Boston: Academic; 2018. p. 153–62.
126. Wei K, et al. Epicardial FSTL1 reconstitution regenerates the adult mammalian heart. *Nature*. 2015;525(7570):479–85.
127. Cox TR, Ertler JT. Remodeling and homeostasis of the extracellular matrix: implications for fibrotic diseases and cancer. *Dis Model Mech*. 2011;4(2):165–78.
128. Gao L, et al. Myocardial tissue engineering with cells derived from human-induced pluripotent stem cells and a native-like, high-resolution, 3-dimensionally printed scaffold. *Circ Res*. 2017;120(8):1318–25.
129. Giacomelli E, et al. Three-dimensional cardiac microtissues composed of cardiomyocytes and endothelial cells co-differentiated from human pluripotent stem cells. *Development*. 2017;144(6):1008–17.
130. Pati F, et al. Printing three-dimensional tissue analogues with decellularized extracellular matrix bioink. *Nat Commun*. 2014;5:3935.
131. Weissman IL. Normal and neoplastic stem cells. *Novartis Found Symp*. 2005;265:35–50; discussion 50–4, 92–7.
132. Knappe N, et al. Directed dedifferentiation using partial reprogramming induces invasive phenotype in melanoma cells. *Stem Cells*. 2016;34(4):832–46.
133. Clement F, et al. Stem cell manipulation, gene therapy and the risk of cancer stem cell emergence. *Stem Cell Investig*. 2017;4:67.



Nanobiomaterial Advances in Cardiovascular Tissue Engineering

5

Michael J. Hill, Morteza Mahmoudi,
and Parisa P. S. S. Abadi

Introduction

Heart failure remains one of the deadliest, most expensive, and medically challenging problems in the modern world [1]. Occlusion of coronary arteries (e.g., as a result of atherosclerosis) leads to ischemic myocardial infarction (MI) which in turn can cause an irreversible substantial epicardial and myocardial tissue damage and loss of function [2]. The irreversibility of the loss of tissue is mainly due to the innately low self-renewal of adult cardiomyocytes (CMs), as human radioisotope studies show that less than half of the myocardium is renewed during the normal adult lifespan [3].

Various drugs (e.g., β -blockers and aldosterone), bare-metal stents, and drug eluting stents have been used to induce regeneration of CMs damaged by MI [4, 5]. Additionally, left ventricular polymeric restraints have been developed to prevent

M. J. Hill

Department of Mechanical Engineering-Engineering Mechanics, Michigan Technological University, Houghton, MI, USA

e-mail: mijhill@mtu.edu

M. Mahmoudi

Department of Anesthesiology, Brigham and Women's Hospital, Harvard Medical School, Boston, MA, USA

Precision Health Program, Department of Radiology, College of Human Medicine, Michigan State University, East Lansing, MI, USA

e-mail: mahmou22@msu.edu

P. P. S. S. Abadi (✉)

Department of Mechanical Engineering-Engineering Mechanics, Michigan Technological University, Houghton, MI, USA

Department of Biomedical Engineering, Department of Materials Science and Engineering, Michigan Technological University, Houghton, MI, USA

e-mail: pabadi@mtu.edu

the negative remodeling events post-MI [6]. However, long-term use of drugs can have side effects and excessive costs. Surgical interventions can be also dangerous [7–9]. Cell therapy is an alternative approach that consists of injecting a bolus of cells intravenously, so they can home to the site of injury and become engrafted to replace damaged cells or exert therapeutic paracrine effects to retrieve the functions of stunned or hibernated CMs in the pre-infarcted area of myocardium [10–13]. This approach can be efficacious with cell types such as human umbilical vein endothelial cells (HUVECs) or bone marrow derived mesenchymal stem cells (MSCs), since these cells can be obtained from patients, have limited but clinically relevant expansion capacity *in vitro*, and have been shown to engraft at the injury site [14, 15]. Cell therapy has a high potential for regeneration of post-MI ischemic damage to the myocardium. However, due to the notoriously low renewal capacity of adult CMs, producing clinically relevant numbers of mature adult CMs is difficult. Thus, conventional cell therapy approaches have been thwarted, because of the inability of adult CMs to remain mature *in vitro* while undergoing expansion [16]. Under culture conditions where CMs remain mature, they remain viable only a few days, and under conditions where they proliferate and expand, they become immature [17, 18].

Because of the senescent nature of adult human CMs, researchers have turned to utilizing various stem cell types which can be expanded and then differentiated into CMs. The main stem cell types proposed for use in regenerative medicine are human embryonic stem cells (hESCs), human induced pluripotent stem cells (hiPSCs), and MSCs [19, 20]. hESCs once held a great promise as a source of species-specific biological cells which could be differentiated into adult cell types for regenerative therapy. The failures of this technology have since been evidenced due to ethical controversies, risk of immune rejection, immature phenotype resembling CMs of the primary heart tube, and tumor formation [21–23]. Unlike hESCs, patient-specific cells such as iPSCs and MSCs can partially avoid immune rejection and ethical controversies, as we can extract the cells from the patients and create patient-specific CMs [24–26]. Although these patient-specific CMs provided better opportunities to reduce the cardiac scar size, one of their main issues is the immature nature of the differentiated cells. Maturation of patient-specific CMs to a particular lineage cannot be achieved without providing stem cell or early stage differentiated CM cues on multiple spatial scales, from the molecular and nanoscale to the microscale [27–29]. Therefore, the field of tissue engineering (TE) has sought sources of patient-specific cells which can be engineered with spatiotemporal cues on the nanoscale. The nanoscale is the spatial domain of biological information and molecular recognition, thus giving the cells the ability to be expanded in a coordinated manner, and finally to mature into functional adult cells [30].

Two of the major candidate cell types currently carrying the most promise for cardiac TE are patient-specific human iPSCs and MSCs. In recent years it has become evident that each cell source carries drawbacks and advantages. Adult multipotent stem cells, such as MSCs, and progenitor cells have a capacity to differentiate into mature cardiac cell types; however limited self-renewal and potential for expansion remain a major hurdle [31]. iPSCs, obtained from patient cells such as skin or immune cells, can be reprogrammed to the pluripotent state and exhibit unlimited self-renewal. The reprogrammed cells display the capacity for *in vitro* expansion to

therapeutically relevant cell numbers and the ability to differentiate into immune-compatible CMs [32, 33]. The major drawbacks of iPSC-derived CMs include the immaturity of the resultant CMs, batch-to-batch variations, and lack of reproducibility [16, 34, 35]. The immaturity can cause low functionality, teratoma formation, arrhythmia, and low cardiac regenerative capacity [16, 34, 35].

The immature phenotype of iPSC-derived CMs produced from various biochemical cocktails (typically modulating the Wnt and TGF- β signaling pathways), using traditional culture materials, include microscopic details such as pleomorphic morphology, nanoscopic details such as disorganized, smaller sarcomeres, and clustered mitochondria, as well as molecular level Ca⁺⁺ transport isotropy. This is in contrast to the cylindrical adult CMs with aligned, larger sarcomeres, distributed mitochondria, and directional Ca⁺⁺ signaling [16, 36–38]. In addition, current methods of injecting a CM bolus for heart regeneration result in low retention and engraftment rates, lower than 10% in mice models [39]. Such a low survival percentage is due not solely to low engraftment but also to the immune reaction after the integration of the therapeutic cells into the tissue [40]. The idea that nanoenvironmental scaffolds which mimic the adult cardiac milieu can enhance iPSCs differentiation and maturation and serve as delivery platforms or enhancers for engraftment has been a major factor in the development of nanobiomaterials. In addition to iPSCs, human adult MSCs and CMs derived from animal models are being studied for their interactions with nanobiomaterials. As nanotechnology has advanced over the past few decades, with discoveries of new materials and methodologies, applications to TE have followed close behind.

Advances in Nanobiotechnology

The nanotechnology paradigm began in the 1960s, and the name was coined in the 1970s in connection with processing materials with nanometer accuracy [41]. The definition of nanotechnology is utilizing materials with one or more geometric dimensions smaller than 100 nm [42]. An alternative definition is, the building of materials from their atoms or molecules to suit an application (bottom-up nanotechnology), rather than devising applications based on a material's macroscopic property [43]. Since then, many nanomaterials have been discovered (e.g., buckyballs, carbon nanotubes, and graphene) and planned to be implemented in the field of TE beginning in the 2000s and cardiac TE within the past few years [44–47]. Aside from the discovery of new materials, in the past few decades, nanotechnological advances such as the manipulation of single molecules with atomic force microscopy (AFM), the deposition of nanoliter volumes of ink using nano three-dimensional (3D) printing, and improved methods for producing nanotopography (e.g., electrospinning, polymer-demixing, and colloidal lithography) have also led to a widespread interest and growth in nanobiotechnology for TE applications [48–50]. The main promise is to mimic the explosive growth in the electronics industry by controlling biological molecules on the smallest scales, a currently urgent initiative for cardiac TE considering the growing epidemic of heart disease in the younger populations of western countries [51, 52].

Utilization of biomaterials with nanoscale features and organized structures that can mimic natural biological structures on the smallest scales results in unique material properties unobtainable by mimicking gross morphological features of tissue or organs, alone. This is because incrementally changing the structure on a lower spatial scale can have nonlinear outcomes on material and biological properties, providing the possibility of mimicking diseased rather than healthy tissue nanostructure [53]. Therefore, the ubiquity of nanosurfaces in biological systems, such as the nanoscale domains of proteins responsible for molecular recognition, makes utilizing nanoscale approaches a necessity [30, 54]. In general, nanobiomaterials can create tissues with structures that mimic many physiological tissue characteristics including cell orientation, cell morphology, diffusion of gases/nutrients, extracellular matrix (ECM) topological structure, and mechanical/electrical properties [55–58].

The Heart at the Nanoscale

The heart is a complex three-dimensional organ with a multiscale structure consisting of CMs and supporting cell types and ECM. Cardiac muscle ECM has a role as both scaffold for the CMs to physically bind them into an organ unit and an intrinsic role in force transmission, CM mechanotransduction to control gene expression, propagation of electrical signals via inducing alignment of CM gap junctions, etc. [59, 60]. The collagenous matrix of the heart consists of the endomysium, a network weave-like structure wrapped around CMs, collagen struts connecting CMs, perimysium consisting of larger collagen fibrils, and the epimysium consisting of the largest and most ordered fibers [61]. This morphological multiscale structure is preserved among species and mechanical strength differences are mainly due to the concentration of collagen in the structure.

The importance of the cardiac ECM is highlighted by the finding that reversible ischemic CM injury results in structural changes to the collagenous network including uncoiling of fibers and discontinuities in the structure [62]. Such nano- and microscale differences between healthy and diseased ECM are important considerations in TE when the goal is either to model diseased tissue or engineer tissue replacements. For instance, the fractal dimension of liver tissue ECM as assessed by imaging software has been used to distinguish healthy from fibrotic tissue [63]. In addition to CMs, another important cell type are the Purkinje fibers and other cells which compose the conduction system of the heart and are also integrated with the nanoscale ECM into fractal-like networks [64]. These cells are responsible for propagating the electrical impulse of the Sino-atrial (SA) node and synchronizing CM contraction in a spatiotemporal manner [65]. With the discovery of conductive nanomaterials with various geometries similar to native cardiac ECM, this conduction system can also be mimicked with nanobiomaterial scaffolds that act as “artificial” Purkinje fibers to help synchronize CM electrical communication [66, 67]. Recent advances in TE have exploited the discovery of such materials to better mimic the properties of native heart tissue [56, 68].

While the actual arrangement of CMs, their connectivity, and the macroscopic structure of the heart have remained controversial, it is evident that the properties of functional heart tissue result from a unique microscopic structure that is ordered spatially down to the nanoscale. Therefore, a more physiologically functional tissue will result by taking this order into account [69, 70]. Little is known about how the nanoscale features of the heart relate to the structure and function at higher spatial scales, which is critically important for mimicking the natural structure of the heart, making the task of the cardiac tissue engineer even more difficult [71]. Despite this impediment, considerable progress has been made in the field of nanobiomaterials over the past few decades [72–74]. The increased understanding of cell signal transduction has integrated the nanoscale role of ECM and the physical nanoenvironment with biochemical signaling [75]. The central task of the cardiac tissue engineer is therefore to provide a nanoenvironment which induces proper biochemical/physical signal integration for producing a functionally mature cardiac tissue. This integration of signals will determine whether a stem cell becomes a mature CM and help the cardiac function.

The three main emerged strategies for nanoscale TE of cardiac tissue are the following: (i) creating nanoscale topography or patterns that guide cells into more mature morphological structures; (ii) using nanomaterials or composite scaffolds with conductive nanoenvironments; and (iii) utilizing nanoparticulate systems to engineer or deliver payloads to CMs.

Engineering Nanotopography of Cardiac Tissue Scaffolds

Perfectly smooth solid surfaces are rarely found in nature and are difficult to produce using current engineering techniques. Most surfaces even with fabrication techniques designed to reduce surface heterogeneities will have some degree of nano- or atomic scale heterogeneity, and on most engineered topographies, there will be multiscale features (Fig. 5.1d) [76, 77]. The biological influences of such surface nanoscale topographies are relevant to TE and can be utilized to mimic the natural ECM and control cell behavior through contact guidance in cardiac TE applications. Creating nanofibrous surfaces (Fig. 5.1a) and nanoscale surface structures such as tubes and pillars (Fig. 5.1b) and grooves (Fig. 5.1c) are some of the methods for engineering nanotopography of surfaces and systematically studying its effect on cardiac tissue regeneration.

The field of contact guidance probably first began with the culture of cells on spider webs during the early twentieth century where it was noted that cells aligned along the length of the fibers [78]. From the 1960s forward, the realization that surface topography and gradients control cell behavior gradually developed [79–81]. The cell cytoskeleton must be specifically oriented in space for proper signaling and maturation to ensue and cells will tend to align along structures of minimal curvature to prevent cytoskeletal deformation [82]. The creation of nanotopographical cues on a biomaterial surface is the extension of contact guidance down to the nanoscale motivated by biomimicry of the natural ECM. In

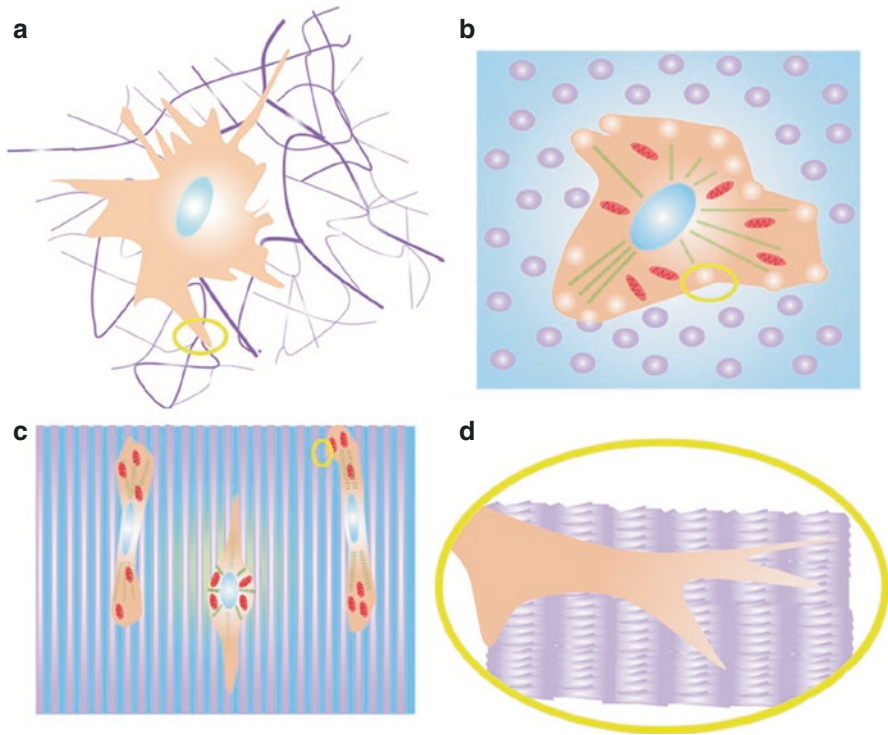


Fig. 5.1 (a) Schematic representation of CM cultured on nanofibrous scaffold where cell pseudo-pods are aligning along the fibers. (b) Schematic representation of CM cultured on nanostructure, showing alignment of cytoskeletal structures (sarcomeres are green mitochondria are dark red) with the topography. (c) Schematic representation of CM alignment on nanogrooves showing parallel alignment and spreading of CMs and cytoskeletal structures. (d) Magnified view (from yellow circles in a–c) of cells on nanostructures showing the features of topography interacting with cell membrane. Feature sizes are not to scale

this section, recent advances in nanotopographical strategies for biomimicry of heart ECM and cardiac TE will be discussed.

Nanofibrous Scaffolds

One of the most widely used strategies for mimicking natural cardiac ECM topography on the nanoscale is the creation of nanofibrous scaffolds using electrospinning of polymers or other fabrication techniques [83]. Such scaffolds can be fabricated with varying degrees of fiber orientation/alignment, porosity or space-filling character, and surface properties/hydrophilicity [84, 85]. The motivation for using this strategy is to mimic the complex multiscale fibrous network of the cardiac ECM. The main objective is to create nanotopographic cues on the scaffold surface to use contact guidance to control CM maturation. This includes focal adhesion

formation, CM aspect ratio, ion channel gene expression, and cytoskeletal arrangement [86–88]. In addition, stem cell differentiation can be directly influenced by topography via mechanotransduction mediated by focal adhesion kinase [89].

Given the goal of creating as realistic and natural a scaffold as possible, one natural choice for a fibrous TE cardiac scaffold is an injectable form of the decellularized cardiac ECM which can reassemble *in vivo* after injecting [90]. Such a scaffold presents not only native nanofibrous topography but also the solid phase protein molecular recognition sites (typically 50 nm² or less) of the native cardiac milieu [30]. This strategy was used to compare fetal and adult bovine cardiac ECM as a 3D scaffold for CMs which naturally have organized, periodic nanoscale cell-recognition sites in the gel molecular backbone [88]. hiPSC derived CMs were seeded onto two-dimensional (2D) layers or in 3D gels composed of the decellularized and digested scaffold proteins. Initial studies prior to digestion showed that adult ECM had more organized bundles of ECM proteins whereas fetal ECM was more disorganized. The 3D gels led to mature CM gene expression relative to 2D layers as determined via quantitative polymerase chain reaction (qPCR) with multifold enhanced expression of mature cytoskeletal, cell adhesion, and Ca⁺⁺ handling and other ion channel genes, including Kir2.1, an ion channel with higher expression in mature CM, thought to prevent arrhythmia [91]. In addition, adult ECM had greater positive influence than fetal ECM on CM maturity.

While reconstituted natural ECM intrinsically carries the molecular recognition sites of the native myocardium, the methods for decellularization and processing create variability in mechanical properties and biocompatibility. To gain more engineering control over TE scaffold creation, synthetic polymers can also be used to fabricate biomimetic nanofibrous scaffolds [92]. Poly (lactic-glycolic acid) (PLGA) is one of the most common biodegradable TE materials which can also be used for nanofibrous scaffold creation via electrospinning [93]. Aligned PLGA nanofibrous scaffolds coated with gelatin were used for the maturation of hiPSC derived CMs. Resultant CMs were aligned with PLGA nanofibers via contact guidance relative to flat, smooth culture plates which was observed in scanning electron microscopic images (Fig. 5.2a). Sarcomeres were larger on the PLGA scaffold, closer to the size of native sarcomeres (~ 2 μm) than on flat surfaces and mitochondria were also aligned with the fibers showing more dense cristae. The rate of beating of CMs on the aligned structures was also approximately 50% higher than on a traditional, flat culture surface.

Electrospun polyurethane (PU) scaffolds have also been fabricated as scaffolds for mouse ESCs differentiation to CMs [96]. PU is a copolymer consisting of polyol, diisocyanate, and chain extender which self-organize into micro- and nanoscopic hard (diisocyanate and chain extender) and soft segment (polyol) [97]. Polycaprolactone diol (PCL) soft segment with a lysine-based diisocyanate and phenyl-alanine-based chain extender was used to create biodegradable electrospun PU. Such scaffolds could be spun with diameters ranging from hundreds of nm to μm; however, the multiscale hard/soft segment morphology can add another layer of nano- and microscopic complexity with incompletely known effects on protein adsorption and cell adhesion [98, 99]. Mouse ESCs could be differentiated to

CMs on these scaffolds with improved maturation characteristics on scaffolds with aligned fibers relative to those with more random orientation.

Surface Nanostructures

A second form of nanotopography which can give spatial control over the cues presented to CMs is creating nanogrooves or nanopillars on the substrate surface which can have varying diameter and separation [100, 101]. These controlled nanotopographies can be used to study fundamental mechanisms of cell interaction

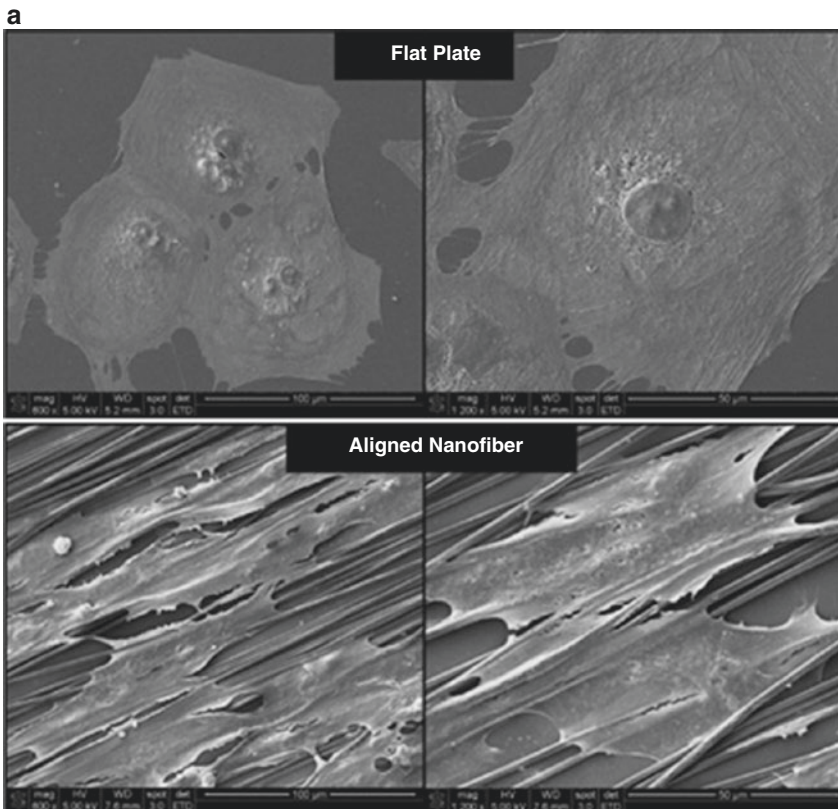


Fig. 5.2 Engineering nanotopography for Cardiac TE scaffolds: (a) SEM images of CMs on flat surfaces (top) and nanofibrous PLGA scaffolds (bottom), showing distinct alignment of CMs on nanofibers by contact guidance (Reprinted with permission from [93]). (b) CMs cultured on nanogrooves of varying geometry stained for α -actinin and F-actin (Reprinted with permission from [94]). Copyright 2016 American Chemical Society). (c) iPSC-CM on flat, 2D cell-imprinted, and multiscale cell-imprinted PDMS surfaces showing beating analysis in the insets. (d) qPCR analysis of CMs on various patterned PDMS substrates where multiscale imprinted PDMS had the highest expression of cardiac markers (c and d reprinted with permission from [95]). Copyright 2018 WILEY-VCH Verlag GmbH & Co. KGaA, Weinheim)

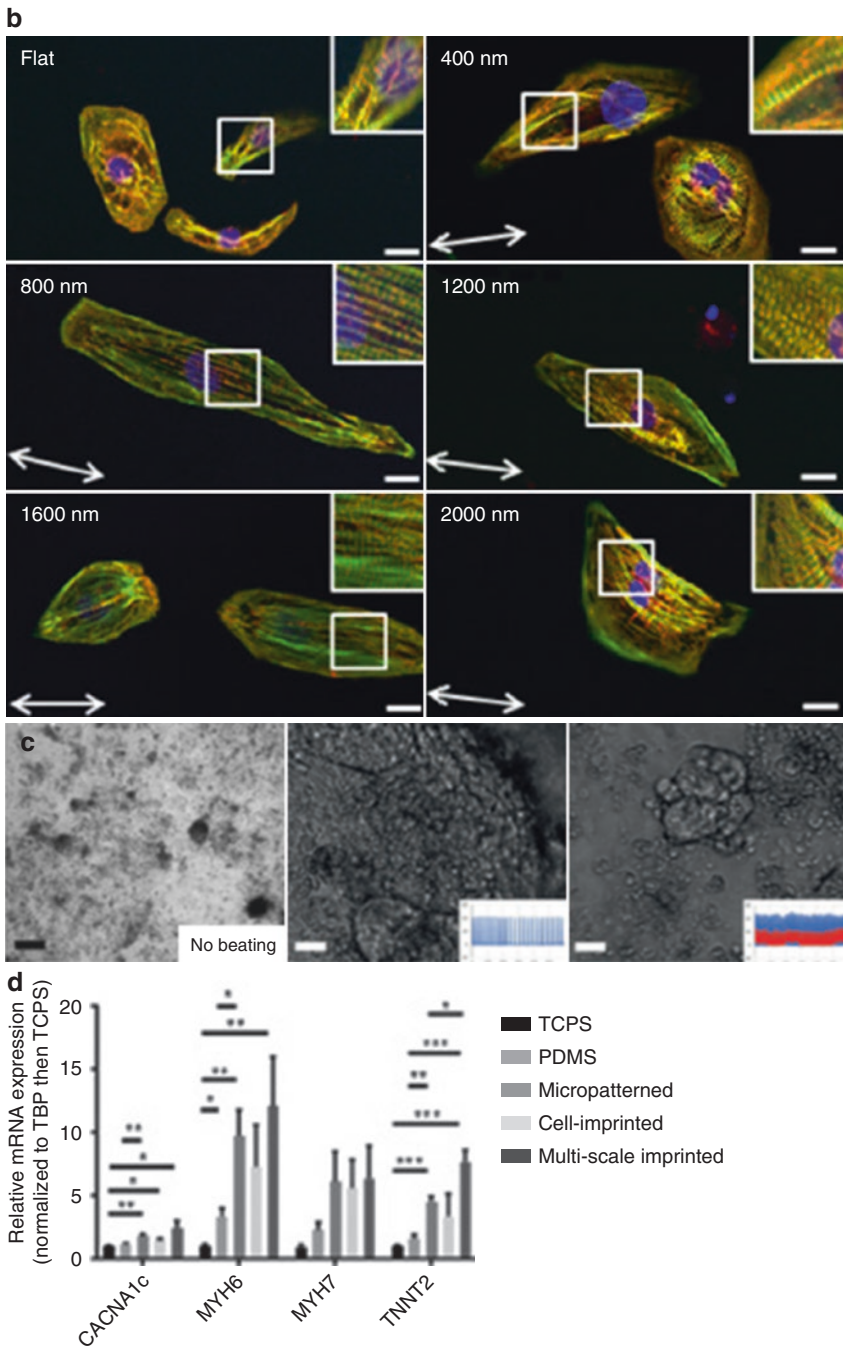


Fig. 5.2 (continued)

with topographies of different dimensions and geometries [86]. One such strategy utilized poly(ethylene glycol) (PEG) diacrylate-based aligned nanofibers formed with surface nanogrooves as scaffolds developed from a UV cross-linking capillary molding technique [27]. The groove/ridge width was 150/50–800/800 and the depth of grooves was 200–500 nm in height. The hydrophilic nature of PEG creates a high water content scaffold with aligned fibers similar in diameter to native collagen. Neonatal rat ventricular CMs were used to create highly aligned beating cardiac monolayers. Cell cytoskeletal proteins such as sarcomeric α -actinin and F-actin are also highly aligned on such nanotopographic surfaces relative to control unpatterned surfaces.

The creation of nanogrooved surfaces has also been combined with variation of substrate stiffness to examine the important influence of the deformability of the nanostructured surfaces using photolithography techniques [102]. PU and polystyrene nanogrooved surfaces were fabricated to compare nanotopographical surfaces with differential stiffness. Rat CMs were cultured on engineered substrates. The surface nanogrooves of 100 or 350 nm depth controlled the cell alignment, regardless of surface stiffness, with 350 nm giving greater alignment than 100 nm grooves. However, CM contractility differed between PU (softer, ~ 4 MPa) and polystyrene (stiffer, ~ 2 GPa) and synchronous contractility was longer maintained on the former, indicating that the stiffness of topographical features is also an important parameter. When human ESCs were differentiated on poly (acrylamide) gels of variable stiffness, expression of Brachyury (a marker of mesendodermal fate) on day 1 peaked on gels of intermediate stiffness, which also lead to the highest expression of Troponin T expressing CM [103]. However the impact was less significant if differentiation was initiated on TCP, to the point of cardiac progenitor stage, and subsequently transferred to substrates of variable stiffness.

Nanogrooves imprinted in PU-acrylate (PUA) with self-assembled (due to a PUA binding domain) chimeric peptides promoted cell adhesion [94]. Various groove/ridge widths were fabricated from a few hundred nm to 2 μm , all of which had uniform adhesion of hiPSC derived CMs after coating with the peptide. Each nanogroove substrate enhanced CM morphological anisotropy. The 800 nm grooves resulted in greatest cell-spread area as demonstrated by immunofluorescent staining of α -actinin and F-actin (Fig. 5.2b).

Creating shapes other than grooves, such as nanopillars, has also been recently achieved using a UV-curable PEG derivative [100]. The tapered pillars, created by capillary lithography were ~ 100 nm wide and a few hundred nm in height. Rat CMs were seeded on the nanopillar substrate and observed by environmental scanning electron microscopy (ESEM) to be migrating across PEG pillars, causing them to bend. Due to the non-fouling characteristics of PEG, cell adhesion was restricted and ephemeral. The posts, however, could be used to study the dynamics of cell focal adhesions on nanopillars. Immunofluorescence studies revealed that cytoskeletal filaments were aligned with the underlying PEG nanopillars.

Molecular and Cellular Imprinting

Molecular imprinting has also emerged as a rising strategy for TE including cardiac regenerative medicine. Molecular imprinting began in the 1930s, when it was discovered that silica gelled in the presence of a specific molecule will have increased selective adsorption of the molecule [104]. In general, the method usually consists of curing a cross-linkable polymer on a molecular template and subsequently removing the template to obtain geometrically defined cavities which mimic binding sites of the molecular template [105]. Importantly, the cavities will have complementary binding sights (lock-and-key type specificity) and chemical recognition of the template species. In this way, molecularly imprinted surfaces can act as “artificial antibodies.” Molecular imprinting has been used for separation/sorting systems, bio sensing, drug delivery, and catalysis [105]. Recently, this methodology has been extended to the imprinting of bacterial and mammalian cells for selective adsorption or adhesion [106]. Cardiac applications for molecular imprinting include templated polymers to detect cardiac troponin T and myoglobin, while previous cell imprinting applications included the imprinting of mature CMs for iPSC differentiation as well as mature chondrocytes and keratinocytes for MSC differentiation [95, 106–109].

Cells in different 2D or 3D microenvironments can be imprinted to achieve different results. One photolithographic method created cell-imprinted surfaces with multiscale topography by seeding primary human CMs on a 3D semicylindrical micro-molded poly(dimethyl siloxane) (PDMS) surface with a pattern aspect ratio similar to *in vivo* CM morphology. PDMS was poured over adult primary human CMs, aligned within the 3D patterns, and cured to create a mold of the mature cells with topography at the μm and sub- μm level, which could be used as a substrate for the differentiation of iPSCs to CMs. In addition to the asymmetrical microscale mature cell-shaped pattern, the nanoscale topography of the adhesion molecules of primary human CM was used as complementary binding sights for the iPSCs throughout their differentiation to CMs. CMs produced on these substrates started beating earlier, showed enhanced expression of cardiac markers, and mature calcium handling characteristics relative to traditional culturing surfaces. Contractile function of CMs was analyzed at day 16 of differentiation on multiscale imprinted PDMS, and was compared with CMs generated on tissue culture plastic (TCP), showing no beating (Fig. 5.2c). QPCR data (Fig. 5.2d) showed highest expression of cardiac markers on multiscale CM imprinted PDMS compared to TCP, micropatterned PDMS, or PDMS imprinted by adult primary human CMs on 2D surfaces.

Conductive Nanomaterials

Over the past few decades, the discovery of graphene and the earlier discovery of carbon nanotubes have led to an explosion in research in conductive materials that is predicted to revolutionize the electronics industry [110]. This excitement has fueled a parallel interest in the field of nanobiomaterials. The reason for this interest is the

concept of engineering a tissue on the nanoscale that can mimic the complex electrical activity and signal propagation of the native heart [65, 111]. Materials such as graphene, carbon nanotubes (CNTs), gold nanorods, and silver nanoparticles have become routinely used fillers or as pure materials in scaffold design [112–120]. Such materials have a niche in cardiac TE due to the need for CMs to propagate electrical signals to synchronize cell-cell communication (in the absence of a native conduction system). There is also need for conductive tissue elements to interface with a patient's heart tissue for TE cardiac grafts [121]. This strategy is becoming popular due to the high electrical impedance of most traditional cross-linkable materials used for TE purposes, such as hydrogels and various synthetic polymers which can interfere with the conduction velocity of engineered CM tissues.

Spherical Conductive Nanomaterials

Spherical conductive nanoparticles have been incorporated in biomaterials for different applications such as creating scaffolds with actuation, with antibiotic properties, or with reduced impedance to enhance CM cell-cell communication [122, 123]. They are typically incorporated into a fibrous matrix or a hydrogel material [115]. One study used gold nanoparticles (AuNPs) combined with an autologous ECM matrix to create conductive immune-compatible scaffolds which can be used with patient-specific cells. AuNPs were decorated on the scaffolds by e-beam evaporation. Cardiac patches were made by seeding neonatal rat CM on Au-coated ECM. These scaffolds could maintain the population of CMs, against being overpopulated by fibroblasts, relative to control non-conductive scaffolds. Additionally, the Au-coated ECM resulted in greater contractile forces and lower excitation threshold for induced contraction by external electrical stimuli. Ca^{++} transients on scaffolds decorated with 4 and 10 nm AuNPs were two to threefold greater than that on pristine ECM, demonstrating an overall more mature electrophysiological behavior. The cytoskeletal alignment and organization of CX-43 also increased with increasing AuNP concentration (Fig. 5.3a).

Silver (Ag) nanoparticles have attracted attention due to their antimicrobial and possible anti-inflammatory effects [126, 127]. One method of producing a natural conductive ECM is to use collagen protected with nano-Ag for electrospinning, which can produce electrical conductivity at low μmolar Ag concentration [128]. The Ag nanoparticles were added to the collagen solution prior to electrospinning followed by a glutaraldehyde cross-linking process [129]. Neonatal rat CMs were plated on the Ag containing scaffolds and controls with no Ag. After electrical pacing, the CMs on the Ag-containing scaffolds exhibited greater expression of gap junction protein CX-43 and protein Ki67 (a marker of proliferation) compared to control collagen fibers. The Ki67 expression increase may have been due to increased survival and growth of the neonatal CMs. In addition,

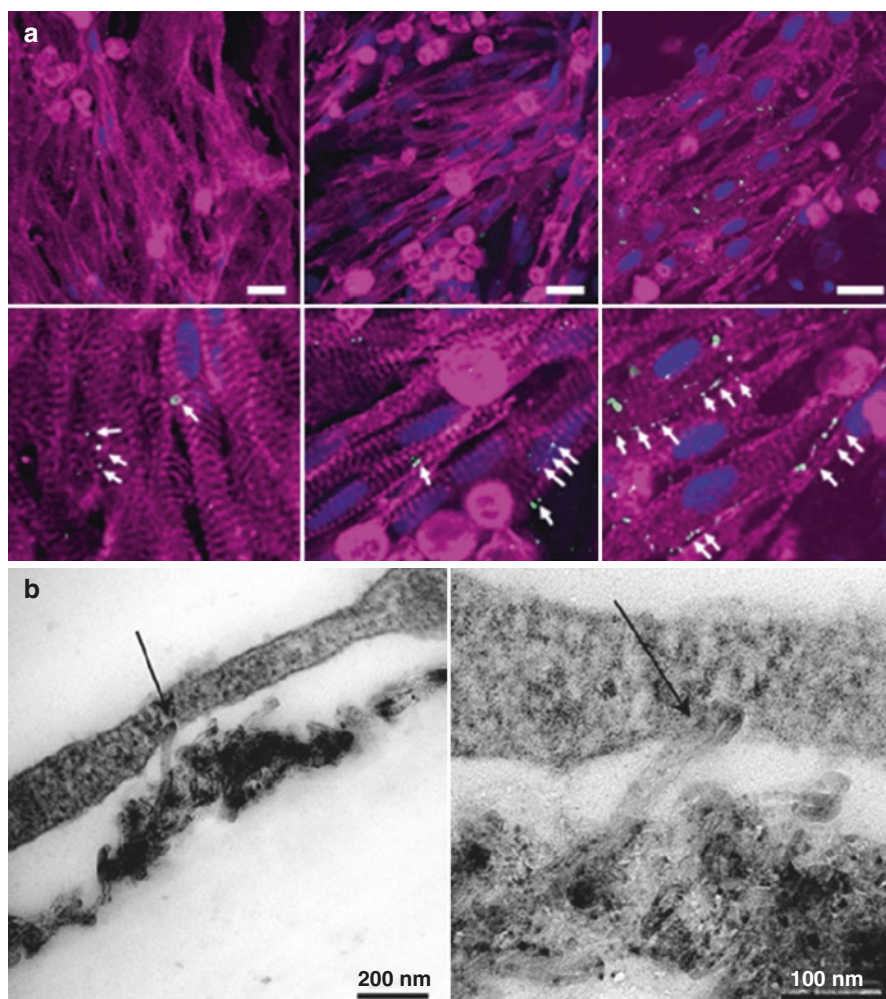


Fig. 5.3 Conductive nanomaterial strategies: (a) immunofluorescent staining of α -actinin and CX-43 on pristine (left), 4 nm AuNP (center), and 10 nm AuNP (right). Arrows point to CX-43 fluorescence (Reprinted with permission from [122]. Copyright 2014 American Chemical Society). (b) TEM images showing the close approximation between CM membrane and CNT substrate creating electrical shortcuts (Reprinted with permission from [124]. Copyright 2013 American Chemical Society). (c) α -actinin staining of CMs on control culture dish (left) and graphene substrates (right), showing sarcomere length is significantly greater on graphene substrates (Reprinted with permission from [125]. Copyright 2017 American Chemical Society). (d) SEM of CNT-Gel-MA networks showing fractal-like structure of CNTs (left) and CNT-Gel-MA supporting adherent CMs as free-floating bioactuator, capable of spontaneous movement in suspension (Reprinted with permission from [47]. Copyright 2013 American Chemical Society)

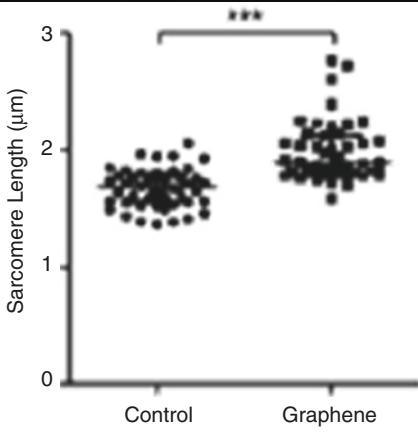
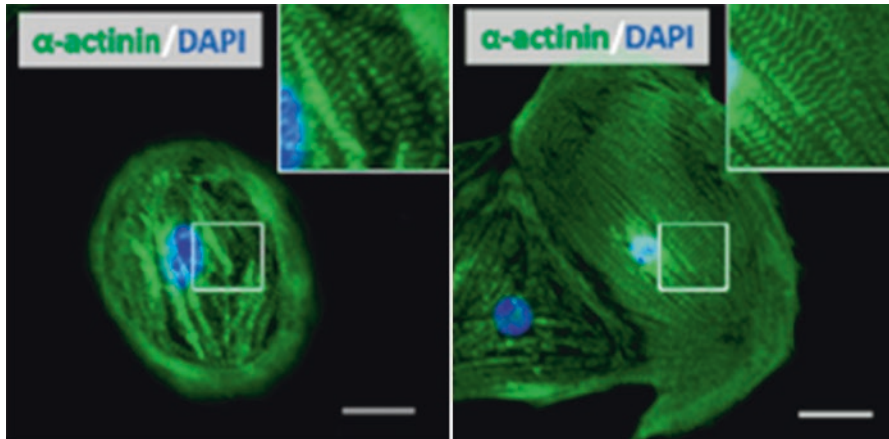


Fig. 5.3 (continued)

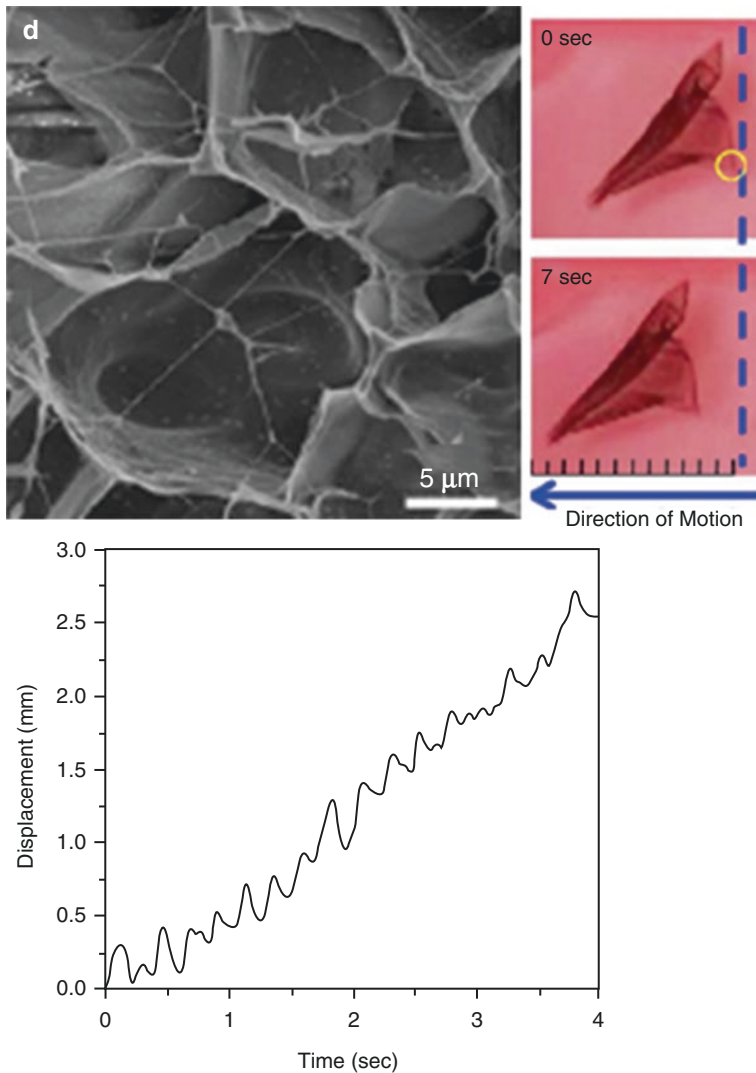


Fig. 5.3 (continued)

antibacterial properties of Ag nanofiber scaffolds were evident by the ability to prevent *Pseudomonas aeruginosa* biofilm formation [130, 131].

High-Aspect Ratio Conductive Nanomaterials

Conductive one-dimensional (1D) or 2D nanomaterials with high aspect ratios have recently been used as substrates for CM maturation or iPSC differentiation to CM. For 1D materials, CMs were matured on CNT layers attached to glass [124,

132]. Since CNTs do not passively bind with glass, they were first functionalized using 1,3-dipolar cycloaddition of azomethine ylides [133]. They can then form 100 to 200 nm films on the glass and be defunctionalized by heating under N₂ resulting in a layer of pristine CNTs. Transmission electron microscopic (TEM) images showed that rat ventricular CM membranes had close approximation to CNT bundles that were periodically distributed over the basal surface (Fig. 5.3b). CMs also had greater proliferative capacity on CNTs than control gelatin films, while fibroblasts had no proliferative advantage on CNTs versus gelatin. Smooth conductive control surfaces such as amorphous carbon and indium tin oxide were also compared and did not demonstrate the enhanced proliferative effect on CMs; however fibroblast proliferation rate on those surfaces was slightly increased. In addition to this enhanced proliferative effect, CMs on CNTs exerted more negative action potentials and higher probability of firing an action potential relative to CMs on control surfaces.

To study 2D materials, both hESCs and hiPSCs were differentiated to CMs on 2D graphene substrates [125, 134]. hiPSCs were differentiated by small molecule modulators of Wnt signaling pathway while hESCs were differentiated by removing fibroblast growth factor from the medium and adding fetal bovine serum. Both cell types showed increased expression of cardiac markers and hiPSCs had increased alignment of sarcomeres as shown by α -actinin staining (Fig. 5.3c) and larger mitochondria that were aligned with myofibril bundles. The hESCs had higher early expression of cardiac mesodermal gene MESP1, higher SOX 17, similar ectodermal genes, and higher later expression of CX-43, NKX2.5, cardiac and troponin T, indicating a promotion of mesodermal and eventually cardiac mesodermal fate. However, beating CMs were not observed in the absence of small molecule inhibitors or cytokines typically used for CM differentiation, indicating that graphene alone, promoted cardiac differentiation but not complete maturation. Graphene was also shown to enhance BMP4 signaling in hiPSCs relative to oxidized graphene, showing a direct role of substrate conductivity in cardiac differentiation. This is despite the fact that CMs on smooth conductive surfaces (such as amorphous carbon) did not have enhanced maturation, demonstrating that scaffold conductivity and nanostructure can have diverse pathways in affecting cell function [124].

One of the most popular strategies for creating conductive TE substrates is mixing a natural hydrogel material with conductive nanomaterials. One of the major drawbacks using 3D nanomaterials such as spherical particles is the high filler concentration required to achieve percolation and highly reduced impedance [135]. The obvious drawbacks to such high nanofiller concentrations for biomedical applications are the high cost of nanomaterial as well as the release of nanomaterials which can interface with cells in vitro or tissues in vivo, in an uncontrolled manner. Substituting 1D or 2D conductive nanomaterials with high aspect ratios can substantially reduce the percolation threshold for nanomaterial concentration, allowing for conductive composites with reduced risk of particle accumulation in the system. One of the early trials utilized gold nanowires, mixed with alginate, to create electrical connectivity between CMs via mechanically and electrically connecting the individual pores containing CMs [121]. The resultant neonatal rat heart cells

demonstrated increased alignment and expression of cardiac markers. It was suggested that such engineered tissues could be used as a regenerative cardiac patch that will be degraded and replaced with natural ECM with the exception of the gold-nanowires.

This strategy was subsequently extended to other ECM molecules containing a variety of nanomaterials with high aspect ratios (1D or 2D nanomaterials), which are a preferred filler due to the lower concentration percolation threshold, minimizing the amount of nanomaterial in the system. For instance, CNTs were used with a gelatin methacrylate (Gel-MA)-based scaffold for maturation of rat neonatal CMs [47]. Gel-Ma is a UV-curable gelatin derivative that can be mixed with CNTs and cured to form a composite hydrogel. SEM images of dried Gel-MA laden with CNTs revealed nanotube networks had a morphology reminiscent of Purkinje fiber networks in the heart (Fig. 5.3d). Gel-MA-CNT scaffolds, fabricated at $\sim 50 \mu\text{m}$ thickness, showed enhanced expression of cardiac proteins as well as enhanced alignment, lower excitation threshold, and more synchronous CM beating behavior. In addition, the scaffold exerted a protective effect against free radicals, possibly due to absorption via the CNTs. The engineered tissue could then be released from the substrate to form a spontaneously beating, floating bioactuator (Fig. 5.3d). This strategy was later extended to create biomimetic swimming bioactuators utilizing the Gel-MA-CNT-based CM sheets as the actuator in the shape of a batoid fish [136].

Conductive nanomaterial culture substrates can also be used for purposes other than contact guidance or maturation/differentiation of cells. In one case, a platinum nanopillar electrode array was fabricated using photolithographic methods for the purpose of culturing hiPSC and hESC-derived CMs and having the ability to measure action potentials in a more efficient, high throughput manner than traditional patch-clamp techniques [137]. The fabricated nanopillars were 200 nm in diameter and 1.5 μm in height and the surface of the substrate was electrically insulated to isolate the signal of the nanopillar electrodes. The nanopillars created nanoholes in the CMs via electroporation prior to measuring action potentials. The potential recording from the nanoelectrode array was compared with that obtained from traditional patch-clamp technique, showing that action potential shape was of different amplitude but identical shape. The array was also capable of determining CM subpopulation, determining what percentage of CMs were atrial, ventricular, or pacemaker types. This system was also able to differentiate between normal CMs versus those with long QT syndrome.

Engineering Nanocarriers for Cardiac Tissue Repair

Using nanoparticles to deliver molecules and engineer tissues is another nanobiotechnological strategy where rapid progress has been made. The basic concept involves encapsulating delivery agents inside colloidal scale matter with variable dimensions and geometry, which can be made to protect the payload until it reaches the desired location in the body. Such targeted delivery in which collateral damage

is completely avoided is called a “magic bullet” and is often considered the *holy-grail* of nanomedicine and has been increasingly used in cardiac TE [138, 139].

Therapeutic payloads such as interleukin 10 (IL-10) have recently been used inside blends of biodegradable poly(D-lactic acid) (PLA) and PLGA to target cell types that form coronary atherosclerotic plaques [140]. A targeting polymer consisting of PLGA, PEG, and collagen IV (PLGA-PEG-Col-IV) was mixed into the blends at a small percentage to impart the specificity of the nanoparticle. The basic concept is to target collagen IV basement membrane protein, which will be exposed due to injury/inflammation at the site [141]. These particles were capable of reducing reactive oxygen species of macrophages in vitro by ~30–60%. Additionally, in a mouse model of atherosclerosis, the fibrous cap thickness could be increased, while the necrotic area of the plaque was reduced (Fig. 5.4a).

Decorating cell surfaces with nanoparticles, which can then control cell binding behavior or be internalized by the cells stimulating signaling cascades, is another engineering strategy which has been developed [142, 144]. In one case, iron oxide nanoparticles were used for increasing the expression of CX-43 in cardiomyoblasts, with inherently low CX-43 expression, to enhance therapeutic efficacy and cell-cell communication [142]. Iron oxide nanocubes were the particle chosen for this study, due to their higher colloidal stability and magnetization. Particles are internalized by the cardiomyoblasts after exposure with endosomal localization, which partially ionizes them due to the lower pH. These iron ions caused JNK-mediated CX-43 expression. To examine the influence of this increased gap junction protein expression cardiomyoblasts were cultured with MSCs (cMSCs) after taking up two dyes, one of which can pass through gap junctions (Calcein-AM). After 48 hours, more MSCs had calcein AM when plated with iron oxide nanoparticle containing cardiomyoblasts than those plated with control cardiomyoblasts (Fig. 5.4b). The MSCs were then sorted from the cardiomyoblasts, and those which had communicated with iron oxide containing cardiomyoblasts had greater expression of cardiac genes. The results of the injection of iron oxide nanocube treated MSCs versus control groups in a model of rat ventricular infarction were then examined histologically (Fig. 5.4c). The extent of collagenous remodeling and blue-colored fibrotic scar tissue formation was reduced in the treatment groups versus control MSCs.

Magnetotactic bacteria (MB) are another naturally occurring nanobiomaterial that have recently gained attention. MB are bacteria that naturally synthesize magnetic nanoparticles at density sufficient to allow their alignment with the Earth’s magnetic field. They were examined as a contrast agent for cardiac TE by infecting CMs with the non-pathologic bacteria (commercially available “Magnelles®”) [143]. The nanoparticles inside the bacteria were visible in TEM images and by immunofluorescence (within CM cytoplasm, Fig. 5.4d). CMs could then be injected in a mouse model and their magnetic resonance imaging could be compared with that of cells injected after decoration with iron oxide particles. The iron oxide particles tend to remain in the tissue even after cell death while the MB are present only with living cells, giving a more objective determination of the engraftment efficiency.

Cardiac hypertrophy is another variant of heart disease caused by adaptation of the heart to pathological mechanical stress levels caused by various conditions. Its uncontrolled progression can lead to heart attack or death. An endogenous peptide, apelin, with a short plasma half-life and incompletely known function was recently encapsulated in liposomal nanocarriers with PEG surface decoration for use in a model of cardiac hypertrophy [145]. Previous studies had shown that loss

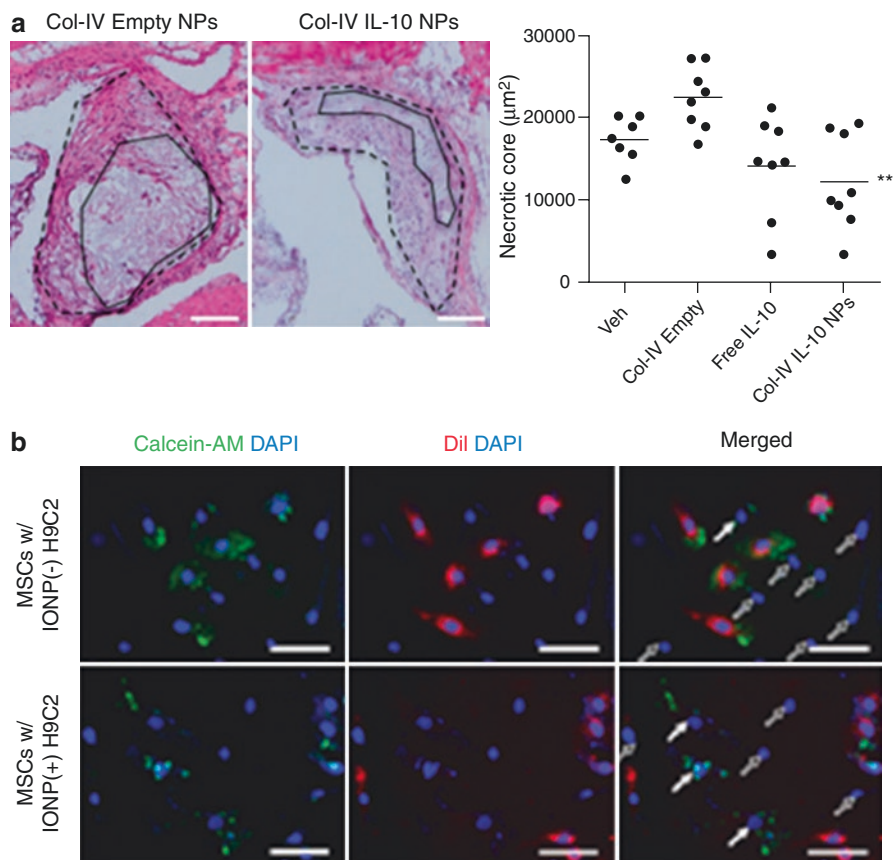


Fig. 5.4 Engineering Nanocarriers for Cardiac Tissue Repair: **(a)** Histological slices of sacrificed mouse heart with H&E staining comparing size of necrotic core between treatment and control groups where necrotic core was substantially reduced for targeted IL-10 containing NPs (Reprinted with permission from [140]. Copyright 2016 American Chemical Society). **(b)** 48 hours after staining cardiomyoblasts in coculture with MSCs, having green but no red dye denotes MSCs with gap junction crosstalk, while having DAPI but no stain denotes MSCs with no gap junction crosstalk. **(c)** Histological sections of rat heart 2 weeks after treatment with MSCs, stained with Masson's trichrome stain to assess the extent of collagenous fibrous tissue formation **(b** and **c** reprinted with permission from [142]. Copyright 2015 American Chemical Society). **(d)** TEM images of magnetotactic bacteria showing the synthesized magnetic nanoparticles (top) and immunofluorescence showing the Magnellex® (red) inside CMs (Reprinted with permission from [143])

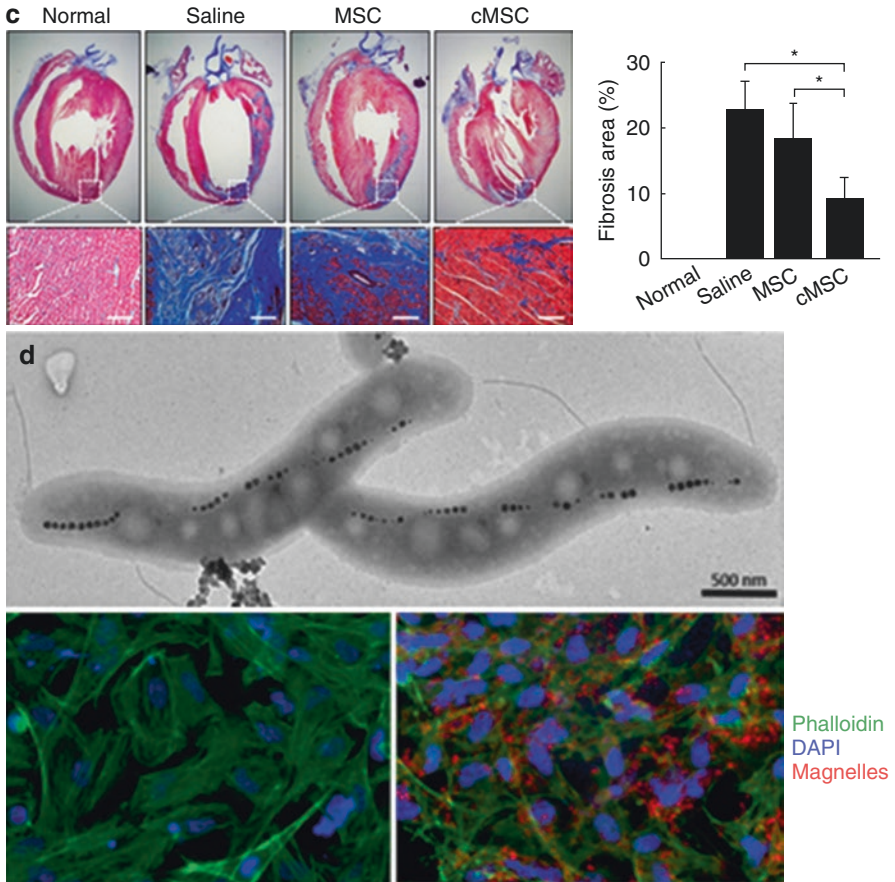


Fig. 5.4 (continued)

of function of the peptide or its receptor is associated with cardiovascular diseases [146, 147]. Specifically [Pyr 1]-apelin-13 was used in a transverse aortic constriction mouse model. The nanoencapsulated apelin (lipoPEG-PA13) was compared with direct administration of PA13 and saline injection. LipoPEG-PA13 attenuated the adaptive hypertrophic response compared to the two control groups and resulted in a sustainably elevated level of plasma PA13 up to 6 days post injection [148]. The extent of fibrotic scar tissue was also significantly less with the nanoencapsulated peptide relative to the free peptide, demonstrating the controlled and sustainable release which could overcome the short plasma half-life of the peptide.

Future Outlook

Top-down strategies for cardiac TE, such as decellularized heart tissue, are popular and plausible strategies to utilize the native architecture of the heart, in the absence of fundamental principles for engineering cardiac tissues [149]. However gaining

more engineering and manufacturing control and avoiding immunogenicity issues have led to the continuous search for bottom-up engineering strategies. A greater understanding of fundamental mechanisms of cell interactions with nanofeatures and assessment of in vivo performance of the nanomaterials will be required to advance the nanobiomaterial technologies. This knowledge could particularly accelerate the use of nanomaterials for obtaining sufficient quantities of patient-specific mature CMs. In vitro experiments typically use purified proteins to coat scaffold surfaces and defined cell culture medium. These strategies can work for producing CMs in vitro, but would not be able to predict the fate of CMs or nanostructured grafts in vivo, where they will be exposed to a complex mixture of thousands of plasma proteins and many cell types. Upon administration in vivo and exposure to the blood, nanostructured materials will be spontaneously coated with protein corona [150]. Recent studies suggest that the biological identity of this corona may change based on patient disease phenotype [151, 152]. An increased emphasis on realistic nanosystems with biomimetic structures that examine more faithful conditions will move the field of cardiac nanobiomaterials closer to a stage of viability and ubiquity.

Despite the significant progress in using various nanobiomaterials in cardiovascular TE applications, the clinical use of such material systems has not been achieved. To advance toward clinical applications, socioeconomic aspects of the technology as well as the time frame and speed of development should be considered. Furthermore, the specific needs of patients and physicians should be assessed as guiding factors in the design of the material, treatment, or implantable device.

Acknowledgments This work was supported by American Heart Association grant # 17SDG33660925 / P.P.S.S. Abadi /2017.

References

1. Dalen JE, Alpert JS, Goldberg RJ, Weinstein RS. The epidemic of the 20th century: coronary heart disease. *Am J Med.* 2014;127(9):807–12.
2. Holmes JW, Laksman Z, Gepstein L. Making better scar: emerging approaches for modifying mechanical and electrical properties following infarction and ablation. *Prog Biophys Mol Biol.* 2016;120(1–3):134–48.
3. Bergmann O, Bhardwaj RD, Bernard S, Zdunek S, Barnabé-Heider F, Walsh S, Zupicich J, Alkass K, Buchholz BA, Druid H. Evidence for cardiomyocyte renewal in humans. *Science.* 2009;324(5923):98–102.
4. Anderson JL, Morrow DA. Acute myocardial infarction. *N Engl J Med.* 2017;376(21):2053–64.
5. Chen Q-Z, Harding SE, Ali NN, Lyon AR, Boccaccini AR. Biomaterials in cardiac tissue engineering: ten years of research survey. *Mater Sci Eng R Rep.* 2008;59(1–6):1–37.
6. Christman KL, Lee RJ. Biomaterials for the treatment of myocardial infarction. *J Am Coll Cardiol.* 2006;48(5):907–13.
7. van Erven L, Schaliq MJ. Amiodarone: an effective antiarrhythmic drug with unusual side effects. *Heart.* 2010;96(19):1593–600.
8. Goldhill D. Preventing surgical deaths: critical care and intensive care outreach services in the postoperative period. *Br J Anaesth.* 2004;95(1):88–94.
9. Rankin JS, Hammill BG, Ferguson TB Jr, Glower DD, O'Brien SM, DeLong ER, Peterson ED, Edwards FH. Determinants of operative mortality in valvular heart surgery. *J Thorac Cardiovasc Surg.* 2006;131(3):547–57.

10. Tachibana A, Santoso MR, Mahmoudi M, Shukla P, Wang L, Bennett M, Goldstone AB, Wang M, Fukushi M, Ebert AD. Paracrine effects of the pluripotent stem cell-derived cardiac myocytes salvage the injured myocardium. *Circ Res.* 2017;121(6):e22–36.
11. Gneocchi M, Zhang Z, Ni A, Dzau VJ. Paracrine mechanisms in adult stem cell signaling and therapy. *Circ Res.* 2008;103(11):1204–19.
12. Tang YL, Zhao Q, Qin X, Shen L, Cheng L, Ge J, Phillips MI. Paracrine action enhances the effects of autologous mesenchymal stem cell transplantation on vascular regeneration in rat model of myocardial infarction. *Ann Thorac Surg.* 2005;80(1):229–37.
13. Serpooshan V, Wu SM. *Cell Stem Cell.* 2014;15(6):671–3.
14. Tang ZC, Liao W-Y, Tang AC, Tsai S-J, Hsieh PC. The enhancement of endothelial cell therapy for angiogenesis in hindlimb ischemia using hyaluronan. *Biomaterials.* 2011;32(1):75–86.
15. Wei X, Yang X, Han Z-P, Qu F-F, Shao L, Shi Y-F. Mesenchymal stem cells: a new trend for cell therapy. *Acta Pharmacol Sin.* 2013;34(6):747.
16. Yang X, Pabon L, Murry CE. Engineering adolescence: maturation of human pluripotent stem cell-derived cardiomyocytes. *Circ Res.* 2014;114(3):511–23.
17. Volz A, Piper HM, Siegmund B, Schwartz P. Longevity of adult ventricular rat heart muscle cells in serum-free primary culture. *J Mol Cell Cardiol.* 1991;23(2):161–73.
18. Zhang Y, Li T-S, Lee S-T, Wawrowsky KA, Cheng K, Galang G, Malliaras K, Abraham MR, Wang C, Marbán E. Dedifferentiation and proliferation of mammalian cardiomyocytes. *PLoS One.* 2010;5(9):e12559.
19. Yamanaka S. Induced pluripotent stem cells: past, present, and future. *Cell Stem Cell.* 2012;10(6):678–84.
20. Bianco P, Robey PG, Simmons PJ. Mesenchymal stem cells: revisiting history, concepts, and assays. *Cell Stem Cell.* 2008;2(4):313–9.
21. Fijnvandraat AC, van Ginneken AC, de Boer PA, Ruijter JM, Christoffels VM, Moorman AF, Lekanne Deprez RH. Cardiomyocytes derived from embryonic stem cells resemble cardiomyocytes of the embryonic heart tube. *Cardiovasc Res.* 2003;58(2):399–409.
22. Swijnenburg R-J, Tanaka M, Vogel H, Baker J, Kofidis T, Gunawan F, Lebl DR, Caffarelli AD, de Bruin JL, Fedoseyeva EV. Embryonic stem cell immunogenicity increases upon differentiation after transplantation into ischemic myocardium. *Circulation.* 2005;112(9 suppl):I-166–72.
23. Nussbaum J, Minami E, Laflamme MA, Virag JA, Ware CB, Masino A, Muskheli V, Pabon L, Reinecke H, Murry CE. Transplantation of undifferentiated murine embryonic stem cells in the heart: teratoma formation and immune response. *FASEB J.* 2007;21(7):1345–57.
24. Ma D, Wei H, Lu J, Ho S, Zhang G, Sun X, Oh Y, Tan SH, Ng ML, Shim W. Generation of patient-specific induced pluripotent stem cell-derived cardiomyocytes as a cellular model of arrhythmogenic right ventricular cardiomyopathy. *Eur Heart J.* 2012;34(15):1122–33.
25. Zhou H, Rao MS. Can cord blood banks transform into induced pluripotent stem cell banks? *Cytotherapy.* 2015;17(6):756–64.
26. Ehnert S, Glanemann M, Schmitt A, Vogt S, Shanny N, Nussler NC, Stöckle U, Nussler A. The possible use of stem cells in regenerative medicine: dream or reality? *Langenbeck's Arch Surg.* 2009;394(6):985–97.
27. Kim D-H, Lipke EA, Kim P, Cheong R, Thompson S, Delannoy M, Suh K-Y, Tung L, Levchenko A. Nanoscale cues regulate the structure and function of macroscopic cardiac tissue constructs. *Proc Natl Acad Sci.* 2010;107(2):565–70.
28. Dalby MJ, Gadegaard N, Oreffo RO. Harnessing nanotopography and integrin–matrix interactions to influence stem cell fate. *Nat Mater.* 2014;13(6):558.
29. Murtuza B, Nichol JW, Khademhosseini A. Micro-and nanoscale control of the cardiac stem cell niche for tissue fabrication. *Tissue Eng Part B Rev.* 2009;15(4):443–54.
30. Conte LL, Chothia C, Janin J. The atomic structure of protein-protein recognition sites I. *J Mol Biol.* 1999;285(5):2177–98.
31. Roobrouck VD, Ulloa-Montoya F, Verfaillie CM. Self-renewal and differentiation capacity of young and aged stem cells. *Exp Cell Res.* 2008;314(9):1937–44.
32. Zhang J, Wilson GF, Soerens AG, Koonce CH, Yu J, Palecek SP, Thomson JA, Kamp TJ. Functional cardiomyocytes derived from human induced pluripotent stem cells. *Circ Res.* 2009;104(4):e30–41.

33. Maherali N, Hochedlinger K. Guidelines and techniques for the generation of induced pluripotent stem cells. *Cell Stem Cell*. 2008;3(6):595–605.
34. Villa-Diaz L, Ross A, Lahann J, Krebsbach P. Concise review: the evolution of human pluripotent stem cell culture: from feeder cells to synthetic coatings. *Stem Cells*. 2013;31(1):1–7.
35. Kyttälä A, Moraghebi R, Valensisi C, Kettunen J, Andrus C, Pasumarthy KK, Nakanishi M, Nishimura K, Ohtaka M, Weltner J. Genetic variability overrides the impact of parental cell type and determines iPSC differentiation potential. *Stem Cell Rep*. 2016;6(2):200–12.
36. Gherghiceanu M, Barad L, Novak A, Reiter I, Itskovitz-Eldor J, Binah O, Popescu L. Cardiomyocytes derived from human embryonic and induced pluripotent stem cells: comparative ultrastructure. *J Cell Mol Med*. 2011;15(11):2539–51.
37. Lundy SD, Zhu W-Z, Regnier M, Laflamme MA. Structural and functional maturation of cardiomyocytes derived from human pluripotent stem cells. *Stem Cells Dev*. 2013;22(14):1991–2002.
38. Lian X, Hsiao C, Wilson G, Zhu K, Hazeltine LB, Azarin SM, Raval KK, Zhang J, Kamp TJ, Palecek SP. Robust cardiomyocyte differentiation from human pluripotent stem cells via temporal modulation of canonical Wnt signaling. *Proc Natl Acad Sci*. 2012;109(27):E1848–57.
39. Hong KU, Li Q-H, Guo Y, Patton NS, Mokter A, Bhatnagar A, Bolli R. A highly sensitive and accurate method to quantify absolute numbers of c-kit+ cardiac stem cells following transplantation in mice. *Basic Res Cardiol*. 2013;108(3):346.
40. Zanganeh S, Hutter G, Spittler R, Lenkov O, Mahmoudi M, Shaw A, Pajarinen JS, Nejadnik H, Goodman S, Moseley M. Iron oxide nanoparticles inhibit tumour growth by inducing pro-inflammatory macrophage polarization in tumour tissues. *Nat Nanotechnol*. 2016;11(11):986.
41. Tolochko N. History of nanotechnology, Nanoscience and nanotechnology. *Encyclopaedia of life Support Systems (EOLSS)*, Developed under the auspices of the UNESCO, SEOLSS Published, oxford (2009) p. 3–4.
42. Webster TJ. *Nanomedicine: what's in a definition?* Dove Press; 2006.
43. Von Hippel A. Molecular engineering. *Science*. 1956;123(3191):315–7.
44. Van Noorden R. Chemistry: the trials of new carbon. *Nature News*. 2011;469(7328):14–6.
45. MacDonald RA, Laurenzi BF, Viswanathan G, Ajayan PM, Stegemann JP. Collagen-carbon nanotube composite materials as scaffolds in tissue engineering. *J Biomed Mater Res A*. 2005;74(3):489–96.
46. Correa-Duarte MA, Wagner N, Rojas-Chapana J, Morszeck C, Thie M, Giersig M. Fabrication and biocompatibility of carbon nanotube-based 3D networks as scaffolds for cell seeding and growth. *Nano Lett*. 2004;4(11):2233–6.
47. Shin SR, Jung SM, Zalabany M, Kim K, Zorlutuna P, Kim SB, Nikkha M, Khabiry M, Azize M, Kong J. Carbon-nanotube-embedded hydrogel sheets for engineering cardiac constructs and bioactuators. *ACS Nano*. 2013;7(3):2369–80.
48. Norman JJ, Desai TA. Methods for fabrication of nanoscale topography for tissue engineering scaffolds. *Ann Biomed Eng*. 2006;34(1):89–101.
49. Neuman KC, Nagy A. Single-molecule force spectroscopy: optical tweezers, magnetic tweezers and atomic force microscopy. *Nat Methods*. 2008;5(6):491.
50. Lee K-S, Kim RH, Yang D-Y, Park SH. Advances in 3D nano/microfabrication using two-photon initiated polymerization. *Prog Polym Sci*. 2008;33(6):631–81.
51. Rosamond WD. Trends in heart failure incidence in the community. *Am Heart Assoc*. 2017.
52. Christiansen MN, Køber L, Weeke P, Vasan RS, Jeppesen JL, Smith JG, Gislason GH, Torp-Pedersen C, Andersson C. Age-specific trends in incidence, mortality, and comorbidities of heart failure in Denmark, 1995 to 2012. *Circulation*. 2017;135(13):1214–23.
53. Liang H, Upmanyu M, Huang H. Size-dependent elasticity of nanowires: nonlinear effects. *Phys Rev B*. 2005;71(24):241403.
54. Saei AA, Yazdani M, Lohse SE, Bakhtiary Z, Serpooshan V, Ghavami M, Asadian M, Mashaghi S, Dreaden EC, Mashaghi A, Mahmoudi M. Nanoparticle surface functionality dictates cellular and systemic toxicity. *Chem Mater*. 2017;29(16):6578–95.
55. Mengsteab PY, Uto K, Smith AS, Frankel S, Fisher E, Nawas Z, Macadangang J, Ebara M, Kim D-H. Spatiotemporal control of cardiac anisotropy using dynamic nanotopographic cues. *Biomaterials*. 2016;86:1–10.

56. Jafarkhani M, Salehi Z, Kowsari-Esfahan R, Shokrgozar MA, Mohammadi MR, Rajadas J, Mozafari M. Strategies for directing cells into building functional hearts and parts. *Biomater Sci.* 2018;6:1664–90.
57. Li W-J, Jiang YJ, Tuan RS. Cell–Nanofiber-based cartilage tissue engineering using improved cell seeding, growth factor, and bioreactor technologies. *Tissue Eng A.* 2008;14(5):639–48.
58. Zhong S, Zhang Y, Lim CT. Fabrication of large pores in electrospun nanofibrous scaffolds for cellular infiltration: a review. *Tissue Eng Part B Rev.* 2011;18(2):77–87.
59. Huijing PA. Muscle as a collagen fiber reinforced composite: a review of force transmission in muscle and whole limb. *J Biomech.* 1999;32(4):329–45.
60. Parker KK, Ingber DE. Extracellular matrix, mechanotransduction and structural hierarchies in heart tissue engineering. *Philos Trans R Soc Lond B Biol Sci.* 2007;362(1484):1267–79.
61. Borg TK. Development of the connective tissue network in the neonatal hamster heart. *Dev Dyn.* 1982;165(4):435–43.
62. Zhao M, Zhang H, Robinson TF, Factor SM, Sonnenblick EH, Eng C. Profound structural alterations of the extracellular collagen matrix in postischemic dysfunctional (“stunned”) but viable myocardium. *J Am Coll Cardiol.* 1987;10(6):1322–34.
63. Moal F, Chappard D, Wang J, Vuillemin E, Michalak-Provost S, Rousselet MC, Oberti F, Cales P. Fractal dimension can distinguish models and pharmacologic changes in liver fibrosis in rats. *Hepatology.* 2002;36(4):840–9.
64. Goldberger AL. Fractal Electrodynamics of the Heartbeats. *Ann N Y Acad Sci.* 1990;591(1):402–9.
65. Monteiro LM, Vasques-Nóvoa F, Ferreira L, Nascimento DS. Restoring heart function and electrical integrity: closing the circuit. *NPJ Regen Med.* 2017;2(1):9.
66. Cui Z, Ni NC, Wu J, Du G-Q, He S, Yau TM, Weisel RD, Sung H-W, Li R-K. Polypyrrole-chitosan conductive biomaterial synchronizes cardiomyocyte contraction and improves myocardial electrical impulse propagation. *Theranostics.* 2018;8(10):2752.
67. Liu Y, Liang X, Wang S, Hu K. Electrospun poly (lactic-co-glycolic acid)/multiwalled carbon nanotube nanofibers for cardiac tissue engineering. *J Biomater Tissue Eng.* 2016;6(9):719–28.
68. Shin SR, Zihlmann C, Akbari M, Assawes P, Cheung L, Zhang K, Manoharan V, Zhang YS, Yükksekaya M, Wan Kt. Reduced graphene oxide-gelMA hybrid hydrogels as scaffolds for cardiac tissue engineering. *Small.* 2016;12(27):3677–89.
69. Anderson RH, Sanchez-Quintana D, Redmann K, Lunkenheimer PP. How are the myocytes aggregated so as to make up the ventricular mass?, *Seminars in Thoracic & Cardiovascular Surgery: Pediatric Cardiac Surgery Annual: Elsevier;* 2007. p. 76–86.
70. Kocica MJ, Corno AF, Carreras-Costa F, Ballester-Rodes M, Moghbel MC, Cueva CN, Lackovic V, Kanjuh VI, Torrent-Guas F. The helical ventricular myocardial band: global, three-dimensional, functional architecture of the ventricular myocardium. *Eur J Cardiothorac Surg.* 2006;29(Supplement_1):S21–40.
71. Hunter PJ, Borg TK. Integration from proteins to organs: the physiome project. *Nat Rev Mol Cell Biol.* 2003;4(3):237.
72. Sapir Y, Polyak B, Cohen S. *Nanomaterials for cardiac tissue engineering, Nanomaterials in Tissue Engineering.* Cambridge: Woodhead Publishing Limited; 2013. p. 244–75.
73. Zhou J, Chen J, Sun H, Qiu X, Mou Y, Liu Z, Zhao Y, Li X, Han Y, Duan C. Engineering the heart: evaluation of conductive nanomaterials for improving implant integration and cardiac function. *Sci Rep.* 2014;4:3733.
74. Zhang Y, Tang Y, Wang Y, Zhang L. Nanomaterials for cardiac tissue engineering application. *Nano-Micro Lett.* 2011;3(4):270–7.
75. Schwartz MA, Schaller MD, Ginsberg MH. Integrins: emerging paradigms of signal transduction. *Annu Rev Cell Dev Biol.* 1995;11(1):549–99.
76. Chibowski E, Jurak M. Comparison of contact angle hysteresis of different probe liquids on the same solid surface. *Colloid Polym Sci.* 2013;291(2):391–9.
77. Curtis A. Tutorial on the biology of nanotopography. *IEEE Trans Nanobioscience.* 2004;3(4):293–5.
78. Harrison RG. On the stereotropism of embryonic cells. *Science.* 1911;34(870):279–81.

79. Ebendal T. The relative roles of contact inhibition and contact guidance in orientation of axons extending on aligned collagen fibrils in vitro. *Exp Cell Res.* 1976;98(1):159–69.
80. Dunn G, Ebendal T. Contact guidance on oriented collagen gels. *Exp Cell Res.* 1978;111(2):475–9.
81. Carter SB. Haptotaxis and the mechanism of cell motility. *Nature.* 1967;213(5073):256–60.
82. Dunn G, Heath J. A new hypothesis of contact guidance in tissue cells. *Exp Cell Res.* 1976;101(1):1–14.
83. Zhao G, Zhang X, Lu TJ, Xu F. Recent advances in electrospun nanofibrous scaffolds for cardiac tissue engineering. *Adv Funct Mater.* 2015;25(36):5726–38.
84. Pham QP, Sharma U, Mikos AG. Electrospinning of polymeric nanofibers for tissue engineering applications: a review. *Tissue Eng.* 2006;12(5):1197–211.
85. Fleischer S, Shapira A, Regev O, Nseir N, Zussman E, Dvir T. Albumin fiber scaffolds for engineering functional cardiac tissues. *Biotechnol Bioeng.* 2014;111(6):1246–57.
86. Biggs MJP, Richards RG, Dalby MJ. Nanotopographical modification: a regulator of cellular function through focal adhesions. *Nanomedicine.* 2010;6(5):619–33.
87. Goversen B, van der Heyden MA, van Veen TA, de Boer TP. The immature electrophysiological phenotype of iPSC-CMs still hampers in vitro drug screening: special focus on I K1. *Pharmacol Ther.* 2017;183:127–36.
88. Fong AH, Romero-López M, Heylman CM, Keating M, Tran D, Sobrino A, Tran AQ, Pham HH, Fimbres C, Gershon PD. Three-dimensional adult cardiac extracellular matrix promotes maturation of human induced pluripotent stem cell-derived cardiomyocytes. *Tissue Eng A.* 2016;22(15–16):1016–25.
89. Teo BKK, Wong ST, Lim CK, Kung TY, Yap CH, Ramagopal Y, Romer LH, Yim EK. Nanotopography modulates mechanotransduction of stem cells and induces differentiation through focal adhesion kinase. *ACS Nano.* 2013;7(6):4785–98.
90. Singelyn JM, DeQuach JA, Seif-Naraghi SB, Littlefield RB, Schup-Magoffin PJ, Christman KL. Naturally derived myocardial matrix as an injectable scaffold for cardiac tissue engineering. *Biomaterials.* 2009;30(29):5409–16.
91. Lieu DK, Fu J-D, Chiamvimonvat N, Tung KWC, McNerney GP, Huser T, Keller G, Kong C-W, Li RA. Mechanism-based facilitated maturation of human pluripotent stem cell-derived cardiomyocytes. *Circ Arrhythm Electrophysiol.* 2013; <https://doi.org/10.1161/CIRCEP.112.973420>.
92. Lutolf M, Hubbell J. Synthetic biomaterials as instructive extracellular microenvironments for morphogenesis in tissue engineering. *Nat Biotechnol.* 2005;23(1):47.
93. Khan M, Xu Y, Hua S, Johnson J, Belevych A, Janssen PM, Gyorke S, Guan J, Angelos MG. Evaluation of changes in morphology and function of human induced pluripotent stem cell derived cardiomyocytes (hiPSC-CMs) cultured on an aligned-nanofiber cardiac patch. *PLoS One.* 2015;10(5):e0126338.
94. Carson D, Hnilova M, Yang X, Nemeth CL, Tsui JH, Smith AS, Jiao A, Regnier M, Murry CE, Tamerler C. Nanotopography-induced structural anisotropy and sarcomere development in human cardiomyocytes derived from induced pluripotent stem cells. *ACS Appl Mater Interfaces.* 2016;8(34):21923–32.
95. Abadi PP, Garbern JC, Behzadi S, Hill MJ, Tresback JS, Heydari T, Ejtehadi MR, Ahmed N, Copley E, Aghaverdi H. Engineering of mature human induced pluripotent stem cell-derived cardiomyocytes using substrates with multiscale topography. *Adv Funct Mater.* 2018;28(19)
96. Parrag IC, Zandstra PW, Woodhouse KA. Fiber alignment and coculture with fibroblasts improves the differentiated phenotype of murine embryonic stem cell-derived cardiomyocytes for cardiac tissue engineering. *Biotechnol Bioeng.* 2012;109(3):813–22.
97. Bonart R, Müller E. Phase separation in urethane elastomers as judged by low-angle X-ray scattering. I. Fundamentals. *J Macromol Sci Part B: Phys.* 1974;10(1):177–89.
98. Dicesare P, Fox WM, Hill MJ, Krishnan GR, Yang S, Sarkar D. Cell-material interactions on biphasic polyurethane matrix. *J Biomed Mater Res A.* 2013;101(8):2151–63.
99. Hill MJ, Cheah C, Sarkar D. Interfacial energetics approach for analysis of endothelial cell and segmental polyurethane interactions. *Colloids Surf B Biointerfaces.* 2016;144:46–56.

100. Kim D-H, Kim P, Suh KY, Choi SK, Lee SH, Kim B Modulation of adhesion and growth of cardiac myocytes by surface nanotopography, *Engineering in Medicine and Biology Society*, 2005. IEEE-EMBS 2005. 27th Annual International Conference of the, IEEE, 2006, p. 4091–94.
101. Martinez E, Engel E, Planell J, Samitier J. Effects of artificial micro-and nano-structured surfaces on cell behaviour. *Ann Anat*. 2009;191(1):126–35.
102. Wang P-Y, Yu J, Lin J-H, Tsai W-B. Modulation of alignment, elongation and contraction of cardiomyocytes through a combination of nanotopography and rigidity of substrates. *Acta Biomater*. 2011;7(9):3285–93.
103. Hazeltine LB, Badur MG, Lian X, Das A, Han W, Palecek SP. Temporal impact of substrate mechanics on differentiation of human embryonic stem cells to cardiomyocytes. *Acta Biomater*. 2014;10(2):604–12.
104. Lisichkin G, Novotortsev RY, Bernadyuk S. Chemically modified oxide surfaces capable of molecular recognition. *Colloid J*. 2004;66(4):387–99.
105. Chen L, Wang X, Lu W, Wu X, Li J. Molecular imprinting: perspectives and applications. *Chem Soc Rev*. 2016;45(8):2137–211.
106. Mahmoudi M, Bonakdar S, Shokrgozar MA, Aghaverdi H, Hartmann R, Pick A, Witte G, Parak WJ. Cell-imprinted substrates direct the fate of stem cells. *ACS Nano*. 2013;7(10):8379–84.
107. Silva BV, Rodríguez BA, Sales GF, Maria Del Pilar TS, Dutra RF. An ultrasensitive human cardiac troponin T graphene screen-printed electrode based on electropolymerized-molecularly imprinted conducting polymer. *Biosens Bioelectron*. 2016;77:978–85.
108. Mashinchian O, Bonakdar S, Taghinejad H, Satarifard V, Heidari M, Majidi M, Sharifi S, Peirovi A, Saffar S, Taghinejad M. Cell-imprinted substrates act as an artificial niche for skin regeneration. *ACS Appl Mater Interfaces*. 2014;6(15):13280–92.
109. Moreira FT, Sharma S, Dutra RA, Noronha JP, Cass AE, Sales MGF. Protein-responsive polymers for point-of-care detection of cardiac biomarker. *Sensors Actuators B Chem*. 2014;196:123–32.
110. Sun DM, Liu C, Ren WC, Cheng HM. A review of carbon nanotube-and graphene-based flexible thin-film transistors. *Small*. 2013;9(8):1188–205.
111. Jin G, Li K. The electrically conductive scaffold as the skeleton of stem cell niche in regenerative medicine. *Mater Sci Eng C*. 2014;45:671–81.
112. Mena F, Abdelghani A, Mena B. Graphene nanomaterials as biocompatible and conductive scaffolds for stem cells: impact for tissue engineering and regenerative medicine. *J Tissue Eng Regen Med*. 2015;9(12):1321–38.
113. Harrison BS, Atala A. Carbon nanotube applications for tissue engineering. *Biomaterials*. 2007;28(2):344–53.
114. Navaei A, Saini H, Christenson W, Sullivan RT, Ros R, Nikkhah M. Gold nanorod-incorporated gelatin-based conductive hydrogels for engineering cardiac tissue constructs. *Acta Biomater*. 2016;41:133–46.
115. Fleischer S, Shevach M, Feiner R, Dvir T. Coiled fiber scaffolds embedded with gold nanoparticles improve the performance of engineered cardiac tissues. *Nanoscale*. 2014;6(16):9410–4.
116. Saravanan S, Nethala S, Pattnaik S, Tripathi A, Moorthi A, Selvamurugan N. Preparation, characterization and antimicrobial activity of a bio-composite scaffold containing chitosan/nano-hydroxyapatite/nano-silver for bone tissue engineering. *Int J Biol Macromol*. 2011;49(2):188–93.
117. Liu S, Navaei A, Meng X, Nikkhah M, Chae J. Wireless passive stimulation of engineered cardiac tissues. *ACS Sens*. 2017;2(7):1006–12.
118. Tan Y, Richards D, Xu R, Stewart-Clark S, Mani SK, Borg TK, Menick DR, Tian B, Mei Y. Silicon nanowire-induced maturation of cardiomyocytes derived from human induced pluripotent stem cells. *Nano Lett*. 2015;15(5):2765–72.
119. Tian B, Liu J, Dvir T, Jin L, Tsui JH, Qing Q, Suo Z, Langer R, Kohane DS, Lieber CM. Macroporous nanowire nanoelectronic scaffolds for synthetic tissues. *Nat Mater*. 2012;11(11):986.
120. Hou J, Xie Y, Ji A, Cao A, Fang Y, Shi E. Carbon-nanotube-wrapped spider silks for directed cardiomyocyte growth and electrophysiological detection. *ACS Appl Mater Interfaces*. 2018;10(8):6793–8.

121. Dvir T, Timko BP, Brigham MD, Naik SR, Karajanagi SS, Levy O, Jin H, Parker KK, Langer R, Kohane DS. Nanowired three-dimensional cardiac patches. *Nat Nanotechnol.* 2011;6(11):720.
122. Shevach M, Fleischer S, Shapira A, Dvir T. Gold nanoparticle-decellularized matrix hybrids for cardiac tissue engineering. *Nano Lett.* 2014;14(10):5792–6.
123. Samal SK, Goranov V, Dash M, Russo A, Shelyakova T, Graziosi P, Lungaro L, Riminucci A, Uhlarz M, Bañobre-López M. Multilayered magnetic gelatin membrane scaffolds. *ACS Appl Mater Interfaces.* 2015;7(41):23098–109.
124. Martinelli V, Cellot G, Toma FM, Long CS, Caldwell JH, Zentilin L, Giacca M, Turco A, Prato M, Ballerini L. Carbon nanotubes promote growth and spontaneous electrical activity in cultured cardiac myocytes. *Nano Lett.* 2012;12(4):1831–8.
125. Wang J, Cui C, Nan H, Yu Y, Xiao Y, Poon E, Yang G, Wang X, Wang C, Li L. Graphene sheet-induced global maturation of cardiomyocytes derived from human induced pluripotent stem cells. *ACS Appl Mater Interfaces.* 2017;9(31):25929–40.
126. Wong KK, Cheung SO, Huang L, Niu J, Tao C, Ho CM, Che CM, Tam PK. Further evidence of the anti-inflammatory effects of silver nanoparticles. *ChemMedChem.* 2009;4(7):1129–35.
127. Rai M, Yadav A, Gade A. Silver nanoparticles as a new generation of antimicrobials. *Biotechnol Adv.* 2009;27(1):76–83.
128. Allison S, Ahumada M, Andronic C, McNeill B, Variola F, Griffith M, Ruel M, Hamel V, Liang W, Suuronen EJ. Electroconductive nanoengineered biomimetic hybrid fibers for cardiac tissue engineering. *J Mater Chem B.* 2017;5(13):2402–6.
129. Rath G, Hussain T, Chauhan G, Garg T, Goyal AK. Collagen nanofiber containing silver nanoparticles for improved wound-healing applications. *J Drug Target.* 2016;24(6):520–9.
130. Hajipour MJ, Fromm KM, Ashkarran AA, Jimenez de Aberasturi D, de Larramendi IR, Rojo T, Serpooshan V, Parak WJ, Mahmoudi M. Antibacterial properties of nanoparticles. *Trends Biotechnol.* 2012;30(10):499–511.
131. Mahmoudi M, Serpooshan V. Silver-coated engineered magnetic nanoparticles are promising for the success in the fight against antibacterial resistance threat. *ACS Nano.* 2012;6(3):2656–64.
132. Martinelli V, Cellot G, Fabbro A, Bosi S, Mestroni L, Ballerini L. Improving cardiac myocytes performance by carbon nanotubes platforms. *Front Physiol.* 2013;4:239.
133. Lovat V, Pantarotto D, Lagostena L, Cacciari B, Grandolfo M, Righi M, Spalluto G, Prato M, Ballerini L. Carbon nanotube substrates boost neuronal electrical signaling. *Nano Lett.* 2005;5(6):1107–10.
134. Lee T-J, Park S, Bhang SH, Yoon J-K, Jo I, Jeong G-J, Hong BH, Kim B-S. Graphene enhances the cardiomyogenic differentiation of human embryonic stem cells. *Biochem Biophys Res Commun.* 2014;452(1):174–80.
135. Cong H, Pan T. Photopatternable conductive PDMS materials for microfabrication. *Adv Funct Mater.* 2008;18(13):1912–21.
136. Shin SR, Migliori B, Miccoli B, Li YC, Mostafalu P, Seo J, Mandla S, Enrico A, Antona S, Sabarish R. Electrically driven microengineered bioinspired soft robots. *Adv Mater.* 2018;30(10):1704189.
137. Lin ZC, McGuire AF, Burrige PW, Matsa E, Lou H-Y, Wu JC, Cui B. Accurate nanoelectrode recording of human pluripotent stem cell-derived cardiomyocytes for assaying drugs and modeling disease. *Microsyst Nanoeng.* 2017;3:16080.
138. Tavano L, Muzzalupo R. Multi-functional vesicles for cancer therapy: the ultimate magic bullet. *Colloids Surf B: Biointerfaces.* 2016;147:161–71.
139. Godin B, Sakamoto JH, Serda RE, Grattoni A, Bouamrani A, Ferrari M. Emerging applications of nanomedicine for the diagnosis and treatment of cardiovascular diseases. *Trends Pharmacol Sci.* 2010;31(5):199–205.
140. Kamaly N, Fredman G, Fojas JJR, Subramanian M, Choi WI, Zepeda K, Vilos C, Yu M, Gadde S, Wu J. Targeted interleukin-10 nanotherapeutics developed with a microfluidic chip enhance resolution of inflammation in advanced atherosclerosis. *ACS Nano.* 2016;10(5):5280–92.
141. Kamaly N, Fredman G, Subramanian M, Gadde S, Pesic A, Cheung L, Fayad ZA, Langer R, Tabas I, Farokhzad OC. Development and in vivo efficacy of targeted polymeric inflammation-resolving nanoparticles. *Proc Natl Acad Sci.* 2013;110(16):6506–11.

142. Han J, Kim B, Shin J-Y, Ryu S, Noh M, Woo J, Park J-S, Lee Y, Lee N, Hyeon T. Iron oxide nanoparticle-mediated development of cellular gap junction crosstalk to improve mesenchymal stem cells' therapeutic efficacy for myocardial infarction. *ACS Nano*. 2015;9(3):2805–19.
143. Mahmoudi M, Tachibana A, Goldstone AB, Woo YJ, Chakraborty P, Lee KR, Foote CS, Pieciewicz S, Barrozo JC, Wakeel A. Novel MRI contrast agent from magnetotactic bacteria enables in vivo tracking of iPSC-derived cardiomyocytes. *Sci Rep*. 2016;6:26960.
144. Cheng K, Shen D, Hensley MT, Middleton R, Sun B, Liu W, De Couto G, Marbán E. Magnetic antibody-linked nanomatchmakers for therapeutic cell targeting. *Nat Commun*. 2014;5:4880.
145. Serpooshan V, Sivanesan S, Huang X, Mahmoudi M, Malkovskiy AV, Zhao M, Inayathullah M, Wagh D, Zhang XJ, Metzler S. [Pyr1]-Apelin-13 delivery via nano-liposomal encapsulation attenuates pressure overload-induced cardiac dysfunction. *Biomaterials*. 2015;37:289–98.
146. Kuba K, Zhang L, Imai Y, Arab S, Chen M, Maekawa Y, Leschnik M, Leibbrandt A, Markovic M, Schwaighofer J. Impaired heart contractility in Apelin gene-deficient mice associated with aging and pressure overload. *Circ Res*. 2007;101(4):e32–42.
147. Japp A, Cruden N, Barnes G, Van Gemeren N, Mathews J, Adamson J, Johnston N, Denvir M, Megson I, Flapan A. Acute cardiovascular effects of apelin in humans: potential role in patients with chronic heart failure. *Circulation*. 2010;121(16):1818–27.
148. Jayakumar Rajadas PR-L, Serpooshan V. Compositions and methods for treating cardiovascular and pulmonary diseases and disorders with apelin; 2016.
149. Ott HC, Matthiesen TS, Goh S-K, Black LD, Kren SM, Netoff TI, Taylor DA. Perfusion-decellularized matrix: using nature's platform to engineer a bioartificial heart. *Nat Med*. 2008;14(2):213.
150. Casals E, Pfaller T, Duschl A, Oostingh GJ, Puentes V. Time evolution of the nanoparticle protein corona. *ACS Nano*. 2010;4(7):3623–32.
151. Hajipour MJ, Laurent S, Aghaie A, Rezaee F, Mahmoudi M. Personalized protein coronas: a “key” factor at the nanobiointerface. *Biomater Sci*. 2014;2(9):1210–21.
152. Serpooshan V, Mahmoudi M, Zhao M, Wei K, Sivanesan S, Motamedchaboki K, Malkovskiy AV, Gladstone AB, Cohen JE, Yang PC, Rajadas J, Bernstein D, Woo YJ, Ruiz-Lozano P. Protein corona influences cell-biomaterial interactions in nanostructured tissue engineering scaffolds. *Adv Funct Mater*. 2015;25(28):4379–89.



Bioengineering 3D Cardiac Microtissues Using Bioassembly

6

Longjun Gu, Jinghan Feng, Donghui Zhang, and Pu Chen

Introduction

Bioengineering of three-dimensional (3D) microtissues has developed rapidly in recent years due to the increasing demands of drug screening [1–3], regenerative medicine [4–7], and basic biomedical research [8–10]. Specifically, bioengineering of 3D cardiac microtissues has been regarded as a potential strategy to repair impaired heart and prolong patient survival via cardiac regenerative therapies [11, 12]. Furthermore, 3D cardiac microtissue is also a preferred physiologically relevant model for preclinical screening of cardiotoxicity [13]. Drug-induced cardiotoxicity is one of the primary reasons for the failure of drug development [14–17], leading the rate of cardiotoxicity-related withdrawal to reach 33.3% since 1997 [18, 19]. Thus, a better cardiac model that enables high-throughput preclinical drug screening is needed in the drug discovery pipeline to replace or supplement traditional two-dimensional (2D) monolayer culture and animal models. Emerging 3D cardiac microtissues that better mimic the human native cardiac physiology in vitro can improve the predictive accuracy of preclinical drug evaluation. In addition, 3D cardiac microtissues constructed with patient-derived cardiomyocytes have unique advantages in modeling gene-associated cardiac diseases for personalized therapy.

L. Gu · J. Feng · P. Chen (✉)

Department of Biomedical Engineering, School of Basic Medical Sciences,
Wuhan University, Wuhan, China

Institute of Hepatobiliary Diseases of Wuhan University, Transplant Center of Wuhan
University, Hubei Key Laboratory of Medical Technology on Transplantation, Wuhan, China
e-mail: longjun_gu@whu.edu.cn; jinghanfeng@whu.edu.cn; puchen@whu.edu.cn

D. Zhang

College of Life Sciences, Hubei University, Wuhan, China
e-mail: dongh.zhang@hubu.edu.cn

In recent years, biofabrication approaches have attracted great attention and have been broadly used in bioengineering of 3D cardiac microtissues to address the aforementioned demands [20, 21]. The definition of biofabrication is the generation of defined biological products from living cells, biomaterials, bioactive molecules, and extracellular matrix (ECM) by one of two distinct strategies: bioprinting and bioassembly [22–25]. The formation of functional tissue products is usually accompanied by subsequent tissue maturation procedures after fabrication [24, 26, 27].

Bioprinting is one of the widely adopted technical routes in biofabrication [21, 28–30] and is defined as the assembly of living and nonliving materials into structure- and component-defined cytoarchitectures with a prescribed 2D or 3D structure via computer-aided transfer processes [24, 27]. Different bioprinting techniques have been used in the preparation of 3D cardiac microtissues [31], including inkjet bioprinting [32], microextrusion bioprinting [33–36], and laser-assisted bioprinting [37]. These bioprinting techniques usually require a significant portion of the biomaterials and living cells to be a part of the bioink. However, many types of widely used natural biomaterials (e.g., Matrigel, collagen, gelatin, alginate, and chitosan) potentially induce adverse biological effects such as immunogenicity, fibrous tissue formation, toxicity of degradation products, and host inflammatory responses which affect their long-term function for *in vivo* applications [38]. Ong et al. have developed a biomaterial-free 3D bioprinting method for generating 3D cardiac microtissues. Living cells are initially patterned on a needle array, which greatly increases the difficulty of the operation and the complexity of bioprinting [39, 40]. Many more challenges still exist for 3D bioprinting of cardiac tissues: (1) Traditional bioprinting techniques cannot effectively control intercellular proximity; therefore, it is difficult to accurately emulate the *in vivo* arrangement of cardiomyocytes (CMs) and intercellular interactions. (2) Cell damage or death can be caused by a high printing speed. (3) A long operation process is needed for large-scale designed product. (4) Physiologically relevant cell density is difficult to be obtained due to the abundant usage of biomaterials in the bioink. Especially for cardiac tissue, cell density is much higher than that of any other tissues and the fraction of ECM is very low [41]. For these reasons, alternative approaches are urgently needed in the construction of cardiac microtissues.

Bioassembly has recently emerged as a well-accepted technical alternative to biofabrication. The first clear definition of bioassembly was provided by the International Society for Biofabrication in 2016 [26]. Bioassembly represents the manufacture of hierarchical structures with defined 2D or 3D organization using the automatic assembly of preformed cell-containing fabrication units, which are generated through cell-driven self-organization or via the preparation of hybrid cell-material building blocks, representatively by utilizing enabling techniques [26, 27]. Compared with bioprinting, a large number of cells can be assembled into a closely packed cytoarchitecture in a short time by bioassembly. In addition, cell containing building blocks can also be closely packed into a 2D or 3D construct in

a noninvasive way [26, 27]. Most importantly, microtissues with a physiologically relevant cell packing density and low ECM fraction can be easily prepared by bioassembly approaches. These advantages make bioassembly an optimal choice for constructing cardiac microtissues.

Over the past decade, several emerging bioassembly techniques have been developed for bioengineering cardiac microtissues: acoustic field-guided assembly [42–44], magnetic field-guided assembly [45–47], gravity-driven assembly [48, 49], and molecular recognition-assisted self-assembly [50, 51]. Cardiac constructs prepared by these approaches have been cultured *in vitro* for the maturation and formation of cardio-specific functions. These cardiac microtissues have been demonstrated as an *in vitro* model for basic medical research and preclinical drug screening. In addition, these cardiac microtissues have also been utilized as building blocks for cardiac regenerative therapy. Until now, an in-depth summary of these bioassembly techniques for the fabrication of cardiac microtissues has been lacking.

In this chapter, we aim to provide a systematic review on bioengineering 3D cardiac microtissues using various bioassembly techniques (Fig. 6.1). A comprehensive comparison of the pros and cons of these techniques is presented. Maturation is an essential procedure for 3D cardiac microtissues to exert organ-specific functions, a topic that is also touched upon briefly in the chapter. Additionally, three types of typical applications of 3D cardiac microtissues are mentioned. We also discuss the challenges and prospects for the application of bioassembly techniques in cardiac tissue engineering. We believe that this chapter will be helpful for postgraduate and undergraduate students as well as clinicians and medical researchers who wish to gain a fundamental understanding of 3D cardiac microtissue biofabrication using bioassembly approaches.

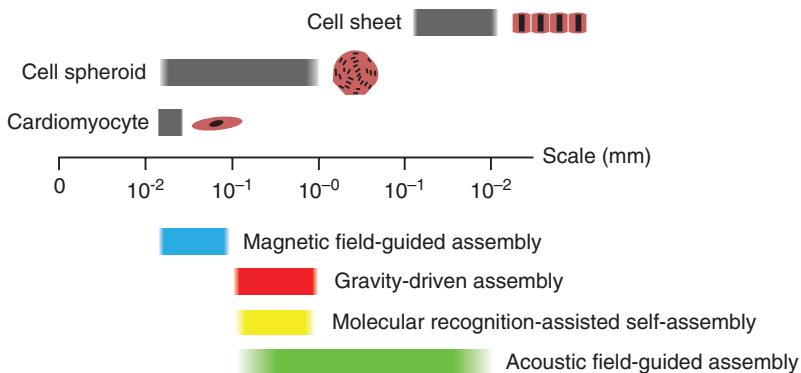


Fig. 6.1 Four types of bioassembly techniques for the generation of 3D cardiac microtissues. The sizes of the cardiomyocytes, cell spheroids, and cell sheets are shown above the axis, while the sizes of the 3D cardiac microtissues fabricated by each bioassembly technique are shown below the axis

Bioassembly Techniques for 3D Cardiac Microtissues

Bioengineering human physiologically relevant 3D cardiac microtissues potentially facilitates a wide range of biomedical applications, including the probing of cardiac disease mechanisms, screening of cardiac toxicity of drug candidates, and repair of cardiac damage. In recent years, numerous bioassembly techniques have been developed to fabricate cardiac microtissues from building materials, including CMs, biomaterials, and bioactive molecules (Fig. 6.2). These bioassembly techniques usually employ interactions between cardiac cells and external fields as well as the intercellular interaction to form predefined cytoarchitectures. The formed cytoarchitectures are usually immobilized via a sol-gel transition and are transferred to a cell incubator for further tissue culture and maturation. In this section, we provide a comprehensive summary of current bioassembly techniques and discuss aspects, such as their working principle, instrumentation, operating procedure, and typical examples. Additionally, we also discuss the merits and drawbacks of each bioassembly technique (Table 6.1).

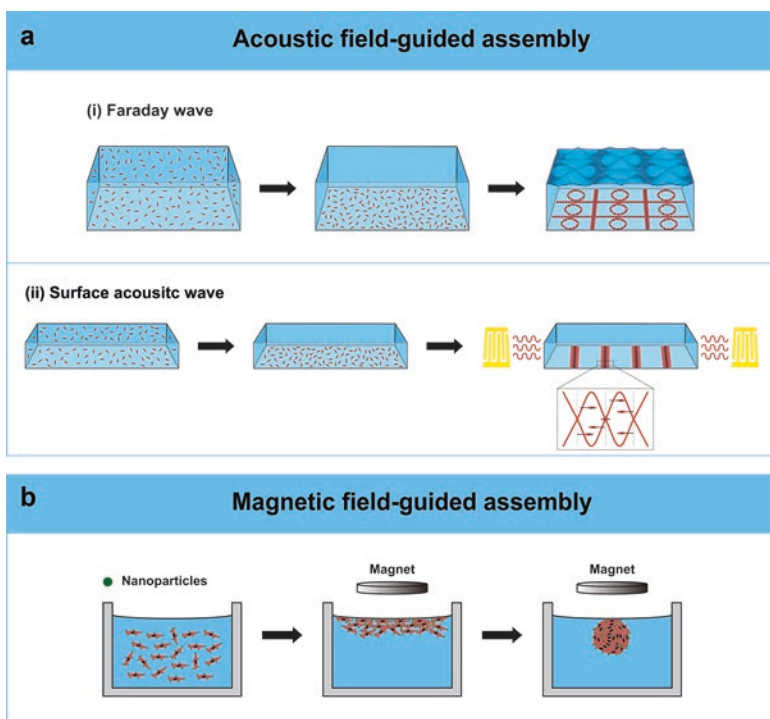


Fig. 6.2 Commonly used techniques in bioassembly and their brief use in cardiac microtissues fabrication. (a) Acoustic field-guided assembly (Faraday wave and surface acoustic wave), (b) magnetic field-guided assembly, (c) gravity-driven assembly (hanging drop and micromolding assembly), and (d) molecular recognition-assisted self-assembly

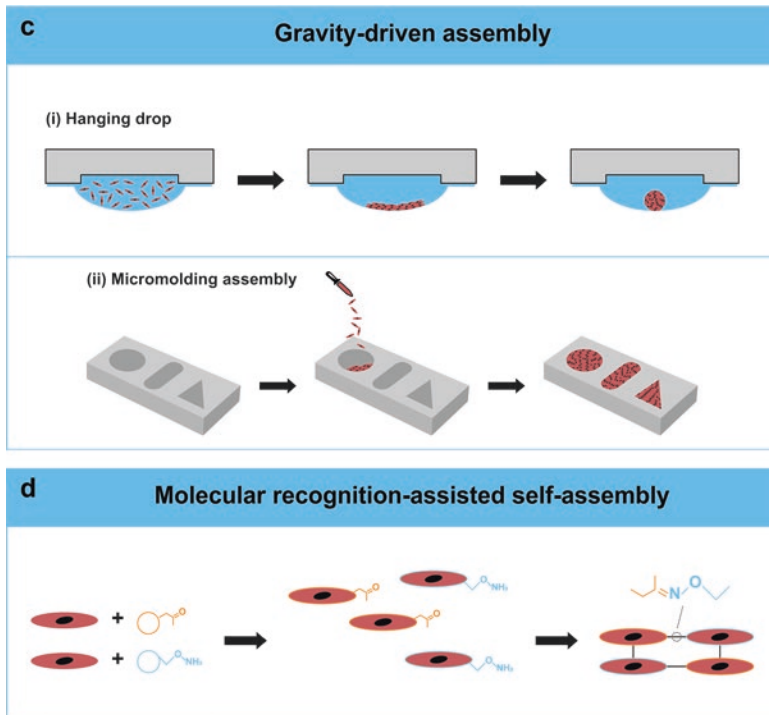


Fig. 6.2 (continued)

Acoustic Field-Guided Assembly

Acoustic waves have long been utilized in biomedical research to manipulate or detect biological systems due to their biocompatibility, tunability, and multiformity. Vibrational frequency and amplitude are two pivotal parameters that determine the intrinsic characteristic of acoustic waves. According to the range of vibrational frequency and the type of propagation medium, acoustic waves can be categorized into different wave types. Currently, three types of acoustic waves, Faraday wave [52], surface acoustic wave (SAW) [44], and bulk acoustic wave [53, 54], are used as bio-fabrication tools to assemble cells into various cytoarchitectures. Among these tools, Faraday waves and SAW have been demonstrated to fabricate cardiac microtissues.

Faraday Wave

Faraday wave is a nonlinear standing wave existing at the air-liquid interface that is generated by oscillatory vertical acceleration of a liquid layer [55]. Faraday waves take various forms such as circle, square, bar, or other more complex geometries. These waveforms are determined by vibrational parameters (i.e., vibrating frequency and acceleration amplitude), boundary geometries, and fluid properties (i.e., surface tension, viscosity, and density) [56]. In Faraday wave-based assembly,

Table 6.1 Comparison of four types of bioassembly techniques

Bioassembly techniques	Advantages	Limitations	Refs
Acoustic field-guided assembly (Faraday wave)	Noninvasive High speed Physiologically relevant cell density	No control over spatial organization of heterogeneous building units	[42, 43]
Acoustic field-guided assembly (SAW)	Noninvasive High speed	Single geometry	[44]
Magnetic field-guided assembly	High speed	Potential cytotoxicity Low throughput	[46]
Gravity-driven assembly (hanging drop)	Ease of operation High throughput Precise control over microtissue size	Single geometry	[72]
Gravity-driven assembly (micromolding assembly)	Ease of operation Precise control over microtissue size Multiple geometries	Requires templates	[77, 79]
Molecular recognition-assisted self-assembly	Highly specific Noninvasive	Requires surface modification	[86]

microscale bioentities can be assembled either at the air-liquid interface as a monolayer structure [57] or at the bottom of a liquid container as a closely packed multilayer structure [52]. The use of this technique for the assembly of polymeric beads [57], single cells [42, 43], and cell spheroids [52] has been reported previously.

Chen et al. employed Faraday wave pattern as a liquid-based template to assemble microscale particles (microparticles) into a closely packed monolayer structure at the liquid surface. In principle, the beads drift to a region with minimized force potential, which is determined by Faraday wave pattern [57]. The pattern of microparticles can be flexibly tuned by varying the vibrational frequency or geometric boundary of the liquid container. Thereafter, the same group reported the application of this technique to assemble hepatic spheroids into 3D hepatic microtissues at the bottom of a liquid container. Hepatic spheroids have been successfully constructed into 3D hepatic microtissues [52]. Assembly of striated 3D cardiac microtissues has also been reported by using human induced pluripotent stem cell-derived cardiomyocytes (hiPSC-CMs) [42, 43]. Briefly, a fibrin prepolymer solution containing hiPSC-CMs with a density of 1.7×10^6 cells/mL was transferred to the assembly chamber. After cell sedimentation, Faraday waves with stripe-like waveforms were generated in the chamber by applying vertical mechanical vibration. The hiPSC-CMs, subjected to Faraday waves, were assembled into a 3D construct with a predefined pattern. The cellular construct was subsequently immobilized by gelation of the fibrin prepolymer solution for further tissue culture. The generated cardiac tissues demonstrated some critical nature cardiac functions, including the expression of connexin 43 (CX43) and α -actinin, spontaneous beating and high metabolic activity compared to unassembled CMs. Faraday wave-based bioassembly provides a noninvasive and rapid approach to fabricate functional cardiac microtissues with a cell density close to that of human cardiac tissues.

Surface Acoustic Wave

SAW is a type of acoustic wave that travels along an elastic material surface [58]. An interdigital transducer (IDT) is a widely used device to generate SAW from electric signals. The IDT is fabricated on a piezoelectric (PZT) substrate by a lift-off or etching process [59]. The wavelength of the SAW can be easily determined by periodic spacing of the interdigital electrodes of the IDT, while the amplitude of the SAW is tuned by input electric signals. When two series of SAWs travel in opposite directions, a standing surface acoustic wave (SSAW) forms through the interference of the two SAWs. Cells in the SSAW are trapped in regions with the lowest force potential as defined by the interaction between the acoustic radiation field and the cells. Based on this mechanism, SSAW has been used for microparticle focusing [60] and 2D or 3D single-cell patterning [61–63].

Recently, Naseer et al. demonstrated spatial patterning of CMs and cardiac fibroblasts (CFs) using an SAW device [44]. To generate these patterns, a cell mixture was first suspended in a prepolymer solution of photocrosslinkable gelatin methacrylate (GelMA). The GelMA solution was added to the chamber and covered with glass slide. Then, SAWs were generated by applying sinusoidal electric signals to the LiNbO_3 substrate. Cardiac cells were driven to the pressure node of the SSAW and stripe shaped cytoarchitectures were formed. Subsequently, the cardiac cells were immobilized by crosslinking the GelMA prepolymer solution via ultraviolet (UV) exposure. The cell-encapsulating GelMA hydrogel was transferred to an incubator for tissue maturation. Expression of F-actin was validated in the generated cardiac microtissues. The SAW-based bioassembly enables the manipulation of single cells to form cytoarchitectures with a high spatial resolution. However, this technique is limited to the generation of line or cross-shaped patterns, which hampers its application in the bioengineering of complex cytoarchitectures in native cardiac tissues.

Magnetic Field-Guided Assembly

Magnetic field-guided assembly is a technique that explores an external magnetic field to drive suspended cells into a closely packed construct with a spatially defined geometry. In a magnetic field-guided assembly, the movements of the cells are initially determined by the magnetic force. When the magnetic force on the cells is balanced with other forces such as buoyant force or gravity, the cells ultimately aggregate in the region. Target cells can be either labeled with magnetic nanoparticles or suspended in a magnetic contrast medium like gadolinium solution. The assembled cytoarchitectures are determined by the location and shape of the magnets. For example, Souza et al. explored the use of a ring-shaped magnet for biofabricating of a ring-shaped tumor microtissues by magnetic levitation [64]. Until now, more than 20 types of cells including stem cells [64], primary cells [65], and cell lines [66] have been used in the magnetic assembly. Specifically, Hogan et al. [46] demonstrated the magnetic assembly of rat CMs into cardiac microtissues for cardiac tissue engineering. Freshly isolated primary

rat CMs were labeled with magnetic iron oxide (MIO)-based nanoparticles via endocytosis. These MIO-containing cells were uniformly suspended in cell culture medium and then levitated at the air-liquid interface by applying a disk magnet on top of the liquid container. Levitated cells were closely packed by the magnetic field, and they finally formed spherical cardiac microtissue that could contract spontaneously and expressed cardio-specific proteins such as α -actinin and fibronectin. As levitation of CMs relies on the cellular uptake of magnetic nanoparticles, complete removal of nanoparticles from CMs poses a challenge for utilizing these microtissues in regenerative therapy. The throughput of the current device was 24 microtissues per batch, which can be further scaled up if this technique is combined with a 96-well or 384-well plate.

Gravity-Driven Assembly

In a gravity-driven assembly, cell assembly is realized by the gravitational sedimentation of cells to the bottom of a nonadhesive restriction interface, which can be an air-liquid interface used in the hanging drop technique or a polymeric template used for micromolding. Gravity-driven assembly has the advantages of being free from external bulk equipment, easy to operate and scale-up [67], and able to precisely control the microtissue size [48].

Hanging Drop

The hanging drop technique is a well-commercialized gravity-driven assembly method. In this method, hanging drops can be generated in a homemade mold [68], cell culture dish [69], microwell arrays [70, 71], or microfluidic plate [67]. Suspended cells are cultured in a hanging drop that adheres to a flat surface. The settling cells are driven by gravity and then aggregate at the bottom as hemisphere-shaped hanging drops. After a period of incubation, the cells spontaneously self-organize into a spheroid. This technique has been utilized for generation of cardiac spheroids with physiologically relevant characteristics, including spontaneous beating, production of cardio-specific ECM, and expression of specific proteins such as CX 43 and F-actin, from CMs derived from different species, such as human, rat, and mouse [72, 73]. In addition, the hanging drop plate can be further integrated with other microdevices to realize more sophisticated functions. Yazdi et al. developed a microfluidic hanging drop network integrated with a micropump for precise flow control. The micropump relies on surface tension at the air-liquid interface to drive the culture medium flow through hanging drop networks [74]. In addition, Schmid et al. integrated microelectrodes in tissue culture chambers for situ monitoring of the beating rate of cardiac microtissues [75]. The hanging drop technique enables precise control over the size of formed microtissues. However, the geometry of microtissues is limited to the simple spherical shape.

Micromolding Assembly

In a micromolding process, microtissue templates are first fabricated using a variety of cell nonadhesive and biocompatible materials, such as poly(ethylene glycol) (PEG) [76–78], polydimethylsiloxane (PDMS) [79], and agarose [80]. The templates contain an assembly chamber with predefined geometries. After being added to the template, suspended cells settle down to the bottom of the assembly chamber by gravity and generate microtissues with defined structures and sizes [76, 80–84]. Huebsch et al. generated 3D microheart muscle arrays using a micromolding process [79]. In this study, a PDMS template was fabricated by soft lithography and replica molding and was bonded to a polystyrene (PS) substrate. iPSC-CMs and fibroblasts were seeded in the assembly chambers, where they formed dog-bone-shaped cardiac microtissues. The 3D cardiac microtissues exhibited physiologically relevant cardiac functions, including a reproducible inotropic response when stimulated with a β -adrenergic agonist, spontaneous beating, and expression of specific proteins such as α -actinin, F-actin, and phospho-connexin 43. The micromolding assembly technique meets the requirement for bioengineering complex cellular structures in native cardiac tissues. However, the fabrication of the templates increases the cost of the experiment.

Molecular Recognition-Assisted Self-Assembly

Molecular recognition-assisted self-assembly explores bio-orthogonal functional groups for generating predefined intercellular linkages between heterogeneous cells. The cell membrane is specifically modified with biorthogonal functional groups to selectively link cells. Dutta et al. successfully employed this technique to generate millimeter-scale, closely packed multilayered architecture with a predefined heterogeneous arrangement [85]. Following this work, Rogozhnikov et al. used the same technique for the assembly of functional cardiac microtissues from primary rat CMs, human umbilical vein endothelial cells (HUVECs) and fibroblasts [86]. All three cell types were treated with liposomes, which contained ketone or oxyamine groups. Chemical groups could be installed rapidly onto the cell surface by liposome delivery and fusion. Then, surface-engineered cells would be aggregated via oxime ligation. The bonding between ketone and oxyamine groups is a bio-orthogonal reaction that does not interfere with native biological processes. After 24 hours of culturing, 3D cardiac microtissues formed. CMs constituting cardiac microtissues could express cardio-specific ECM, and native propagation of Na^+ , K^+ , and Ca^{2+} ions across the cardiac microtissues was detected. Moreover, the cardiac microtissues expressed specific proteins such as CX43 and cardiac troponin T (cTnT). Notably, the molecular recognition-assisted self-assembly technique offers a noninvasive way for the bioassembly of 3D microtissues from most mammalian cell types. However, this approach cannot be used to fabricate cardiac microtissues with complex shapes and structures (e.g., tubes and rings) [40].

Maturation and Characterization of 3D Cardiac Microtissues

Maturation is an essential procedure for the formation of functional 3D cardiac microtissues. Generally, bioassembly techniques can form only a predefined heterogeneous cell arrangement or cytoarchitecture, and no intercellular connections are created between the CMs immediately after bioassembly. The formed cytoarchitecture is immobilized and transferred to a cell incubator for tissue maturation. During this process, intercellular connections (such as CX 43 and CX45) are established between the CMs. Simultaneously, CMs modify their local microenvironment by secreting their own ECM. Furthermore, biochemical factors [87] and biophysical stimulation [88] are usually required to treat cardiac microtissues for enhancing cellular maturation.

Immunohistochemical analysis is commonly used to evaluate the function of 3D cardiac microtissues. Various tissues are immunostained for the detection of cardio-specific marker expression. For example, CX 43 is a gap junction protein localized in cardiomyocyte mitochondria and is essential for intercellular connection and cardiac function [89]. The α -actinin plays an important role in the formation and maintenance of Z-lines [90], and its expression indicates the maturation of cardiac microtissues. Cardiac troponin T is a specific marker of CMs that presents in healthy cardiac tissues and is essential in cardiac muscle contraction and sarcomere assembly [91]. In addition to using immunofluorescence staining, Lu et al. studied gene expression in 3D cardiac microtissues such as myosin light chain 2 V (MLC2V), myosin heavy chain 6 (MYH6), myosin heavy chain 7 (MYH7), and the homeobox protein NKX2.5 to demonstrate the development of the tissues [92]. Further, cardiac contractility can reflect the function of cardiac microtissues [93]. For a healthy adult, the heart rate is 60–100 bpm and the contractile stress is between 6000 and 8000 Pa. In general, the contractile function of cardiac microtissues can be improved by increasing the purity of CMs and inducing CM alignment. Moreover, indicators such as contractile force [94–96] and action potential conduction [97, 98] can be used to demonstrate physiologically relevant characteristics of cardiac microtissues [99].

Applications of 3D Cardiac Microtissues

Cardiac Regenerative Therapy

After heart injury, human's heart is hardly to recover as the limitation of cardiomyocytes' proliferation block. At the same time, no clinical therapy is able to satisfactorily treat acute or chronic heart injury, including acute myocardial infarction, viral myocarditis, and heart failure. Cardiac regenerative therapy represents an emerging approach that holds great promise for restoring cardiac functions by transplanting bioengineered cardiac tissues to the injured site.

Vascularization has always been the most important consideration for all kinds of transplanted tissues. Using bioassembly, Sharon Fleischer et al. fabricated a

vascularized cardiac patch composed of different modular layers, including an endothelial cell layer, a cardiac layer, and a dexamethasone (DEX) layer [83]. The DEX layers were responsible for attenuating the activation of macrophages. A series of critical cardiac functions, such as electrical coupling in the z-direction between cardiac layers and expression of CX43 and α -sarcomeric actinin, were demonstrated on the generated cardiac patch in vitro. After orthotropic transplantation to a rat, vascular endothelial growth factor (VEGF) particles in the endothelial cell layers promoted the vascularization of the cardiac patch. In addition, the cardiac patch could be cultured in vivo for at least 2 weeks. 3D cardiac microtissues fabricated by bioassembly provide a promising in vitro approach for cardiac regenerative therapy.

Cardiac Physiological Study

The heart is one of the most vital organs to human body. Therefore, it is necessary to understand the biological functions and control mechanisms of the heart. Specifically, elongated tissue morphology, fast conduction velocity, and efficient contractility are the three most critical parameters that need to be evaluated in artificial cardiac tissue. 3D cardiac microtissue with a high cell-packing density and predefined pattern is more similar to native cardiac tissue than 2D cardiac model in terms of geometry and function. Therefore, 3D cardiac microtissues fabricated by bioassembly are regarded as a promising in vitro model to study cardiac physiological characteristics.

Huebsch et al. fabricated dogbone-shaped cardiac microtissues composed of iPSC-CMs and fibroblasts on a PDMS template by using a micromolding assembly [79]. The physiological function of the cardiac microtissues was analyzed in situ within the template. Neighboring cardiac microtissues could beat spontaneously without disturbing each other. In contrast, when a syncytium formed between two adjacent microtissues, a correlation in contractile motion was demonstrated. To determine the contractile force of the CMs directly, the two sides of the cardiac microtissue were connected to a force transducer and a moveable arm, respectively. In addition, the cardiac microtissues were cultured in a bath filled with Tyrode's solution. In this test, cardiac microtissues showed a typical Frank-Starling response, which represents the correlation between contractile force and cardiac microtissue length as determined by external stretching. In addition, contractile force increased when the extracellular calcium concentration was higher. Moreover, cardiac microtissues treated with a β -adrenergic agonist showed a dose-dependent inotropic response. In summary, the cardiac microtissues used in this work present a potential application for studying cardiac physiology in vitro.

Drug Screening

Cardiotoxicity presents a major cause for the failure of drug candidates, which not only limited to cardiac disease related drugs but also the other medicine which have

the possibility to lead to cardiotoxicity. However, 2D cardiac cell monolayers cannot faithfully recapitulate the complicated environment of the native cardiac tissue. Therefore, a realistic preclinical model is needed in order to improve the prediction accuracy of preclinical drug screening. Compared with a 2D monolayer culture, 3D cardiac microtissues cultured *in vitro* can better mimic native cardiac physiology and have been widely used in preclinical drug screening.

Rogozhnikov et al. utilized 3D cardiac microtissues, which were fabricated by molecular recognition-assisted self-assembly, as testing models to evaluate the effects of two drugs on beating rate [86]. In this study, 2D cardiac monolayers were used as the control group. One of these drugs, isoprenaline, is a nonselective β -adrenoreceptor agonist and is used to treat bradycardia. The other drug, doxorubicin, a chemotherapy medication used for cancer treatment, can cause severe side effects such as cardiotoxicity and lead to congestive heart failure. Cardiac microtissues that were exposed to isoprenaline (5 nM and 10 nM) or doxorubicin (100 μ M and 200 μ M) for 25 min showed an increase or decrease in beating rate, respectively. Moreover, with the increase in drug concentration, the effect was more significant. Compared with 2D cardiac models, 3D cardiac microtissues treated with isoprenaline were less sensitive to changes in pulse because drug transport to cells in a monolayer is greater than that in a 3D tissue. This result indicated that 2D monolayers cannot mimic organ function as completely as 3D cardiac microtissues. 3D cardiac microtissue has become a preferred physiologically relevant model for *in vitro* cardiotoxicity assessment.

Challenges and Future Perspectives

Although great advances have been made in inventing bioassembly techniques for generating physiologically relevant human cardiac microtissues, several challenges still need to be addressed. One of the challenges is to generate a functional vascular network in cardiac microtissues. The maturation and long-term survival of cardiac microtissues are dependent on the ability of the vascular system to provide efficient oxygen and nutrient exchange inside the tissues [100, 101]. Despite great progress, the challenges of vascularization and neoangiogenesis in assembled cardiac microtissues remain unmet [43, 86].

Additionally, none of the current bioassembly approaches can form arbitrary complex cytoarchitectures to faithfully recapitulate native multiscale heterogeneous cytoarchitectures. Most of the generated cardiac microtissues can recapitulate only some of the morphological features or functions native to cardiac tissue. None of the assembled cardiac tissues have been fully validated at the genetic, transcriptional, and metabolic levels. The formation of high-fidelity cardiac tissues requires improvement in current bioassembly techniques and a combination of multiple bioassembly approaches that can engineer complex multiscale cardiac architectures from native physiologically relevant cardiac cell populations. Melde et al. constructed arbitrary patterns of silicone particles by using an acoustic assembly technique and specific algorithms [102]. This method has great potential for the

generation of 3D cardiac microtissues with spatially defined geometry. In addition, DNA-programmed assembly may be an alternative method for fabricating cardiac microtissues with programmed shapes [103].

In summary, bioassembly approaches represent an emerging technical route in the field of biofabrication and are effective tools for generating cardiac microtissues. Cardiac microtissues have been proven useful in many research fields. We believe that with the rapid development in cell biology and bioengineering technology, cardiac microtissues that closely mimic the native heart tissue structure and function will be generated in vitro using bioassembly methods. Meanwhile, this technical route will vigorously promote the development of basic biomedical research and clinical therapies.

Acknowledgment We gratefully acknowledge financial support from the National Key Research and Development Program of China (No. 2018YFA0109000) and the National Natural Science Foundation of China (No. 31871018).

References

1. Khademhosseini A, Langer R. A decade of progress in tissue engineering. *Nat Protoc*. 2016;11(10):1775–81.
2. Underhill GH, Khetani SR. Bioengineered liver models for drug testing and cell differentiation studies. *Cell Mol Gastroenterol Hepatol*. 2018;5(3):426–439 e1.
3. Breslin S, O'Driscoll L. Three-dimensional cell culture: the missing link in drug discovery. *Drug Discov Today*. 2013;18(5–6):240–9.
4. Guven S, et al. Multiscale assembly for tissue engineering and regenerative medicine. *Trends Biotechnol*. 2015;33(5):269–79.
5. Ogoke O, Oluwole J, Parashurama N. Bioengineering considerations in liver regenerative medicine. *J Biol Eng*. 2017;11:46.
6. Parsa H, Ronaldson K, Vunjak-Novakovic G. Bioengineering methods for myocardial regeneration. *Adv Drug Deliv Rev*. 2016;96:195–202.
7. Madl CM, Heilshorn SC, Blau HM. Bioengineering strategies to accelerate stem cell therapeutics. *Nature*. 2018;557(7705):335–42.
8. Kharaziha M, et al. Nano-enabled approaches for stem cell-based cardiac tissue engineering. *Adv Healthc Mater*. 2016;5(13):1533–53.
9. Mazzoleni G, Di Lorenzo D, Steimberg N. Modelling tissues in 3D: the next future of pharmaco-toxicology and food research? *Genes Nutr*. 2009;4(1):13–22.
10. Ralph JC, de Lange WJ. 3D engineered cardiac tissue models of human heart disease: learning more from our mice. *Trends Cardiovasc Med*. 2013;23(2):27–32.
11. Curtis MW, Russell B. Cardiac tissue engineering. *J Cardiovasc Nurs*. 2009;24(2):87–92.
12. Hirt MN, Hansen A, Eschenhagen T. Cardiac tissue engineering: state of the art. *Circ Res*. 2014;114(2):354–67.
13. Brown GE, Khetani SR. Microfabrication of liver and heart tissues for drug development. *Philos Trans R Soc Lond Ser B Biol Sci*. 2018;373(1750):20170225.
14. Abassi YA, et al. Dynamic monitoring of beating periodicity of stem cell-derived cardiomyocytes as a predictive tool for preclinical safety assessment. *Br J Pharmacol*. 2012;165(5):1424–41.
15. CsobonyeiOVA M, Polak S, Danisovic L. Toxicity testing and drug screening using iPSC-derived hepatocytes, cardiomyocytes, and neural cells. *Can J Physiol Pharmacol*. 2016;94(7):687–94.
16. Li X, et al. Cardiotoxicity screening: a review of rapid-throughput in vitro approaches. *Arch Toxicol*. 2016;90(8):1803–16.

17. Himmel HM. Drug-induced functional cardiotoxicity screening in stem cell-derived human and mouse cardiomyocytes: effects of reference compounds. *J Pharmacol Toxicol Methods*. 2013;68(1):97–111.
18. Qureshi ZP, et al. Market withdrawal of new molecular entities approved in the United States from 1980 to 2009. *Pharmacoepidemiol Drug Saf*. 2011;20(7):772–7.
19. MacDonald JS, Robertson RT. Toxicity testing in the 21st century: a view from the pharmaceutical industry. *Toxicol Sci*. 2009;110(1):40–6.
20. Bajaj P, et al. 3D biofabrication strategies for tissue engineering and regenerative medicine. *Annu Rev Biomed Eng*. 2014;16:247–76.
21. Pedde RD, et al. Emerging biofabrication strategies for engineering complex tissue constructs. *Adv Mater*. 2017;29(19).
22. Mironov V, et al. Biofabrication: a 21st century manufacturing paradigm. *Biofabrication*. 2009;1(2):022001.
23. Ferris CJ, et al. Biofabrication: an overview of the approaches used for printing of living cells. *Appl Microbiol Biotechnol*. 2013;97(10):4243–58.
24. Moroni L, et al. Biofabrication: a guide to technology and terminology. *Trends Biotechnol*. 2018;36(4):384–402.
25. Wu LQ, Payne GF. Biofabrication: using biological materials and biocatalysts to construct nanostructured assemblies. *Trends Biotechnol*. 2004;22(11):593–9.
26. Groll J, et al. Biofabrication: reappraising the definition of an evolving field. *Biofabrication*. 2016;8(1):013001.
27. Moroni L, et al. Biofabrication strategies for 3D in vitro models and regenerative medicine. *Nat Mater*. 2018;3(5):21–37.
28. Murphy SV, Atala A. 3D bioprinting of tissues and organs. *Nat Biotechnol*. 2014;32(8):773–85.
29. Patra S, Young V. A review of 3D printing techniques and the future in biofabrication of bioprinted tissue. *Cell Biochem Biophys*. 2016;74(2):93–8.
30. Guillemot F, Mironov V, Nakamura M. Bioprinting is coming of age: report from the international conference on bioprinting and biofabrication in Bordeaux (3B'09). *Biofabrication*. 2010;2(1):010201.
31. Serpooshan V, et al. Bioengineering cardiac constructs using 3D printing. *J 3D Printing Med*. 2017;1(2):123–39.
32. Xu T, et al. Fabrication and characterization of bio-engineered cardiac pseudo tissues. *Biofabrication*. 2009;1(3):035001.
33. Colosi C, et al. Microfluidic bioprinting of heterogeneous 3D tissue constructs using low-viscosity bioink. *Adv Mater*. 2016;28(4):677–84.
34. Zhang YS, et al. Bioprinting 3D microfibrillar scaffolds for engineering endothelialized myocardium and heart-on-a-chip. *Biomaterials*. 2016;110:45–59.
35. Gaetani R, et al. Cardiac tissue engineering using tissue printing technology and human cardiac progenitor cells. *Biomaterials*. 2012;33(6):1782–90.
36. Pati F, et al. Printing three-dimensional tissue analogues with decellularized extracellular matrix bioink. *Nat Commun*. 2014;5:3935.
37. Gaebel R, et al. Patterning human stem cells and endothelial cells with laser printing for cardiac regeneration. *Biomaterials*. 2011;32(35):9218–30.
38. Norotte C, et al. Scaffold-free vascular tissue engineering using bioprinting. *Biomaterials*. 2009;30(30):5910–7.
39. Ong CS, et al. Creation of cardiac tissue exhibiting mechanical integration of spheroids using 3D bioprinting. *J Vis Exp*. 2017;(125).
40. Ong CS, et al. Biomaterial-free three-dimensional bioprinting of cardiac tissue using human induced pluripotent stem cell derived cardiomyocytes. *Sci Rep*. 2017;7(1):4566.
41. Neuman RE, Logan MA. The determination of collagen and elastin in tissues. *J Biol Chem*. 1950;186(2):549–56.
42. Zhu Y, et al. Tissue engineering of 3D organotypic microtissues by acoustic assembly. *Methods Mol Biol*. 2017. https://doi.org/10.1007/7651_2017_68.

43. Serpooshan V, et al. Bioacoustic-enabled patterning of human iPSC-derived cardiomyocytes into 3D cardiac tissue. *Biomaterials*. 2017;131:47–57.
44. Naseer SM, et al. Surface acoustic waves induced micropatterning of cells in gelatin methacryloyl (GelMA) hydrogels. *Biofabrication*. 2017;9(1):015020.
45. Yamamoto Y, et al. Preparation of artificial skeletal muscle tissues by a magnetic force-based tissue engineering technique. *J Biosci Bioeng*. 2009;108(6):538–43.
46. Hogan M, Souza G, Birla R. Assembly of a functional 3D primary cardiac construct using magnetic levitation. *AIMS Bioeng*. 2016;3(3):277–88.
47. Turker E, Arslan-Yildiz A. Recent advances in magnetic levitation: a biological approach from diagnostics to tissue engineering. *ACS Biomater Sci Eng*. 2018;4(3):787–99.
48. Kelm JM, Fussenegger M. Microscale tissue engineering using gravity-enforced cell assembly. *Trends Biotechnol*. 2004;22(4):195–202.
49. Kelm JM, et al. Tissue-transplant fusion and vascularization of myocardial microtissues and macro-tissues implanted into chicken embryos and rats. *Tissue Eng*. 2006;12(9):2541–53.
50. Luo W, et al. Remote control of tissue interactions via engineered photo-switchable cell surfaces. *Sci Rep*. 2014;4:6313.
51. O'Brien PJ, et al. Spheroid and tissue assembly via click chemistry in microfluidic flow. *Bioconjug Chem*. 2015;26(9):1939–49.
52. Chen P, et al. Biotunable acoustic node assembly of organoids. *Adv Healthc Mater*. 2015;4(13):1937–43.
53. Bouyer C, et al. A Bio-Acoustic Levitational (BAL) assembly method for engineering of multilayered, 3D brain-like constructs, using human embryonic stem cell derived neuroprogenitors. *Adv Mater*. 2016;28(1):161–7.
54. Olofsson K, et al. Acoustic formation of multicellular tumor spheroids enabling on-chip functional and structural imaging. *Lab Chip*. 2018;18(16):2466–76.
55. Binks D, vandeWater W. Nonlinear pattern formation of Faraday waves. *Phys Rev Lett*. 1997;78(21):4043–6.
56. Westra M-T, Binks DJ, Van De Water W. Patterns of Faraday waves. *J Fluid Mech*. 2003;496:1–32.
57. Chen P, et al. Microscale assembly directed by liquid-based template. *Adv Mater*. 2014;26(34):5936–41.
58. Lin SC, Mao X, Huang TJ. Surface acoustic wave (SAW) acoustophoresis: now and beyond. *Lab Chip*. 2012;12(16):2766–70.
59. Kirschner J. Surface Acoustic Wave Sensors (SAWS). *Micromechanical systems*. 2010.
60. Shi J, et al. Focusing microparticles in a microfluidic channel with standing surface acoustic waves (SSAW). *Lab Chip*. 2008;8(2):221–3.
61. Ding XY, et al. On-chip manipulation of single microparticles, cells, and organisms using surface acoustic waves. *Proc Natl Acad Sci U S A*. 2012;109(28):11105–9.
62. Collins DJ, et al. Two-dimensional single-cell patterning with one cell per well driven by surface acoustic waves. *Nat Commun*. 2015;6:8686.
63. Guo F, et al. Three-dimensional manipulation of single cells using surface acoustic waves. *Proc Natl Acad Sci U S A*. 2016;113(6):1522–7.
64. Souza GR, et al. Three-dimensional tissue culture based on magnetic cell levitation. *Nat Nanotechnol*. 2010;5(4):291–6.
65. Tseng H, et al. Assembly of a three-dimensional multitype bronchiole coculture model using magnetic levitation. *Tissue Eng Part C Methods*. 2013;19(9):665–75.
66. Daquinag AC, Souza GR, Kolonin MG. Adipose tissue engineering in three-dimensional levitation tissue culture system based on magnetic nanoparticles. *Tissue Eng Part C Methods*. 2013;19(5):336–44.
67. Frey O, et al. Reconfigurable microfluidic hanging drop network for multi-tissue interaction and analysis. *Nat Commun*. 2014;5:4250.
68. Desroches BR, et al. Functional scaffold-free 3-D cardiac microtissues: a novel model for the investigation of heart cells. *Am J Physiol Heart Circ Physiol*. 2012;302(10):H2031–42.

69. Foty R. A simple hanging drop cell culture protocol for generation of 3D spheroids. *J Vis Exp*. 2011;(51).
70. Tung YC, et al. High-throughput 3D spheroid culture and drug testing using a 384 hanging drop array. *Analyst*. 2011;136(3):473–8.
71. Emmert MY, et al. Human stem cell-based three-dimensional microtissues for advanced cardiac cell therapies. *Biomaterials*. 2013;34(27):6339–54.
72. Kelm JM, et al. Design of artificial myocardial microtissues. *Tissue Eng*. 2004;10(1–2):201–14.
73. Beauchamp P, et al. Development and characterization of a scaffold-free 3D spheroid model of induced pluripotent stem cell-derived human cardiomyocytes. *Tissue Eng Part C Methods*. 2015;21(8):852–61.
74. Rismani Yazdi S, et al. Adding the ‘heart’ to hanging drop networks for microphysiological multi-tissue experiments. *Lab Chip*. 2015;15(21):4138–47.
75. Schmid YRF, et al. Electrical impedance spectroscopy for microtissue spheroid analysis in hanging-drop networks. *ACS Sensors*. 2016;1(8):1028–35.
76. Karp JM, et al. Controlling size, shape and homogeneity of embryoid bodies using poly(ethylene glycol) microwells. *Lab Chip*. 2007;7(6):786–94.
77. Ma Z, et al. Self-organizing human cardiac microchambers mediated by geometric confinement. *Nat Commun*. 2015;6:7413.
78. Hoang P, et al. Generation of spatial-patterned early-developing cardiac organoids using human pluripotent stem cells. *Nat Protoc*. 2018;13(4):723–37.
79. Huebsch N, et al. Miniaturized iPSC-cell-derived cardiac muscles for physiologically relevant drug response analyses. *Sci Rep*. 2016;6:24726.
80. Rivron NC, et al. Tissue deformation spatially modulates VEGF signaling and angiogenesis. *Proc Natl Acad Sci U S A*. 2012;109(18):6886–91.
81. Khademhosseini A, et al. Microscale technologies for tissue engineering and biology. *Proc Natl Acad Sci U S A*. 2006;103(8):2480–7.
82. Bao M, et al. 3D microniches reveal the importance of cell size and shape. *Nat Commun*. 2017;8(1):1962.
83. Fleischer S, et al. Modular assembly of thick multifunctional cardiac patches. *Proc Natl Acad Sci U S A*. 2017;114(8):1898–903.
84. Lee BW, et al. Modular assembly approach to engineer geometrically precise cardiovascular tissue. *Adv Healthc Mater*. 2016;5(8):900–6.
85. Dutta D, et al. Synthetic chemoselective rewiring of cell surfaces: generation of three-dimensional tissue structures. *J Am Chem Soc*. 2011;133(22):8704–13.
86. Rogozhnikov D, et al. Scaffold free bio-orthogonal assembly of 3-dimensional cardiac tissue via cell surface engineering. *Sci Rep*. 2016;6:39806.
87. Ribeiro MC, et al. Functional maturation of human pluripotent stem cell derived cardiomyocytes in vitro—correlation between contraction force and electrophysiology. *Biomaterials*. 2015;51:138–50.
88. Godier-Furnemont AF, et al. Physiologic force-frequency response in engineered heart muscle by electromechanical stimulation. *Biomaterials*. 2015;60:82–91.
89. Boengler K, Heusch G, Schulz R. Connexin 43 and ischemic preconditioning: effects of age and disease. *Exp Gerontol*. 2006;41(5):485–8.
90. Melo TG, et al. Disarray of sarcomeric alpha-actinin in cardiomyocytes infected by *Trypanosoma cruzi*. *Parasitology*. 2006;133(Pt 2):171–8.
91. Sehnert AJ, et al. Cardiac troponin T is essential in sarcomere assembly and cardiac contractility. *Nat Genet*. 2002;31(1):106–10.
92. Lu HF, et al. Engineering a functional three-dimensional human cardiac tissue model for drug toxicity screening. *Biofabrication*. 2017;9(2):025011.
93. Liao B, Zhang DH, Bursac N. Functional cardiac tissue engineering. *Regen Med*. 2012;7(2):187–206.
94. Sasaki D, et al. Contractile force measurement of human induced pluripotent stem cell-derived cardiac cell sheet-tissue. *PLoS One*. 2018;13(5):e0198026.

95. Lind JU, et al. Cardiac microphysiological devices with flexible thin-film sensors for higher-throughput drug screening. *Lab Chip*. 2017;17(21):3692–703.
96. Lee S, et al. Contractile force generation by 3D hiPSC-derived cardiac tissues is enhanced by rapid establishment of cellular interconnection in matrix with muscle-mimicking stiffness. *Biomaterials*. 2017;131:111–20.
97. Zhang D, et al. Tissue-engineered cardiac patch for advanced functional maturation of human ESC-derived cardiomyocytes. *Biomaterials*. 2013;34(23):5813–20.
98. Shadrin IY, et al. Cardiopatch platform enables maturation and scale-up of human pluripotent stem cell-derived engineered heart tissues. *Nat Commun*. 2017;8(1):1825.
99. Zhang D, Pu WT. Exercising engineered heart muscle to maturity. *Nat Rev Cardiol*. 2018;15(7):383–4.
100. Kang HW, et al. A 3D bioprinting system to produce human-scale tissue constructs with structural integrity. *Nat Biotechnol*. 2016;34(3):312–9.
101. Lee S, et al. Microfluidic-based vascularized microphysiological systems. *Lab Chip*. 2018;18(18):2686–709.
102. Melde K, et al. Acoustic fabrication via the assembly and fusion of particles. *Adv Mater*. 2018;30(3):1704507.
103. Todhunter ME, et al. Programmed synthesis of three-dimensional tissues. *Nat Methods*. 2015;12(10):975–81.



From Bench to Clinic: Translation of Cardiovascular Tissue Engineering Products to Clinical Applications

7

Amanda N. Steele and Y. Joseph Woo

Introduction

Cardiovascular disease is a major global health crisis and continues to be the leading cause of mortality, accounting for 31.5% of deaths worldwide [1]. An estimated 23 million Americans suffer from ischemic heart disease, a number that is expected to rise up to 46% by 2030 [2]. Annual healthcare expenditures due to ischemic heart disease are staggering, amounting to over a quarter of a trillion dollars, and are projected to double in the next 10 years [1, 2]. The mortality rate of coronary heart disease (CHD) has fallen substantially over the last several decades, which can largely be attributed to improvements in primary prevention strategies and secondary interventions [3, 4]. However, despite improved survival, many patients will succumb to heart failure due to the inability to reverse or prevent the progressive functional deterioration following ischemic cardiomyopathy. Revascularization techniques such as percutaneous coronary intervention (PCI) and coronary artery bypass grafting (CABG) are only possible in 60–80% of patients, and even then, treatments are often initiated late into disease progression [5]. Furthermore, interventions such as PCI and CABG focus on macrovascular reperfusion and neglect the presence of significant microvascular malperfusion. While large vessels are reperfused, this

A. N. Steele · Y. J. Woo (✉)
Department of Cardiothoracic Surgery, Stanford University,
Stanford, CA, USA

Department of Bioengineering, Stanford University,
Stanford, CA, USA
e-mail: anstele@stanford.edu; joswoo@stanford.edu

microvascular perfusion deficit can lead to endothelial cell (EC) dysfunction, cardiomyocyte death, and adverse ventricular remodeling, ultimately leading to heart failure [6–8]. Thus, there is an extraordinary clinical need to investigate adjunct therapies to regenerate, repair, and reverse the maladaptive responses secondary to ischemic cardiomyopathy.

Over the past two decades, cardiovascular tissue engineering technology has demonstrated exciting progress and is now widely used in preclinical research. Advances in stem cell biology, angiogenesis, and regenerative signaling, as well as biomaterials science, have enabled translation from preclinical validation studies to clinical application. As such, there has been tremendous interest in applying diverse tissue engineering products to the ischemic heart. This chapter will focus on the various tissue engineering strategies that address the limitations of current therapies to regenerate functional myocardial tissue.

Cytokine and Growth Factor Therapy

Due to our improved understanding of the mechanisms and signaling pathways that underlie blood vessel formation and tissue regeneration, protein therapy has emerged as a promising strategy to repair the ischemic myocardium [9]. Administering therapeutic cytokines and growth factors (GFs) can modulate inflammatory responses and biological processes and, therefore, can alter disease progression [10–12]. Specifically, angiogenic cytokines and GFs stimulate the formation or remodeling of blood vessels either through angiogenesis (creation of blood vessels from existing vessel), vasculogenesis (de novo formation of new blood vessels), or arteriogenesis (arterioles remodeling into larger collateral arteries). These processes encourage therapeutic micro-revascularization of the ischemic heart thereby enhancing tissue oxygenation and reducing cardiomyocyte death [13]. Thus far, many angiogenic cytokines have been discovered and evaluated including vascular endothelial growth factor (VEGF), fibroblast growth factor (FGF), placental growth factor (PGF), hepatocyte growth factor (HGF), and stromal cell-derived factor-1 α (SDF-1) [13, 14]. Of these, VEGF is one of the most widely studied angiogenic cytokines and functions via its receptor on endothelial cells (EC) to produce nitric oxide, enhance EC survival, mobilize endothelial progenitor cells (EPC), induce EPC mitosis, and enhance vascular permeability and vasodilation [14]. A number of positive functional results in preclinical animal studies of myocardial infarction initiated a multitude of human trials involving VEGF treatment. While several studies demonstrated that VEGF was safe and promoted symptomatic relief via reduced ischemia, many of these effects were transient as determined in more rigorous phase II clinical trials [15–18].

HGF has also been evaluated in the treatment of heart diseases due to its pronounced anti-apoptotic, chemotactic, and proliferative effects on cardiac-relevant cell types, in addition to its ability to promote angiogenesis [19–21]. The beneficial pleiotropic effects of HGF have led to its translation to phase I clinical trials in which HGF therapy using adenovirus vector (Ad-HGF) was delivered as an adjunct

therapy to CABG [22, 23]. Preliminary safety and efficacy results confirmed the long-term safety of intracoronary delivery of Ad-HGF for treating severe coronary disease in addition to an improvement in ejection fraction [23].

Finally, SDF-1 has unique pro-angiogenic behavior due to its capacity to potently stimulate migration of EPCs and other hematopoietic cells to participate in angio- and vasculogenesis, ultimately resulting in reduced ventricular remodeling and fibrosis [24–26]. Notably, SDF-1 binding and stimulation of EPCs require the expression of its receptor, CCR4, which is upregulated on EPCs during hypoxia. Thus, SDF-1 appears to be a key candidate for therapeutic targeting in ischemic heart disease [27]. Clinical studies of SDF-1 therapy have been actively conducted using non-viral gene transfer and plasmid expressing SDF-1. Phase I trials have found SDF-1 delivery to be safe with improvements in symptoms [28]. These encouraging results promoted a phase II study of SDF-1 in patients with ischemic cardiomyopathy, in which a small improvement in ejection fraction was observed at 12 months [29].

Additionally, proliferative, or cell-cycle inducing GFs have also demonstrated therapeutic benefit in preclinical and clinical studies of ischemic heart disease. The four extracellular factors known to induce proliferation of differentiated cardiomyocytes include insulin-like growth factor-1 (IGF-1), FGF-1, periostin, and neuregulin-1 (NRG-1). Interestingly, all of these ligands require signal mediation via PI3-kinase [30–32]. The most widely studied cell-cycle inducing GF in human clinical trials is NRG-1, an agonist for receptor tyrosine kinases of the epidermal growth factor receptor family. The importance of NRG-1 signaling in the adult heart first became apparent when women with cancer receiving NRG-1 receptor blocking antibody, Herceptin, developed cardiomyopathy [30, 33]. A number of promising preclinical studies spurred a cascade of human clinical trials to test the safety and efficacy of NRG-1 in patients with cardiomyopathy [34–37]. A phase II, randomized, double-blinded, placebo-controlled study in patients with chronic heart failure demonstrated that delivery of recombinant human NRG-1 enhanced left ventricular function and limited negative remodeling [36]. Phase III trials studying efficacy of patients with chronic heart failure are ongoing and an interim analysis showed a statistically significant decrease in mortality [37, 38].

Stem Cell Therapy

Over the past few decades, there has been a surge in the development of stem cell therapies to treat cardiovascular disease, many of which have quickly progressed to clinical trials. The initial goal of cellular therapy was to deliver cells to repopulate and regenerate the damaged and diseased area; however, due to poor retention rates, beneficial effects observed from cell therapy are likely due to paracrine factors which mobilize endogenous repair mechanisms [39–41]. A number of different cell lineages have been evaluated in clinical studies thus far, including mesenchymal stem cells (MSCs), bone marrow-derived stem cells (BMSCs), skeletal myoblasts, adipose-derived stem cells (ASCs), and cardiac stem cells (CSCs) [41, 42]. Of these,

the most widely studied are MSCs and BMSCs, which in large, have demonstrated feasibility and safety [43, 44]. MSCs are especially advantageous because they can differentiate into all cells of the mesodermal lineage and release a broad range of growth factors and cytokines that modulate cardiomyocyte apoptosis, inflammation, and angiogenesis [42, 43]. Furthermore, MSCs lack major histocompatibility complex class II antigens and therefore do not require immunosuppression if harvested from an allogenic source, thereby enabling potential off-the-shelf products [45]. In 2014, 30 patients with end-stage heart failure were randomized to receive an intramyocardial injection of 25 million MSCs or cell medium concurrent with left ventricular device (LVAD) implantation. This was an early-phase, multicenter, double-blinded study aimed to explore safety and efficacy and the first trial to evaluate allogenic MSCs in patients undergoing LVAD with advanced heart failure [43]. Based on the greater number of MSC patients experiencing successful temporary LVAD weans at 90 days, the study concluded that administration of MSCs was feasible and safe with a trend toward functional efficacy [43]. Interestingly, a recent randomized phase II blinded study highlighted the crucial role of MSC dose and concentration in the functional response to cell therapy. This trial demonstrated that in patients with ischemic cardiomyopathy, a dose of 100 million MSCs resulted in enhanced ejection fraction compared to those who received the 20 million doses [46]. Optimizing cell dose is critical to advance in the field of cell therapy and opens the field for further phase III investigation.

Compared to MSCs, BMSCs are more difficult to isolate and clinical trials involving BMSCs have led to more inconsistent results in terms of functional benefit [47]. BMSCs contain a number of different stem and progenitor populations, and preclinical studies indicate that the therapeutic benefit likely derives from angiogenic paracrine signaling [48]. A phase I and phase II randomized trial aimed to compare MSCs with BMSCs by evaluating patients receiving MSC injection to a placebo group versus patients receiving BMSCs to placebo. At the 12-month follow-up, viable tissue mass, walk distance, and regional myocardial function significantly improved only in the MSC group, not in the BMSC group [49]. These results support the importance of a specific cell source for the treatment of ischemic cardiomyopathy.

A few trials investigated the regenerative potential of skeletal myoblasts in hopes that they would repopulate post-infarction scar tissue with functional contractile cells. However, further evaluation of this stem cell population was discontinued due to the high number of adverse cardiac events (i.e., arrhythmias) secondary to myoblast transplantation and the emergence of other stem cell sources (e.g., MSC) that are easier to obtain [50]. One such lineage is adipose-derived stem cells (ASCs), which can be harvested from adipose tissue of patients with minimal invasiveness [45]. ASCs are also capable of differentiating into mesodermal lineages, and have demonstrated superiority to BMSCs in preclinical studies [51]. The first prospective, randomized, placebo-controlled, double-blind study evaluating the safety and feasibility of ASC in patients with advanced ischemic cardiomyopathy was completed in 2014 [52]. ASCs were isolated via patient liposuction aspirates and prepared for

immediate administration. A total of 27 patients were enrolled in the study, and at a 6-month follow-up, patients who received ASC injections ($n = 21$) had modest improvements in myocardial perfusion, scar size, and left ventricular contractility [52]. This study confirmed the safety and feasibility of ASC treatment, and has encouraged follow-up studies involving larger patient sample sizes and ASCs from allogenic sources [53].

The adult heart was generally considered a terminally differentiated organ, incapable of self-renewal until the discovery and delineation of CSCs [54, 55]. Anversa et al. were the first to describe the CSC population, defined as Lin^{NEG}c-kit^{POS} cells, which were self-renewing and multipotent with the ability to give rise to myocytes, smooth muscle cells, and endothelial cells [55]. Results from initial preclinical studies were promising, demonstrating that delivery of CSCs to the infarcted myocardium could regenerate tissue, reduce infarct size, and enhance left ventricular function [55–57]. The first in-human, phase I randomized, open-label trial of autologous c-kit⁺ cells in patients with heart failure was initiated in 2009 in patients undergoing CABG [58]. A total of 33 patients were enrolled in the SCPIO study, and cardiac magnetic resonance revealed that patients who received autologous CSC infusion had a striking improvement in both global and regional left ventricular function [58, 59]. Furthermore, CSC infusion also resulted in an increase in viable tissue that persisted for at least 12 months [58]. Encouraging phase I clinical results from CSCs have warranted further, larger studies [60, 61]. However, due to a recently reported concern with the reproducibility of some of the CSC studies, a moratorium has been issued from the National Institutes of Health (NIH) on the use of CSC in cell therapy trials.

Despite the number of clinical studies which have evaluated stem cell therapy, initial enthusiasm has declined due to disappointing and conflicting clinical results [41]. This is likely due to a number of factors, but a major challenge is cell retention. Cell retention is influenced by the mode of administration which has been distributed among intracoronary, intramyocardial, transendocardial, and transepicardial injection techniques in clinical studies [42, 62]. Intracoronary delivery has severe limitations because it relies on successful homing of the cells to the damaged tissue and subsequent extravasation. If the cells successfully navigate these obstacles, they are then subjected to a hostile microenvironment, further reducing their chance of survival and eliminating a therapeutic effect. Direct injection into cardiac tissue may be a preferred method of delivery due to the cells being deposited directly to the intended site. However, injecting cells through a needle subjects them to significant shear forces that can fatally disrupt the cellular membrane, resulting in post-transplantation viability as low as 1–32% [63–65]. Therefore, to fully harness the therapeutic potential of stem cell delivery, we must first determine an optimal transplantation technique that protects cells during delivery and supports engraftment into the myocardium thereafter. Finally, because studies have pointed to a difference in efficacy among stem cell types, clinical studies would further benefit from determination of the optimal cell type for cardiac-specific indications [41, 45, 60].

Hydrogels

A major limitation of both direct protein therapy and stem cell therapy is the therapeutic effect and is transient, which may explain why clinical trials with both types of therapies have resulted in modest clinical improvements [13, 16, 17, 66]. In the case of protein therapy, delivered cytokines and GFs are subject to diffusion away from the intended site, rapid *in vivo* degradation and reduced *in vivo* stability [67]. Similarly, stem cells injected into the ischemic myocardium are subjected to a harsh microenvironment with damaged extracellular matrix (ECM), thereby resulting in poor retention rates and rapid cell death [65, 66]. An extremely promising strategy to overcome the limitations of both protein and stem cell therapy is to encapsulate these treatments within hydrogels.

Hydrogels are water-swollen, insoluble networks of cross-linked polymers used for a variety of biomedical applications [68]. Due to their tissue-like elasticity, biocompatibility and biomimetic permeability, hydrogels are ideal delivery vehicles for cells, cytokines, and other biomolecules for regenerative medicine. Hydrogels can be derived from natural and/or synthetic polymers and are largely classified based on chemical or physical cross-linking mechanisms [69]. While biologically derived hydrogels are advantageous due to their bioactivity and the ability to communicate with surrounding cells via cell surface receptors, natural hydrogels suffer from limited mechanical tunability and batch-to-batch variation [68–71]. Synthetic hydrogels are advantageous due to their easily tunable mechanics, degradation, and immobilization of cargo, which optimizes controlled delivery [68, 69]. Yet, compared to natural hydrogels, synthetic hydrogels may have reduced biocompatibility [70, 71]. As a result of these challenges, significant research has gone into developing hybrid hydrogels, which incorporate both natural and synthetic polymer components, thereby harnessing the advantages of each. Thus, hybrid hydrogels can mimic tissues in both mechanical and biological properties [71].

To date, there have only been a few clinical trials evaluating the safety and efficacy of hydrogels for the treatment of cardiomyopathy, though there has been an abundance of small animal studies [68, 69, 72–74]. In 2015, an alginate-based hydrogel delivered via direct intramyocardial injection was evaluated in patients with advanced heart failure. The purpose of the hydrogel was to serve as a prosthetic scaffold to prevent further left ventricular dilation. Patients receiving the hydrogel treatment demonstrated improved exercise capacity and symptoms at a 6-month follow-up, though further clinical studies are needed to validate these results [75]. More recently, a phase I trial was initiated evaluating the safety and feasibility of a cardiac extracellular matrix hydrogel to treat patients who have experienced a large ST elevation myocardial infarction. The hydrogel was delivered trans-endocardially and secondary endpoints will look at efficacy variables of end systolic volume, end diastolic volume, ejection fraction, and scar mass. The estimated completion date of this study is October 2018, and the reporting of results should follow within the following year [76].

One explanation as to why hydrogels have not yet been applied widely to clinical cardiomyopathy research is due to suboptimal mechanical properties. In addition to

biocompatibility, perhaps the most important characteristic of hydrogels for cardiac tissue engineering is the ability to be delivered in a minimally invasive manner, which may explain why so few have made it to clinical trials. Injectability significantly facilitates their translation into clinical practice because it eliminates the need for an open-chest surgery. This requirement has been uniquely addressed by a novel class of hydrogels which undergo shear-thinning and self-healing behavior. Shear-thinning, self-healing hydrogels have reversible cross-links which indicate that the cross-links can break and re-form depending on the applied shear stress [68, 77]. For example, when the formed hydrogel is placed under a shear stress, as in the case of injection, the cross-links break apart, and the hydrogel undergoes a phase change to a liquid state, enabling easy injection. As soon as the hydrogel exits the syringe, the cross-links immediately re-form, and the hydrogel is once again in a solid gel state.

Our group recently reported on a novel shear-thinning hydrogel, termed SHIELD (shear-thinning hydrogel for injectable encapsulation and long-term delivery), to deliver an engineered HGF fragment to the ischemic myocardium (Fig. 7.1) [67]. We demonstrated that SHIELD could prolong the release of the HGF fragment

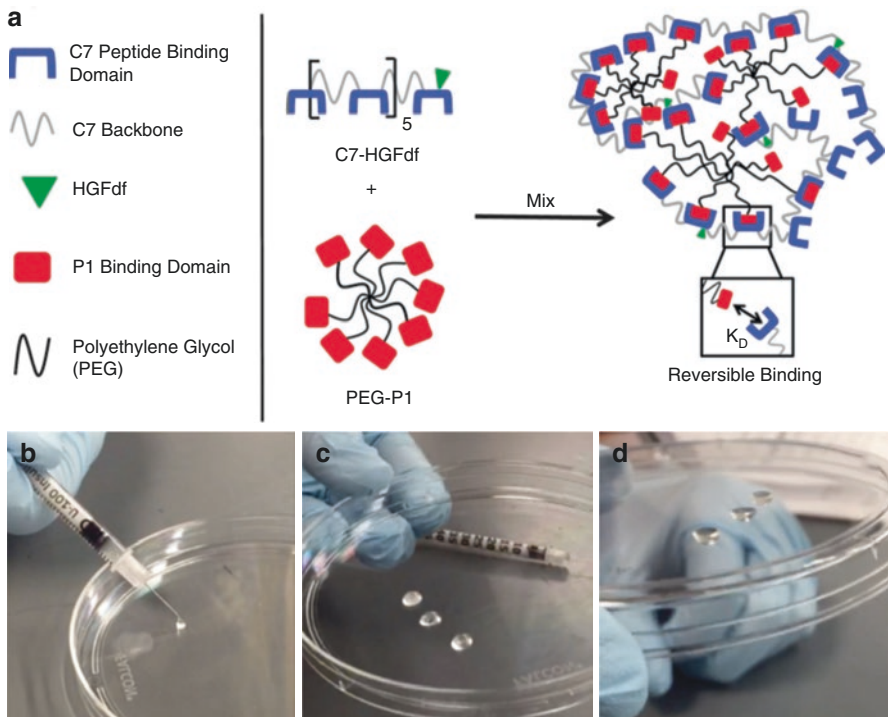


Fig. 7.1 (a) Shear-thinning hydrogel for injectable encapsulation and long-term delivery (SHIELD) is composed of an engineered protein and peptide-conjugated polymer. (b–d) Shear-thinning and self-healing behavior of SHIELD during injection. (Adapted from Steele et al. [67])

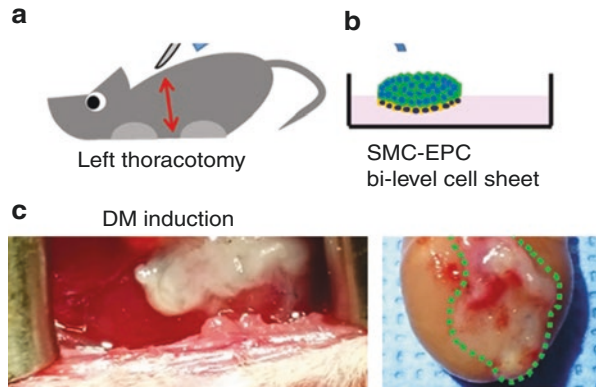
for over 2 weeks, and minimally invasive delivery of this treatment resulted in enhanced angiogenesis, reduced infarct size, and improved left ventricular function [67]. Burdick et al. published on the design of a shear-thinning hydrogel which underwent a guest-host assembly mechanism to facilitate ex vivo injection and rapid in vivo material retention [78]. In a large animal sheep model, the hydrogel was delivered percutaneously via an Agilis™ NxT steerable inducer and BRK™ trans-septal needle. In a porcine model, it was shown that hydrogel injections helped to reduce negative left ventricular remodeling following myocardial infarction (MI) [79]. While a hydrogel with the ideal mechanical and biological properties is still under development, the advent of new shear-thinning hydrogel technologies enables the opportunity for translation to clinical trials. Bioengineered shear-thinning, self-healing hydrogels have the potential to deliver therapeutic peptides and cells in a minimally invasive, percutaneous approach, thereby providing an effective clinical option for patients suffering from cardiomyopathy.

Cell Sheets

Another strategy to enhance cellular retention following transplantation is to utilize cell sheet technology, which avoids the loss of cell-cell communication and extracellular matrix and evades shear forces during injection, thereby extending the therapeutic window. Furthermore, cell sheets have also demonstrated the ability to eliminate arrhythmogenicity of some injection-based methods [80]. Cell sheets are constructed using a temperature-responsive, polymer-coated cell culture dish which interacts with cells differentially based on the culture temperature. To create the sheets, cells are plated on special culture dishes coated with poly-*N*-isopropylacrylamide. At 37 °C, the surface of the polymer is hydrophobic, allowing the cells to adhere. Once the cells reach confluency, the cells are spontaneously detached by placing the culture dishes at 20 °C, which changes the conformation of the thermoresponsive polymer, creating a hydrophilic surface. As a result, a free monolayer sheet lifts off the culture plate and floats freely into the aqueous media, preserving cell-cell junctions and extracellular matrix [81–83].

Thus far, a variety of cells have been used to create cell sheets, including myoblasts, cardiomyocytes, ASCs, chondrocytes, smooth muscle cells (SMCs), EPCs, and MSCs [82, 84–89]. Furthermore, multi-layer, multi-lineage cell sheets can be created to optimize the spatial arrangement of delivered cells and to induce the development of structurally mature tissue [84]. Our group recently published a study involving layered SMC-EPC sheets, hypothesizing that joint delivery of these cells would mimic the native architecture of mature blood vessels, thereby acting as a potent angiogenic construct (Fig. 7.2) [86]. We tested this bone marrow-derived, bi-level cell sheet in a small animal model of myocardial infarction and observed significant attenuation of cardiac fibrosis, enhanced left ventricular function, and preservation of left ventricular dimensions [86]. This study demonstrated the ability to obtain a novel, multi-lineage cell therapy derived from a translationally practical

Fig. 7.2 (a) Cell sheet implantation technique. (b) Cell sheet covering left ventricular (LV) wall. (c) Visibility of cell sheet 1-week post-implantation. (Adapted from Kawamura et al. [85])



source and its ability to limit adverse remodeling and improve function after a myocardial infarction.

Based on the number of encouraging results from preclinical studies, the first in-man study of cell sheets for cardiomyopathy was completed in 2012 [90]. In this case report, a 56-year-old male suffering from idiopathic dilated cardiomyopathy, with LVAD support, underwent autologous myoblast cell sheet implantation delivered via a left lateral thoracotomy. Three months after LVAD support plus cell sheet transplantation, his ejection fraction improved from 20 to 46%, resulting in the explantation of his LVAD [90]. This case study revealed the safety and potential efficacy of an autologous cell sheet to be created from a patient's own skeletal myoblasts, delivered to the myocardium [90].

To further study autologous myoblast cell sheet transplantation for treating cardiomyopathy, a phase I clinical study was initiated by Sawa et al. [91]. In this study, 27 patients with ischemic ($n = 15$) and nonischemic ($n = 12$) cardiomyopathy etiologies were enrolled. None of the patients experienced procedure-related complications nor arrhythmic events up to 1-month post-procedure. One year after treatment, the ischemic cardiomyopathy patients demonstrated significant improvements in left ventricular dimensions and increases in global ejection fraction compared to baseline parameters. However, in the nonischemic group, patients did not demonstrate improvements in geometry nor function. Nonetheless, the safety and feasibility results within this study motivate future clinical studies to assess larger patient cohorts. Notably, this study encourages initiation of future trials to evaluate the potential of other cell lineages, or combinations of lineages, for cell sheet transplantation to treat cardiomyopathy.

3D Scaffolds/Cardiac Patches

In efforts to reconstruct the native architecture of the myocardium and enhance the survival of cells during transplantation, biomaterial 3D scaffolds have been employed for cardiac tissue engineering. Scaffold-based cardiac therapies generally involve suspending cells within a matrix consisting of naturally occurring biomaterials or

synthetic polymers [92, 93]. The goal of these scaffolds, or patches, is to maintain the cellular microenvironment to support differentiation, orientation, and proliferation, and to prevent anoikis [93]. However, major limitations of cardiac patches include size restrictions due to adequate nutrient diffusion and interference with electrical signal transduction [94, 95]. Nonetheless, efforts to overcome these drawbacks, including vascularized patches and electrical field stimulation, are being utilized to promote nutrient delivery and synchronize electrical activity, respectively [94, 96].

The most common scaffold used for the fabrication of cardiac patches is collagen, which comprises a majority of the myocardial extracellular matrix [97]. Murry and colleagues demonstrated the ability to seed embryonic stem cell-derived and human-induced pluripotent stem cell-derived cardiomyocytes in a three-dimensional collagen matrix and, via uniaxial tension and cyclic stretching, showed enhanced cardiomyocyte alignment. Following delivery to the rat myocardium, this cardiac patch was perfused by the host circulation 1-week posttransplantation, indicating engraftment into the host tissue [98]. The first clinical study involving a tissue-engineered cardiac patch was published in 2008. The Myocardial Assistance by Grafting a New Bioartificial Upgraded Myocardium (MAGNUM) trial was a phase 1, non-randomized study evaluating the safety and efficacy of a BMSC-seeded collagen matrix concurrent with CABG. Ten patients with post-ischemic myocardial scars received the tissue-engineered implant and ten patients received a cell-alone injection. Patients who received the cell-seeded matrix exhibited an increase in ventricular wall thickness and improvement in left ventricular end-diastolic volume compared to the cell-only group. This initial study demonstrated that implantation of a cardiac patch was safe and appeared to improve the efficacy of cellular cardiomyoplasty [99].

A second common scaffold for cardiac patches is fibrin, which is created by polymerizing individual fibrinogen monomers in the presence of thrombin. As fibrinogen converts to fibrin, the fibrin molecules chemically cross-link to form a solid mesh which can be used to support cell survival or deliver therapeutic growth factors *in vivo* [92, 100]. Recently, Zhang et al. generated a cardiac muscle patch of clinically relevant dimensions by culturing cardiomyocytes, smooth muscle cells, and endothelial cells in a fibrin matrix. *In vitro*, the patch demonstrated the ability to generate action potentials and beat synchronously and developed intercalated disk-like structures. The researchers then tested this patch in a large animal porcine model of myocardial infarction. Animals that received the engineered patch had significant improvements in left ventricular function, infarct size, myocardial wall stress, and myocardial hypertrophy. Furthermore, the treatment was not associated with significant changes in arrhythmogenicity [101].

In January 2018, Larghero et al. published results from a clinical study evaluating the safety of human embryonic stem cell-derived cardiac progenitor cells embedded in a fibrin patch in patients with severe ischemic left ventricular dysfunction. Six patients received the fibrin patch which was epicardially delivered during CABG. After a median 18-month follow-up, the investigators concluded that the patches exhibit both short- and medium-term safety and therefore warrant future efficacy studies that are adequately powered.

Acellular bioactive scaffolds have also demonstrated an efficacy in preclinical models of myocardial infarction [74, 102]. Rather than harnessing the paracrine signaling mechanisms of cell therapy, acellular scaffolds utilize ECM as the basis of cellular cues to support endogenous repair processes [103]. Acellular bioactive scaffolds are normally created by decellularizing biological tissue, which maintains the complex structure and composition of ECM [104]. Furthermore, tissue characterization studies have demonstrated that decellularization processes do not disrupt native bioactive constituents contained within ECM, such as VEGF and FGF-2 [102, 105]. Using a bioinductive ECM patch in a preclinical porcine model of ischemia reperfusion, Mewhort et al. showed that the acellular patch could promote vasculogenesis and myocardial recovery [106]. These findings encouraged the initiation of the first-in-man pilot clinical feasibility trial, currently ongoing, where this acellular bioactive ECM scaffold is implanted concurrent with CABG. Primary and secondary outcome measurements from this study include feasibility of application of the ECM scaffold, infarct area, regional myocardial function, and treatment-related adverse events [107].

Conclusion

In summary, the current gold standard treatments for ischemic heart disease fail to adequately restore functional heart tissue, leaving patients at risk for developing end-stage heart failure. Tissue engineering strategies are continuing to evolve for the benefit of the field of cardiovascular medicine and surgery and may very well become permanent adjunct therapies. Protein and stem cell therapy can mobilize endogenous repair mechanisms to enhance recovery following ischemia. Hydrogels, cell sheets, and scaffolds can be harnessed to enhance retention and delivery of proteins and stem cells, thereby prolonging and maximizing the therapeutic effect. Continued development and optimization of these tissue engineering techniques will yield promising clinical outcomes.

References

1. Benjamin EJ, et al. Heart disease and stroke statistics-2017 update: a report from the American Heart Association. *Circulation*. 2017;135:e146–603.
2. Benjamin EJ, et al. Heart disease and stroke statistics-2018 update: a report from the American Heart Association. *Circulation*. 2018;137:e67–e492.
3. Wilmot KA, O’Flaherty M, Capewell S, Ford ES, Vaccarino V. Coronary heart disease mortality declines in the United States from 1979 through 2011: evidence for stagnation in young adults, especially women. *Circulation*. 2015;132:997–1002.
4. Vandvik PO, et al. Primary and secondary prevention of cardiovascular disease: antithrombotic therapy and prevention of thrombosis, 9th ed: American College of Chest Physicians Evidence-Based Clinical Practice Guidelines. *Chest*. 2012;141:e637S–68S.
5. Boodhwani M, Sodha NR, Laham RJ, Sellke FW. The future of therapeutic myocardial angiogenesis. *Shock*. 2006;26:332–41.

6. Araszkiwicz A, et al. Effect of impaired myocardial reperfusion on left ventricular remodeling in patients with anterior wall acute myocardial infarction treated with primary coronary intervention. *Am J Cardiol.* 2006;98:725–8.
7. Wu KC, et al. Prognostic significance of microvascular obstruction by magnetic resonance imaging in patients with acute myocardial infarction. *Circulation.* 1998;97:765–72.
8. Bolognese L, et al. Impact of microvascular dysfunction on left ventricular remodeling and long-term clinical outcome after primary coronary angioplasty for acute myocardial infarction. *Circulation.* 2004;109:1121–6.
9. Beohar N, Rapp J, Pandya S, Losordo DW. Rebuilding the damaged heart: the potential of cytokines and growth factors in the treatment of ischemic heart disease. *J Am Coll Cardiol.* 2010;56:1287–97.
10. Srinivas G, Anversa P, Frishman WH. Cytokines and myocardial regeneration: a novel treatment option for acute myocardial infarction. *Cardiol Rev.* 2009;17:1–9.
11. Jayasankar V, et al. Induction of angiogenesis and inhibition of apoptosis by hepatocyte growth factor effectively treats postischemic heart failure. *J Card Surg.* 2005;20:93–101.
12. Atluri P, et al. Neovasculogenic therapy to augment perfusion and preserve viability in ischemic cardiomyopathy. *Ann Thorac Surg.* 2006;81:1728–36.
13. Atluri P, Woo YJ. Pro-angiogenic cytokines as cardiovascular therapeutics: assessing the potential. *BioDrugs.* 2008;22:209–22.
14. Toyota E, Matsunaga T, Chilian WM. Myocardial angiogenesis. *Mol Cell Biochem.* 2004;264:35–44.
15. Kastrup J, et al. Direct intramyocardial plasmid vascular endothelial growth factor-A165 gene therapy in patients with stable severe angina pectoris a randomized double-blind placebo-controlled study: the Euroinject One trial. *J Am Coll Cardiol.* 2005;45:982–8.
16. Giusti II, et al. High doses of vascular endothelial growth factor 165 safely, but transiently, improve myocardial perfusion in no-option ischemic disease. *Hum Gene Ther Methods.* 2013;24:298–306.
17. Stewart DJ, et al. VEGF gene therapy fails to improve perfusion of ischemic myocardium in patients with advanced coronary disease: results of the NORTHERN trial. *Mol Ther.* 2009;17:1109–15.
18. Henry TD, et al. The VIVA trial: vascular endothelial growth factor in ischemia for vascular angiogenesis. *Circulation.* 2003;107:1359–65.
19. Jin H, Wyss JM, Yang R, Schwall R. The therapeutic potential of hepatocyte growth factor for myocardial infarction and heart failure. *Curr Pharm Des.* 2004;10:2525–33.
20. Zhou N, Wang Y, Cheng W, Yang Z. Hepatocyte growth factor (HGF) promotes cardiac stem cell differentiation after myocardial infarction by increasing mTOR activation in p27kip haploinsufficient mice. *Genes Genomics.* 2015;37:905–12.
21. Gallo S, Sala V, Gatti S, Crepaldi T. Hgf/met axis in heart function and cardioprotection. *Biomedicine.* 2014;2:247–62.
22. Kim JS, et al. Intramyocardial transfer of hepatocyte growth factor as an adjunct to CABG: phase I clinical study. *Gene Ther.* 2013;20:717–22.
23. Meng H, et al. Safety and efficacy of intracoronary Ad-HGF administration for treating severe coronary disease: results from long-term follow-up of a phase I clinical trial. *J Clin Trials.* 2017;07.
24. Yamaguchi J, et al. Stromal cell-derived factor-1 effects on ex vivo expanded endothelial progenitor cell recruitment for ischemic neovascularization. *Circulation.* 2003;107:1322–8.
25. Zheng H, Fu G, Dai T, Huang H. Migration of endothelial progenitor cells mediated by stromal cell-derived factor-1 α /CXCR4 via PI3K/Akt/eNOS signal transduction pathway. *J Cardiovasc Pharmacol.* 2007;50:274–80.
26. Hiesinger W, et al. Myocardial tissue elastic properties determined by atomic force microscopy after stromal cell-derived factor 1 α angiogenic therapy for acute myocardial infarction in a murine model. *J Thorac Cardiovasc Surg.* 2012;143:962–6.
27. Tang YL, et al. Hypoxic preconditioning enhances the benefit of cardiac progenitor cell therapy for treatment of myocardial infarction by inducing CXCR4 expression. *Circ Res.* 2009;104:1209–16.

28. Penn MS, et al. An open-label dose escalation study to evaluate the safety of administration of nonviral stromal cell-derived factor-1 plasmid to treat symptomatic ischemic heart failure. *Circ Res.* 2013;112:816–25.
29. Chung ES, et al. Changes in ventricular remodelling and clinical status during the year following a single administration of stromal cell-derived factor-1 non-viral gene therapy in chronic ischaemic heart failure patients: the STOP-HF randomized phase II trial. *Eur Heart J.* 2015;36:2228–38.
30. Bersell K, Arab S, Haring B, Kühn B. Neuregulin1/ErbB4 signaling induces cardiomyocyte proliferation and repair of heart injury. *Cell.* 2009;138:257–70.
31. Pasumarthi KBS, Field LJ. Cardiomyocyte cell cycle regulation. *Circ Res.* 2002;90:1044–54.
32. Kühn B, et al. Periostin induces proliferation of differentiated cardiomyocytes and promotes cardiac repair. *Nat Med.* 2007;13:962–9.
33. Keefe DL. Trastuzumab-associated cardiotoxicity. *Cancer.* 2002;95:1592–600.
34. Liu X, et al. Neuregulin-1/erbB-activation improves cardiac function and survival in models of ischemic, dilated, and viral cardiomyopathy. *J Am Coll Cardiol.* 2006;48:1438–47.
35. Jabbour A, et al. Parenteral administration of recombinant human neuregulin-1 to patients with stable chronic heart failure produces favourable acute and chronic haemodynamic responses. *Eur J Heart Fail.* 2011;13:83–92.
36. Gao R, et al. A phase II, randomized, double-blind, multicenter, based on standard therapy, placebo-controlled study of the efficacy and safety of recombinant human neuregulin-1 in patients with chronic heart failure. *J Am Coll Cardiol.* 2010;55:1907–14.
37. Gao R, et al. A phase iii, randomized, double-blind, multicenter, placebo-controlled study of the efficacy and safety of neucardin™ in patients with chronic heart failure. *J Am Coll Cardiol.* 2018;71:A668.
38. Clinical trial to evaluate the efficacy and safety of recombinant human neuregulin-1 for subcutaneous administration in patients with chronic systolic heart failure – full text view – ClinicalTrials.gov. At <https://clinicaltrials.gov/ct2/show/NCT01214096>.
39. Mirosou M, Jayawardena TM, Schmeckpeper J, Gnechchi M, Dzau VJ. Paracrine mechanisms of stem cell reparative and regenerative actions in the heart. *J Mol Cell Cardiol.* 2011;50:280–9.
40. Tachibana A, et al. Paracrine effects of the pluripotent stem cell-derived cardiac myocytes salvage the injured myocardium. *Circ Res.* 2017;121:e22–36.
41. Rosen MR, Myerburg RJ, Francis DP, Cole GD, Marbán E. Translating stem cell research to cardiac disease therapies: pitfalls and prospects for improvement. *J Am Coll Cardiol.* 2014;64:922–37.
42. Alrefai MT, et al. Cardiac tissue engineering and regeneration using cell-based therapy. *Stem Cells Cloning.* 2015;8:81–101.
43. Ascheim DD, et al. Mesenchymal precursor cells as adjunctive therapy in recipients of contemporary left ventricular assist devices. *Circulation.* 2014;129:2287–96.
44. Sürder D, et al. Intracoronary injection of bone marrow-derived mononuclear cells early or late after acute myocardial infarction: effects on global left ventricular function. *Circulation.* 2013;127:1968–79.
45. Hao M, Wang R, Wang W. Cell therapies in cardiomyopathy: current status of clinical trials. *Anal Cell Pathol (Amst).* 2017;2017:9404057.
46. Florea V, et al. Dose comparison study of allogeneic mesenchymal stem cells in patients with ischemic cardiomyopathy (the TRIDENT study). *Circ Res.* 2017;121:1279–90.
47. Lu Y, et al. A systematic review of randomised controlled trials examining the therapeutic effects of adult bone marrow-derived stem cells for non-ischaemic dilated cardiomyopathy. *Stem Cell Res Ther.* 2016;7:186.
48. Korf-Klingebiel M, et al. Bone marrow cells are a rich source of growth factors and cytokines: implications for cell therapy trials after myocardial infarction. *Eur Heart J.* 2008;29:2851–8.
49. Heldman AW, et al. Transendocardial mesenchymal stem cells and mononuclear bone marrow cells for ischemic cardiomyopathy: the TAC-HFT randomized trial. *JAMA.* 2014;311:62–73.
50. Menasché P, et al. The Myoblast Autologous grafting in ischemic Cardiomyopathy (MAGIC) trial: first randomized placebo-controlled study of myoblast transplantation. *Circulation.* 2008;117:1189–200.

51. Mazo M, et al. Transplantation of adipose derived stromal cells is associated with functional improvement in a rat model of chronic myocardial infarction. *Eur J Heart Fail.* 2008;10:454–62.
52. Perin EC, et al. Adipose-derived regenerative cells in patients with ischemic cardiomyopathy: the PRECISE trial. *Am Heart J.* 2014;168:88–95.e2.
53. Allogeneic stem cell therapy in heart failure – full text view – ClinicalTrials.gov. At <https://clinicaltrials.gov/ct2/show/NCT03092284?id=NCT03092284&rank=1&load=cart>.
54. Carvalho AB, Fleischmann BK, Carlos Campos de Carvalho A. Resident stem cells and regenerative therapy. Oxford/Waltham: Elsevier; 2013. p. 141–55. <https://doi.org/10.1016/B978-0-12-416012-5.00008-6>.
55. Beltrami AP, et al. Adult cardiac stem cells are multipotent and support myocardial regeneration. *Cell.* 2003;114:763–76.
56. Dawn B, et al. Cardiac stem cells delivered intravascularly traverse the vessel barrier, regenerate infarcted myocardium, and improve cardiac function. *Proc Natl Acad Sci U S A.* 2005;102:3766–71.
57. Tang X-L, et al. Intracoronary administration of cardiac progenitor cells alleviates left ventricular dysfunction in rats with a 30-day-old infarction. *Circulation.* 2010;121:293–305.
58. Chugh AR, et al. Administration of cardiac stem cells in patients with ischemic cardiomyopathy: the SCIPIO trial: surgical aspects and interim analysis of myocardial function and viability by magnetic resonance. *Circulation.* 2012;126:S54–64.
59. Bolli R, et al. Cardiac stem cells in patients with ischaemic cardiomyopathy (SCIPIO): initial results of a randomised phase 1 trial. *Lancet.* 2011;378:1847–57.
60. Bolli R, et al. Rationale and design of the CONCERT-HF trial (combination of mesenchymal and c-kit+ cardiac stem cells as regenerative therapy for heart failure). *Circ Res.* 2018;122:1703–15.
61. Cambria E, et al. Translational cardiac stem cell therapy: advancing from first-generation to next-generation cell types. *NPJ Regen Med.* 2017;2:17.
62. Smart N, Riley PR. The stem cell movement. *Circ Res.* 2008;102:1155–68.
63. Aguado BA, Mulyasmita W, Su J, Lampe KJ, Heilshorn SC. Improving viability of stem cells during syringe needle flow through the design of hydrogel cell carriers. *Tissue Eng Part A.* 2012;18:806–15.
64. Maisonneuve BGC, Roux DCD, Thorn P, Cooper-White JJ. Effects of cell density and biomacromolecule addition on the flow behavior of concentrated mesenchymal cell suspensions. *Biomacromolecules.* 2013;14:4388–97.
65. Foster AA, Marquardt LM, Heilshorn SC. The diverse roles of hydrogel mechanics in injectable stem cell transplantation. *Curr Opin Chem Eng.* 2017;15:15–23.
66. MacArthur JW, Goldstone AB, Cohen JE, Hiesinger W, Woo YJ. Cell transplantation in heart failure: where do we stand in 2016? *Eur J Cardiothorac Surg.* 2016;50:396–9.
67. Steele AN, et al. A novel protein-engineered hepatocyte growth factor analog released via a shear-thinning injectable hydrogel enhances post-infarction ventricular function. *Biotechnol Bioeng.* 2017;114:2379–89.
68. Rodell CB, et al. Shear-thinning supramolecular hydrogels with secondary autonomous covalent crosslinking to modulate viscoelastic properties in vivo. *Adv Funct Mater.* 2015;25:636–44.
69. MacArthur JW, et al. Injectable bioengineered hydrogel therapy in the treatment of ischemic cardiomyopathy. *Curr Treat Options Cardiovasc Med.* 2017;19:30.
70. Hasan A, et al. Injectable hydrogels for cardiac tissue repair after myocardial infarction. *Adv Sci (Weinh).* 2015;2:1500122.
71. Saludas L, Pascual-Gil S, Prósper F, Garbayo E, Blanco-Prieto M. Hydrogel based approaches for cardiac tissue engineering. *Int J Pharm.* 2017;523:454–75.
72. Camci-Unal G, Annabi N, Dokmeci MR, Liao R, Khademhosseini A. Hydrogels for cardiac tissue engineering. *NPG Asia Mater.* 2014;6:e99.
73. Izkovits JL, et al. Injectable hydrogel properties influence infarct expansion and extent of postinfarction left ventricular remodeling in an ovine model. *Proc Natl Acad Sci U S A.* 2010;107:11507–12.

74. Hernandez MJ, Christman KL. Designing acellular injectable biomaterial therapeutics for treating myocardial infarction and peripheral artery disease. *JACC Basic Transl Sci.* 2017;2:212–26.
75. Anker SD, et al. A prospective comparison of alginate-hydrogel with standard medical therapy to determine impact on functional capacity and clinical outcomes in patients with advanced heart failure (AUGMENT-HF trial). *Eur Heart J.* 2015;36:2297–309.
76. A phase I, open-label study of the effects of percutaneous administration of an extracellular matrix hydrogel, VentiGel, following myocardial infarction. At <https://clinicaltrials.gov/ct2/show/NCT02305602>.
77. Guvendiren M, Lu HD, Burdick JA. Shear-thinning hydrogels for biomedical applications. *Soft Matter.* 2012;8:260–72.
78. Rodell CB, Kaminski AL, Burdick JA. Rational design of network properties in guest-host assembled and shear-thinning hyaluronic acid hydrogels. *Biomacromolecules.* 2013;14:4125–34.
79. Rodell CB, et al. Injectable shear-thinning hydrogels for minimally invasive delivery to infarcted myocardium to limit left ventricular remodeling. *Circ Cardiovasc Interv.* 2016;9(10):e004058.
80. Narita T, et al. The use of cell-sheet technique eliminates arrhythmogenicity of skeletal myoblast-based therapy to the heart with enhanced therapeutic effects. *Int J Cardiol.* 2013;168:261–9.
81. Shimizu T, et al. Fabrication of pulsatile cardiac tissue grafts using a novel 3-dimensional cell sheet manipulation technique and temperature-responsive cell culture surfaces. *Circ Res.* 2002;90:e40.
82. Memon IA, et al. Repair of impaired myocardium by means of implantation of engineered autologous myoblast sheets. *J Thorac Cardiovasc Surg.* 2005;130:1333–41.
83. Matsuura K, Masuda S, Shimizu T. Cell sheet-based cardiac tissue engineering. *Anat Rec (Hoboken).* 2014;297:65–72.
84. Shudo Y, et al. Spatially oriented, temporally sequential smooth muscle cell-endothelial progenitor cell bi-level cell sheet neovascularizes ischemic myocardium. *Circulation.* 2013;128:S59–68.
85. Kawamura M, et al. Tissue-engineered smooth muscle cell and endothelial progenitor cell bi-level cell sheets prevent progression of cardiac dysfunction, microvascular dysfunction, and interstitial fibrosis in a rodent model of type 1 diabetes-induced cardiomyopathy. *Cardiovasc Diabetol.* 2017;16:142.
86. Shudo Y, et al. Layered smooth muscle cell-endothelial progenitor cell sheets derived from the bone marrow augment postinfarction ventricular function. *J Thorac Cardiovasc Surg.* 2017;154:955–63.
87. Shudo Y, et al. Isolation and trans-differentiation of mesenchymal stromal cells into smooth muscle cells: utility and applicability for cell-sheet engineering. *Cytotherapy.* 2016;18:510–7.
88. Ishida O, et al. Adipose-derived stem cell sheet transplantation therapy in a porcine model of chronic heart failure. *Transl Res.* 2015;165:631–9.
89. Haraguchi Y, Shimizu T, Yamato M, Okano T. Regenerative therapies using cell sheet-based tissue engineering for cardiac disease. *Cardiol Res Pract.* 2011;2011:845170.
90. Sawa Y, et al. Tissue engineered myoblast sheets improved cardiac function sufficiently to discontinue LVAS in a patient with DCM: report of a case. *Surg Today.* 2012;42:181–4.
91. Miyagawa S, et al. Phase I clinical trial of autologous stem cell-sheet transplantation therapy for treating cardiomyopathy. *J Am Heart Assoc.* 2017;6(4):e003918.
92. Zhang J. Engineered tissue patch for cardiac cell therapy. *Curr Treat Options Cardiovasc Med.* 2015;17:399.
93. Rane AA, Christman KL. Biomaterials for the treatment of myocardial infarction: a 5-year update. *J Am Coll Cardiol.* 2011;58:2615–29.
94. Radisic M, et al. Functional assembly of engineered myocardium by electrical stimulation of cardiac myocytes cultured on scaffolds. *Proc Natl Acad Sci U S A.* 2004;101:18129–34.

95. Christman KL, Lee RJ. Biomaterials for the treatment of myocardial infarction. *J Am Coll Cardiol*. 2006;48:907–13.
96. Kim JJ, Hou L, Huang NF. Vascularization of three-dimensional engineered tissues for regenerative medicine applications. *Acta Biomater*. 2016;41:17–26.
97. Zimmermann WH, et al. Three-dimensional engineered heart tissue from neonatal rat cardiac myocytes. *Biotechnol Bioeng*. 2000;68:106–14.
98. Tulloch NL, et al. Growth of engineered human myocardium with mechanical loading and vascular coculture. *Circ Res*. 2011;109:47–59.
99. Chachques JC, et al. Myocardial assistance by grafting a new bioartificial upgraded myocardium (MAGNUM trial): clinical feasibility study. *Ann Thorac Surg*. 2008;85:901–8.
100. Zhang G, et al. Controlled release of stromal cell-derived factor-1 alpha in situ increases c-kit+ cell homing to the infarcted heart. *Tissue Eng*. 2007;13:2063–71.
101. Gao L, et al. Large cardiac muscle patches engineered from human induced-pluripotent stem cell-derived cardiac cells improve recovery from myocardial infarction in swine. *Circulation*. 2018;137:1712–30.
102. Svystonyuk DA, Mewhort HEM, Fedak PWM. Using acellular bioactive extracellular matrix scaffolds to enhance endogenous cardiac repair. *Front Cardiovasc Med*. 2018;5:35.
103. Akhyari P, Kamiya H, Haverich A, Karck M, Lichtenberg A. Myocardial tissue engineering: the extracellular matrix. *Eur J Cardiothorac Surg*. 2008;34:229–41.
104. Badylak SF, Freytes DO, Gilbert TW. Extracellular matrix as a biological scaffold material: structure and function. *Acta Biomater*. 2009;5:1–13.
105. Voytik-Harbin SL, Brightman AO, Kraine MR, Waisner B, Badylak SF. Identification of extractable growth factors from small intestinal submucosa. *J Cell Biochem*. 1997;67:478–91.
106. Mewhort HEM, et al. Epicardial infarct repair with bioinductive extracellular matrix promotes vasculogenesis and myocardial recovery. *J Heart Lung Transplant*. 2016;35:661–70.
107. Epicardial infarct repair using CorMatrix®-ECM: clinical feasibility study – full text view – ClinicalTrials.gov. At <https://clinicaltrials.gov/ct2/show/NCT02887768>.



Cardiac Patch-Based Therapies of Ischemic Heart Injuries

8

Wuqiang Zhu, Danielle Pretorius, and Jianyi Zhang

Ischemic Heart Diseases

The mammalian hearts extract about 60–80% of the oxygen delivered by arterial blood, which is relatively high comparing to other organs such as skeletal muscle (2–5% at rest), kidney (2–3%), intestine (4–6%), and skin (1–2%). The ability to increase oxygen extraction as a means to increase oxygen delivery is limited. Therefore, mammalian hearts are sensitive to ischemic injuries. Diseases that affect coronary blood flow cause immediate loss of myocytes, which results in serious manifestations such as angina, palpitation, shortness of breath, or sudden death. As little as 20 minutes of hypoxia may induce irreversible injury of myocytes.

Although myocytes in the neonatal mammalian hearts are able to regenerate after ischemic myocardial injury, they withdraw from cell cycle during adolescence and adulthood. Therefore, cardiomyocyte (CM) loss due to ischemic injury is typically replaced by fibrotic scar tissue. The loss of contractile myocytes leads to impaired left ventricular (LV) systolic function. The decrease in cardiac function, in turn, activates a series of compensatory responses, e.g., the activation of sympathetic nervous system and renin-angiotensin system (RAS) to stimulate contractility, peripheral arterial vasoconstriction, and retention of salt and water. These subsequently increase energy requirements. Besides, the increased workload, neurohormonal stimulation, and inflammation lead to overproduction of reactive oxygen species (ROS) and reduced antioxidant capacity. ROS may stimulate CM hypertrophy, fibroblast proliferation, and collagen synthesis, and reduces bioavailability of nitric oxide (NO), an important substrate for vasodilation. Together, these changes lead

W. Zhu · D. Pretorius · J. Zhang (✉)

Department of Biomedical Engineering, School of Medicine, School of Engineering,
University of Alabama at Birmingham, Birmingham, AL, USA

e-mail: dpret@uab.edu; jayzhang@uab.edu

© Springer Nature Switzerland AG 2019

V. Serpooshan, S. M. Wu (eds.), *Cardiovascular Regenerative Medicine*,
https://doi.org/10.1007/978-3-030-20047-3_8

141

to LV remodeling which renders significant impact on myocyte biology as well as geometry and architecture of LV chamber. LV remodeling may be reversed by medicine, LV assist devices, and more recently, via cell-based therapy.

Engineered Heart Tissue

Overview

Tissue engineering is an interdisciplinary field that mainly focuses on developing new and improving upon current designs for living tissue mimics. Most of these models are designed with specific purposes in mind, including but not limited to drug testing, tissue/organ repair, or even replacement. With such a mammoth goal in mind, it comes as no surprise that specialists across many fields, like stem cell biology, engineering, biomaterials, as well as clinicians, have been working endlessly to achieve this task. The past 20 years have witnessed great advances in the field of tissue engineering. Thus far, almost all tissues in the human body can be engineered.

The main function of the heart is to pump the blood to the coronary and peripheral circuits, thus generating the arterial pressure to maintain the perfusion of organs including the heart itself. The pumping function of the heart depends on oxygen supply from coronary arteries. Despite the major advances in cardiovascular medicine and interventional cardiology techniques, ischemic heart diseases, due to the insufficient perfusion within the myocardium, are one of the leading causes of death worldwide. While heart transplantation has been demonstrated to be an effective therapeutic approach for patients with terminal heart failure, the clinical application of this method is limited by the shortage of organ donors compared to the high demands. Data from preclinical studies and some clinical trials show that cell-based therapy is promising for treating terminal heart diseases where loss of CMs is prominent. However, low rate of cell engraftment is one of the major concerns of this approach.

With cardiac tissue engineering, the focus lies with designing and producing *functional* human heart tissue – functional in a physical, structural, and physiological sense. The early studies of engineered heart tissues (EHTs) utilized CMs derived from embryonic chick hearts [1] or neonatal rat hearts [2]. These studies proved the concept of generating a 3-dimensional (3D) cardiac tissue in the laboratory using cells, extracellular matrix (ECM), and bioreactors. The idea of a CM populated matrix (CMPM) was introduced in the late 1990s by Eschenhagen and colleagues [1]. For these designs, they used embryonic chick CMs and a collagen hydrogel. The EHT term was introduced by Zimmermann et al. [2] in 2000 to describe their 3D system of coherently and spontaneously beating neonatal rat myocytes – a system more relevant for mammalian heart repair. In this work, a collagen-Matrigel matrix was used to culture the rat myocytes. A key finding in the study was the positive force-length relationship and negative force-frequency relationship generally observed in EHTs, which is also used as a guiding principle for EHT fabrication.

Over the years, both the techniques and technology used to fabricate cardiac tissue improved and the field advanced past proof-of-concept studies, allowing to produce patches that more closely resembled native human myocardial tissue. The new generation of EHTs utilized human cells, such as mesenchymal stem cells (MSCs), embryonic stem cells, and human-induced pluripotent stem cells (hiPSCs), which made them more clinically attractive. In the recently completed ESCORT trial, Menasche et al. tested hESC-derived cardiac progenitor cells (CD15+/Isl-1+) in a fibrin patch implanted epicardially in six patients with end-stage heart failure [3]. A modest functional recovery was observed which was postulated to be mediated by paracrine mechanisms. Compared to human ESCs, the hiPSCs are more attractive as they can be derived from patients themselves for autologous transplantation. The density and spatial distribution of the cells in tissue constructs were increased by cultivation in bioreactors with perfusion (interstitial flow) of culture medium and by co-culture with endothelial cells (ECs) to promote vascularization. The differentiation and maturation of the cardiac patches were further improved by mechanical and electrical stimulation. The advances made over the last few years have enabled the generation of tissues with sophisticated architecture and functional properties approaching those of native hearts.

Cell Sources

Skeletal myoblasts and primary cardiac cells enjoyed much of the limelight in the early 1990s, with skeletal myoblasts being the first cell type to be tested as a potential treatment against heart diseases. Initial studies examined skeletal myoblasts, grafted to the host after injection, either into a normal or injured myocardium [4–6]. Several clinical studies demonstrated the functional benefits of skeletal myoblasts in treating ischemic heart diseases. For example, Menasche et al. reported that intramyocardial injection of autologous skeletal myoblasts enhances cardiac contractile function in a patient with myocardial infarction (MI) [7]. Recently published data from clinical trials in Japan confirmed the beneficial effects of transplanting autologous skeletal myoblasts into patients with ischemic heart diseases [8–10]. However, these promising results should be taken with a grain of salt, as increased risk of ventricular arrhythmia has also been observed in preclinical and clinical studies of myoblast transplantation [11–13]. Due to their lack in connexin 43 (Cx43), skeletal myoblasts cannot form gap junctions with host myocardium, leading to these cells rarely being used in clinical trials.

The feasibility of using primary CMs for myocardial repair was established by Soonpaa et al. [14]. In their study, grafted fetal mouse CMs survived and formed intercalated discs with host mouse myocardium. EHTs have been made with neonatal rat CMs, using a floating collagen matrix. These structures displayed rhythmic contractions and electrocardiogram-like potentials *in vitro* [15, 16]. EHTs laden with fetal CMs have been shown to attenuate LV remodeling in infarcted rat hearts [17, 18]. Despite all these merits, clinical application of primary cardiac cell-based EHTs is limited due to the insufficient availability of human primary cardiac cells.

MSCs are the most commonly used cells in cell-based clinical trials for myocardial repair [19, 20]. These stem cells are defined by their multipotency, capacity for self-renewal, and low immunogenicity. Due to the fact that they do not persist long in target tissues, MSCs limit the risk of any long-term complications after administration [21, 22]. MSCs can be obtained from various organs with bone marrow aspirates. Adipose tissue is the most common source [23, 24]. Bone marrow also contains numerous of other cell types (e.g., bone marrow stromal cells [25, 26], hematopoietic stem cells [27], and endothelial progenitor cells [28]) that have been investigated in preclinical and/or clinical studies of cardiac disease but these are generally not used for myocardial tissue engineering. Intramyocardial injections of autologous bone marrow-derived MSCs (BM-MSCs), done by Tomita et al., showed improved cardiac function in a rat cryoinjury model [29]. Clinical studies by Hare et al. demonstrated that both allogeneic and autologous BM-MSCs enhance cardiac function and attenuate LV remodeling in ischemic cardiomyopathy patients [30], where paracrine effects have been thought to contribute to the cardiac protective nature of the MSCs. Overexpression of the Akt gene in transplanted MSCs has also been shown to enhance their pro-angiogenic effects in MI rats [31].

In 2004, Liu et al. fabricated and evaluated the potential of an EHT made out of autologous BM-MSCs seeded in a fibrin matrix [20]. These fibrin patches were applied to the injury sites in a swine model of MI. The EHTs were associated with improvements in contractile function and with a robust increase in neovascularization. Autologous MSCs have been shown to differentiate into ECs and smooth muscle cells (SMCs) when administered as fragmented sheets to MI swine hearts and preserved cardiac function by attenuating LV remodeling [32]. The first generation of EHTs containing human MSCs were generated in 2011, when Godier-Furnémont et al. [33] applied a mixture of human MSCs, fibrinogen, and thrombin to a 300- μm -thick section of decellularized human heart tissue. Delivery of this EHT construct to nude rats with acute and chronic MI was associated with cardiac functional improvement 4 weeks after transplantation. Additionally, this study showed that treating the MSCs with transforming growth factor β (TGF- β) promoted the release of pro-angiogenic factors, yet no evidence of MSC-CMs were found. From this study, it was concluded that a native tissue matrix can be used as a cell delivery vehicle and thusly promote both the local and long-ranging cell function, a phenomenon that has been extended to other therapeutic cells and formulations of the native tissue matrix. In addition to bone marrow, MSCs derived from other tissues such as umbilical cord matrix [34] or lining [35, 36], adipose [37], placenta [38], and amnion [39, 40] have been shown to attenuate LV remodeling and improve cardiac function after transplantation into MI animals.

Human pluripotent stem cells, including embryonic stem cells (ESCs) and iPSCs, can be used to generate potentially unlimited numbers and types of cells for regenerative medicine purposes. ESCs are collected from the inner cell mass of embryo and can differentiate into all cell types of human body aside from extra-embryonic tissues [41]. A pilot study in 1996 reported that intramyocardial injection of purified ESC-CMs formed stable intracardiac grafts in mice, thus outlining the value of ESCs in cardiovascular regenerative medicine [42]. The field advanced

in the past 23 years, with numerous preclinical studies showing hESC-CMs not only engrafted in MI rats [43, 44], guinea pigs [45], and monkeys [46], but also attenuated LV remodeling. However, large engraftment of hESC-CMs was associated with increased frequency of arrhythmia [46]. The first EHTs containing mouse ESC-CMs were generated in 2006 [47], and the first EHTs with human ESC-CMs were generated 1 year later [48]. After mechanical stimulation, these engineered tissues functionally and structurally resembled immature native cardiac tissue. Transplantation of EHTs with hESC-CMs has been shown to enhance engraftment rate, leading to long-term survival and progressive maturation of CMs [49]. ESCs can also be obtained via parthenogenesis-asexual, uniparental reproduction from an unfertilized oocyte, a process that occurs naturally in some lower organisms [50, 51], but can be chemically stimulated in mice and nonhuman primates [52–55] and may alleviate ethical issues regarding the destruction of fertilized human embryos. CMs derived from parthenogenetic stem cells have been used to generate force-generating myocardium that improved cardiac function after transplantation into infarcted mouse hearts [56]. These data demonstrate this unique cell type as an attractive resource for tissue engineering-based myocardial repair.

iPSCs can be generated from the patient's own somatic cells (dermal or cardiac fibroblasts, blood cells, etc.) via the overexpression of four transcriptional regulators, Oct4, Sox2, Klf4, and Myc [57]. The efficiency of differentiation and subsequent function of iPSC-derived cells may be influenced by epigenetic factors that the iPSCs retain from their tissues of origin [58–60]. Overall, the ease of iPSC derivation and the ethical (no destruction of viable embryos) as well as immunological (can be derived from patients themselves) advantages have made iPSCs a popular cell type utilized for heart muscle repair. In 2011, the first EHTs containing hiPSC-derived cells were generated by combining CMs (hiPSC-CMs), human umbilical vein ECs (HUVECs), and MSCs or murine embryonic fibroblasts (MEFs) in a type I collagen scaffold [61]. One week after transplantation onto the hearts of athymic rats, these EHTs formed grafts containing human microvessels perfused by rat blood. In another long-term, large animal study, sheets of hiPSC-CMs were transplanted into infarcted swine hearts [62]. Grafted cells were detectable 8 weeks after transplantation. This treatment significantly improved LV remodeling, neovascularization, and contractile function. Transplantation of hiPSC-derived vascular cells (ECs and SMCs) has also been proven to enhance cardiac function and promote angiogenesis in MI swine models [63]. For this reason, vascular cells are typically added into hiPSC-CMs containing EHTs to aid in vascularization of scaffolds *in vivo* and hence, also enhance the survival of the transplanted cells [64, 65]. However, in a recent report, the addition of ECs did not increase the survival of hiPSC-based EHTs transplanted onto guinea pig hearts [65]. The first clinical trial is also underway and Menasche et al. reported on patients treated with a human ESC-CM graft, which suggested safety and efficacy of using hiPSC products [66, 67].

In 2006, Zimmermann and colleagues reported, for the first time, on how cell composition affected the physiology of EHTs [68]. CMs constitute ~30–40% of the total number of cells and ~80% of the total volume of the adult mammalian heart

[69]. The remaining non-myocyte population is composed primarily of ECs and fibroblasts [70]. It is generally agreed that non-myocytes are important for EHTs both in vitro and in vivo [48, 71–76]. To date, most studies demonstrated that a mixed cell population representing the diversity of the native myocardium (CMs, fibroblasts, and ECs) rather than the CMs alone enhances the outcomes of the tissue engineering process and the survival of cells upon transplantation [71, 72, 76–78]. MSCs have also been used as supporting cells in EHTs [61]. In the context of engineering cardiac tissues based on hESC-derived CMs, enhanced matrix remodeling and functional properties were demonstrated in cultures with 75% CMs and 25% hESC-derived CD90+ mesodermal cells [72]. Table 8.1 summarizes the representative preclinical and clinical studies utilizing cell-based therapies.

Scaffolds

Cardiac tissues can be constructed (i) from one or more sheets of cells that are grown in monolayers and released from the culture surface [79], (ii) by seeding the cells into the ECM of decellularized myocardial tissue [80, 81] or, most commonly, (iii) by suspending cells in a scaffold. The importance of material selection is quite often underestimated. A 3D matrix provides an environment for cells to live and function. Therefore, the quality and physiology of matrix is important for full function of cells in EHTs. The material chosen for fabrication forms a vital part of the foundation of the entire study and often, can be a determining factor in its success. Materials, whether biologically or synthetically derived, have chemical and physical traits that impart to the rest of the system as a whole, i.e., interaction between the ECM and the cells [82, 83]. Material interactions occur on multiple levels – the nano-, micro-, and macroscale. All these forces contribute to properties like elasticity, porosity, and degradability. By combining material selection with proper fabrication methods, the system properties can be tailored to match those of native tissues. Materials such as collagen [84], fibrin [20], and polyglycolic acid [85] have been widely investigated. Some novel compositions (e.g., silk fibroin and hyaluronic acid [86], and alginate/chitosan polyelectrolyte complexes [87]) have recently been introduced. For nanofibrous scaffolds, fiber diameter can be controlled via electrospinning [88, 89], a technique that enables manufacturing of scaffolds with mechanical properties that closely mimic the native ECM [90]. Electrospun scaffolds have porous architectures with a high surface area to volume ratio to promote cell adhesion and migration.

Material functionalization, especially with regard to physical properties like elasticity, plays a key role in the cell viability of EHTs [91, 92]. Elasticity in the case of the heart can be an indicator of both age and disease, where an increase in the elastic modulus, also known as the Young's modulus, could be indicative of fibrosis or a decrease in the elastic function of the tissue [92]. Matrix stiffness also plays a major role in determining the fate of stem cell lineages. Engler et al. [93] found that naive MSCs specify lineage and commit to phenotypes with extreme sensitivity to tissue-level elasticity. From their research it was shown that soft matrices that mimic the brain are neurogenic, stiffer matrices that mimic muscle are myogenic,

Table 8.1 Representative studies of cardiac cell therapy

Cell type	Cell source (trial #)	Cell number	Delivery route	Disease or myocardial injury model	Follow-up	Summary/observation			Publication year
						Heart function	Others		
Skeletal myoblast	Autologous skeletal muscle from dogs [4]	$0.5-1.5 \times 10^6$	IM	Cryo-injury in dogs	14 weeks	NA	Survival of skeletal myoblasts within cardiac scar area of injured heart at 6-8 weeks but not at 14 weeks after cell injection	1992	
	Mouse C2C12 cells [5]	$4-10 \times 10^4$	IM	No injury in mice	3 months	NA	Survival of skeletal myoblasts in normal heart at 3 months after cell injection	1993	
	Autologous skeletal muscle from rabbits [6]	1×10^7	IM	Cryo-injury in rabbits	6 weeks	Improved PRSW	Engraftment of skeletal myoblasts improved cardiac function	1998	
	Autologous skeletal muscle from patients [7]	8×10^6	IM (after coronary bypass)	MI in patient ($n = 1$)	5 months	Improved LVFS	First clinical study of skeletal myoblast for myocardial repair	2001	
	Skeletal muscle from newborn rats [11]	5×10^6	IM	MI in rats	26-30 days	NA	Grafted skeletal myoblasts displayed contractile activity but lacks of electromechanical coupling with host myocardium	2003	
	Autologous skeletal muscle from mice [12]	$1-5 \times 10^5$	IM	Cryo-injury in mice	2 weeks	Improved LVEF	Engraftment of skeletal myoblasts genetically engineered to express Cx43 conferred protection against induced VT	2007	

(continued)

Table 8.1 (continued)

Cell type	Cell source (trial #)	Cell number	Delivery route	Disease or myocardial injury model	Follow-up	Summary/observation		Publication year
						Heart function	Others	
	Autologous skeletal muscle from patients (NCT00102128) [13]	4 or 8×10^6	IM (after coronary bypass)	MI in patients ($n = 97$)	3 months	No improvement of heart function comparing to bypass alone	Engraftment of skeletal myoblasts is associated with increased risk of arrhythmia	2011
	Autologous skeletal muscle and bone marrow cells from patients (UMIN000001859) [8]	$2.7\text{--}30 \times 10^7$	IM	Ischemic cardiomyopathy in patients ($n = 4$)	6–12 months	Improved LVEF in 3 patients	No sustained VT	2011
	Autologous skeletal muscle from patients (UMIN000008013) [9]	3×10^8	Cell sheet	Ischemic cardiomyopathy in patients ($n = 7$)	26 weeks	Improved LVEF	Improved patient status (NYHA functional class, 6-minute walk distance)	2015
	Autologous skeletal muscle from patients (UMIN000000660) [10]	$4.5\text{--}7.5 \times 10^8$	Cell sheet	Dilated cardiomyopathy in patients ($n = 4$)	3 months	Improved LVEF in 3 patients	Transplantation of skeletal myoblasts reduces cardiac hypertrophy	2017
Primary cardiac cells	Fetal mouse CMs [14]	$1\text{--}10 \times 10^4$	IM	MI in mice	Up to 19 days	NA	Grafted fetal CMs survived and formed intercalated discs with host myocardium	1994
	Neonatal rat CMs [17]	4×10^7	Gelatin mesh	MI in rats	5 weeks	No significant change	Surviving grafts enhanced angiogenesis	1999
	Neonatal rat CMs [18]	3×10^5	Alginate scaffolds	MI in rats	2 months	No significant change	Surviving grafts reduced LV dilation and enhanced angiogenesis	2000

Bone marrow hematopoietic stem cells (BM-HSC)	Mouse BM-HSCs (CD31 ^{low} , c-kit ⁺ , Sca-1 ⁺) [27]	2000	IV	MI in irradiated mice	4 weeks	NA	Transplanted cells migrated into ischemic myocardium and differentiated to cardiomyocytes (at low rate, ~0.02%) and endothelial cells (3.3%)	2001
	Human BM-derived CD34+ endothelial progenitor cells [28]	1 × 10 ⁵	IM	MI in rats	4 weeks	Improved LVFS	Increased angiogenesis	2003
Mesenchymal stem cells (MSCs)	Rat BM-MSCs overexpressing Akt [31]	2.5–5 × 10 ⁶	IM	MI in rats	3 weeks	Improved LVSP and LV -dp/dt	Reduced infarction size and improved LV remodeling	2003
	Swine BM-MSCs [20]	5 × 10 ⁶	Fibrin patch	MI in swines	~18 days	Improved systolic wall thickness	Enhanced angiogenesis	2004
	Human amnion-derived MSCs [39]	1 × 10 ⁶	IM	MI in rats	2 months	NA	Engrafted cells differentiate into cardiomyocyte-like cells	2005
	Mouse adipose-derived MSCs [37]	2 × 10 ⁵	IM	MI in rats	30 days	Improved LVEF	Improved LV remodeling. Grafted cells differentiated into smooth muscle cells and endothelial cells	2006
	Human placenta-derived MSCs [38]	1 × 10 ⁶	IM	MI in rats	4 weeks	Improved LVEF and LVFS	Improved LV remodeling and enhanced angiogenesis	2007
	Human BM-MSCs [33]	1 × 10 ⁶	Fibrin hydrogel in decellularized sheet of human myocardium	MI in rats	4 weeks	Improved LVFS	Enhanced angiogenesis in infarction area but not normal myocardium	2011
	Human umbilical cord matrix-derived MSCs [34]	5 × 10 ⁶	IM	MI in rabbits	30 days	Improved LVEF and LVFS	Improved LV remodeling	2011

(continued)

Table 8.1 (continued)

Cell type	Cell source (trial #)	Cell number	Delivery route	Disease or myocardial injury model	Follow-up	Summary/observation		Publication year
						Heart function	Others	
	Human BM-MSCs (NCT01087996) [30]	Allogeneic vs. autologous BM-MSCs at three different doses (2×10^7 , 1×10^8 , 2×10^8)	TEM	Ischemic cardiomyopathy in patients	13 months	No difference between two cell types	Low-dose MSCs (20 million cells) produced greatest reductions in LV volumes and increased EF. Allogeneic MSCs did not stimulate significant donor-specific alloimmune reactions	2012
	Human umbilical cord lining-derived MSCs [35, 36]	$2-2.5 \times 10^6$	Fibrin patch	MI in rats	4 weeks	Improved LVEF and LVFS	Improved LV remodeling and enhanced angiogenesis	2013
Embryonic stem cell (ESC)-derived cells	Purified mouse ESC-derived CMs (mESC-CMs) [42]	1×10^4	IM	Dystrophic mdx mice	7 weeks	NA	mESC-CMs (>99% pure) formed stable intracardiac graft in mdx recipient mice	1996
	Human ESC-derived CMs (hESC-CMs) [43]	1.5×10^6	IM	MI in rats	2 months	Improved LVFS	hESC-CMs engrafted in MI rat heart and improved LV remodeling	2007
	Human ESC-CMs [44]	1×10^7	IM	MI in rats	4 weeks	Improved LVFS	Prosurvival cocktail enhances the therapeutic efficacy of hESC-CMs	2007
	Human ESC-CMs [45]	1×10^8	IM	Cryoinjury in guinea pigs	4 weeks	Improved LVEF	Engraftment of hESC-CMs electrically coupled with host myocardium, and reduced the incidence of both spontaneous and induced VT	2012
	Human ESC-CMs [46]	1×10^9	IM	MI in monkeys	Up to 3 months	No significant change	hESC-CMs remuscularized infarcted heart. Large engraftment is associated with higher frequency of arrhythmia	2014

	Human ESC-CMs [49, 175]	2.5×10^6	Engineered heart muscle ring	MI in rats	220 days	No significant changes of LVEF. Preserved heart function revealed by tagged MRI imaging	Transplantation of EHTs increased engraftment rate and led to long-term survival and progressive maturation of hESC-CMs	2015
	Human ESC-derived Isl-1+ SSEA-1+ cells (NCT02057900) [66]	4×10^6	Fibrin patch	Ischemic HF in diabetic patients ($n = 1$)	3 months	Improved LVEF	No complications (e.g., episodes of VT, et al). Improved 6-minute walking test, and increased wall motion and NYHA functional class	2015
	Human ESC-derived Isl-1+ SSEA-1+ cells (NCT02057900) [3]	8.2×10^6	Fibrin patch	Ischemic HF in patients ($n = 6$)	8.5–21.5 months	NA	No complications	2018
Induced pluripotent stem cells (iPSC)-derived cells	Human iPSC-derived CM (hiPSC-CMs) [61]	2×10^6	A mixture of gel (collagen and basement membrane extract) and cells (2 million hiPSC-CMs or hESC-CMs, 1 million HUVECs, and 1 million MSCs orMEFs)	Normal rats	1 week	NA	Both types of EHTs (hiPSC-CMs vs. hESC-CMs) formed grafts that contained human microvessels and were perfused by the native circulation	2011
	hiPSC-CMs [62]	Unknown	Cell sheet	MI in swines	8 weeks	Improved LVEF	Poor engraftment rate. Improved LV remodeling and function due to paracrine effects	2012

(continued)

Table 8.1 (continued)

Cell type	Cell source (trial #)	Cell number	Delivery route	Disease or myocardial injury model	Follow-up	Summary/observation		Publication year
						Heart function	Others	
	Human iPSC-derived vascular cells (hIPSC-VCs) [63]	4×10^6 vascular cells (ECs and SMCs)	In a fibrin patch	MI in swines	4 weeks	Improved LVEF	Increased angiogenesis via recruitment of c-kit+ cells to border zone	2013
	Human iPSC-derived trilineage of cardiac cells (CMs:ECs:SMCs) [64]	6×10^6 (CMs:ECs:SMCs = 2:1:1)	IM and injection site covered by IGF-containing fibrin patch	MI in swines	4 weeks	Improved LVEF	Improved myocardial metabolism and angiogenesis. Reduced infarct size, ventricular wall stress, and apoptosis. No ventricular arrhythmias	2014
	Human iPSC-derived cardiomyocytes and endothelial cells [65]	5×10^6 (CMs) and 2×10^6 (ECs)	Fibrin patch	MI in guinea pigs	4 weeks	Improved FAC	EHTs displayed large engraftment and electrically coupled with host myocardium	2016
	Human iPSC-derived tri-lineages of cardiac cells [77]	4×10^6 (CMs), 2×10^6 (ECs), and 2×10^6 (SMCs)	Large fibrin patch (4 cm \times 4 cm \times 1.25 mm)	MI in swines	4 weeks	Improved LVEF	Improved angiogenesis. Reduced infarct size and apoptosis	2017

BM Bone marrow, *CMs* cardiomyocytes, *ECs* endothelial cells, *EDV* end-diastolic volume, *ESV* end-systolic volume, *FAC* fractional area change, *HF* heart failure, *IM* intramyocardial injection, *LVEDP* developed pressure, *LV+* *dP/dt* LV rate of pressure rise, *LV dP/dt* LV rate of pressure decay, *LVEDD* left ventricle end-diastolic dimension, *LVEDS* left ventricle end-systolic dimension, *LVEF* left ventricular ejection fraction, *LVEFS* left ventricular fraction shortening, *LVSF* left ventricular systolic pressure, *PRSW* preload recruitable stroke work, *LVEDP* improved left ventricular end-diastolic pressure, *MI* myocardial infarction, *STEMI* ST-segment elevation myocardial infarction, *SMCs* smooth muscle cells, *TEM* transendomyocardial injection, *VT* ventricular tachycardia

and, comparatively, rigid matrices that mimic collagenous bone were osteogenic. Incorporation or fabrication of elastic fibers is vital to the success of cardiac-based tissues. Long and Tranquillo [94] reported that the production of elastic fibers and their crosslinking was highly influenced by the matrix used during cell culture, and by the addition of growth factors like TGF- β 1 and insulin. Biodegradability is another important property that needs to be considered in material selection. The degree of degradation and the time over which it occurs may also be important factors to consider.

Potential Mechanisms

Although current pharmacological heart failure treatment regimens may delay disease progression, they do not generate new myocytes, nor do they allow for the maintenance of a sustained recovery of cardiac function. The capability of transplanted ESC- and iPSC-based tissues to remuscularize injured hearts, to some extent, has been proven by many preclinical studies performed on different species such as mice, rats, guinea pigs [45, 65], swine [64, 77, 95], and nonhuman primates [46, 96, 97]. On the other hand, transplantation of nonviable (irradiated) EHTs [49] and EHTs containing hiPSC-ECs and -SMCs without CMs [63] improved cardiac function in infarcted animals, suggesting that implanted stem cells were largely beneficial via their secretome. It is well-known that transplanted MSCs promote vasculogenesis by differentiating into ECs and SMCs in recipient hearts [98, 99]. Several studies have indicated that the paracrine activity of transplanted cells is mediated, at least in part, by exosomes. Exosomes are nano-sized (<100–150 nm diameter) regulatory vesicles that are secreted by most types of cells [77, 100]. These vesicles contain many different materials, including a variety of proteins and RNAs [101]. Recent research efforts have focused on leveraging exosomes as a powerful therapeutic tool for cardiac diseases. The results from pilot studies conducted by Sahoo et al. indicated that exosomes secreted by human CD34+ bone-marrow cells promote angiogenesis in ischemic hearts by increasing the viability, proliferation, and angiogenic activity of ECs [102]. This pro-angiogenesis was mediated by selectively enriched angiomiRs such as miR-126-3p in CD34+ cells [103]. Exosomes from CD34+ were most effectively internalized by ECs in the ischemic tissue to induce their proliferation. Similarly, Khan et al. have shown that murine ESC exosomes increase angiogenesis and CM survival and improve cardiac function in infarcted mice [104]. Beneficial effects of exosomes have been demonstrated in both small and large animal models with myocardial injuries [77, 104, 105]. For example, exosomes from human cardiospheres attenuated LV remodeling and improved cardiac function in swine models with acute and chronic MI [105]. It was recently reported that engrafted hiPSC-derived cardiac cell lineages (i) activate the cell cycle of endogenous CMs in the recipient host [106], (ii) enhance angiogenesis, (iii) reduce scar bulging and wall stress of infarct boarder zone and CM overstretch, and (iv) reduce CM apoptosis. All of these contribute to the significant reduction of infarct size, increased cardiac function, and improved myocardial ATP

turnover [63]. Collectively, these data suggest that mechanisms of the beneficial effects of cell- and tissue-therapy may vary depending on cell types. The strategies of delivering mixed cells may optimize the positive effects via providing both remuscularization and paracrine effects [107, 108]. More extensive investigations are needed to determine the optimal cellular sources for cardiovascular therapy. Furthermore, exosome-based therapies of the heart may be improved by using biomaterial systems to provide sustained delivery of exosomes and extend retention times to several weeks.

Human Cardiac Tissue Patch

Human cardiac tissue patch is a type of engineered myocardium containing human CMs and stroma cells at certain ratio. Most engineered myocardium can be classified into one of the two categories, cell sheets or cell-containing scaffolds. In a broad sense, sheet-based patches are thin structures that are made with the purpose of stacking or sandwiching multiple layers on top of each other to increase the overall thickness of the structure. An early demonstration of this was the study done by Okano et al. [109] in the early 1990s, where temperature-sensitive poly(*N*-isopropyl acrylamide) (PIPAAm) was used to coat culture dishes prior to culturing various cells on them, followed by reducing the temperature from 37 °C to 32 °C. PIPAAm has a lower critical solution temperature at 32 °C. At temperatures below 32 °C, PIPAAm effectively becomes miscible and hydrated, a property making it an extremely attractive option as a biomaterial, were it not for its cytotoxic nature [110]. Stacking cardiac cell sheets have proven successful in producing pulsatile, electrically coupled 3D vascular graft structures, allowing for synchronous beating throughout the structure [111, 112]. As is tradition, nothing can come without paying a price, and the price of increased structural thickness comes in the form of reduced vascularization and perfusion, which itself, can also be hindered by the epicardium after applying the graft to the heart surface. To increase vascularization of these grafted tissues, various cell types like ECs have been added to the designs [71, 113]. These additions not only help with recruitment of vasculature, but also deposit their own ECM components like collagen, fibrin, and laminin while in culture, contributing to the structural integrity of the grafted structure. It should be noted that the matrix stiffness, although necessary for structural integrity, can be detrimental if not measured or regulated properly, as it influences the cell's and finally the graft's fate [114]. Compared to cell sheets, cell-containing 3D patches tend to be thicker, as they are fabricated by suspending cells in a biomaterial matrix, or by using decellularized tissues. In the case of biomaterial matrix patches, materials like fibrin or mixtures of fibrin and collagen are becoming increasingly popular in cardiac applications [77, 115–118]. Synthetic polymers like polyglycolic acid (PGA) and polyurethane (PU) are also viable options, especially with relative ease with which many of these materials can be functionalized [85, 119].

Manufacturing

Ideally, scaffold architectures should be tailored to effectively guide the orientation of CMs. Toward this goal, many methods have been developed to generate anisotropic tissue structures similar to the native myocardium, even in the absence of specific physical cues such as electrical or mechanical stimulation. Engelmayr et al. pioneered the use of microfabrication in 2008 with the creation of 3D cardiac tissue engineered scaffolds [120]. The scaffolds were pre-treated with cardiac fibroblasts followed by seeding with enriched neonatal rat CMs. This method yielded contractile cardiac grafts with mechanical properties closely resembling those of the native rat right ventricle. Additionally, cell alignment could also be manipulated. Badie et al. developed a method to replicate the microstructure of heart tissue *in vitro* [121, 122]. By adjusting the width and spacing of fibronectin lines in a specific 2D plane, cell elongation, distribution of gap junctions, and cell distribution could be altered without affecting cell direction. This approach enabled systematic study of the structure-function relationship in healthy and structurally remodeled hearts. High degrees of anisotropy have been found to correlate with high longitudinal conduction velocities (~35 cm/s) in neonatal rat CMs cultured on micro-molded poly(ethylene glycol) (PEG) hydrogels [123]. Here, submicron corrugated structures, measuring 800 nm by 800 nm, forced the cells to align and form focal adhesions along the groove/ridge direction, with the cytoskeletal alignment following [123]. Recently, Montgomery et al. developed a new shape-memory scaffold that allows for the injection of fully functional tissues [124]. Cardiac patches made using these shape-memory scaffolds (1 cm × 1 cm) have been delivered through orifices as small as 1 mm. The hydrogels were then able to recover their initial shape following injection without affecting CM viability or function. Later alterations were made to the material to further increase the polymer elasticity, making it an even more attractive option for scaffold fabrication [125].

Recently, Gao et al. developed a novel multiphoton-excited, 3D printing technique to generate a native-like, ECM scaffold with submicron resolution [78]. A human cardiac muscle patch (hCMP) was then fabricated by seeding the scaffold with hiPSC-derived CMs, SMCs, and ECs. hCMPs fabricated with these scaffolds yielded significant recovery from ischemic myocardial injury in a murine model of MI.

Patch Size

Patches can be trained to mature to morphologically and functionally resemble native myocardium. Both preclinical and clinical studies have demonstrated that transplanted patches attenuate LV remodeling and improve cardiac function in animal models and human patients. Preclinical studies indicate that the engraftment rate can be substantially higher when the cells are administered as an EHT compared to the cell injection or infusion [77, 99, 126]. A simple and scalable technology is needed to rapidly engineer highly functional human heart tissues suitable for

large animal preclinical studies and future clinical applications. Gao et al. generated an hCMP of clinically relevant dimensions (4 cm × 2 cm × 1.25 mm) [77]. In these hCMPs, mixed CMs, SMCs, and ECs derived from hiPSCs were encapsulated in a fibrin scaffold. They cultured the constructs on a dynamic (rocking) platform. The hCMPs began to beat synchronously within 1 day of fabrication. After 7 days of culture, *in vitro* assessments indicated the mechanisms related to the improvements in electromechanical coupling, calcium-handling, and force generation (1.18 nN/input myocyte) suggesting a maturation during the culture. Epicardial implantation of hCMPs in a porcine model of MI was associated with significant improvements in LV function, infarct size, myocardial wall stress, myocardial hypertrophy, and reduced apoptosis in the peri-scar boarder zone myocardium. Shadrin et al. produced a 7 × 7 mm cardiopatch (1 × 10⁶ cells per patch including hiPSC-CMs, SMCs, and fibroblasts) [115]. At 3 weeks after epicardial implantation, cardiopatches exhibited robust survival and vascularization. Since large patch typically requires high number of CMs, it is necessary to establish a protocol for large-scale production of CMs from hiPSCs. A bioreactor-based culture and differentiation of hiPSCs may be a feasible strategy.

Vascularization

Ensuring that EHTs, either *in vitro* or *in vivo*, are supplied with enough oxygen and nutrients remains a major challenge, even though the heart has a robust neovascularization capacity. If the transplanted EHTs survive the first few days, vascular density due to neovascularization in the graft tends to be similar to that of naïve cardiac tissue [77, 127, 128]. With scaffold-based tissues, vascularity and cell survival tend to be greater in constructs that contain both CMs and non-myocytes (e.g., ECs, SMCs, pericytes, and fibroblasts) than in constructs composed of CMs alone [61, 127, 129–131]. This enhanced in vascularization with the addition of non-myocytes might, in part, be linked to the fact that ECs and SMCs release cytokines that stimulate neovascularization and recruit endogenous cardiac progenitor cells [132]. Other non-myocytes like pericytes and fibroblasts produce vascular endothelial growth factor (VEGF), platelet-derived growth factor (PDGF), angiopoietin 1 (Ang-1), and perhaps other mitogenic factors that stimulate the proliferation of ECs while inhibiting apoptosis [48, 133].

As with everything, there is a balance, and these cells, both myocytes and non-myocytes, affect each other. Myocytes appear to contribute to the vessel growth, as angiogenesis significantly increased in infarcted rat hearts after treatment with sheets of murine ESC-CMs and ECs mural cells, but not when CMs were omitted [134]. The work done by Iseoka et al. showed that the cellular makeup of the EHTs directly influences engraftment as well as functionality when transplanted into the rat MI model [135]. This group showed that tissue consisting of 50–70% hiPSC-CMs and 30–50% non-myocytes tends to engraft more stably, while also leading to functional improvements as opposed by tissue with either more than 90% or less than 25% myocytes.

Vascularized cardiac tissues have also been created by combining neonatal rat cardiac cells with a mixture of Matrigel, insulin-like growth factor-1 (IGF-1), stromal cell-derived factor 1 (SDF-1), and VEGF, followed by implantation into the rat omentum for 7 days to induce the ingrowth of native blood vessels [136]. Testing of prevascularized tissue in this rat model showed that the tissues were structurally and electrically integrated into the host myocardium 4 weeks after transplantation, and that they improved cardiac function and remodeling. Overall, vascularization during *in vitro* culture or following implantation remains a critical requirement for the survival and function of cardiac tissue grafts.

Functional Assessment

The main application of EHTs is to provide a functional human cardiac muscle for myocardial repair, drug testing, and physiological studies. For therapeutic purpose, EHTs must be large enough for covering the injured area in human hearts and capable of generating a contraction force ($\geq 2\text{--}4$ mN/mm²) and propagating electrical signals (at conduction velocities of ≥ 25 cm/s) [137]. Recently, Gao et al. reported a protocol for comprehensive assessment of patch function. In their study, transmembrane action potential, conduction velocity, and duration of action potential were assessed by optical mapping. Intercellular coupling was determined by a linear array system of electric sensors. Functional maturation was evaluated via measurements of force generation. Other assessments of maturation status of hiPSC-CMs include morphological (cell morphology, size, sarcomere length, expression of maturation markers) and functional assays (action potential, calcium handling, and contractility) as reported elsewhere [138, 139]. It is generally accepted that electrical and/or mechanical stimulations induce CM maturation in engineered heart tissues [77, 140–142]. Recent reports indicate that hormonal [143] or electromechanical conditioning [144] of hiPSC-CMs promotes advanced maturation (i.e., formation of T-tubule network), but the effect of these treatments on patch survival and function *in vivo* is unknown.

Patch Implantation

In preclinical studies, engineered heart tissues including tissue patches, cell sheets, and decellularized matrices were typically sutured to the epicardium to cover the injured area [145]. In a recent clinical trial, Menasche et al. reported the procedure of delivering hESC-CMs in a fibrin patch to ischemic patient hearts [3]. After opening the chest, they first identified a piece of pericardium in the patient matching the size of the fibrin patch. Then, they sutured the pericardium around one-half the circumference of the infarct area to create a “pocket.” The fibrin patch was slid into the pocket and the pericardial flap was then folded over and finally stitched to the remaining one-half of the infarct circumference. Thus far, cell-based therapy has been safe and effective in clinical trials and significant complications have been

reported. However, the requirement of open-heart surgery may significantly limit their clinical application to patients who had contraindications to surgery or in an area without appropriate surgical equipment. Another important issue is the ideal timing for cell therapy. Several clinical trials were designed to study the impact of cell delivery time on therapeutic effects [146, 147]. It is likely that the ideal timing varies case by case depending on disease type and stage.

A valid animal model is important for studying the engraftment and function of transplanted human cells and cardiac tissues in injured hearts. Immunocompromised rodents including nonobese diabetic (NOD)/severe combined immunodeficiency (SCID) or NOD/SCID gamma mice and athymic nude rats are commonly used. To test the immunogenicity of transplanted human cells, human immune systems are established in immunodeficient mice via transplantation of human hematolymphoid cells, which is called humanized mice [148]. Although rodents are the most practical animal model for studies of efficacy and mechanisms of cardiac repair, they are not representative of human physiology. The fact that rodent hearts are anatomically and physiologically different from human raised the concerns. Large animals such as porcine or nonhuman primates are probably more relevant models for preclinical studies [46, 62, 77, 149, 150]. The relatively fast short cycle, and the similarity of human and porcine coronary anatomy and electrophysiology renders them the popular and suitable models for examining the efficacy and mechanisms of cardiac cell therapy.

Engraftment Rate

The field of cardiac tissue engineering really came to light in the early 1990s with issues like myocardial regeneration, or rather the lack thereof, becoming a key question that needed answering [4, 5]. Today, even after much time has passed and many advances have been made in the field, we are still faced with the question: “can a few good cells mend a broken heart?” [151]. At present, the most popular preclinical delivery methods include direct intramyocardial injection as well as intravascular infusion. However, cell engraftment in these cases is low and may be the most probable cause of treatment failure [126]. Some of the major contributors to transplanted cell death include inadequate cell attachment to the host tissue, severe ischemia, and excessive inflammation. If the interaction between the transplanted cells and the host ECM is weak, a form of programmed cell death called anoikis can be triggered [152]. Damaged tissue does not generally allow for the cells to adhere as strongly to it as is the case with normal, healthy tissue [153]. Another potential risk factor is the blood supply to the newly transplanted cells, i.e., whether the area becomes ischemic or not. Transport, to and from damaged sites, is usually severely hampered, and even though hypoxia is considered necessary to preserve the stem cell characteristics, harsh ischemic environments activate cell death pathways, leading to reduced cell engraftment [154, 155]. Additionally, injuries like MI are followed by acute inflammatory responses where cells like neutrophils and monocytes are recruited to the damaged area. This is followed by the production

of various inflammatory cytokines and chemokines to recruit more inflammatory cells, the secretion of several proteolytic enzymes, ROSs, as well as the activation of phagocytosis to remove dead cells and tissue debris [156, 157].

In the past two decades, much effort has been investigated to enhance engraftment rates. Engraftment can be improved by increasing cell survival and retention, multiplication of the doses of cell administration, and stimulating the proliferation of grafted cells. Preconditioning of hiPSC-CMs with a rho-kinase inhibitor called Y-27632 enhanced their survival and retention in MI murine hearts [158]. Y-27632 treatment inhibits apoptosis and enhances expression of cell adhesion molecules. Co-administration of cells with anti-apoptotic cocktail has also been demonstrated to enhance the survival of grafted cells [44]. Retention can also be improved by using some form of a carrier or vehicle to transport, protect and potentially provide nutrients to the cells until they can settle down in their new environment. These carriers can come in multiple forms, including, but not limited to polymer-based particles and a variety of hydrogel-based matrices [77, 115, 159, 160]. The biomaterials can also be modified and functionalized according to the desired properties of the system, allowing the designer to tailor properties like elasticity, porosity, hydrophobicity/hydrophilicity, biodegradability, and surface charge, for example, making these systems extremely diverse and dynamic [161, 162].

Microenvironment and cell-cell interactions are important for tissue differentiation and maturation during embryonic development. A way to mimic these conditions is to culture the CMs in 3D clusters (i.e., spheroids) rather than in monolayers or as individual cells. The idea of generating cell spheroids *in vitro* was first introduced in 1959 [163]. Early studies with enzymatically dissociated rat ventricular CMs relied on the cells' own capacity to reassemble into small tissue-like aggregates without scaffolds [164]. Recently, it was reported that cultivating the hiPSC-derived cardiac cells in the form of spheroids promoted CM differentiation and maturation [165]. Furthermore, comparing to isolated cells, CM spheroids formed larger graft after being injected to injured animal hearts, especially when the spheroids were encapsulated in an alginate-chitosan micromatrix prior to transplantation [166–169]. Recently, Mattapally et al. reported that fibrin patches containing hiPSC-CM spheroids displayed better survival comparing to the direct intramyocardial injection of hiPSC-CMs in a murine MI model, thus established the feasibility of using hiPSC-CM spheroids and spheroid fusions for cardiac tissue engineering [170]. Spheroids are also compatible with bioprinting technology [170]. hCMPs can be generated by a 3D bioprinter, using spheroids of hiPSC-CMs, HUVECs, and human adult ventricular fibroblasts [169]. These patches displayed spontaneous beating, and ventricular-like action potentials, and remained stably engrafted with evidence of vascularization 1 week after transplantation onto rat hearts. Recently, preclinical studies from the Bolli laboratory showed that repeated intraventricular cell injections guided by echocardiography resulted in a greater cumulative effect on LV function and remodeling than a single cell injection [171–173]. Several clinical trials were initiated to evaluate the efficacy and safety of a single dose versus repeated dose regimen of cell delivery in patients with acute MI (RELIEF/NCT01652209), heart failure (REPEAT/NCT01693042, REMEDIUM/NCT02248532), and dilated cardiomyopathy (REMEDIUM/NCT02248532).

One of the major goals of cell- or tissue-based therapy is to replace fibrotic scar tissue with electromechanically functional and vascularized cardiac muscle and, thus, provide a long-term benefit. However, the lack of long-term, stable, and large grafts, consisting of transplanted cells and tissues, makes it difficult to study the contribution of remuscularization toward functional improvement in the recipient hearts. To address this question, Zhu et al. reported that inducing proliferation of hiPSC-CMs via targeted expression of a cell cycle gene, *CCND2*, significantly enhanced their potency for myocardial repair as evidenced by remuscularization of injured myocardium in mice [174]. Recently, hESC-CMs have also been shown to form large grafts 3 months after intramyocardial injection into infarcted macaque heart. Together, these data suggest that pluripotent stem cell-derived CMs hold great potential to regenerate loss of myocardium. It is possible that large grafts may induce cardiac arrhythmia. If that is the case, more thorough investigations are needed to optimize the size and location of grafts which provide best treatment without inducing arrhythmias.

Summary

The convergence of science and engineering shaped the field of tissue engineering. The advance in biomaterial and molecular biology will accelerate the development of tissue engineering. Preclinical studies demonstrate that EHTs, including cardiac cell patches, form stable long-term CM grafts in the injured hearts of rodents and large mammals and improve cardiac function. Established protocols to generate hiPSCs and their cardiac derivatives pave the way for autologous transplantation in patients with cardiac diseases. More clinical trials are needed in order to answer the following critical questions: (1) the appropriate cell types and scaffolds, (2) the ideal timing for tissue transplantation, (3) the location for tissue transplantation, and (4) the safety and efficacy of engineered cardiac tissues.

References

1. Eschenhagen T, Fink C, Remmers U, Scholz H, Wattchow J, Weil J, Zimmermann W, Dohmen HH, Schafer H, Bishopric N, Wakatsuki T, Elson EL. Three-dimensional reconstitution of embryonic cardiomyocytes in a collagen matrix: a new heart muscle model system. *FASEB J*. 1997;11:683–94.
2. Zimmermann WH, Fink C, Kralisch D, Remmers U, Weil J, Eschenhagen T. Three-dimensional engineered heart tissue from neonatal rat cardiac myocytes. *Biotechnol Bioeng*. 2000;68:106–14.
3. Menasche P, Vanneau V, Hagege A, Bel A, Cholley B, Parouchev A, Cacciapuoti I, Al-Daccak R, Benhamouda N, Blons H, Agbulut O, Tosca L, Trouvin JH, Fabreguettes JR, Bellamy V, Charron D, Tartour E, Tachdjian G, Desnos M, Larghero J. Transplantation of human embryonic stem cell-derived cardiovascular progenitors for severe ischemic left ventricular dysfunction. *J Am Coll Cardiol*. 2018;71:429–38.
4. Marelli D, Desrosiers C, el-Alfy M, Kao RL, Chiu RC. Cell transplantation for myocardial repair: an experimental approach. *Cell Transplant*. 1992;1:383–90.

5. Koh GY, Klug MG, Soonpaa MH, Field LJ. Differentiation and long-term survival of c2c12 myoblast grafts in heart. *J Clin Invest.* 1993;92:1548–54.
6. Taylor DA, Atkins BZ, Hungspreugs P, Jones TR, Reedy MC, Hutcheson KA, Glower DD, Kraus WE. Regenerating functional myocardium: improved performance after skeletal myoblast transplantation. *Nat Med.* 1998;4:929–33.
7. Menasche P, Hagege AA, Scorsin M, Pouzet B, Desnos M, Duboc D, Schwartz K, Vilquin JT, Marolleau JP. Myoblast transplantation for heart failure. *Lancet.* 2001;357:279–80.
8. Fujita T, Sakaguchi T, Miyagawa S, Saito A, Sekiya N, Izutani H, Sawa Y. Clinical impact of combined transplantation of autologous skeletal myoblasts and bone marrow mononuclear cells in patients with severely deteriorated ischemic cardiomyopathy. *Surg Today.* 2011;41:1029–36.
9. Sawa Y, Yoshikawa Y, Toda K, Fukushima S, Yamazaki K, Ono M, Sakata Y, Hagiwara N, Kinugawa K, Miyagawa S. Safety and efficacy of autologous skeletal myoblast sheets (tcd-51073) for the treatment of severe chronic heart failure due to ischemic heart disease. *Circ J.* 2015;79:991–9.
10. Yoshikawa Y, Miyagawa S, Toda K, Saito A, Sakata Y, Sawa Y. Myocardial regenerative therapy using a scaffold-free skeletal-muscle-derived cell sheet in patients with dilated cardiomyopathy even under a left ventricular assist device: a safety and feasibility study. *Surg Today.* 2018;48(2):200–10.
11. Leobon B, Garcin I, Menasche P, Vilquin JT, Audinat E, Charpak S. Myoblasts transplanted into rat infarcted myocardium are functionally isolated from their host. *Proc Natl Acad Sci U S A.* 2003;100:7808–11.
12. Roell W, Lewalter T, Sasse P, Tallini YN, Choi BR, Breitbach M, Doran R, Becher UM, Hwang SM, Bostani T, von Maltzahn J, Hofmann A, Reining S, Eiberger B, Gabris B, Pfeifer A, Welz A, Willecke K, Salama G, Schrickel JW, Kotlikoff MI, Fleischmann BK. Engraftment of connexin 43-expressing cells prevents post-infarct arrhythmia. *Nature.* 2007;450:819–24.
13. Menasche P, Alfieri O, Janssens S, McKenna W, Reichenspurner H, Trinquart L, Vilquin JT, Marolleau JP, Seymour B, Larghero J, Lake S, Chatellier G, Solomon S, Desnos M, Hagege AA. The myoblast autologous grafting in ischemic cardiomyopathy (magic) trial: first randomized placebo-controlled study of myoblast transplantation. *Circulation.* 2008;117:1189–200.
14. Soonpaa MH, Koh GY, Klug MG, Field LJ. Formation of nascent intercalated disks between grafted fetal cardiomyocytes and host myocardium. *Science.* 1994;264:98–101.
15. Souren JE, Schneijdenberg C, Verkleij AJ, Van Wijk R. Factors controlling the rhythmic contraction of collagen gels by neonatal heart cells. *In Vitro Cell Dev Biol.* 1992;28A:199–204.
16. Souren JE, Peters RC, Van Wijk R. Collagen gels populated with rat neonatal heart cells can be used for optical recording of rhythmic contractions which also show ecg-like potentials. *Experientia.* 1994;50:712–6.
17. Li RK, Jia ZQ, Weisel RD, Mickle DA, Choi A, Yau TM. Survival and function of bioengineered cardiac grafts. *Circulation.* 1999;100:II63–9.
18. Leor J, Aboulafia-Etzion S, Dar A, Shapiro L, Barbash IM, Battler A, Granot Y, Cohen S. Bioengineered cardiac grafts: a new approach to repair the infarcted myocardium? *Circulation.* 2000;102:III56–61.
19. Davani S, Marandin A, Mersin N, Royer B, Kantelip B, Herve P, Etievent JP, Kantelip JP. Mesenchymal progenitor cells differentiate into an endothelial phenotype, enhance vascular density, and improve heart function in a rat cellular cardiomyoplasty model. *Circulation.* 2003;108(Suppl 1):II253–8.
20. Liu J, Hu Q, Wang Z, Xu C, Wang X, Gong G, Mansoor A, Lee J, Hou M, Zeng L, Zhang JR, Jerosch-Herold M, Guo T, Bache RJ, Zhang J. Autologous stem cell transplantation for myocardial repair. *Am J Physiol Heart Circ Physiol.* 2004;287:H501–11.
21. Ankrum JA, Ong JF, Karp JM. Mesenchymal stem cells: immune evasive, not immune privileged. *Nat Biotechnol.* 2014;32:252–60.
22. von Bahr L, Batsis I, Moll G, Hagg M, Szakos A, Sundberg B, Uzunel M, Ringden O, Le Blanc K. Analysis of tissues following mesenchymal stromal cell therapy in humans indicates limited long-term engraftment and no ectopic tissue formation. *Stem Cells.* 2012;30:1575–8.

23. Hass R, Kasper C, Bohm S, Jacobs R. Different populations and sources of human mesenchymal stem cells (msc): a comparison of adult and neonatal tissue-derived msc. *Cell Commun Signal*. 2011;9:12.
24. Golpanian S, Wolf A, Hatzistergos KE, Hare JM. Rebuilding the damaged heart: mesenchymal stem cells, cell-based therapy, and engineered heart tissue. *Physiol Rev*. 2016;96:1127–68.
25. Lindner U, Kramer J, Rohwedel J, Schlenke P. Mesenchymal stem or stromal cells: toward a better understanding of their biology? *Transfus Med Hemother*. 2010;37:75–83.
26. Friedenstein AJ, Chailakhjan RK, Lalykina KS. The development of fibroblast colonies in monolayer cultures of guinea-pig bone marrow and spleen cells. *Cell Tissue Kinet*. 1970;3:393–403.
27. Jackson KA, Majka SM, Wang H, Pocius J, Hartley CJ, Majesky MW, Entman ML, Michael LH, Hirschi KK, Goodell MA. Regeneration of ischemic cardiac muscle and vascular endothelium by adult stem cells. *J Clin Invest*. 2001;107:1395–402.
28. Kawamoto A, Tkebuchava T, Yamaguchi J, Nishimura H, Yoon YS, Milliken C, Uchida S, Masuo O, Iwaguro H, Ma H, Hanley A, Silver M, Kearney M, Losordo DW, Isner JM, Asahara T. Intramyocardial transplantation of autologous endothelial progenitor cells for therapeutic neovascularization of myocardial ischemia. *Circulation*. 2003;107:461–8.
29. Tomita S, Li RK, Weisel RD, Mickle DA, Kim EJ, Sakai T, Jia ZQ. Autologous transplantation of bone marrow cells improves damaged heart function. *Circulation*. 1999;100:II247–56.
30. Hare JM, Fishman JE, Gerstenblith G, DiFede Velazquez DL, Zambrano JP, Suncion VY, Tracy M, Ghersin E, Johnston PV, Brinker JA, Breton E, Davis-Sproul J, Schulman IH, Byrnes J, Mendizabal AM, Lowery MH, Rouy D, Altman P, Wong Po Foo C, Ruiz P, Amador A, Da Silva J, McNiece IK, Heldman AW, George R, Lardo A. Comparison of allogeneic vs autologous bone marrow-derived mesenchymal stem cells delivered by transendocardial injection in patients with ischemic cardiomyopathy: the poseidon randomized trial. *JAMA*. 2012;308:2369–79.
31. Mangi AA, Noiseux N, Kong D, He H, Rezvani M, Ingwall JS, Dzau VJ. Mesenchymal stem cells modified with akt prevent remodeling and restore performance of infarcted hearts. *Nat Med*. 2003;9:1195–201.
32. Huang CC, Tsai HW, Lee WY, Lin WW, Chen DY, Hung YW, Chen JW, Hwang SM, Chang Y, Sung HW. A translational approach in using cell sheet fragments of autologous bone marrow-derived mesenchymal stem cells for cellular cardiomyoplasty in a porcine model. *Biomaterials*. 2013;34:4582–91.
33. Godier-Furnemont AF, Martens TP, Koeckert MS, Wan L, Parks J, Arai K, Zhang G, Hudson B, Homma S, Vunjak-Novakovic G. Composite scaffold provides a cell delivery platform for cardiovascular repair. *Proc Natl Acad Sci U S A*. 2011;108:7974–9.
34. Latifpour M, Nematollahi-Mahani SN, Deilamy M, Azimzadeh BS, Eftekhar-Vaghefi SH, Nabipour F, Najafipour H, Nakhaee N, Yaghoubi M, Eftekhar-Vaghefi R, Salehinejad P, Azizi H. Improvement in cardiac function following transplantation of human umbilical cord matrix-derived mesenchymal cells. *Cardiology*. 2011;120:9–18.
35. Martinez EC, Vu DT, Wang J, Lilyanna S, Ling LH, Gan SU, Tan AL, Phan TT, Lee CN, Kofidis T. Grafts enriched with subamniotic-cord-lining mesenchymal stem cell angiogenic spheroids induce post-ischemic myocardial revascularization and preserve cardiac function in failing rat hearts. *Stem Cells Dev*. 2013;22:3087–99.
36. Lilyanna S, Martinez EC, Vu TD, Ling LH, Gan SU, Tan AL, Phan TT, Kofidis T. Cord lining-mesenchymal stem cells graft supplemented with an omental flap induces myocardial revascularization and ameliorates cardiac dysfunction in a rat model of chronic ischemic heart failure. *Tissue Eng Part A*. 2013;19:1303–15.
37. Yamada Y, Wang XD, Yokoyama S, Fukuda N, Takakura N. Cardiac progenitor cells in brown adipose tissue repaired damaged myocardium. *Biochem Biophys Res Commun*. 2006;342:662–70.
38. Ventura C, Cantoni S, Bianchi F, Lionetti V, Cavallini C, Scarlata I, Foroni L, Maioli M, Bonsi L, Alviano F, Fossati V, Bagnara GP, Pasquinelli G, Recchia FA, Perbellini A. Hyaluronan mixed esters of butyric and retinoic acid drive cardiac and endothelial fate in term placenta

- human mesenchymal stem cells and enhance cardiac repair in infarcted rat hearts. *J Biol Chem.* 2007;282:14243–52.
39. Zhao P, Ise H, Hongo M, Ota M, Konishi I, Nikaido T. Human amniotic mesenchymal cells have some characteristics of cardiomyocytes. *Transplantation.* 2005;79:528–35.
 40. Fujimoto KL, Miki T, Liu LJ, Hashizume R, Strom SC, Wagner WR, Keller BB, Tobita K. Naive rat amnion-derived cell transplantation improved left ventricular function and reduced myocardial scar of postinfarcted heart. *Cell Transplant.* 2009;18:477–86.
 41. Evans MJ, Kaufman MH. Establishment in culture of pluripotential cells from mouse embryos. *Nature.* 1981;292:154–6.
 42. Klug MG, Soompa MH, Koh GY, Field LJ. Genetically selected cardiomyocytes from differentiating embryonic stem cells form stable intracardiac grafts. *J Clin Invest.* 1996;98:216–24.
 43. Caspi O, Huber I, Kehat I, Habib M, Arbel G, Gepstein A, Yankelson L, Aronson D, Beyar R, Gepstein L. Transplantation of human embryonic stem cell-derived cardiomyocytes improves myocardial performance in infarcted rat hearts. *J Am Coll Cardiol.* 2007;50:1884–93.
 44. Laflamme MA, Chen KY, Naumova AV, Muskheli V, Fugate JA, Dupras SK, Reinecke H, Xu C, Hassanipour M, Police S, O'Sullivan C, Collins L, Chen Y, Minami E, Gill EA, Ueno S, Yuan C, Gold J, Murry CE. Cardiomyocytes derived from human embryonic stem cells in pro-survival factors enhance function of infarcted rat hearts. *Nat Biotechnol.* 2007;25:1015–24.
 45. Shiba Y, Fernandes S, Zhu WZ, Filice D, Muskheli V, Kim J, Palpant NJ, Gantz J, Moyes KW, Reinecke H, Van Biber B, Dardas T, Mignone JL, Izawa A, Hanna R, Viswanathan M, Gold JD, Kotlikoff MI, Sarvazyan N, Kay MW, Murry CE, Laflamme MA. Human es-cell-derived cardiomyocytes electrically couple and suppress arrhythmias in injured hearts. *Nature.* 2012;489:322–5.
 46. Chong JJ, Yang X, Don CW, Minami E, Liu YW, Weyers JJ, Mahoney WM, Van Biber B, Cook SM, Palpant NJ, Gantz JA, Fugate JA, Muskheli V, Gough GM, Vogel KW, Astley CA, Hotchkiss CE, Baldessari A, Pabon L, Reinecke H, Gill EA, Nelson V, Kiem HP, Laflamme MA, Murry CE. Human embryonic-stem-cell-derived cardiomyocytes regenerate non-human primate hearts. *Nature.* 2014;510:273–7.
 47. Guo XM, Zhao YS, Chang HX, Wang CY, LL E, Zhang XA, Duan CM, Dong LZ, Jiang H, Li J, Song Y, Yang XJ. Creation of engineered cardiac tissue in vitro from mouse embryonic stem cells. *Circulation.* 2006;113:2229–37.
 48. Caspi O, Lesman A, Basevitch Y, Gepstein A, Arbel G, Habib IH, Gepstein L, Levenberg S. Tissue engineering of vascularized cardiac muscle from human embryonic stem cells. *Circ Res.* 2007;100:263–72.
 49. Riegler J, Tiburcy M, Ebert A, Tzatzalos E, Raaz U, Abilez OJ, Shen Q, Kooreman NG, Neofytou E, Chen VC, Wang M, Meyer T, Tsao PS, Connolly AJ, Couture LA, Gold JD, Zimmermann WH, Wu JC. Human engineered heart muscles engraft and survive long term in a rodent myocardial infarction model. *Circ Res.* 2015;117:720–30.
 50. Kim K, Lerou P, Yabuuchi A, Lengerke C, Ng K, West J, Kirby A, Daly MJ, Daley GQ. Histocompatible embryonic stem cells by parthenogenesis. *Science.* 2007;315:482–6.
 51. Chapman DD, Shivji MS, Louis E, Sommer J, Fletcher H, Prodohl PA. Virgin birth in a hammerhead shark. *Biol Lett.* 2007;3:425–7.
 52. Leeb M, Wutz A. Derivation of haploid embryonic stem cells from mouse embryos. *Nature.* 2011;479:131–4.
 53. Dighe V, Clepper L, Pedersen D, Byrne J, Ferguson B, Gokhale S, Penedo MC, Wolf D, Mitalipov S. Heterozygous embryonic stem cell lines derived from nonhuman primate parthenotes. *Stem Cells.* 2008;26:756–66.
 54. Lin G, OuYang Q, Zhou X, Gu Y, Yuan D, Li W, Liu G, Liu T, Lu G. A highly homozygous and parthenogenetic human embryonic stem cell line derived from a one-pronuclear oocyte following in vitro fertilization procedure. *Cell Res.* 2007;17:999–1007.
 55. Lin H, Lei J, Wininger D, Nguyen MT, Khanna R, Hartmann C, Yan WL, Huang SC. Multilineage potential of homozygous stem cells derived from metaphase ii oocytes. *Stem Cells.* 2003;21:152–61.

56. Didie M, Christalla P, Rubart M, Muppala V, Doker S, Unsold B, El-Armouche A, Rau T, Eschenhagen T, Schwoerer AP, Ehmke H, Schumacher U, Fuchs S, Lange C, Becker A, Tao W, Scherschel JA, Soonpaa MH, Yang T, Lin Q, Zenke M, Han DW, Scholer HR, Rudolph C, Steinemann D, Schlegelberger B, Kattman S, Witty A, Keller G, Field LJ, Zimmermann WH. Parthenogenetic stem cells for tissue-engineered heart repair. *J Clin Invest*. 2013;123:1285–98.
57. Takahashi K, Yamanaka S. Induction of pluripotent stem cells from mouse embryonic and adult fibroblast cultures by defined factors. *Cell*. 2006;126:663–76.
58. Bar-Nur O, Russ HA, Efrat S, Benvenisty N. Epigenetic memory and preferential lineage-specific differentiation in induced pluripotent stem cells derived from human pancreatic islet beta cells. *Cell Stem Cell*. 2011;9:17–23.
59. Kim K, Doi A, Wen B, Ng K, Zhao R, Cahan P, Kim J, Aryee MJ, Ji H, Ehrlich LI, Yabuuchi A, Takeuchi A, Cunniff KC, Hongguang H, McKinney-Freeman S, Naveiras O, Yoon TJ, Irizarry RA, Jung N, Seita J, Hanna J, Murakami P, Jaenisch R, Weissleder R, Orkin SH, Weissman IL, Feinberg AP, Daley GQ. Epigenetic memory in induced pluripotent stem cells. *Nature*. 2010;467:285–90.
60. Zhang L, Guo J, Zhang P, Xiong Q, Wu SC, Xia L, Roy SS, Tolar J, O'Connell TD, Kyba M, Liao K, Zhang J. Derivation and high engraftment of patient-specific cardiomyocyte sheet using induced pluripotent stem cells generated from adult cardiac fibroblast. *Circ Heart Fail*. 2015;8:156–66.
61. Tulloch NL, Muskheili V, Razumova MV, Korte FS, Regnier M, Hauch KD, Pabon L, Reinecke H, Murry CE. Growth of engineered human myocardium with mechanical loading and vascular coculture. *Circ Res*. 2011;109:47–59.
62. Kawamura M, Miyagawa S, Miki K, Saito A, Fukushima S, Higuchi T, Kawamura T, Kuratani T, Daimon T, Shimizu T, Okano T, Sawa Y. Feasibility, safety, and therapeutic efficacy of human induced pluripotent stem cell-derived cardiomyocyte sheets in a porcine ischemic cardiomyopathy model. *Circulation*. 2012;126:S29–37.
63. Xiong Q, Ye L, Zhang P, Lepley M, Tian J, Li J, Zhang L, Swingen C, Vaughan JT, Kaufman DS, Zhang J. Functional consequences of human induced pluripotent stem cell therapy: myocardial atp turnover rate in the in vivo swine heart with postinfarction remodeling. *Circulation*. 2013;127:997–1008.
64. Ye L, Chang YH, Xiong Q, Zhang P, Zhang L, Somasundaram P, Lepley M, Swingen C, Su L, Wendel JS, Guo J, Jang A, Rosenbush D, Greder L, Dutton JR, Zhang J, Kamp TJ, Kaufman DS, Ge Y, Zhang J. Cardiac repair in a porcine model of acute myocardial infarction with human induced pluripotent stem cell-derived cardiovascular cells. *Cell Stem Cell*. 2014;15:750–61.
65. Weinberger F, Breckwoldt K, Pecha S, Kelly A, Geertz B, Starbatty J, Yorgan T, Cheng KH, Lessmann K, Stolen T, Scherrer-Crosbie M, Smith G, Reichenspurner H, Hansen A, Eschenhagen T. Cardiac repair in guinea pigs with human engineered heart tissue from induced pluripotent stem cells. *Sci Transl Med*. 2016;8:363ra148.
66. Menasche P, Vanneaux V, Hagege A, Bel A, Cholley B, Cacciapuoti I, Parouchev A, Benhamouda N, Tachdjian G, Tosca L, Trouvin JH, Fabreguettes JR, Bellamy V, Guillemain R, Suberbielle Boissel C, Tartour E, Desnos M, Larghero J. Human embryonic stem cell-derived cardiac progenitors for severe heart failure treatment: first clinical case report. *Eur Heart J*. 2015;36:2011–7.
67. Menasche P, Vanneaux V, Fabreguettes JR, Bel A, Tosca L, Garcia S, Bellamy V, Farouz Y, Pouly J, Damour O, Perier MC, Desnos M, Hagege A, Agbulut O, Bruneval P, Tachdjian G, Trouvin JH, Larghero J. Towards a clinical use of human embryonic stem cell-derived cardiac progenitors: a translational experience. *Eur Heart J*. 2015;36:743–50.
68. Naito H, Melnychenko I, Didie M, Schneiderbanger K, Schubert P, Rosenkranz S, Eschenhagen T, Zimmermann WH. Optimizing engineered heart tissue for therapeutic applications as surrogate heart muscle. *Circulation*. 2006;114:172–8.
69. Banerjee I, Fuseler JW, Price RL, Borg TK, Baudino TA. Determination of cell types and numbers during cardiac development in the neonatal and adult rat and mouse. *Am J Physiol Heart Circ Physiol*. 2007;293:H1883–91.

70. Pinto AR, Ilinykh A, Ivey MJ, Kuwabara JT, D'Antoni ML, Debuque R, Chandran A, Wang L, Arora K, Rosenthal NA, Tallquist MD. Revisiting cardiac cellular composition. *Circ Res.* 2016;118:400–9.
71. Stevens KR, Kreutziger KL, Dupras SK, Korte FS, Regnier M, Muskheli V, Nourse MB, Bendixen K, Reinecke H, Murry CE. Physiological function and transplantation of scaffold-free and vascularized human cardiac muscle tissue. *Proc Natl Acad Sci U S A.* 2009;106:16568–73.
72. Thavandiran N, Dubois N, Mikryukov A, Masse S, Beca B, Simmons CA, Deshpande VS, McGarry JP, Chen CS, Nanthakumar K, Keller GM, Radisic M, Zandstra PW. Design and formulation of functional pluripotent stem cell-derived cardiac microtissues. *Proc Natl Acad Sci U S A.* 2013;110:E4698–707.
73. Lesman A, Habib M, Caspi O, Gepstein A, Arbel G, Levenberg S, Gepstein L. Transplantation of a tissue-engineered human vascularized cardiac muscle. *Tissue Eng Part A.* 2010;16:115–25.
74. Iyer RK, Chiu LL, Radisic M. Microfabricated poly(ethylene glycol) templates enable rapid screening of triculture conditions for cardiac tissue engineering. *J Biomed Mater Res A.* 2009;89:616–31.
75. Iyer RK, Chiu LL, Vunjak-Novakovic G, Radisic M. Biofabrication enables efficient interrogation and optimization of sequential culture of endothelial cells, fibroblasts and cardiomyocytes for formation of vascular cords in cardiac tissue engineering. *Biofabrication.* 2012;4:035002.
76. Iyer RK, Odedra D, Chiu LL, Vunjak-Novakovic G, Radisic M. Vascular endothelial growth factor secretion by nonmyocytes modulates connexin-43 levels in cardiac organoids. *Tissue Eng Part A.* 2012;18:1771–83.
77. Gao L, Gregorich ZR, Zhu W, Mattapally S, Oduk Y, Lou X, Kannappan R, Borovjagin AV, Walcott GP, Pollard AE, Fast VG, Hu X, Lloyd SG, Ge Y, Zhang J. Large cardiac-muscle patches engineered from human induced-pluripotent stem-cell-derived cardiac cells improve recovery from myocardial infarction in swine. *Circulation.* 2018;137(16):1712–30.
78. Gao L, Kupfer ME, Jung JP, Yang L, Zhang P, Da Sie Y, Tran Q, Ajeti V, Freeman BT, Fast VG, Campagnola PJ, Ogle BM, Zhang J. Myocardial tissue engineering with cells derived from human-induced pluripotent stem cells and a native-like, high-resolution, 3-dimensionally printed scaffold. *Circ Res.* 2017;120:1318–25.
79. Masuda S, Shimizu T, Yamato M, Okano T. Cell sheet engineering for heart tissue repair. *Adv Drug Deliv Rev.* 2008;60:277–85.
80. Wang B, Borazjani A, Tahai M, Curry AL, Simionescu DT, Guan J, To F, Elder SH, Liao J. Fabrication of cardiac patch with decellularized porcine myocardial scaffold and bone marrow mononuclear cells. *J Biomed Mater Res A.* 2010;94:1100–10.
81. Oberwallner B, Brodarac A, Choi YH, Saric T, Anic P, Morawietz L, Stamm C. Preparation of cardiac extracellular matrix scaffolds by decellularization of human myocardium. *J Biomed Mater Res A.* 2014;102:3263–72.
82. Rosso F, Giordano A, Barbarisi M, Barbarisi A. From cell-ecm interactions to tissue engineering. *J Cell Physiol.* 2004;199:174–80.
83. DeMali KA, Adams JC. Cell–cell and cell–matrix interactions. *Mol Biol Cell.* 2012;23:965.
84. Maureira P, Marie PY, Yu F, Poussier S, Liu Y, Groubatch F, Falanga A, Tran N. Repairing chronic myocardial infarction with autologous mesenchymal stem cells engineered tissue in rat promotes angiogenesis and limits ventricular remodeling. *J Biomed Sci.* 2012;19:93.
85. Fukuhara S, Tomita S, Nakatani T, Fujisato T, Ohtsu Y, Ishida M, Yutani C, Kitamura S. Bone marrow cell-seeded biodegradable polymeric scaffold enhances angiogenesis and improves function of the infarcted heart. *Circ J.* 2005;69:850–7.
86. Chi NH, Yang MC, Chung TW, Chen JY, Chou NK, Wang SS. Cardiac repair achieved by bone marrow mesenchymal stem cells/silk fibroin/hyaluronic acid patches in a rat of myocardial infarction model. *Biomaterials.* 2012;33:5541–51.
87. Ceccaldi C, Bushkalova R, Alfaro C, Lairez O, Calise D, Bourin P, Frugier C, Rouzaud-Laborde C, Cussac D, Parini A, Sallerin B, Fullana SG. Evaluation of polyelectrolyte complex-based scaffolds for mesenchymal stem cell therapy in cardiac ischemia treatment. *Acta Biomater.* 2014;10:901–11.

88. Kai D, Wang QL, Wang HJ, Prabhakaran MP, Zhang Y, Tan YZ, Ramakrishna S. Stem cell-loaded nanofibrous patch promotes the regeneration of infarcted myocardium with functional improvement in rat model. *Acta Biomater.* 2014;10:2727–38.
89. Guex AG, Frobert A, Valentin J, Fortunato G, Hegemann D, Cook S, Carrel TP, Tevæearai HT, Giraud MN. Plasma-functionalized electrospun matrix for biograft development and cardiac function stabilization. *Acta Biomater.* 2014;10:2996–3006.
90. Kai D, Jin G, Prabhakaran MP, Ramakrishna S. Electrospun synthetic and natural nanofibers for regenerative medicine and stem cells. *Biotechnol J.* 2013;8:59–72.
91. Wells RG. The role of matrix stiffness in regulating cell behavior. *Hepatology (Baltimore, Md).* 2008;47:1394–400.
92. Sherratt MJ. Tissue elasticity and the ageing elastic fibre. *Age.* 2009;31:305–25.
93. Engler AJ, Sen S, Sweeney HL, Discher DE. Matrix elasticity directs stem cell lineage specification. *Cell.* 2006;126:677–89.
94. Long JL, Tranquillo RT. Elastic fiber production in cardiovascular tissue-equivalents. *Matrix Biol.* 2003;22:339–50.
95. Wang X, Hu Q, Mansoor A, Lee J, Wang Z, Lee T, From AH, Zhang J. Bioenergetic and functional consequences of stem cell-based vegf delivery in pressure-overloaded swine hearts. *Am J Physiol Heart Circ Physiol.* 2006;290:H1393–405.
96. Shiba Y, Gomibuchi T, Seto T, Wada Y, Ichimura H, Tanaka Y, Ogasawara T, Okada K, Shiba N, Sakamoto K, Ido D, Shiina T, Ohkura M, Nakai J, Uno N, Kazuki Y, Oshimura M, Minami I, Ikeda U. Allogeneic transplantation of ips cell-derived cardiomyocytes regenerates primate hearts. *Nature.* 2016;538:388–91.
97. Liu YW, Chen B, Yang X, Fugate JA, Kalucki FA, Futakuchi-Tsuchida A, Couture L, Vogel KW, Astley CA, Baldessari A, Ogle J, Don CW, Steinberg ZL, Seslar SP, Tuck SA, Tsuchida H, Naumova AV, Dupras SK, Lyu MS, Lee J, Hailey DW, Reinecke H, Pabon L, Fryer BH, MacLellan WR, Thies RS, Murry CE. Human embryonic stem cell-derived cardiomyocytes restore function in infarcted hearts of non-human primates. *Nat Biotechnol.* 2018;36:597–605.
98. Wang X, Hu Q, Nakamura Y, Lee J, Zhang G, From AH, Zhang J. The role of the sca-1+/cd31- cardiac progenitor cell population in postinfarction left ventricular remodeling. *Stem Cells.* 2006;24:1779–88.
99. Zeng L, Hu Q, Wang X, Mansoor A, Lee J, Feygin J, Zhang G, Suntharalingam P, Boozer S, Mhashikar A, Panetta CJ, Swingen C, Deans R, From AH, Bache RJ, Verfaillie CM, Zhang J. Bioenergetic and functional consequences of bone marrow-derived multipotent progenitor cell transplantation in hearts with postinfarction left ventricular remodeling. *Circulation.* 2007;115:1866–75.
100. Kishore R, Garikipati VN, Gumpert A. Tiny shuttles for information transfer: exosomes in cardiac health and disease. *J Cardiovasc Transl Res.* 2016;9:169–75.
101. van der Pol E, Boing AN, Harrison P, Sturk A, Nieuwland R. Classification, functions, and clinical relevance of extracellular vesicles. *Pharmacol Rev.* 2012;64:676–705.
102. Sahoo S, Klychko E, Thorne T, Misener S, Schultz KM, Millay M, Ito A, Liu T, Kamide C, Agrawal H, Perlman H, Qin G, Kishore R, Losordo DW. Exosomes from human cd34(+) stem cells mediate their proangiogenic paracrine activity. *Circ Res.* 2011;109:724–8.
103. Mathiyalagan P, Liang Y, Kim D, Misener S, Thorne T, Kamide CE, Klyachko E, Losordo DW, Hajjar RJ, Sahoo S. Angiogenic mechanisms of human cd34(+) stem cell exosomes in the repair of ischemic hindlimb. *Circ Res.* 2017;120:1466–76.
104. Khan M, Nickoloff E, Abramova T, Johnson J, Verma SK, Krishnamurthy P, Mackie AR, Vaughan E, Garikipati VN, Benedict C, Ramirez V, Lambers E, Ito A, Gao E, Misener S, Luongo T, Elrod J, Qin G, Houser SR, Koch WJ, Kishore R. Embryonic stem cell-derived exosomes promote endogenous repair mechanisms and enhance cardiac function following myocardial infarction. *Circ Res.* 2015;117:52–64.
105. Gallet R, Dawkins J, Valle J, Simsolo E, de Couto G, Middleton R, Tseliou E, Luthringer D, Kreke M, Smith RR, Marban L, Ghaleh B, Marban E. Exosomes secreted by cardiosphere-derived cells reduce scarring, attenuate adverse remodelling, and improve function in acute and chronic porcine myocardial infarction. *Eur Heart J.* 2017;38:201–11.

106. Sugiura T, Hibino N, Breuer CK, Shinoka T. Tissue-engineered cardiac patch seeded with human induced pluripotent stem cell derived cardiomyocytes promoted the regeneration of host cardiomyocytes in a rat model. *J Cardiothorac Surg.* 2016;11:163.
107. Bolli R, Hare JM, March KL, Pepine CJ, Willerson JT, Perin EC, Yang PC, Henry TD, Traverse JH, Mitrani RD, Khan A, Hernandez-Schulman I, Taylor DA, DiFede DL, Lima JAC, Chugh A, Loughran J, Vojvodic RW, Sayre SL, Bettencourt J, Cohen M, Moye L, Ebert RF, Simari RD. Cardiovascular Cell Therapy Research N. Rationale and design of the concert-hf trial (combination of mesenchymal and c-kit(+)) cardiac stem cells as regenerative therapy for heart failure). *Circ Res.* 2018;122:1703–15.
108. Natsumeda M, Florea V, Rieger AC, Tompkins BA, Banerjee MN, Golpanian S, Fritsch J, Landin AM, Kashikar ND, Karantalis V, Loescher VY, Hatzistergos KE, Bagno L, Sanina C, Mushtaq M, Rodriguez J, Rosado M, Wolf A, Collon K, Vincent L, Kanelidis AJ, Schulman IH, Mitrani R, Heldman AW, Balkan W, Hare JM. A combination of allogeneic stem cells promotes cardiac regeneration. *J Am Coll Cardiol.* 2017;70:2504–15.
109. Okano T, Yamada N, Sakai H, Sakurai Y. A novel recovery system for cultured cells using plasma-treated polystyrene dishes grafted with poly(n-isopropylacrylamide). *J Biomed Mater Res.* 1993;27:1243–51.
110. Cooperstein MA, Canavan HE. Assessment of cytotoxicity of (n-isopropyl acrylamide) and poly(n-isopropyl acrylamide)-coated surfaces. *Biointerphases.* 2013;8:19.
111. Shimizu T, Yamato M, Isoi Y, Akutsu T, Setomaru T, Abe K, Kikuchi A, Umezumi M, Okano T. Fabrication of pulsatile cardiac tissue grafts using a novel 3-dimensional cell sheet manipulation technique and temperature-responsive cell culture surfaces. *Circ Res.* 2002;90:e40.
112. Haraguchi Y, Shimizu T, Yamato M, Kikuchi A, Okano T. Electrical coupling of cardiomyocyte sheets occurs rapidly via functional gap junction formation. *Biomaterials.* 2006;27:4765–74.
113. Kreuziger KL, Muskheli V, Johnson P, Braun K, Wight TN, Murry CE. Developing vasculature and stroma in engineered human myocardium. *Tissue Eng A.* 2011;17:1219–28.
114. Goldmann WH. Chapter four – mechanosensation: a basic cellular process. In: Engler AJ, Kumar S, editors. *Progress in molecular biology and translational science.* Academic Press; 2014. p. 75–102.
115. Shadrin IY, Allen BW, Qian Y, Jackman CP, Carlson AL, Juhas ME, Bursac N. Cardiopatch platform enables maturation and scale-up of human pluripotent stem cell-derived engineered heart tissues. *Nat Commun.* 2017;8:1825.
116. Zhang G, Wang X, Wang Z, Zhang J, Suggs APL. A pegylated fibrin patch for mesenchymal stem cell delivery. *Tissue Eng.* 2006;12:9–19.
117. Blondiaux E, Pidal L, Autret G, Rahmi G, Balvay D, Audureau E, Wilhelm C, Guerin CL, Bruneval P, Silvestre JS, Menasche P, Clement O. Bone marrow-derived mesenchymal stem cell-loaded fibrin patches act as a reservoir of paracrine factors in chronic myocardial infarction. *J Tissue Eng Regen Med.* 2017;11:3417–27.
118. Rane AA, Christman KL. Biomaterials for the treatment of myocardial infarction: a 5-year update. *J Am Coll Cardiol.* 2011;58:2615–29.
119. Bezuidenhout D, Davies N, Black M, Schmidt C, Oosthuysen A, Zilla P. Covalent surface heparinization potentiates porous polyurethane scaffold vascularization. *J Biomater Appl.* 2010;24:401–18.
120. Engelmayr GC Jr, Cheng M, Bettinger CJ, Borenstein JT, Langer R, Freed LE. Accordion-like honeycombs for tissue engineering of cardiac anisotropy. *Nat Mater.* 2008;7:1003–10.
121. Badie N, Satterwhite L, Bursac N. A method to replicate the microstructure of heart tissue in vitro using dtmri-based cell micropatterning. *Ann Biomed Eng.* 2009;37(12):2510.
122. Badie N, Bursac N. Novel micropatterned cardiac cell cultures with realistic ventricular microstructure. *Biophys J.* 2009;96:3873–85.
123. Kim DH, Lipke EA, Kim P, Cheong R, Thompson S, Delannoy M, Suh KY, Tung L, Levchenko A. Nanoscale cues regulate the structure and function of macroscopic cardiac tissue constructs. *Proc Natl Acad Sci U S A.* 2010;107:565–70.

124. Montgomery M, Ahadian S, Davenport Huyer L, Lo Rito M, Civitaresse RA, Vanderlaan RD, Wu J, Reis LA, Momen A, Akbari S, Pahnke A, Li RK, Caldarone CA, Radisic M. Flexible shape-memory scaffold for minimally invasive delivery of functional tissues. *Nat Mater.* 2017;16:1038–46.
125. Davenport Huyer L, Zhang B, Korolj A, Montgomery M, Drecun S, Conant G, Zhao Y, Reis L, Radisic M. Highly elastic and moldable polyester biomaterial for cardiac tissue engineering applications. *ACS Biomater Sci Eng.* 2016;2(5):780–8.
126. Nguyen PK, Rhee JW, Wu JC. Adult stem cell therapy and heart failure, 2000 to 2016: a systematic review. *JAMA Cardiol.* 2016;1:831–41.
127. Wendel JS, Ye L, Tao R, Zhang J, Zhang J, Kamp TJ, Tranquillo RT. Functional effects of a tissue-engineered cardiac patch from human induced pluripotent stem cell-derived cardiomyocytes in a rat infarct model. *Stem Cells Transl Med.* 2015;4:1324–32.
128. Wendel JS, Ye L, Zhang P, Tranquillo RT, Zhang JJ. Functional consequences of a tissue-engineered myocardial patch for cardiac repair in a rat infarct model. *Tissue Eng A.* 2014;20:1325–35.
129. Zimmermann WH, Didie M, Wasmeier GH, Nixdorff U, Hess A, Melnychenko I, Boy O, Neuhuber WL, Weyand M, Eschenhagen T. Cardiac grafting of engineered heart tissue in syngenic rats. *Circulation.* 2002;106:1151–7.
130. Masumoto H, Ikuno T, Takeda M, Fukushima H, Marui A, Katayama S, Shimizu T, Ikeda T, Okano T, Sakata R, Yamashita JK. Human ips cell-engineered cardiac tissue sheets with cardiomyocytes and vascular cells for cardiac regeneration. *Sci Rep.* 2014;4:6716.
131. Wang Q, Yang H, Bai A, Jiang W, Li X, Wang X, Mao Y, Lu C, Qian R, Guo F, Ding T, Chen H, Chen S, Zhang J, Liu C, Sun N. Functional engineered human cardiac patches prepared from nature's platform improve heart function after acute myocardial infarction. *Biomaterials.* 2016;105:52–65.
132. Xiong Q, Ye L, Zhang P, Lepley M, Swingen C, Zhang L, Kaufman DS, Zhang J. Bioenergetic and functional consequences of cellular therapy: activation of endogenous cardiovascular progenitor cells. *Circ Res.* 2012;111:455–68.
133. Darland DC, Massingham LJ, Smith SR, Piek E, Saint-Geniez M, D'Amore PA. Pericyte production of cell-associated vegf is differentiation-dependent and is associated with endothelial survival. *Dev Biol.* 2003;264:275–88.
134. Masumoto H, Matsuo T, Yamamizu K, Uosaki H, Narazaki G, Katayama S, Marui A, Shimizu T, Ikeda T, Okano T, Sakata R, Yamashita JK. Pluripotent stem cell-engineered cell sheets reassembled with defined cardiovascular populations ameliorate reduction in infarct heart function through cardiomyocyte-mediated neovascularization. *Stem Cells.* 2012;30:1196–205.
135. Iseoka H, Miyagawa S, Fukushima S, Saito A, Masuda S, Yajima S, Ito E, Sougawa N, Takeda M, Harada A, Lee JK, Sawa Y. Pivotal role of non-cardiomyocytes in electromechanical and therapeutic potential of induced pluripotent stem cell-derived engineered cardiac tissue. *Tissue Eng Part A.* 2018;24(3-4):287–300.
136. Dvir T, Kedem A, Ruvinov E, Levy O, Freeman I, Landa N, Holbova R, Feinberg MS, Dror S, Etzion Y, Leor J, Cohen S. Prevascularization of cardiac patch on the omentum improves its therapeutic outcome. *Proc Natl Acad Sci U S A.* 2009;106:14990–5.
137. Zhang J, Zhu W, Radisic M, Vunjak-Novakovic G. Can we engineer a human cardiac patch for therapy? *Circ Res.* 2018;123:244–65.
138. Kadota S, Pabon L, Reinecke H, Murry CE. In vivo maturation of human induced pluripotent stem cell-derived cardiomyocytes in neonatal and adult rat hearts. *Stem Cell Rep.* 2017;8:278–89.
139. Cho GS, Lee DI, Tampakakis E, Murphy S, Andersen P, Uosaki H, Chelko S, Chakir K, Hong I, Seo K, Chen HV, Chen X, Basso C, Houser SR, Tomaselli GF, O'Rourke B, Judge DP, Kass DA, Kwon C. Neonatal transplantation confers maturation of psc-derived cardiomyocytes conducive to modeling cardiomyopathy. *Cell Rep.* 2017;18:571–82.
140. Radisic M, Park H, Shing H, Consi T, Schoen FJ, Langer R, Freed LE, Vunjak-Novakovic G. Functional assembly of engineered myocardium by electrical stimulation of cardiac myocytes cultured on scaffolds. *Proc Natl Acad Sci U S A.* 2004;101:18129–34.

141. Hirt MN, Boeddinghaus J, Mitchell A, Schaaf S, Bornchen C, Muller C, Schulz H, Hubner N, Stenzig J, Stoehr A, Neuber C, Eder A, Luther PK, Hansen A, Eschenhagen T. Functional improvement and maturation of rat and human engineered heart tissue by chronic electrical stimulation. *J Mol Cell Cardiol.* 2014;74:151–61.
142. Ruan JL, Tulloch NL, Razumova MV, Saiget M, Muskheli V, Pabon L, Reinecke H, Regnier M, Murry CE. Mechanical stress conditioning and electrical stimulation promote contractility and force maturation of induced pluripotent stem cell-derived human cardiac tissue. *Circulation.* 2016;134:1557–67.
143. Parikh SS, Blackwell DJ, Gomez-Hurtado N, Frisk M, Wang L, Kim K, Dahl CP, Fiane A, Tonnessen T, Kryshnal DO, Louch WE, Knollmann BC. Thyroid and glucocorticoid hormones promote functional t-tubule development in human-induced pluripotent stem cell-derived cardiomyocytes. *Circ Res.* 2017;121:1323–30.
144. Ronaldson-Bouchard K, Ma SP, Yeager K, Chen T, Song L, Sirabella D, Morikawa K, Teles D, Yazawa M, Vunjak-Novakovic G. Advanced maturation of human cardiac tissue grown from pluripotent stem cells. *Nature.* 2018;556:239–43.
145. Ye L, Zimmermann WH, Garry DJ, Zhang J. Patching the heart: cardiac repair from within and outside. *Circ Res.* 2013;113:922–32.
146. Traverse JH, Henry TD, Ellis SG, Pepine CJ, Willerson JT, Zhao DX, Forder JR, Byrne BJ, Hatzopoulos AK, Penn MS, Perin EC, Baran KW, Chambers J, Lambert C, Raveendran G, Simon DI, Vaughan DE, Simpson LM, Gee AP, Taylor DA, Cogle CR, Thomas JD, Silva GV, Jorgenson BC, Olson RE, Bowman S, Francescon J, Geither C, Handberg E, Smith DX, Baraniuk S, Piller LB, Loghin C, Aguilar D, Richman S, Zierold C, Bettencourt J, Sayre SL, Vojvodic RW, Skarlatos SI, Gordon DJ, Ebert RF, Kwak M, Moye LA, Simari RD. Cardiovascular Cell Therapy R. Effect of intracoronary delivery of autologous bone marrow mononuclear cells 2 to 3 weeks following acute myocardial infarction on left ventricular function: the latetime randomized trial. *JAMA.* 2011;306:2110–9.
147. Traverse JH, Henry TD, Pepine CJ, Willerson JT, Zhao DX, Ellis SG, Forder JR, Anderson RD, Hatzopoulos AK, Penn MS, Perin EC, Chambers J, Baran KW, Raveendran G, Lambert C, Lerman A, Simon DI, Vaughan DE, Lai D, Gee AP, Taylor DA, Cogle CR, Thomas JD, Olson RE, Bowman S, Francescon J, Geither C, Handberg E, Kappenman C, Westbrook L, Piller LB, Simpson LM, Baraniuk S, Loghin C, Aguilar D, Richman S, Zierold C, Spoon DB, Bettencourt J, Sayre SL, Vojvodic RW, Skarlatos SI, Gordon DJ, Ebert RF, Kwak M, Moye LA, Simari RD, Cardiovascular Cell Therapy Research N. Effect of the use and timing of bone marrow mononuclear cell delivery on left ventricular function after acute myocardial infarction: the time randomized trial. *JAMA.* 2012;308:2380–9.
148. Lapidot T, Pflumio F, Doedens M, Murdoch B, Williams DE, Dick JE. Cytokine stimulation of multilineage hematopoiesis from immature human cells engrafted in scid mice. *Science.* 1992;255:1137–41.
149. Kulandavelu S, Karantalis V, Fritsch J, Hatzistergos KE, Loescher VY, McCall F, Wang B, Bagno L, Golpanian S, Wolf A, Grenet J, Williams A, Kupin A, Rosenfeld A, Mohsin S, Sussman MA, Morales A, Balkan W, Hare JM. Pim1 kinase overexpression enhances ckit(+) cardiac stem cell cardiac repair following myocardial infarction in swine. *J Am Coll Cardiol.* 2016;68:2454–64.
150. Karantalis V, Suncion-Loescher VY, Bagno L, Golpanian S, Wolf A, Sanina C, Premer C, Kanelidis AJ, McCall F, Wang B, Balkan W, Rodriguez J, Rosado M, Morales A, Hatzistergos K, Natsumeda M, Margitich I, Schulman IH, Gomes SA, Mushtaq M, DiFede DL, Fishman JE, Pattany P, Zambrano JP, Heldman AW, Hare JM. Synergistic effects of combined cell therapy for chronic ischemic cardiomyopathy. *J Am Coll Cardiol.* 2015;66:1990–9.
151. Kedes L, Kloner RA, Starnes VA. Can a few good cells now mend a broken heart? *J Clin Invest.* 1993;92:1115–6.
152. Frisch SM, Sreaton RA. Anokis mechanisms. *Curr Opin Cell Biol.* 2001;13:555–62.
153. Imanaka-Yoshida K, Hiroe M, Yoshida T. Interaction between cell and extracellular matrix in heart disease: multiple roles of tenascin-c in tissue remodeling. *Histol Histopathol.* 2004;19:517–25.

154. Csete M. Oxygen in the cultivation of stem cells. *Ann N Y Acad Sci.* 2005;1049:1–8.
155. Haider HK, Ashraf M. Strategies to promote donor cell survival: combining preconditioning approach with stem cell transplantation. *J Mol Cell Cardiol.* 2008;45:554–66.
156. Mehta JL, Nichols WW, Mehta P. Neutrophils as potential participants in acute myocardial ischemia: relevance to reperfusion. *J Am Coll Cardiol.* 1988;11:1309–16.
157. Nahrendorf M, Swirski FK, Aikawa E, Stangenberg L, Wurdinger T, Figueiredo J-L, Libby P, Weissleder R, Pittet MJ. The healing myocardium sequentially mobilizes two monocyte subsets with divergent and complementary functions. *J Exp Med.* 2007;204:3037–47.
158. Zhao M, Fan C, Ernst PJ, Tang Y, Zhu H, Mattapally S, Oduk Y, Borovjagin AV, Zhou L, Zhang J, Zhu W. Y-27632 preconditioning enhances transplantation of human induced pluripotent stem cell-derived cardiomyocytes in myocardial infarction mice. *Cardiovasc Res.* 2018;115(2):343–56.
159. Christman KL, Lee RJ. Biomaterials for the treatment of myocardial infarction. *J Am Coll Cardiol.* 2006;48:907–13.
160. Wang B, Borazjani A, Tahai M, de Jongh Curry AL, Simionescu DT, Guan J, To F, Elder SH, Liao J. Fabrication of cardiac patch with decellularized porcine myocardial scaffold and bone marrow mononuclear cells. *J Biomed Mater Res A.* 2010;94A:1100–10.
161. Seal BL, Otero TC, Panitch A. Polymeric biomaterials for tissue and organ regeneration. *Mater Sci Eng R Rep.* 2001;34:147–230.
162. Shoichet MS. Polymer scaffolds for biomaterials applications. *Macromolecules.* 2010;43:581–91.
163. Moscona AA. Tissues from dissociated cells. *Sci Am.* 1959;200:132–134 passim.
164. Akins RE, Boyce RA, Madonna ML, Schroedl NA, Gonda SR, McLaughlin TA, Hartzell CR. Cardiac organogenesis in vitro: reestablishment of three-dimensional tissue architecture by dissociated neonatal rat ventricular cells. *Tissue Eng.* 1999;5:103–18.
165. Nguyen DC, Hookway TA, Wu Q, Jha R, Preininger MK, Chen X, Easley CA, Spearman P, Deshpande SR, Maher K, Wagner MB, McDevitt TC, Xu C. Microscale generation of cardiospheres promotes robust enrichment of cardiomyocytes derived from human pluripotent stem cells. *Stem Cell Rep.* 2014;3:260–8.
166. Oltolina F, Zamperone A, Colangelo D, Gregoletto L, Reano S, Pietronave S, Merlin S, Talmon M, Novelli E, Diena M, Nicoletti C, Musaro A, Filigheddu N, Follenzi A, Prat M. Human cardiac progenitor spheroids exhibit enhanced engraftment potential. *PLoS One.* 2015;10:e0137999.
167. Bartulos O, Zhuang ZW, Huang Y, Mikush N, Suh C, Bregasi A, Wang L, Chang W, Krause DS, Young LH, Pober JS, Qyang Y. Isl1 cardiovascular progenitor cells for cardiac repair after myocardial infarction. *JCI Insight.* 2016;1(10).
168. Zhao S, Xu Z, Wang H, Reese BE, Gushchina LV, Jiang M, Agarwal P, Xu J, Zhang M, Shen R, Liu Z, Weissleder N, He X. Bioengineering of injectable encapsulated aggregates of pluripotent stem cells for therapy of myocardial infarction. *Nat Commun.* 2016;7:13306.
169. Ong CS, Fukunishi T, Zhang H, Huang CY, Nashed A, Blazeski A, DiSilvestre D, Vricella L, Conte J, Tung L, Tomaselli GF, Hibino N. Biomaterial-free three-dimensional bioprinting of cardiac tissue using human induced pluripotent stem cell derived cardiomyocytes. *Sci Rep.* 2017;7:4566.
170. Mattapally S, Zhu W, Fast VG, Gao L, Worley C, Kannappan R, Borovjagin AV, Zhang J. Spheroids of cardiomyocytes derived from human-induced pluripotent stem cells improve recovery from myocardial injury in mice. *Am J Physiol Heart Circ Physiol.* 2018;315:H327–39.
171. Tokita Y, Tang XL, Li Q, Wysoczynski M, Hong KU, Nakamura S, Wu WJ, Xie W, Li D, Hunt G, Ou Q, Stowers H, Bolli R. Repeated administrations of cardiac progenitor cells are markedly more effective than a single administration: a new paradigm in cell therapy. *Circ Res.* 2016;119:635–51.
172. Guo Y, Wysoczynski M, Nong Y, Tomlin A, Zhu X, Gumpert AM, Nasr M, Muthusamy S, Li H, Book M, Khan A, Hong KU, Li Q, Bolli R. Repeated doses of cardiac mesenchymal cells are therapeutically superior to a single dose in mice with old myocardial infarction. *Basic Res Cardiol.* 2017;112:18.

173. Bolli R. Repeated cell therapy: a paradigm shift whose time has come. *Circ Res.* 2017;120:1072–4.
174. Zhu W, Zhao M, Mattapally S, Chen S, Zhang J. Ccnd2 overexpression enhances the regenerative potency of human induced pluripotent stem cell-derived cardiomyocytes: remuscularization of injured ventricle. *Circ Res.* 2018;122:88–96.
175. Qin X, Riegler J, Tiburcy M, Zhao X, Chour T, Ndoye B, Nguyen M, Adams J, Ameen M, Denney TS Jr, Yang PC, Nguyen P, Zimmermann WH, Wu JC. Magnetic resonance imaging of cardiac strain pattern following transplantation of human tissue engineered heart muscles. *Circ Cardiovasc Imaging.* 2016;9(11):e004731.



Cell-Based Cardiovascular Regenerative Therapies

9

Ray P. Prajnamitra, Yuan-Yuan Cheng, Li-Lun Chen,
and Patrick C. H. Hsieh

Introduction

Cardiovascular disease is one of the leading causes of death in the world. According to the report published by the American Heart Association, out of an estimated 54 million deaths throughout the world in 2013, cardiovascular diseases contributed to 17.3 million (31.5%) deaths, with ischemic heart disease being the most common cause [1]. As such, there is an urgent need to address this problem.

The left ventricle of an adult human heart contains around two to four billions cardiomyocytes (heart muscle cells). When a person suffers from cardiovascular diseases such as myocardial infarction (MI), as much as one billion of his/her cardiomyocytes die within a few hours [2]. Adult cardiomyocytes are known to have poor proliferation capability, meaning that they possess poor ability to generate new cells to replace the lost cardiomyocytes. Hence, subsequent healing of the heart post-MI mainly takes place through scar formation rather than muscle regeneration. This eventually results in the loss of heart muscle strength and over time, when more and more cardiomyocytes are lost without new ones being regenerated, the patient will eventually develop heart failure.

In some cases, cardiac transplantation is performed as a last resort; however patients who are in need of transplantation far outnumber the available donors. Furthermore, there is always a risk of organ rejection posttransplantation by the recipient's immune system. With this in mind, researchers around the world have focused on alternative therapeutic methods that are capable of preventing the progression of cardiovascular diseases. This can be achieved either by preventing the death of cardiomyocytes or by regenerating the lost cells. This chapter focuses on the latter, specifically on myocardial regeneration by means of differentiation of stem cells and other modified cell types as shown in Fig. 9.1.

R. P. Prajnamitra · Y.-Y. Cheng · L.-L. Chen · P. C. H. Hsieh (✉)
Institute of Biomedical Sciences, Academia Sinica, Taipei, Taiwan
e-mail: pshieh@ibms.sinica.edu.tw

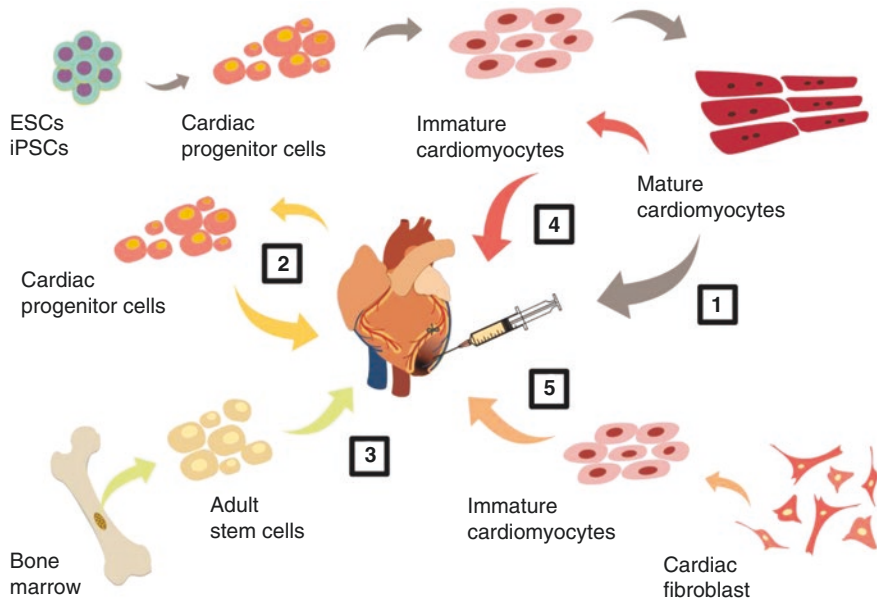


Fig. 9.1 General overview of the cell sources used for cell-based regenerative therapy reviewed in this chapter: (1) pluripotent stem cell-derived cardiomyocytes, (2) cardiac progenitor cells, (3) adult stem cells, (4) proliferative immature cardiomyocytes, and (5) cardiac fibroblast-derived cardiomyocytes

Pluripotent Stem Cells

Pluripotent Stem Cells for Cardiomyocyte Regeneration

Stem cells are defined by their capacity to maintain their undifferentiated state while proliferating, but are also capable of differentiating into various cell types when necessary. Pluripotent stem cells (PSCs) are able to differentiate into different cell lineages, including cardiac cell lineage, and are one of the most promising candidates among various stem cell sources for cardiac regeneration [3]. Embryonic stem cells (ESCs) and induced pluripotent stem cells (iPSCs) are two main PSCs that have been extensively investigated for cardiac regeneration.

ESCs are derived from the inner cell mass of a blastocyst. These pluripotent cells can be directly differentiated into the desired cell types from any lineages. Following the isolation of the inner cell mass, a blastocyst is destroyed and is therefore not able to develop into an embryo (human or murine). This has led to controversies concerning the ethical issues of using human embryo for stem cell research.

Unlike ESCs, iPSCs are derived from somatic cells, such as fibroblasts or peripheral blood. These terminally differentiated cells can regain their pluripotency by undergoing a reprogramming process, through the introduction of several

transcription factors that are important for pluripotency [4–6]. In their seminal work published in 2006, Yamanaka and associates successfully reprogrammed mouse fibroblast to iPSCs by using a cocktail of four transcription factors, Oct3/4, Sox2, c-Myc, and Klf4 [5]. In the years that followed, many other groups also reported successful reprogramming of human somatic cells such as dermal fibroblasts [6–8], peripheral blood cells [9–12], and keratinocytes [13, 14] to iPSCs by using various combinations of transcription factor cocktails. The resulting reprogrammed pluripotent cells are highly similar to ESCs [15] and can subsequently be differentiated into the desired cell types from any lineages. One obvious advantage of iPSCs compared to ESCs is that they do not involve isolation of cells from an embryo and therefore circumvent the aforementioned ethical issues.

Aside from circumventing the ethical issue posed by using ESCs, another advantage of using iPSCs as an alternative is the clinical advantage. It is well known that patients who undergo organ transplantation are at risk of rejection from their own immune system. Similarly, there is a high risk that the transplanted ESC-derived cells are rejected by the patient's immune system [16]. Since iPSCs can be derived from patient's own somatic cells, patient-specific iPSCs can be generated. Together with the aid of immunosuppressant drugs, the risk of rejection by the patient's immune system should be reduced when transplanting autologous iPSC-derived cells [16, 17].

PSCs are able to differentiate into many types of cells including cardiomyocytes. However, poor differentiation and purification of desired cells in culture may result in PSCs differentiating into unintended cell types. If undifferentiated PSCs are transplanted along with differentiated cells, then they may lead to teratoma formation. Efficient differentiation and purification of target cells from unwanted ones are crucial in avoiding the potential formation of teratomas or other types of cancer.

Differentiation of PSCs to Cardiomyocytes and Their Maturation

Both ESCs and iPSCs are capable of differentiation into many types of cells from various lineages, including cardiac lineage. In order to achieve this, there are several important stages that PSCs have to undergo and several important growth factors that have to be administered during the differentiation. There are two most commonly utilized methods for differentiating cardiomyocytes from human PSCs (hPSCs), namely, embryonic body (EB) formation and monolayer culture during the initial stages of PSC differentiation. Either of these strategies lead to the induction of mesoderm which can then be stimulated to cardiac specification and cardiac maturation.

In order for the cells to achieve each of these stages, specific conditions and growth factors are needed, and these have been reported by various groups [18–24]. EB can be formed by culturing hPSCs in StemPro34 culture medium [19–21]. On the other hand, monolayer culture is achieved by culturing them in mTeSR1 or MEF-conditioned (mouse embryonic fibroblast conditioned medium, CM) culture medium which is then replaced with Roswell Park Memorial Institute (RPMI)

medium containing B27 supplement [22, 23]. Either EB or monolayer PSC culture then undergoes mesoderm induction through treatment with WNT activator/GSK3-beta inhibitor such as CHIR99021 or by combination Activin A/BMP4 [19, 20, 22, 23]. The culture media is largely not changed to allow for the accumulation of secreted growth factors. After mesodermal differentiation has been induced, inhibitors of WNT signaling such as IWR-1 or IWP-4 are then added to direct specification toward cardiac differentiation [21, 23]. Finally, factors that promote cardiac differentiation such as VEGF, FGF2, or small molecule triiodothyronine [19–21, 24] are added to enhance the yield of cardiomyocytes.

One of the limitations in using PSC-derived cardiomyocytes (PSC-CMs) for cardiac repair is their immaturity. These cells tend to exhibit the phenotype of fetal cells rather than adult cells. This is to be expected, as adult cardiomyocytes in the human body have undergone years of maturation. In contrast, newly differentiated PSC-CMs have only undergone a few weeks of maturation [25]. Some of the characteristics, among others, that can be used to differentiate immature and mature cells are size, shape, alignment, resting membrane potential, and metabolic substrate [25, 26].

Immature PSC-CMs are small and round-shaped, have disorganized sarcomeres, and possess a resting membrane potential of about -60 mV [25]. They rely on glucose and glycolysis as their main metabolic substrate and metabolism pathway, respectively [26]. When cardiomyocytes mature, they become larger and rod-shaped, with highly organized sarcomeres and a resting membrane potential of about -80 to -90 mV [25]. Their oxidative ability increases as they mature, and therefore, mature cardiomyocytes tend to use fatty acid as their main metabolic substrate and hence the β -oxidation as their metabolism pathway [26].

Transplantation of immature PSC-CMs may result in arrhythmia (irregular heartbeat) and less efficient contraction [24], and therefore, maturation should be achieved either prior or shortly after transplantation to ensure patient's safety. There are several ways to promote the maturation of PSC-CMs, such as treating with small molecules (triiodothyronine) [24], co-culturing cardiomyocytes along with non-cardiomyocytes such as endothelial cells, or electrical and mechanical stimulation [25, 27, 28]. These methods work synergistically to enhance the electrophysiological and mechanical maturation of cardiomyocytes [24, 28].

Alignment of cardiomyocytes is also an important issue, as immature PSC-CMs tend to be disorganized. One study proved the importance of alignment by culturing cardiomyocytes and endothelial cells aligned and nonaligned nanofibrous electrospun patches [29]. The resulting aligned and nonaligned patches were transplanted on rats with MI hearts. It was found that the cardiac function of the hearts treated with aligned patches was improved. On the contrary, hearts treated with nonaligned patches deteriorated after the implantation [29].

PSC-CMs in Regenerative Cardiac Therapy

One of the most common methods to deliver PSC-CMs to the heart is through direct intramyocardial injection. This is usually performed using cells enclosed within a

biomaterial scaffold, such as Matrigel® or collagen, to help retaining the cells in the heart. Over time, the cells secrete extracellular matrices, promoting the formation of cell-cell connection, while the biomaterial scaffold slowly degrades. In the end, biomaterial-free cells are engrafted and transplanted to the heart. Although the scaffold helps in ensuring the retention, it does not provide the support for the cells to form connections with the host cardiomyocytes. Therefore, this may result in poor engraftment as the individual cells will have to form the connections with host cardiomyocytes.

In order to optimize the engraftment of stem cells onto the heart, investigators have embedded cells onto a sheet of polymer scaffold, and the resulting construct is then transplanted [3, 30]. This transplantable scaffold technology enables the retention of cells without relying on enzymatic digestion [30] and ensures long-term engraftment of cells on the heart. Studies have been performed whereby murine ESC cardiomyocyte (mESC-CM) cell sheets were transplanted in rats with MI [30] and human iPSC cardiomyocyte (hiPSC-CM) cell sheets were transplanted in pigs with ischemic cardiomyopathy [31, 32]. In all cases, the utilization of cell sheets improved the engraftment of the cells in the heart while at the same time also improves the heart function [3, 30–32]. A clinical study has been performed using human ESC (hESC) cardiac progenitors embedded on a fibrin patch [33]. The result of this study showed that there was no arrhythmia or tumor formation, given that no cells were found surviving after patch engraftment. However, the issue of long-term efficacy and safety will need to be addressed [33].

Despite all the issues, *in vivo* transplantation of PSC-CMs has been studied using small and large animal models [17, 22, 34–41]. Human ESC-derived cardiomyocytes (hESC-CMs) have been transplanted on the infarct heart of rodents such as mice [34], rats [22, 35], and guinea pigs [36]. Mouse iPSC-derived cardiomyocytes have also been transplanted in MI mice which resulted in improved left ventricular function [37]. These studies have shown that in all cases, PSC-CMs improved heart function postinfarction in small animals [22, 34–37].

In large animals, sheep were used in the study that exploited cardiac-committed murine ESCs (mESCs). In addition pigs were used in studies using human iPSC (hiPSC)-derived cells. Furthermore, nonhuman primates were used in the transplantation study using hESC-CMs and monkey iPSC-derived cardiomyocytes (monkey iPSC-CMs) [17, 38–41]. In sheep with MI, transplantation of mESCs successfully improved the function of the left ventricle [39]. Improvement of the heart function was also observed in pigs with acute MI transplanted with hiPSC-CMs, hiPSC-derived endothelial cells, and hiPSC-derived smooth muscle cells [38]. For the study using nonhuman primates, macaque monkeys (pigtail macaque *Macaca nemestrina* [40, 41] and cynomolgus monkey *Macaca fascicularis* [17]) were selected. Transplantation of hESC-CMs in pigtail macaque monkeys with MI resulted in successful short-term (<90 days) engraftment of cardiomyocytes [40, 41], while monkey iPSC-CMs transplanted in cynomolgus monkeys improved the cardiac contractile function [17]. It should be noted, however, that transplantation of PSC-CMs in large animals may give different result from that in small animals. Transplantation of PSC-CMs in macaque monkeys resulted in arrhythmia that had not previously been observed in rodents [17, 40, 41].

Adult Stem Cells

Bone Marrow-Derived Adult Stem Cells for Angiogenesis and Cardiac Regeneration

Aside from pluripotent stem cells, adult stem cells show relatively limited but useful potential for heart regeneration. The well-established isolation protocol and autologous transplantation have led adult stem cell-based therapy to undergo pre-clinical or clinical trials to test the therapeutic efficiency for heart disease in a clinical setting [42].

Bone marrow (BM)-derived mesenchymal and adult stem cells including unselected or selected mononuclear cells were reported to support angiogenesis and secrete a number of paracrine factors to protect cardiomyocytes from death [43]. They do this by inducing several cytokines and chemokines such as platelet-derived growth factor (PDGF), vascular endothelial growth factor (VEGF), and insulin-like growth factor (IGF-1) for angiogenesis and arteriogenesis, resulting in improved heart function after injury [44, 45]. After transplantation, these BM-derived adult stem cells seldomly differentiate into cardiomyocytes or endothelial cells in the damaged region of the heart, therefore, aiding heart regeneration [46, 47]. Other BM-derived adult stem cells, such as CD34-positive hematopoietic stem cell, would migrate and infiltrate into the infarct area, increasing microvasculature and decreasing fibrosis, ultimately resulting in improved heart function after MI [48].

Cardiac Stem Cells for Heart Regeneration

Endogenous cardiac stem cells (CSCs) were found to express embryonic cardiac progenitor markers and show great efficiency to differentiate into cardiac lineage cells. CSCs, initially reported as c-Kit positive cells, reside in the atrium and ventricular apex of adult hearts [49, 50]. Over time, several other markers were gradually discovered to define CSCs such as Sca-1 or MDR-1 [51], indicating potential ability for multipotency, self-renewal, and limited differentiation into cardiac cells including cardiomyocytes, endothelial cells, and smooth muscle cells [52]. Cardiac stem cells were reported to participate in cardiomyocyte and vasculature formation, and to protect existing cardiomyocytes from death [53]. Nevertheless, using genetic fate-mapping, recent studies suggested that the cardiogenic capability of c-Kit or Sca-1 cells might be quite low [54, 55].

Cardiosphere-Derived Cells for Heart Regeneration

Cardiosphere-derived cells have been isolated and cultured from heart biopsy to form a 3D sphere with 20–150 μm in diameter [56, 57]. The cardiosphere was packed with CSCs inside and coated with cardiac-differentiated cells outside. The outer layer protected the internal CSCs, maintaining their activity and function.

CSCs would proliferate and improve heart function after the cardiosphere had been attached to the fibronectin on the infarct site after injury [58, 59]. The cardiosphere-derived cell therapy is currently undergoing clinical trial and the preliminary results of the trial so far have been encouraging, where significant decrease in scar formation in the infarct area of the heart after injury was observed [59].

Proliferative Cardiomyocytes

Gene Modification for Cardiomyocyte Proliferation and Heart Regeneration

The loss of proliferative ability of adult cardiomyocytes is one of the reasons why heart disease remains a leading cause of death. Although delivery of mature cardiomyocytes may decrease potential problem with synchronization between host and transplanted cells, their limited proliferative ability is still a concern for therapy. Several cell cycle inducers such as cyclin D1 or cyclin A2 or repressor Rb1 were manipulated in cardiomyocytes to regain their proliferative ability; however, the efficacy of the proliferative ability was still low [60–63]. Therefore, upstream cell cycle regulators were taken into consideration to obtain more powerful cardiomyocyte proliferation advancement. Transcription factor E2F4 was found to co-localize with kinetochore in cardiomyocytes, and together, they support mitosis [64]. Knockdown of E2F4 by siRNA significantly affected cardiomyocyte proliferation due to reduction in mitosis. RE1 silencing transcription factor (REST) supports cardiomyocyte proliferation through inhibition of the cell cycle inhibitor p21 [65]. Under REST deletion, p21 knockout rescued cell cycle arrest in cardiomyocytes, indicating the importance of REST-p21 signaling in the proliferative ability of cardiomyocytes. Transcription factor with opposite function reported as Meis1 was found to be capable of inhibiting cyclin-dependent kinase inhibitor and therefore increasing cardiomyocyte proliferation ability [66]. Through careful examination of cardiomyocyte reprogramming process, combined gene modification (FoxM1, Id1, Jnk3 inhibitor) was determined to efficiently increase cardiomyocyte proliferation by inducing each step of cell cycle for heart regeneration after injury [4].

Small RNAs and Signalings Induce Cardiomyocyte Proliferation for Heart Regeneration

Small RNAs also play a role in producing cardiomyocyte progenitors for heart regeneration. Through high throughput screening, several microRNAs such as miR-590 and miR-199a have been shown as candidates that could increase neonatal cardiomyocyte proliferation [67].

Some signaling pathways were reported to be essential for cardiomyocyte proliferation. Hippo signaling induces Yap phosphorylation, which was reported to be present in low level in neonatal mice with high proliferative ability but present in

high level in adult mice [68, 69]. Furthermore, Yap activation stimulates cardiomyocyte proliferation after heart injury, and Hippo/Yap pathway has been shown to possess excellent potential for heart regeneration without causing cardiac hypertrophy [70]. Neuregulin (Nrg1)-ErbB2 signaling is another regulator of cardiomyocyte cell cycle. Nrg1 induction led to increased proliferative ability of cardiomyocytes through its receptor ErbB2 signaling [71, 72]. Induction of ErbB2 led to enlarged size and enhanced proliferation in cardiomyocytes, showing therapeutic potential for improving heart function after MI [73].

Transdifferentiation from Cardiac Fibroblasts to Cardiomyocytes

Aside from manipulating cardiomyocytes in order to regain their proliferative ability as abundant cell source for heart therapy, cardiac fibroblasts have also been taken into consideration for their potential cardiomyocyte transformation. Cardiac fibroblasts and cardiomyocytes are both differentiated from cardiac-committed mesoderm, and the cardiomyocyte progenitor markers (Gata4, Mef2C, and Tbx5, GMT) have been reported as the main factors for cardiomyocyte differentiation. With this in mind, a new technique capable of performing GMT expression in cardiac fibroblasts or dermal fibroblasts was developed. This technique is called transdifferentiation, and it has been used for producing induced cardiomyocyte-like cells (iCMs) with excellent contractility [74]. This technique has been tested successfully *in vitro* and *in vivo* [75]; however, the efficacy of the transdifferentiation should still be improved for better practical clinical application [76].

A different strategy has also been reported where fibroblasts were reprogrammed directly to cardiac progenitor cells using a combination of five genes, Mesp1, Gata4, Tbx5, Nkx2-5, and Baf60c [77]. Transplantation of the resulting cells into mice hearts post-MI showed improved survival. This strategy bypassed the pluripotent stage and therefore could potentially reduce the risk of teratoma formation [77].

Conclusion

Heart disease remains a leading cause of death worldwide and the main reason is the inability of the heart itself to regenerate the lost cardiomyocytes. Cell-based therapy has shown great potential in replacing or complementing the lost cells, and overall in improving heart function after injury. In this chapter, we integrate various cell types including stem cells and modified cell types to demonstrate their potential as cell sources for heart disease. Even though large-scale production of candidate cells is no longer a problem for cell-based therapy, safety, cell retention, survival, engraftment, and maturation after transplantation are the main issues that should be addressed for better and more efficient therapeutic and clinical applications. Although at this point the prospect for iPS cell-based therapy to reach clinical use remains uncertain, ongoing efforts by numerous groups around the world should

ensure improvement in efficacy and safety of this therapeutic approach. We believe that all of the studies so far have set the stage for cardiac cell-based regenerative therapy to succeed and that in the near future, we will be able to demonstrate the ability for cell transplantation to save the lives of people suffering from heart failure.

References

1. Benjamin EJ, Blaha MJ, Chiuve SE, et al. Heart disease and stroke statistics—2017 update: a report from the American Heart Association. *Circulation*. 2017;135:e146–603.
2. Laflamme MA, Murry CE. Heart regeneration. *Nature*. 2011;473:326–35.
3. Masumoto H, Ikuno T, Takeda M, et al. Human iPS cell-engineered cardiac tissue sheets with cardiomyocytes and vascular cells for cardiac regeneration. *Sci Rep*. 2015;4:6716.
4. Cheng Y-Y, Yan Y-T, Lundy DJ, Lo AH, Wang Y-P, Ruan S-C, Lin P-J, Hsieh PCH. Reprogramming-derived gene cocktail increases cardiomyocyte proliferation for heart regeneration. *EMBO Mol Med*. 2017;9:251–64.
5. Takahashi K, Yamanaka S. Induction of pluripotent stem cells from mouse embryonic and adult fibroblast cultures by defined factors. *Cell*. 2006;126:663–76.
6. Takahashi K, Tanabe K, Ohnuki M, Narita M, Ichisaka T, Tomoda K, Yamanaka S. Induction of pluripotent stem cells from adult human fibroblasts by defined factors. *Cell*. 2007;131:861–72.
7. Park I-H, Zhao R, West JA, Yabuuchi A, Huo H, Ince TA, Lerou PH, Lensch MW, Daley GQ. Reprogramming of human somatic cells to pluripotency with defined factors. *Nature*. 2008;451:141–6.
8. Yu J, Vodyanik MA, Smuga-Otto K, et al. Induced pluripotent stem cell lines derived from human somatic cells. *Science*. 2007;318:1917–20.
9. Ye Z, Zhan H, Mali P, Dowey S, Williams DM, Jang Y-Y, Dang CV, Spivak JL, Moliterno AR, Cheng L. Human-induced pluripotent stem cells from blood cells of healthy donors and patients with acquired blood disorders. *Blood*. 2009;114:5473–80.
10. Seki T, Yuasa S, Oda M, et al. Generation of induced pluripotent stem cells from human terminally differentiated circulating T cells. *Cell Stem Cell*. 2010;7:11–4.
11. Loh Y-H, Hartung O, Li H, et al. Reprogramming of T cells from human peripheral blood. *Cell Stem Cell*. 2010;7:15–9.
12. Staerk J, Dawlaty MM, Gao Q, Maetzel D, Hanna J, Sommer CA, Mostoslavsky G, Jaenisch R. Reprogramming of human peripheral blood cells to induced pluripotent stem cells. *Cell Stem Cell*. 2010;7:20–4.
13. Aasen T, Raya A, Barrero MJ, et al. Efficient and rapid generation of induced pluripotent stem cells from human keratinocytes. *Nat Biotechnol*. 2008;26:1276–84.
14. Carey BW, Markoulaki S, Hanna J, Saha K, Gao Q, Mitalipova M, Jaenisch R. Reprogramming of murine and human somatic cells using a single polycistronic vector. *Proc Natl Acad Sci*. 2009;106:157–62.
15. Yamanaka S. Induced pluripotent stem cells: past, present, and future. *Cell Stem Cell*. 2012;10:678–84.
16. Yamanaka S. Strategies and new developments in the generation of patient-specific pluripotent stem cells. *Cell Stem Cell*. 2007;1:39–49.
17. Shiba Y, Gomibuchi T, Seto T, et al. Allogeneic transplantation of iPS cell-derived cardiomyocytes regenerates primate hearts. *Nature*. 2016;538:388–91.
18. BurrIDGE PW, Matsa E, Shukla P, et al. Chemically defined generation of human cardiomyocytes. *Nat Methods*. 2014;11:855–60.
19. Yang L, Soonpaa MH, Adler ED, et al. Human cardiovascular progenitor cells develop from a KDR+ embryonic-stem-cell-derived population. *Nature*. 2008;453:524–8.

20. Kattman SJ, Witty AD, Gagliardi M, Dubois NC, Niapour M, Hotta A, Ellis J, Keller G. Stage-specific optimization of activin/nodal and BMP signaling promotes cardiac differentiation of mouse and human pluripotent stem cell lines. *Cell Stem Cell*. 2011;8:228–40.
21. Willems E, Spiering S, Davidovics H, Lanier M, Xia Z, Dawson M, Cashman J, Mercola M. Small-molecule inhibitors of the Wnt pathway potently promote cardiomyocytes from human embryonic stem cell-derived mesoderm. *Circ Res*. 2011;109:360–4.
22. Laflamme MA, Chen KY, Naumova AV, et al. Cardiomyocytes derived from human embryonic stem cells in pro-survival factors enhance function of infarcted rat hearts. *Nat Biotechnol*. 2007;25:1015–24.
23. Hudson J, Titmarsh D, Hidalgo A, Wolvetang E, Cooper-White J. Primitive cardiac cells from human embryonic stem cells. *Stem Cells Dev*. 2012;21:1513–23.
24. Lee Y-K, Ng K-M, Chan Y-C, Lai W-H, Au K-W, Ho C-YJ, Wong L-Y, Lau C-P, Tse H-F, Siu C-W. Triiodothyronine promotes cardiac differentiation and maturation of embryonic stem cells via the classical genomic pathway. *Mol Endocrinol*. 2010;24:1728–36.
25. Lee DS, Chen JH, Lundy DJ, et al. Defined MicroRNAs induce aspects of maturation in mouse and human embryonic-stem-cell-derived cardiomyocytes. *Cell Rep*. 2015;12:1960–7.
26. Yang X, Pabon L, Murry CE. Engineering adolescence: maturation of human pluripotent stem cell-derived cardiomyocytes. *Circ Res*. 2014;114:511–23.
27. Hsieh PCH, Davis ME, Lisowski LK, Lee RT. Endothelial-cardiomyocyte interactions in cardiac development and repair. *Annu Rev Physiol*. 2006;68:51–66.
28. Kim C, Majdi M, Xia P, Wei KA, Talantova M, Spiering S, Nelson B, Mercola M, Chen HV. Non-cardiomyocytes influence the electrophysiological maturation of human embryonic stem cell-derived cardiomyocytes during differentiation. *Stem Cells Dev*. 2010;19:783–95.
29. Lin YD, Ko MC, Wu ST, et al. A nanopatterned cell-seeded cardiac patch prevents electro-uncoupling and improves the therapeutic efficacy of cardiac repair. *Biomater Sci*. 2014;2:567–80.
30. Masumoto H, Matsuo T, Yamamizu K, et al. Pluripotent stem cell-engineered cell sheets reassembled with defined cardiovascular populations ameliorate reduction in infarct heart function through cardiomyocyte-mediated neovascularization. *Stem Cells*. 2012;30:1196–205.
31. Kawamura M, Miyagawa S, Miki K, et al. Feasibility, safety, and therapeutic efficacy of human induced pluripotent stem cell-derived cardiomyocyte sheets in a porcine ischemic cardiomyopathy model. *Circulation*. 2012;126:S29–37.
32. Kawamura M, Miyagawa S, Fukushima S, et al. Enhanced therapeutic effects of human iPSC cell derived-cardiomyocyte by combined cell-sheets with omental flap technique in porcine ischemic cardiomyopathy model. *Sci Rep*. 2017;7:8824.
33. Menasché P, Vanneau V, Haggège A, et al. Human embryonic stem cell-derived cardiac progenitors for severe heart failure treatment: first clinical case report. *Eur Heart J*. 2015;36:2011–7.
34. van Laake LW, Passier R, Monshouwer-Kloots J, et al. Human embryonic stem cell-derived cardiomyocytes survive and mature in the mouse heart and transiently improve function after myocardial infarction. *Stem Cell Res*. 2007;1:9–24.
35. Caspi O, Huber I, Kehat I, Habib M, Arbel G, Gepstein A, Yankelson L, Aronson D, Beyar R, Gepstein L. Transplantation of human embryonic stem cell-derived cardiomyocytes improves myocardial performance in infarcted rat hearts. *J Am Coll Cardiol*. 2007;50:1884–93.
36. Shiba Y, Fernandes S, Zhu WZ, et al. Human ES-cell-derived cardiomyocytes electrically couple and suppress arrhythmias in injured hearts. *Nature*. 2012;489:322–5.
37. Rojas SV, Kensah G, Rotaermel A, Baraki H, Kutschka I, Zweigerdt R, Martin U, Haverich A, Gruh I, Martens A. Transplantation of purified iPSC-derived cardiomyocytes in myocardial infarction. *PLoS One*. 2017;12:e0173222.
38. Ye L, Chang YH, Xiong Q, et al. Cardiac repair in a porcine model of acute myocardial infarction with human induced pluripotent stem cell-derived cardiovascular cells. *Cell Stem Cell*. 2014;15:750–61.
39. Ménard C, Haggège AA, Agbulut O, et al. Transplantation of cardiac-committed mouse embryonic stem cells to infarcted sheep myocardium: a preclinical study. *Lancet*. 2005;366:1005–12.

40. Chong JJH, Yang X, Don CW, et al. Human embryonic-stem-cell-derived cardiomyocytes regenerate non-human primate hearts. *Nature*. 2014;510:273–7.
41. Liu YW, Chen B, Yang X, et al. Human embryonic stem cell-derived cardiomyocytes restore function in infarcted hearts of non-human primates. *Nat Biotechnol*. 2018;36:597–605.
42. Wagers AJ, Weissman IL. Plasticity of adult stem cells. *Cell*. 2004;116:639–48.
43. Segers VFM, Lee RT. Stem-cell therapy for cardiac disease. *Nature*. 2008;451:937–42.
44. Erbs S, Linke A, Adams V, et al. Transplantation of blood-derived progenitor cells after recanalization of chronic coronary artery occlusion: first randomized and placebo-controlled study. *Circ Res*. 2005;97:756–62.
45. Yao K, Huang R, Qian J, et al. Administration of intracoronary bone marrow mononuclear cells on chronic myocardial infarction improves diastolic function. *Heart*. 2008;94:1147–53.
46. Kocher AA, Schuster MD, Szabolcs MJ, Takuma S, Burkhoff D, Wang J, Homma S, Edwards NM, Itescu S. Neovascularization of ischemic myocardium by human bone-marrow–derived angioblasts prevents cardiomyocyte apoptosis, reduces remodeling and improves cardiac function. *Nat Med*. 2001;7:430–6.
47. Orlic D, Kajstura J, Chimenti S, et al. Bone marrow cells regenerate infarcted myocardium. *Nature*. 2001;410:701–5.
48. Nygren JM, Jovinge S, Breitbach M, Säwén P, Röhl W, Hescheler J, Taneera J, Fleischmann BK, Jacobsen SEW. Bone marrow–derived hematopoietic cells generate cardiomyocytes at a low frequency through cell fusion, but not transdifferentiation. *Nat Med*. 2004;10:494–501.
49. Ellison GM, Vicinanza C, Smith AJ, et al. Adult c-kitpos cardiac stem cells are necessary and sufficient for functional cardiac regeneration and repair. *Cell*. 2013;154:827–42.
50. Smith AJ, Lewis FC, Aquila I, Waring CD, Nocera A, Agosti V, Nadal-Ginard B, Torella D, Ellison GM. Isolation and characterization of resident endogenous c-kit+ cardiac stem cells from the adult mouse and rat heart. *Nat Protoc*. 2014;9:1662–81.
51. Messina E, De Angelis L, Frati G, et al. Isolation and expansion of adult cardiac stem cells from human and murine heart. *Circ Res*. 2004;95:911–21.
52. Beltrami AP, Barlucchi L, Torella D, et al. Adult cardiac stem cells are multipotent and support myocardial regeneration. *Cell*. 2003;114:763–76.
53. Ellison GM, Torella D, Dellegrottaglie S, et al. Endogenous cardiac stem cell activation by insulin-like growth factor-1/hepatocyte growth factor intracoronary injection fosters survival and regeneration of the infarcted pig heart. *J Am Coll Cardiol*. 2011;58:977–86.
54. van Berlo JH, Kanisicak O, Mailliet M, Vagnozzi RJ, Karch J, Lin S-CJ, Middleton RC, Marbán E, Molkenkin JD. C-kit+ cells minimally contribute cardiomyocytes to the heart. *Nature*. 2014;509:337–41.
55. Vagnozzi RJ, Sargent MA, Lin S-CJ, Palpant NJ, Murry CE, Molkenkin JD. Genetic lineage tracing of Sca-1+ cells reveals endothelial but not myogenic contribution to the murine heart. *Circulation*. 2018. <https://doi.org/10.1161/CIRCULATIONAHA.118.035210>.
56. Smith RR, Barile L, Cho HC, Leppo MK, Hare JM, Messina E, Giacomello A, Abraham MR, Marbán E. Regenerative potential of Cardiosphere-derived cells expanded from percutaneous endomyocardial biopsy specimens. *Circulation*. 2007;115:896–908.
57. Davis DR, Zhang Y, Smith RR, Cheng K, Terrovitis J, Malliaras K, Li T-S, White A, Makkar R, Marbán E. Validation of the cardiosphere method to culture cardiac progenitor cells from myocardial tissue. *PLoS One*. 2009;4:e7195.
58. Johnston PV, Sasano T, Mills K, et al. Engraftment, differentiation, and functional benefits of autologous cardiosphere-derived cells in porcine ischemic cardiomyopathy. *Circulation*. 2009;120:1075–83.
59. Chimenti I, Smith RR, Li T-S, Gerstenblith G, Messina E, Giacomello A, Marbán E. Relative roles of direct regeneration versus paracrine effects of human cardiosphere-derived cells transplanted into infarcted mice. *Circ Res*. 2010;106:971–80.
60. Soonpaa MH, Koh GY, Pajak L, Jing S, Wang H, Franklin MT, Kim KK, Field LJ. Cyclin D1 overexpression promotes cardiomyocyte DNA synthesis and multinucleation in transgenic mice. *J Clin Invest*. 1997;99:2644–54.

61. Shapiro SD, Ranjan AK, Kawase Y, Cheng RK, Kara RJ, Bhattacharya R, Guzman-Martinez G, Sanz J, Garcia MJ, Chaudhry HW. Cyclin A2 induces cardiac regeneration after myocardial infarction through cytokinesis of adult cardiomyocytes. *Sci Transl Med.* 2014;6:224ra27.
62. Foglia MJ, Poss KD. Building and re-building the heart by cardiomyocyte proliferation. *Development.* 2016;143:729–40.
63. Mohamed TMA, Ang Y-S, Radzinsky E, Zhou P, Huang Y, Elnenbein A, Foley A, Magnitsky S, Srivastava D. Regulation of cell cycle to stimulate adult cardiomyocyte proliferation and cardiac regeneration. *Cell.* 2018;173:104–116.e12.
64. van Amerongen MJ, Diehl F, Novoyatleva T, Patra C, Engel FB. E2F4 is required for cardiomyocyte proliferation. *Cardiovasc Res.* 2010;86:92–102.
65. Zhang D, Wang Y, Lu P, et al. REST regulates the cell cycle for cardiac development and regeneration. *Nat Commun.* 2017;8:1979.
66. Mahmoud AI, Kocabas F, Muralidhar SA, Kimura W, Koura AS, Thet S, Porrello ER, Sadek HA. Meis1 regulates postnatal cardiomyocyte cell cycle arrest. *Nature.* 2013;497:249–53.
67. Eulalio A, Mano M, Ferro MD, Zentilin L, Sinagra G, Zacchigna S, Giacca M. Functional screening identifies miRNAs inducing cardiac regeneration. *Nature.* 2012;492:376–81.
68. Diez-Cuñado M, Wei K, Bushway PJ, Maurya MR, Perera R, Subramaniam S, Ruiz-Lozano P, Mercola M. miRNAs that induce human Cardiomyocyte proliferation converge on the hippo pathway. *Cell Rep.* 2018;23:2168–74.
69. Heallen T, Zhang M, Wang J, Bonilla-Claudio M, Klysiak E, Johnson RL, Martin JF. Hippo pathway inhibits wnt signaling to restrain cardiomyocyte proliferation and heart size. *Science.* 2011;332:458–61.
70. von Gise A, Lin Z, Schlegelmilch K, et al. YAP1, the nuclear target of Hippo signaling, stimulates heart growth through cardiomyocyte proliferation but not hypertrophy. *Proc Natl Acad Sci.* 2012;109:2394–9.
71. Gemberling M, Karra R, Dickson AL, Poss KD. Nrg1 is an injury-induced cardiomyocyte mitogen for the endogenous heart regeneration program in zebrafish. *elife.* 2015. <https://doi.org/10.7554/eLife.05871>.
72. Wadugu B, Kühn B. The role of neuregulin/ErbB2/ErbB4 signaling in the heart with special focus on effects on cardiomyocyte proliferation. *Am J Physiol Heart Circ Physiol.* 2012;302:H2139–47.
73. D’Uva G, Aharonov A, Lauriola M, et al. ERBB2 triggers mammalian heart regeneration by promoting cardiomyocyte dedifferentiation and proliferation. *Nat Cell Biol.* 2015;17:627–38.
74. Ieda M, Fu J-D, Delgado-Olguin P, Vedantham V, Hayashi Y, Bruneau BG, Srivastava D. Direct reprogramming of fibroblasts into functional cardiomyocytes by defined factors. *Cell.* 2010;142:375–86.
75. Fu J-D, Stone NR, Liu L, Spencer CI, Qian L, Hayashi Y, Delgado-Olguin P, Ding S, Bruneau BG, Srivastava D. Direct reprogramming of human fibroblasts toward a Cardiomyocyte-like state. *Stem Cell Reports.* 2013;1:235–47.
76. Fu J-D, Srivastava D. Direct reprogramming of fibroblasts into cardiomyocytes for cardiac regenerative medicine. *Circ J.* 2015;79:245–54.
77. Lalit PA, Salick MR, Nelson DO, et al. Lineage reprogramming of fibroblasts into proliferative induced cardiac progenitor cells by defined factors. *Cell Stem Cell.* 2016;18:354–67.



Injectable Hydrogels to Treat Myocardial Infarction

10

Miranda D. Diaz and Karen L. Christman

Introduction

Each year, over 700,000 Americans experience myocardial infarction (MI), which remains the leading cause for heart failure worldwide [1]. MI, commonly known as heart attack, is defined by an ischemic event that results in the sudden death of myocardial tissue due to partial or full occlusion of the coronary arteries [2]. As the tissue experiences a sudden reduction of oxygen and nutrient supply, massive death of cardiomyocytes occurs. Within minutes of the onset of ischemic injury, inflammatory cells, such as neutrophils and then macrophages, infiltrate into the infarct. These cells degrade the surrounding extracellular matrix (ECM) as well as trigger the upregulation of apoptotic signals, proteases, and matrix metalloproteinases (MMPs) [2–5]. The infarct consists of a core of necrotic myocardial tissue surrounded by a border zone that contains the tissue at risk. For days to months after MI, further cardiomyocyte death and ECM degradation in the border zone can expand the necrotic core, a process referred to as infarct expansion [5].

Due to the extremely limited capability of adult myocardial tissue to regenerate, fibroblasts will infiltrate the infarct to deposit a stiff fibrous scar, composed primarily of collagen, in the left ventricle (LV) wall. This scar is a dynamic environment that changes for years post-MI with continued collagen turnover and active myofibroblasts [6]. Mostly acellular scar tissue increases the collagen content of the ECM up to 20-fold higher than that in the healthy myocardial ECM, and its tensile strength serves to balance the distending forces of the heart wall as it beats [4, 7]. However, because the fibrotic scar lacks cardiac muscle, the LV begins to dilate in order to maintain stroke volume via the Frank-Starling law [4]. Simultaneously, the LV wall will become thinner as the chamber expands and the remaining bundles of muscle fibers around the

M. D. Diaz · K. L. Christman (✉)

Department of Bioengineering, University of California, San Diego, La Jolla, CA, USA

Sanford Consortium for Regenerative Medicine, San Diego, La Jolla, CA, USA

e-mail: mdd002@eng.ucsd.edu; christman@eng.ucsd.edu

© Springer Nature Switzerland AG 2019

V. Serpooshan, S. M. Wu (eds.), *Cardiovascular Regenerative Medicine*,
https://doi.org/10.1007/978-3-030-20047-3_10

185

infarct slide past each other, otherwise known as myocyte slippage [5]. This dilation further increases the LV wall stresses. Myocyte hypertrophy is initiated in an ultimately insufficient attempt to offset these additional wall stresses, which only triggers a cycle of additional dilation. While dilation initially serves as a compensatory method to maintain cardiac function, continued dilation and thinning leads to heart failure as these effects become deleterious [5]. Ejection fraction (EF), a common functional measurement of the percentage of blood that is pumped from the LV, greatly reduces after MI as the patient progresses toward heart failure as a direct result of LV remodeling. Fibrosis, LV dilation, wall thinning, increased wall stresses, and reduced functional output are all major consequences of negative LV remodeling. This is a therapeutic opportunity for injectable hydrogels. To prevent or reverse negative LV remodeling, injectable hydrogels often target the border zone of the infarct where cell death can still be prevented, and infarct expansion may be reduced. If bioactive, these hydrogels may also serve as scaffolds to positively remodel the infarct.

To investigate the efficacy of these injectable hydrogel therapeutics to treat MI, small animal models using murine species are powerful tools for a primary investigation to show proof of concept. More extensive reviews on these small animal models can be found in the literature [8–10]. However, large animals such as porcine or ovine models are required for preclinical studies of MI treatment, before moving into human patients, since the cardiovascular system of these animals is more mimetic of human systems. In both porcine and ovine models, predictable coronary anatomy and the lack of many pre-existing collateral vessels allow for the generation of infarcts that are easily reproducible in size and location [11]. This can occur through either total occlusion of a coronary artery, typically via surgery, or ischemia-reperfusion, typically achieved with a balloon catheter. Generally, pigs have similar cardiac to body mass ratios, hemodynamics, and development of cardiac injury post-MI to those in humans (both spatially and temporally) [12]. Therefore, to emphasize clinical relevance, this chapter presents a concise review of large animal studies (summarized in Table 10.1) and any subsequent clinical trials (summarized in Table 10.2) involving injectable hydrogel therapeutics for treating MI, with a focus on how design principles may impact efficacy of the material.

Properties of an Injectable Hydrogel

A hydrogel is defined as a hydrophilic polymeric network capable of absorbing water, resulting in a swollen, flexible, and porous material that can closely resemble the physical properties of many soft tissues [13]. A physical hydrogel is one in which the cross-links between polymers are due to ionic interactions, hydrogen bonding, and other non-covalent bonding. These hydrogels are easily influenced by their environment, and their degree of cross-linking may be reversed depending on pH, temperature, or ionic strength. Conversely, chemically cross-linked hydrogels rely on covalent bonding, and gelation is often permanent. However, both physical and chemical hydrogels may be degraded by enzymatic or hydrolytic reactions, depending on the chemical structure of the polymeric backbone.

Table 10.1 Tabulated comparison of large animal preclinical studies evaluating the efficacy of injectable hydrogels to treat myocardial infarction

Material	Delivery	Time of delivery post-MI	Echo/MRI	Functional efficacy	Model	Biologics/cells delivered	Modifications	Refs #
Fibrin/Alginate	Thoracotomy microinjections	7 days	Echo	No significance	Porcine	N/A	N/A	[19]
Alginate	Intracoronary infusion	4 days	Echo	Reduced LV areas	Porcine	N/A	Calcium cross-linked	[20]
Alginate	Open-chest microinjections	Immediate	Echo	N/A	Porcine	MSCs	RGD	[46]
Algisyl-LVR	Open-chest microinjections	Micro-embolization model	Echo	Trends for decreased LV volumes	Canine	N/A	N/A	[24]
Algisyl-LVR	Open-chest microinjections	8 weeks	Echo	No significant differences in LV volumes	Porcine	N/A	N/A	[25]
PEG	Transendocardial catheterization	4 weeks	N/A	N/A	Porcine	HGF/IGF-1	UPy coupled via alkyl spacers	[42]
HA	Thoracotomy microinjections	Immediate	MRI & echo	Reduced LV volumes	Porcine	rTIMP-3	Methacrylated	[40]
HA	Thoracotomy microinjections	Immediate	Echo	Attenuated LVEDV dilation	Porcine	rTIMP-3	Aldehyde, hydrazide functionalization of HA and dextran sulfate; MMP cleavable peptide	[41]
HA	Thoracotomy microinjections	30 minutes	Echo	No significance	Ovine	N/A	Methacrylate	[35]
HA	Thoracotomy microinjections	30 minutes	MRI	Maintained LVEDV compared to saline	Ovine	N/A	Hydroxyethyl methacrylate	[36]
HA	Open-chest microinjections	Immediate	Echo	Reduced LVEDV	Porcine	MNCs	N/A	[45]

(continued)

Table 10.1 (continued)

Material	Delivery	Time of delivery post-MI	Echo/MRI	Functional efficacy	Model	Biologics/cells delivered	Modifications	Refs #
HA (Extracel-HP)	Thoracotomy injection	Immediate	Echo	Decreased LV volumes for multiple treatment groups	Porcine	PRP, AA, ibuprofen, and allopurinol	N/A	[43]
Myocardial matrix	Transendocardial catheterization	2 weeks	Echo	Reduced LV volumes	Porcine	N/A	N/A	[32]
Peptide NFs	Open-chest microinjections	Immediate	Echo	Improved fractional shortening	Porcine	VEGF	N/A	[39]
Peptide NFs	Open-chest microinjections	Immediate	Echo	Reduced LV volumes	Porcine	MNCs	N/A	[47]

Echo echocardiography, *MRI* magnetic resonance imaging

Table 10.2 Tabulated comparison of clinical trials evaluating the safety, feasibility, and efficacy of injectable hydrogels to treat myocardial infarction

Therapeutic	Trial name	Delivery	Time of delivery post-MI	Echo/ MRI	Functional efficacy	Phase	Identifier	Refs (#)
BL-1040 / IK_5001	N/A	Intracoronary infusion	2–5 days	Echo	LV volume preservation up to 6 months postinjection	I/II	NCT00557531	[22]
	PRESERVATION-I	Intracoronary infusion	2–5 days	Echo	No significance in LV volume differences between groups	II	NCT01226563	[23]
Algisyl-LVR	N/A	Open-chest injection during CABG	Symptomatic heart failure	MRI	Trends for decreasing LV volumes at 6 months postinjection (only 3 patients)	II	NCT00847964	[27]
	AUGMENT-HF	Thoracotomy injection	Symptomatic heart failure	Echo	No significance in LV volume differences between groups	II/III	NCT01311791	[26]
VentriGel	N/A	Transendocardial	60 days–3 years	MRI	Study not yet published	I	NCT02305602	N/A

Echo echocardiography, *MRI* magnetic resonance imaging

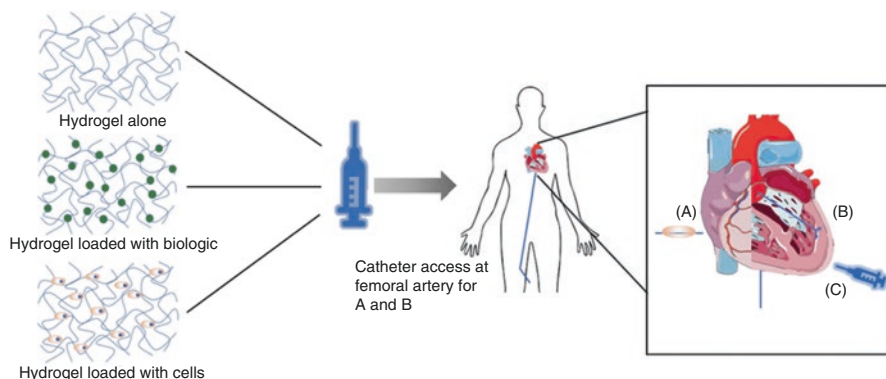


Fig. 10.1 Injectable hydrogel therapeutics can be delivered alone or may be loaded with a biologic payload or stem cells to improve localized retention, as well as prolong the therapeutic delivery. Injectable hydrogels may be delivered minimally invasively through catheter approaches of intracoronary infusion (A) or transendocardial delivery (B). However, the more invasive approach of surgical-based injection is required for some materials (C)

It is critical to keep in mind the changes occurring in the myocardial tissue after MI when designing a biomaterial therapeutic. Injectable hydrogels provide a unique opportunity to recapitulate soft tissue through the tunability of their mechanical properties, porosity, ability to absorb water, and ability to be created by many different polymers, both natural and synthetic [10]. While biomaterial design plays a key role in therapeutic efficacy, it also plays a role in delivery. Catheter delivery of a hydrogel therapeutic is a favorable method versus those that require direct surgical access to the heart. To accomplish this, though, the hydrogel must be injectable not only through a syringe and needle, but also a long narrow catheter. Therefore, the materials would need to have the appropriate viscosity, often accomplished by using shear thinning materials. Further, after injection into the heart wall, the material should gel in situ at physiological temperature ($37\text{ }^{\circ}\text{C}$), pH (7.4), and salt conditions [14]. This gelation time must also be relatively short (less than $\sim 30\text{ s}$) to minimize loss of material to the surrounding vasculature due to the beating of the heart [14]. These injectable hydrogels can be delivered alone or loaded with a drug, biological reagent, or therapeutic cells (Fig. 10.1) that are continuously released to the infarct region over time as the hydrogel is degraded.

Biomaterials Alone

Natural or synthetic biomaterials can be used to provide biochemical cues or alter the local tissue environment to prevent negative LV remodeling and attenuate cardiomyocyte death. Initially, the hypothesis for the mechanism of action of these materials hinged on the mechanical support they could provide to the LV wall. However, later studies suggested bioactivity and cellular interaction play a more dominant role in affecting cardiac function [15, 16], although changes in polymer

mechanical properties are also likely to influence the local cell and tissue response. Natural biomaterials include those derived from polymers found in nature such as alginate, fibrin, and collagen or from decellularization of ECMs. Because these materials are naturally derived, they are also most easily degraded by the body with no toxic byproducts. Protein-based materials contain native peptide sequences that facilitate cell adhesion and infiltration. Synthetic biomaterials are made from polymers not found in nature, such as polyethylene glycol (PEG), or naturally derived polymers that are modified using synthetic compounds to improve their degradation rate or physical strength, such as hyaluronic acid (HA). Hydrogels from these materials can often have much stronger mechanical properties due to the ease of tunability during polymerization and processing [17]. However, they have limited bioactivity. Commonly, synthetic polymers are used to enhance mechanical properties of naturally derived materials or to deliver biologics or cells, as will be discussed in the following sections.

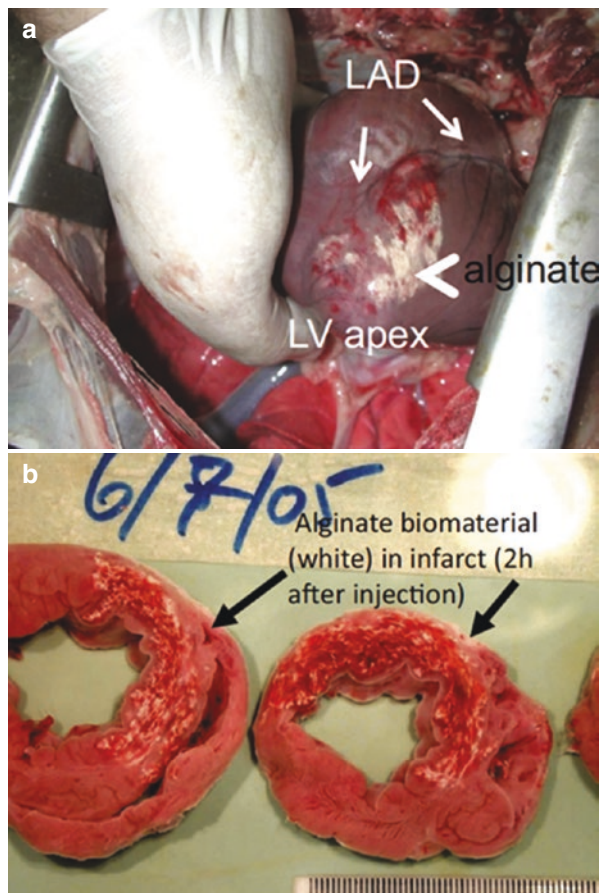
Alginate

Alginate is a polysaccharide that is naturally produced by brown algae and can easily be turned into a hydrogel by using calcium as an ionic cross-linking agent [18]. Although alginate is not naturally produced in humans, it still contains biocompatible structures which can be easily modified with other functional molecules such as RGD peptides to promote cell adhesion. Humans, however, do not have the native enzymes capable of breaking down alginate, and instead, their degradation must be regulated by the design of the cross-linking conditions. Properties such as cross-linking may be altered depending on how long the specific clinical application requires the therapeutic to remain at the site of injury [18].

In an early investigation into the therapeutic potential of alginate, done by Mukherjee et al., alginate was combined with fibrin to form an injectable hydrogel composite material (Fib-Alg) [19]. Fibrin is the body's native wound healing scaffold formed by thrombin cleaving fibrinogen to form a clot. It is commercially used as a sealant and surgical adhesive and often experimentally used as a tissue engineering scaffold. For this study, an invasive delivery option was chosen by reopening the initial thoracotomy site 7 days post-MI, likely because of the quick gelling and dual component nature of the Fib-Alg material, which would make catheter delivery more difficult. Using an injection grid, the composite material was injected using a double barrel syringe, resulting in rapid gelation upon mixing of the fibrin and alginate solutions [19]. The Fib-Alg group showed similar capillary density to the control healthy animals 28 days after MI, while the saline control was significantly reduced compared to the Fib-Alg and healthy controls. This study only provided proof of concept and no statistical significance was achieved on functional echocardiographic measurements.

In a study done by Leor et al., a calcium cross-linked alginate solution was delivered at day 4 post-MI via intracoronary infusion instead of using needle-based injection like most hydrogels (Fig. 10.2) [20]. After MI, inflammatory cytokines

Fig. 10.2 (a) and (b): calcium cross-linked alginate hydrogel. Intracoronary infusion of alginate solution is visible in the porcine heart 2 hours after injection. (Reprinted with permission from Ref. [20])



increase the permeability of the microvasculature of the heart resulting in an increased ability for larger molecules to extravasate through the endothelial cell layer in blood vessels to reach surrounding tissue. This is commonly referred to as “leaky vasculature” [21]. As the alginate solution was infused through a balloon catheter, the material that entered the infarct region gelled because of the high concentration of calcium in the infarct, while the material remaining in the blood stream was likely excreted by the kidneys [20]. This study showed that the calcium cross-linked alginate solution is capable of reversing enlargement of LV end-diastolic and end-systolic area, as measured by echocardiography, and increasing scar thickness up to 2 months after MI in a porcine model. The initial hypothesis of the mechanism of action for the material was that it would act as an LV mechanical wall support. However, staining with α -smooth muscle actin (α SMA) showed increased presence of myofibroblasts in the infarct compared to the control group, which could have accounted for its observed efficacy.

A Phase I/II study using the alginate material (Identifier: NCT00557531), called BL-1040 or IK-5001, showed proof of concept for safe and feasible delivery at least 2 days after successful percutaneous coronary intervention (PCI) and up to 1 week after MI. This study was not a randomized controlled trial, but echocardiographic measurements showed preservation of LV volumes up to 6 months postdelivery [22]. A 303-patient, multicenter, randomized, double-blind, placebo-controlled clinical trial, PRESERVATION-I, was subsequently completed in 2015 (Identifier: NCT01226563). PRESERVATION-I delivered the IK-5001 2–5 days after successful PCI in patients that previously experienced large ST-elevation myocardial infarction (STEMI), as defined by their inclusion criteria. LV dimensions were measured using 3D echocardiography by an independent, blinded echocardiographic core laboratory. The results yielded no significant differences in LV end-diastolic volume index (LVEDVI) changes over 6 months between the saline control and IK-5001-treated groups, indicating the material may not have the ability to prevent negative LV remodeling [23]. The trial publication suggests that the patient cohort chosen for this study may have had infarcts too large for the volume of material they were delivering to have any therapeutic effect. Additionally, the authors recognized that faster delivery of the material, for instance, in the initial PCI during MI, might be more effective since microvascular obstruction several days post-MI may prevent material delivery. In terms of safety, the assessment of IK-5001 concluded that there were increased events of stent thrombosis in IK-5001 treated patients compare to saline treated. Failed primary endpoints halted further evaluation of this material.

An initial investigation into another formulation of alginate, Algisyl-LVR, was done in a canine model of chronic heart failure (CHF) with delivery of material via open-chest direct injection. This study, done by Sabbah et al., showed trends for decreasing LV end-systolic volume (ESV) and end-diastolic volume (EDV), as well as significantly increased LV wall thickness in the alginate-treated groups compared to the saline controls up to 17 weeks postinjection [24]. A subsequent study done by Choy et al. demonstrated efficacy of Algisyl-LVR to act as a permanent scaffold to increase EF in a porcine model of CHF (Fig. 10.3) [25]. In this CHF model, Algisyl-LVR or saline control was delivered via sternotomy 8 weeks after MI. Injections were performed at the mid-ventricular level, with a total of 10–19 intramyocardial injections equally spaced circumferentially around the beating heart (Fig. 10.3a). Because the scaffold is permanent, the inflammatory response for this type of biomaterial resolves with the body forming a fibrous capsule around the material to essentially wall it off from surrounding tissue (Fig. 10.3b). Echocardiographic (2D and 3D) measurements yielded no statistical differences in LV EDV/ESV between treatment groups, while a significant increase in EF was shown in the Algisyl-LVR group compared to the saline control group. The Algisyl-LVR treated animals also exhibited increased LV wall thickness and reduced myofiber stress, indicating some recovery or rescue of function due to treatment [25]. Additionally, 8 weeks after therapeutic delivery, animals that received Algisyl-LVR showed reduced expression of miRNA-195, 21, and 210, which are commonly associated with cardiac stress.

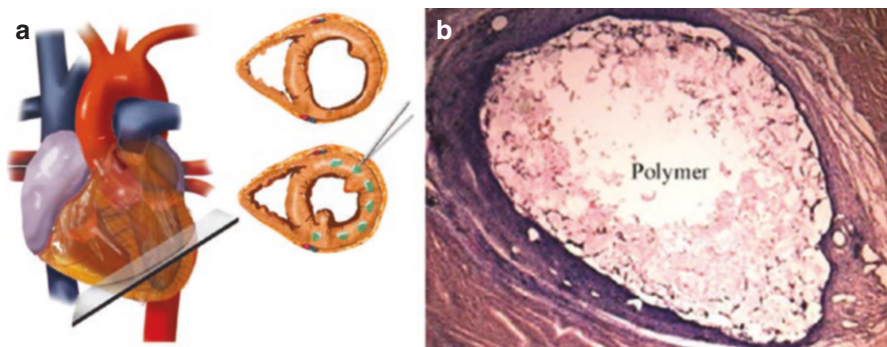


Fig. 10.3 (a) Algisyl-LVR implantation, demonstrating equally spaced injections at mid-ventricular level. (b) H&E stained histological section of treated group myocardium, showing implanted Algisyl-LVR polymer at 100 \times . (Reprinted with permission from Refs. [25, 26])

A first-in-man trial looked into the safety and feasibility of delivering Algisyl-LVR in 11 patients who developed HF from ischemic and non-ischemic dilated cardiomyopathy (DCM) in combination with coronary artery bypass grafting (CABG) via sternotomy (Identifier: NCT00847964). While HF from DCM has some differences in progression from MI, negative LV remodeling still remains a therapeutic target. Publication of the trial results by Lee et al. has shown safety of the material. However, only 3 out of the 11 patients could safely undergo MRI, and consequently, the sample size of functional data is small ($n = 3$) [27]. Although there were no statistically significant differences, the LV wall thickness, EDV, ESV, and myofiber stress showed decreasing trends for up to 6 months postinjection. Due to the success in showing safety and feasibility, Algisyl-LVR has also completed a multicenter, randomized, and controlled Phase II/III clinical trial (AUGMENT-HF), investigating the safety and efficacy of Algisyl-LVR alone to treat advanced heart failure (Identifier: NCT01311791) [26]. Since this material requires thoracotomy to perform direct injection delivery of the material, it was considered unethical to have a control group with saline injection, and instead, the control group consisted of patients who received standard medical care only. The experimental group received standard medical care as well as Algisyl-LVR injections. The primary efficacy endpoint of AUGMENT-HF was changed in peak VO_2 from baseline to 6 months after material injection. Peak VO_2 is a measurement of volume of oxygen delivered to the body during exercise. Increased peak VO_2 has been previously shown to be closely related to a better prognosis for chronic heart failure patients [28]. AUGMENT-HF yielded significant increases in patients treated with Algisyl-LVR compared to saline controls, as well as increased quality of life based on patient surveys standardized by the New York Heart Association (NYHA). However, similar to the preclinical trial of this material, no statistical differences were seen in any echocardiographic measurements of LV dimensions at 3 and 6 months postdelivery. Although not statistically significant, some adverse events were seen in the Algisyl-LVR group with a 30-day absolute mortality rate of 8.75% and surgical complication rate of 25%, compared to no mortality in the control group.

Comparing clinical trials PRESERVATION-I and AUGMENT-HF, it is worth noting some differences and similarities in material design and therapeutic targets. Algisyl-LVR does not degrade and is intended for permanent implantation via surgical-based injection into the heart wall. IK-5001, however, is delivered by intracoronary infusion, which heavily depends on the presence of leaky vasculature immediately following MI. IK-5001 material will eventually degrade over 3–6 months. For this reason, Algisyl-LVR is better suited to treat chronic heart failure patients, while IK-5001 would only be suitable for acute MIs. Both trials indicated increased exercise capacity of patients treated with Algisyl-LVR and IK-5001 compared to the saline controls using a 6-minute walk test. Since PRESERVATION-I failed to produce significant data for the defined primary outcome, a study redesign is required to continue clinical trials for the treatment of MI using the IK-5001 material. It is also important to point out that both trials failed to produce significant improvements in LV volumes or dimensions when compared to their respective control groups, which is a critical determinant of efficacy in treating MI and preventing the development of heart failure. Both materials were hypothesized to act as mechanical supports to prevent negative LV remodeling, but the results of these studies may point to the requirement of additional biochemical activity for effective treatment.

Tissue-Derived ECM

Decellularized ECM hydrogels can be derived from various tissue types, such as heart, pancreas, skeletal muscle, and brain. Since each tissue type has a specific biochemical composition, some studies have shown improved efficacy using a tissue-specific source, possibly related to which germ layer the tissue arose from [29–31]. To create an injectable hydrogel, the tissue undergoes decellularization and enzymatic digestion, which changes the microstructure of the ECM. However, the hydrogel maintains the biochemical complexity of the tissue from which it was derived, and for the most part, the nanostructure of the ECM. This can provide a therapeutic that is highly mimetic of native myocardial ECM. A preclinical porcine study investigated the efficacy of a porcine-derived, decellularized, LV myocardial ECM hydrogel, termed myocardial matrix, to prevent negative LV remodeling and improve cardiac function. The study showed that delivery of the myocardial matrix 2 weeks after MI increased EF and reduced LV volumes 3 months after treatment compared to untreated and saline control groups [32]. Additionally, analysis with Masson's trichrome staining showed a thicker muscle layer in the endocardium of the matrix injected heart (Fig. 10.4) as well as reduced infarct fibrosis. The myocardial matrix hydrogel fully degraded *in vivo* in approximately 3 weeks. However, the effects of repair were longer lasting [32]. To investigate the mechanism of action, a gene expression study was performed in rat model and showed that the material can adjust the inflammatory response toward pro-remodeling. It can also reduce fibrosis, promote cardiomyocyte survival in the infarct, and modulate cardiomyocyte metabolism [33].

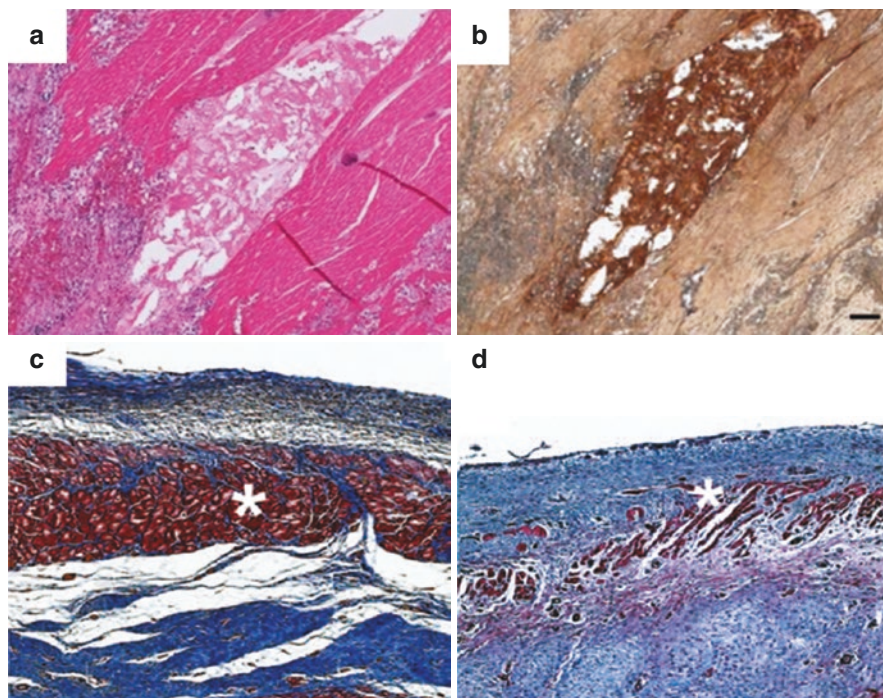


Fig. 10.4 Myocardial matrix hydrogel derived from decellularized porcine myocardial ECM. Myocardial matrix hydrogel mitigated negative LV remodeling in the infarct. H&E (a) and diaminobenzene (b) staining of biotin labeled hydrogel showed the presence of myocardial matrix in the infarct 24 hours after injection. Masson's trichrome staining images of infarcted pig heart with myocardial matrix hydrogel-treated (c) and saline-injected groups (d) showed distinct and thicker muscle layer in matrix-treated hearts. (Reprinted with permission from Refs. [32, 34])

There is a recently completed, Phase I, open-label clinical trial determining the safety and feasibility of the myocardial matrix hydrogel, commercially produced as VentriGel, to treat MI up to 3 years after the initial PCI (Identifier: NCT02305602). VentriGel is delivered minimally invasively via transcatheter injections using the Myostar catheter after 3D NOGA™ mapping to determine injection points based on electrical activity. Results are not yet published, but secondary endpoints will be used as a first investigation into the efficacy of the material from magnetic resonance imaging (MRI) data such as ESV, EDV, and EF. Compared to the alginate products examined in AUGMENT-HF and PRESERVATION-I, VentriGel is being regulated as a biologic in the United States as opposed to a device. This is due to the presence of biochemically active compounds and other proteins found in native ECM. Although this makes the FDA approval process for VentriGel more rigorous, it may provide an advantage in efficacy for preventing negative LV remodeling compared to biomaterials that lack biochemically active compounds.

Hyaluronic Acid

Hyaluronic acid (HA) is a highly abundant, anionic, non-sulfated glycosaminoglycan (GAG) natively found in the ECM of many connective and soft tissues. HA serves as an important signaling molecule for cell migration and proliferation. In order to induce gelation, HA macromers can be chemically modified by attaching groups capable of covalent or non-covalent cross-linking. A common substitution is the introduction of methacrylate. Methacrylate substitution can be controlled with a high degree of accuracy, allowing for increased tunability of the material's physical properties. This allows the gel to better mimic the mechanical properties of the tissue that is targeted for therapy.

Ifkovits et al. designed a study using an left anterior descending (LAD) coronary artery ligation ovine model of acute MI to investigate the efficacies of hydrogels with compressive moduli comparable to that of the cardiac tissue (MeHA low) and approximately 10 times greater than that of healthy myocardium (MeHA high) [35]. Both high and low MeHA had a similar degradation profile that spanned over 8 weeks in vivo, allowing for prolonged presence of the material. The key differences between the two materials were their mechanical properties. MeHA high and low, as well as saline control microinjections directly into the infarct region, were performed 30 minutes following MI through the thoracotomy opening. This study showed that 8 weeks after delivery, the high and low MeHA significantly reduced wall thinning compared to the saline control group. Further, MeHA high significantly reduced infarct length compared to MeHA low and saline control groups. Echocardiographic 3D functional measurements of normalized EF, EDV, and ESV were however not statistically significant. While mechanical properties play a role in repair, the lack of difference between the low and high MeHA groups may suggest that additional biochemical cues can provide a synergistic effect.

In a study done by Dorsey et al., hydroxyethyl methacrylate HA (HeMA HA) was investigated in an acute porcine model with delivery of the biomaterial only 30 minutes after MI, while the thoracotomy site was still open. Infarct was induced via ligation of the LCX coronary artery [36]. This quick delivery time was chosen to minimize the number of procedures the animal had to undergo. However, this limits the clinical relevance of the study, as the average time for cardiac balloon-angioplasty intervention in human patients experiencing MI is more than an hour, and injectable materials via needle-based injection are unlikely to be administered until several days to weeks after MI. The HeMA HA material degraded well before 12 weeks in vivo. However, positive effects of the material were still observed up to 12 weeks after MI, implying lasting effects of the material after degradation. Cine MRI and spatial modulation of magnetization (SPAMM) were used to analyze cardiac dimensions and finite element (FE) measurements of wall stresses. Significant increases in EF for HeMA HA-treated animals were seen starting at 8 weeks, and LV EDV was maintained up to 12 weeks, while in the saline control group, EDV became significantly larger than baseline at 1 week post-MI. Significantly increased

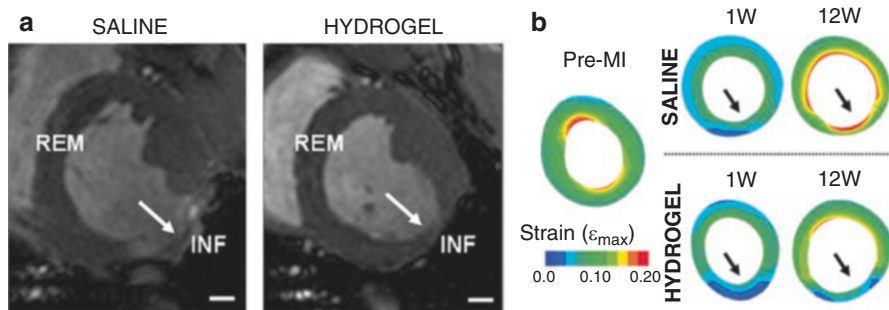


Fig. 10.5 (a) Representative magnetic resonance images showing increased wall thickness and smaller infarct size in hydrogel-treated animals. (b) Finite element simulation of diastolic principle strain maps of baseline and post hydrogel or saline injections, showing increased stiffness in the hydrogel-treated group compared to saline. (Reprinted with permission from Ref. [36])

wall thickness became evident at 12 weeks (Fig. 10.5a). Additionally, some trends indicated increased infarct thickness and stiffness in the direction of the cardiac muscle fibers, but the small sample size yielded no statistical significance (Fig. 10.5b).

Biologics Delivered

While biomaterials alone have the ability to promote repair and prevent negative LV remodeling, therapeutic efficacy may be potentially enhanced by introducing biologics into the material. Biomaterials have been used to deliver plasmids, RNA, or proteins that may act as growth factors, cytokines, or other regulators of cellular activity. Systemic delivery of the therapeutic often results in rapid dilution and degradation in the bloodstream and/or filtration out of the body. Consequently, a high dose is required to obtain the optimal concentration for treatment at the site of disease or injury with possible off target effects depending on localization efficiency. The benefit of delivering a biologic within a hydrogel is that the encapsulation may protect the biologic from degradation or excretion while also allowing a prolonged and localized delivery of the therapeutic [37, 38]. For MI treatment specifically, biomaterials provide an exciting opportunity to prevent the development of heart failure through the prolonged delivery of a therapeutic that targets the negative remodeling of the LV based on specific changes occurring in the infarcted environment.

Self-assembling peptide nanofibers (NFs) of a specific sequence can undergo gelation upon injection and have been investigated as a therapeutic delivery system for recombinant human vascular endothelial growth factor (VEGF) in a study by Lin et al. [39]. The NFs were designed to remain in the infarct for an extended period, with 70% of the material still at the injection site for up to 1 month. In this porcine model, MI was induced via permanent occlusion of the LAD coronary artery with immediate subsequent injection of PBS, NFs alone, VEGF alone, or the

combinatorial NF-VEGF therapy. LV volumes from 2D echocardiographic measurements showed that the EDV and ESV from both the VEGF alone and NF-VEGF groups were significantly lower compared to the saline control group. Additional cardiac functional data showed significant improvement at 28 days post-MI in the NF-VEGF group through improved LV fractional shortening (FS) compared to the other groups. VEGF alone and NF-VEGF injections both significantly improved angiogenesis in the border zone of the infarct, but only the combinatorial therapeutic of NF-VEGF significantly increased arteriogenesis at 28 days post-MI. While this study may not confidently show the efficacy of the combinatorial treatment compared to VEGF alone, it still points to the importance of biochemical cues to promote repair in the infarct.

As previously mentioned, MMPs play a role in LV remodeling after MI due to their ability to degrade ECM components, specifically collagen. Because of this, MMP inhibition may be of interest to prevent negative LV remodeling and promote infarct repair. One study by Eckhouse et al. in a porcine model investigated the immediate injection of recombinant tissue inhibitor of MMP-3 (rTIMP-3), encapsulated in HA hydroxyethyl methacrylate (HEMA) gels by binding rTIMP-3 to the HA backbone via ester-mediated hydrolysis [40]. The injections were administered through the thoracotomy site used for MI. Functional measurements showed reduced wall stresses and reduced LV volumes with echocardiographic and MR imaging. Immunoblotting analysis also showed reduced MMP levels, increased TIMP levels, and reduced macrophage presence in groups treated with the rTIMP-3 gel (Fig. 10.6). Although this implies the rTIMP-3 gel can modulate the inflammatory response, some macrophages have a pro-regenerative capability, so this effect is not clear as positive or negative. However, levels of fibrillar collagen mRNA were reduced in the rTIMP-3 gel without reduced collagen content, showing that this group had less collagen turnover with increased ECM stability.

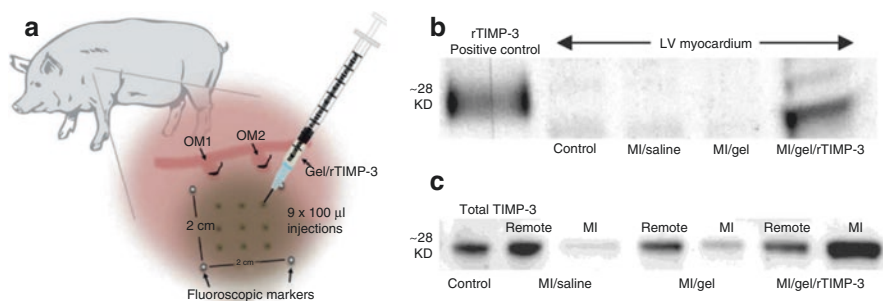


Fig. 10.6 Encapsulated recombinant tissue inhibitor of matrix metalloproteinase-3 (rTIMP-3) in hydroxyethyl methacrylate (HEMA) hydrogel. Immunoblotting of MI and remote regions of injection grid show presence of rTIMP-3 and native TIMP-3 in the infarcted pig hearts. Schematic of injection grid used for HEMA Gel/rTIMP-3 (a) and subsequent immunoblotting for His-tagged rTIMP-3 (b), as well as immunoblotting for rTIMP-3 and native TIMP-3 (c). (Reprinted with permission from Ref. [40])

A similar porcine study from the same research group has also shown the delivery of rTIMP-3 to the infarct via a more specialized hydrogel that is designed to degrade and release rTIMP-3 only in the presence of MMPs, in an attempt to reduce off target effects [41]. The hydrogel was composed of an HA backbone modified with aldehyde (ALD) and hydrazide (HYD) functional groups, as well as dextran sulfate (DS) backbones modified with ALD. MMP sensitivity was induced by the incorporation of an MMP cleavable cross-linking peptide sequence: GGRMSMPV. Direct injection of the material through thoracotomy access requires a double barrel syringe to ensure equal mixing of ALD and HYD groups and gelation *in vivo*. When the hydrogel was injected into non-infarcted hearts, the gel degraded very little, in comparison to injection into infarcted hearts, where there was minimal material left 14 days after MI. Echocardiography was used to assess functional benefits of the hydrogel and rTIMP-3 system. Significant increases in LV EF, attenuated LVEDV dilation, increased wall thickness, and improved pulmonary capillary wedge pressure (PCWP) compared to the saline and hydrogel alone controls all signify the ability of the hydrogel and rTIMP-3 system to mitigate negative LV remodeling up to 28 days post-MI. Normal levels of MMPs were also observed in the hydrogel and rTIMP-3 group compared to the saline and hydrogel alone controls without evidence of any increased levels of rTIMP-3 in the systemic circulation. Looking at gene expression, the hydrogel and rTIMP-3 group showed significant upregulation of myosin heavy chain isoform (MYH14) compared to the control groups, suggesting a more mature and contractile phenotype of myofibroblasts in this treatment group.

Bastings et al. investigated the therapeutic carrying ability of a modified PEG hydrogel that undergoes reversible gelation at physiological pH of 7.4 via cross-linking of ureido-pyrimidinone (UPy) units (Fig. 10.7a) [42]. This UPy hydrogel was loaded with human growth factor (HGF) and insulin-like growth factor-1 (IGF-1) and delivered via transendocardial injections with NOGATM-guided Myostar catheterization 4 weeks after MI in a porcine model. Comparing the GF-loaded UPy-gels with GFs in saline or saline alone controls, favorable remodeling was seen in the loaded UPy-gel group through reduced collagen content and increased myocardial viability, measured via Picrosirius red staining for collagen content (Fig. 10.7f). However, this study had minimal cardiac functional data, which would be critical in determining therapeutic efficacy for moving toward clinical trials.

A permanent occlusion porcine model examined the HA-based commercially available Extracel-HP gel as a delivery vehicle for a cocktail of ascorbic acid, ibuprofen, and allopurinol with platelet rich plasma (PRP) [43]. The ascorbic acid acts as a free radical scavenger to minimize reactive oxidant species (ROS) in the infarct, while the ibuprofen and allopurinol act as anti-inflammatory agents. The PRP contains natural stores of growth factors (GFs) and cytokines responsible for wound healing and angiogenesis. To attempt to control for all various components the treatment groups were as follows: HA hydrogel, PRP alone, cocktail group (ibuprofen, allopurinol, and ascorbic acid), full compound (HA hydrogel with cocktail and PRP), and saline. All injections were delivered through thoracotomy immediately following MI. This study showed the ability of the PRP control and full compound

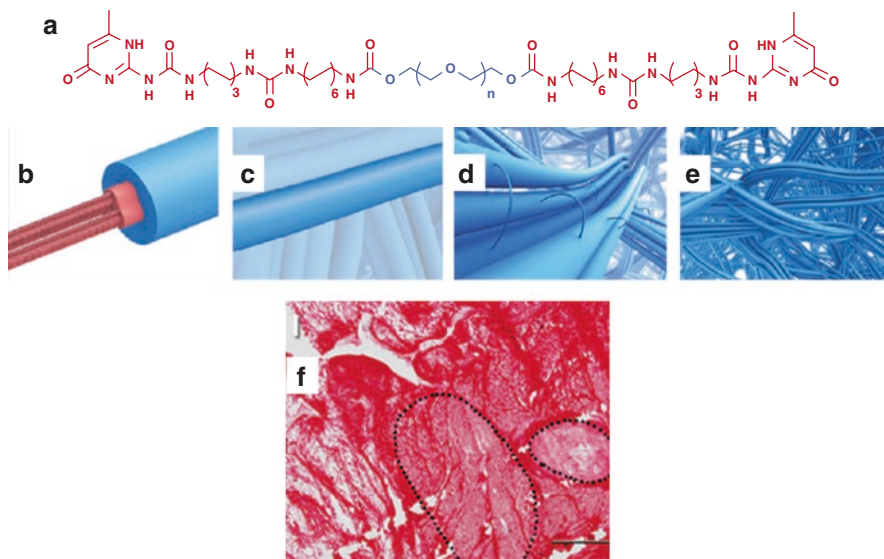


Fig. 10.7 Polyethylene glycol (PEG)-based hydrogel with ureido-pyrimidinone (UPy) cross-linking units to induce reversible gelation at physiological pH. (a) Chemical structure of UPy hydrogel polymer. (b–e) Schematic of hydrogel fibers with UPy-stacks in red, surrounded by hydrophilic PEG, which can then interact with neighboring fibers and ultimately form a hydrogel network. (f) Picrosirius red staining of cryosections of infarcted heart treated with UPy-gel + HGF/IGF shows surviving cardiomyocyte islands denoted by the dashed lines. (Reprinted with permission from Ref. [42])

to promote increased neovascularization in the infarct and border zone. Additionally, assessment of fibrosis with Masson's Trichrome staining showed significantly decreased collagen content in the PRP-only, cocktail, and full compound groups. However, all treatment groups showed significant decreases in LV volumes and increases in EF, compared to the saline control. This could indicate a need for more control groups to properly isolate the component of the full compound that is responsible for functional improvement. The efficacy of the PRP alone control group was associated with the bioactivity of compounds found in PRP that promote neovascularization, as well as the activation of platelets that may result in a fibrin network similar to a hydrogel itself.

Cells Delivered

Stem cell research has proven to be a promising subset of tissue engineering and regenerative medicine. Many preclinical studies have shown that stem or progenitor cells can have reparative properties in cardiac tissue via paracrine effects. However, there are still many problems associated with their implementation, such as identifying a good cell source and scaling up proliferation conditions for widespread

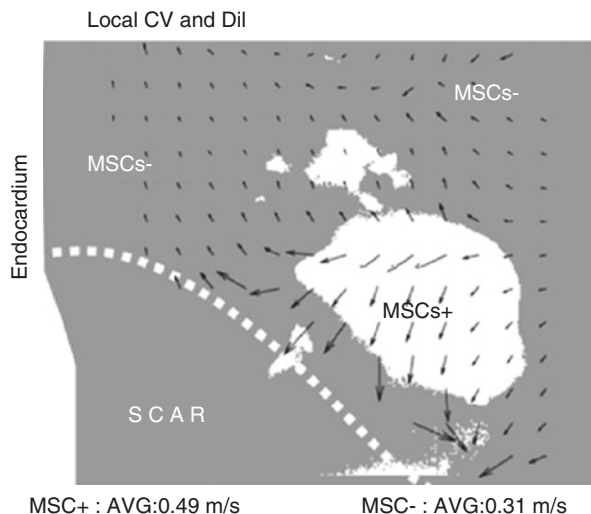
clinical application. Additionally, similar to delivering the biologics described earlier, cells are rapidly cleared from the region of delivery with very poor retention and survival and limited differentiation. Recent studies have shown improvement in cell retention, differentiation, and proliferation by delivering cells within an injectable hydrogel material that is able to serve as a localized scaffold for these cells upon injection [44]. Considering the extremely limited regenerative capacity of the native adult cardiac cells, stem cell delivery could promote MI repair via paracrine effects or, debatably, through direct differentiation.

A study by Chen et al. investigated the open-chest injection of autologous DiI-labeled bone marrow mononuclear cells (MNCs) in a HA hydrogel in a preclinical porcine model of MI [45]. Autologous cells minimize any immune response from the patient. However, isolating and expanding these cells require additional procedures and time for proliferation. With delivery in the hydrogel, the MNCs had a statistically significant, twofold higher retention in the infarct as opposed to MNCs delivered in PBS. Interestingly, the HA+MNC treatment group also showed improved neovascularization. However, these vessels contained mainly unlabeled cells suggesting that the material had an ability to preserve endogenous vasculature, as opposed to direct differentiation into vessel formation. The HA + MNC groups also had improved EF and decreased LV EDV as measured with echocardiography, as well as reduced fibrosis and increased cardiomyocyte diameter. These may suggest a combinatorial effect between the HA and MNCs.

Another study by Panda et al. investigated the conductivity of tissue in the infarct region of a porcine MI model after open-chest injection into the infarct of mesenchymal stem cells (MSCs) in an RGD-modified alginate hydrogel [46]. This material was delivered 4 weeks after MI. This may explain the absence of differences seen in fibrosis between treatment groups, as there is inability to rescue many cardiomyocytes in the border zone at this time point. Echocardiography was performed, but data on LV dimensions or volumes were not reported in the study as a functional assessment. However, there was a high correlation between regions of improved conduction in the border zone and area of MSCs (Fig. 10.8). This suggested the MSCs were possibly able to bridge electrical signaling in cardiac tissues without directly differentiating into impulse generating cardiomyocytes [46].

In another study involving the previously discussed self-assembling peptide NFs, Lin et al. evaluated the efficacy of these fibers to encapsulate autologous MNCs to promote long-term pro-remodeling up to 3 months after MI [47]. In this porcine model, saline control, NFs alone, MNCs alone, or the combined therapeutic (MNCs and NFs) were injected into the infarct region immediately following MI while the chest was still open. The combined therapeutic showed that the NFs increased MNC retention in the infarct approximately 11.3-fold higher than injection of MNCs alone. They also significantly improved LV EF, EDV, and ESV, as measured by echocardiographic analysis at 3 months after MI. The MNC alone treatment, however, only provided functional benefits in the short term. About 30% of the NFs remained at the site of injection 3 months after MI, compared to the more rapidly degraded HA, which may be attributed to the differences in cell retention.

Fig. 10.8 Alginate-based hydrogel modified with cell adhesion peptide, RGD, to encapsulate mesenchymal stem cells (MSCs). Schematic of threshold of DiI fluorescently labeled cells overlaid with map of local conduction velocity vectors shows increased local conduction velocity in areas containing MSCs compared to areas lacking MSCs. (Reprinted with permission from Ref. [46])



The NF alone group still proved to be beneficial for function in the long term via pressure catheterization measurements. Additionally, both NF alone and the combined therapeutic significantly increased wall thickness and reduced collagen deposition compared to the saline and MNC alone controls. The combined therapeutic group, however, promoted neovascularization the most, with the highest capillary, artery, and arteriole density in the peri-infarct region among all groups. Positive staining for α SMA myofibroblasts also suggested the ability of the combined therapeutic to recruit these cells to the infarct. While the combined therapeutic showed the most beneficial long-term effects, evaluating the NF alone group suggested that the material not only provides a scaffold for cell retention but may play a role in preventing negative LV remodeling itself.

Conclusion and Future Outlook

Injectable hydrogels provide an exciting opportunity to treat MI, an ischemic injury that currently afflicts many patients, for which there is no existing therapeutic that can reverse or prevent further progression to HF. These minimally invasive therapeutics can be comprised of natural or synthetic polymers and may contain stem cells or biologics for combinatorial effects. While previous literature suggests that mechanical support to the infarct could prevent negative LV remodeling and promote regeneration, current opinions highlight that biochemical cues are the real key that promote repair through activating pro-regenerative pathways [48]. Encapsulating cells and biologic molecules within hydrogels has the potential to achieve these goals. However, cost remains a large factor with additive biologics in developing a therapeutic that is sustainable for clinical use. Therefore, the therapeutic efficacy of including additional factors must outweigh these costs when compared to delivering a hydrogel alone.

Translation of currently investigated injectable hydrogels also depends largely on their method of delivery. Algisyl-LVR is delivered via invasive surgical-based injection. However, minimally invasive catheter approaches, such as transcatheter delivery or intracoronary balloon infusion (used for the delivery of VentriGel and BL-1040/IK-5001, respectively), are favorable. Such methods reduce the risk for the patient when compared to delivery via injection during a surgery. However, some of these minimally invasive procedures, such as NOGA™ mapping, require a highly specialized cardiologist, which still may limit the translational feasibility. The future outlook for the field of injectable hydrogels to treat MI depends largely on the design of biomaterials to balance cost and translational feasibility, as well as minimize the invasiveness of delivery.

Acknowledgments The authors thank Raymond Wang, and Melissa Hernandez for providing feedback and edits on this chapter. This work was supported by the NIH NHLBI R01HL113468 (KLC) and T32HL105373 (MDD). Dr. Christman is a co-founder, board member, consultant, holds equity interest, and receives income from Ventrix, Inc.

References

1. Anderson JL, Morrow DA. Acute myocardial infarction. *N Engl J Med*. 2017;376(21):2053–64.
2. Frangogiannis NG. The inflammatory response in myocardial injury, repair, and remodeling. *Nat Rev Cardiol*. 2014;11(5):255–65.
3. Frangogiannis NG. Pathophysiology of myocardial infarction. *Compr Physiol*. 2015;5(4):1841–75.
4. St. John Sutton MG, Sharpe N. LV remodeling after MI: pathophysiology and therapy. *Clin Cardiol New Front*. 2000;101:2981–8.
5. Pfeffer MA, Braunwald E. Ventricular remodeling after myocardial infarction. Experimental observations and clinical implications. *Circulation*. 1990;81(4):10.
6. Yao Sun KTW. Infarct scar: a dynamic tissue. *Cardiovasc Res*. 2000;46:6.
7. Whittaker P. Collagen organization in wound healing after myocardial injury. *Basic Res Cardiol*. 1998;93(2):s023.
8. Hernandez MJ, Christman KL. Designing acellular injectable biomaterial therapeutics for treating myocardial infarction and peripheral artery disease. *JACC Basic Transl Sci*. 2017;2(2):212–26.
9. Hasan A, Khattab A, Islam MA, Hweij KA, Zeitouny J, Waters R, et al. Injectable hydrogels for cardiac tissue repair after myocardial infarction. *Adv Sci*. 2015;2(11):1500122.
10. Pena B, Laughter M, Jett S, Rowland TJ, Taylor MRG, Mestroni L, et al. Injectable hydrogels for cardiac tissue engineering. *Macromol Biosci*. 2018;18(6):e1800079.
11. Dixon JA, Spinale FG. Large animal models of heart failure: a critical link in the translation of basic science to clinical practice. *Circ Heart Fail*. 2009;2(3):262–71.
12. Heusch G, Skyschally A, Schulz R. The in-situ pig heart with regional ischemia/reperfusion – ready for translation. *J Mol Cell Cardiol*. 2011;50(6):951–63.
13. Caló E, Khutoryanskiy VV. Biomedical applications of hydrogels: a review of patents and commercial products. *Eur Polym J*. 2015;65:252–67.
14. Chen MH, Wang LL, Chung JJ, Kim YH, Atluri P, Burdick JA. Methods to assess shear-thinning hydrogels for application as injectable biomaterials. *ACS Biomater Sci Eng*. 2017;3(12):3146–60.
15. Rane AA, Chuang JS, Shah A, Hu DP, Dalton ND, Gu Y, et al. Increased infarct wall thickness by a bio-inert material is insufficient to prevent negative left ventricular remodeling after myocardial infarction. *PLoS One*. 2011;6(6):e21571.

16. McGarvey JR, Pettaway S, Shuman JA, Novack CP, Zellars KN, Freels PD, et al. Targeted injection of a biocomposite material alters macrophage and fibroblast phenotype and function following myocardial infarction: relation to left ventricular remodeling. *J Pharmacol Exp Ther*. 2014;350(3):701–9.
17. El-Sherbiny IM, Yacoub MH. Hydrogel scaffolds for tissue engineering: progress and challenges. *Glob Cardiol Sci Pract*. 2013;2013(3):316–42.
18. Augst AD, Kong HJ, Mooney DJ. Alginate hydrogels as biomaterials. *Macromol Biosci*. 2006;6(8):623–33.
19. Mukherjee R, Zavadzkas JA, Saunders SM, McLean JE, Jeffords LB, Beck C, et al. Targeted myocardial microinjections of a biocomposite material reduces infarct expansion in pigs. *Ann Thorac Surg*. 2008;86(4):1268–76.
20. Leor J, Tuvia S, Guetta V, Manczur F, Castel D, Willenz U, et al. Intracoronary injection of in situ forming alginate hydrogel reverses left ventricular remodeling after myocardial infarction in Swine. *J Am Coll Cardiol*. 2009;54(11):1014–23.
21. Claesson-Welsh L. Vascular permeability--the essentials. *Ups J Med Sci*. 2015;120(3):135–43.
22. Frey N, Linke A, Suselbeck T, Muller-Ehmsen J, Vermeersch P, Schoors D, et al. Intracoronary delivery of injectable bioabsorbable scaffold (IK-5001) to treat left ventricular remodeling after ST-elevation myocardial infarction: a first-in-man study. *Circ Cardiovasc Interv*. 2014;7(6):806–12.
23. Rao SV, Zeymer U, Douglas PS, Al-Khalidi H, White JA, Liu J, et al. Bioabsorbable intracoronary matrix for prevention of ventricular remodeling after myocardial infarction. *J Am Coll Cardiol*. 2016;68(7):715–23.
24. Sabbah HN, Wang M, Gupta RC, Rastogi S, Ilsar I, Sabbah MS, et al. Augmentation of left ventricular wall thickness with alginate hydrogel implants improves left ventricular function and prevents progressive remodeling in dogs with chronic heart failure. *JACC Heart Fail*. 2013;1(3):252–8.
25. Choy JS, Leng S, Acevedo-Bolton G, Shaul S, Fu L, Guo X, et al. Efficacy of intramyocardial injection of Algisyl-LVR for the treatment of ischemic heart failure in swine. *Int J Cardiol*. 2018;255:129–35.
26. Anker SD, Coats AJ, Cristian G, Dragomir D, Pusineri E, Piredda M, et al. A prospective comparison of alginate-hydrogel with standard medical therapy to determine impact on functional capacity and clinical outcomes in patients with advanced heart failure (AUGMENT-HF trial). *Eur Heart J*. 2015;36(34):2297–309.
27. Lee LC, Wall ST, Klepach D, Ge L, Zhang Z, Lee RJ, et al. Algisyl-LVR with coronary artery bypass grafting reduces left ventricular wall stress and improves function in the failing human heart. *Int J Cardiol*. 2013;168(3):2022–8.
28. Swank AM, Horton J, Fleg JL, Fonarow GC, Keteyian S, Goldberg L, et al. Modest increase in peak VO₂ is related to better clinical outcomes in chronic heart failure patients: results from heart failure and a controlled trial to investigate outcomes of exercise training. *Circ Heart Fail*. 2012;5(5):579–85.
29. Ungerleider JL, Johnson TD, Hernandez MJ, Elhag DI, Braden RL, Dzieciatkowska M, et al. Extracellular matrix hydrogel promotes tissue remodeling, Arteriogenesis, and perfusion in a rat Hindlimb ischemia model. *JACC Basic Transl Sci*. 2016;1(1–2):32–44.
30. Medberry CJ, Crapo PM, Siu BF, Carruthers CA, Wolf MT, Nagarkar SP, et al. Hydrogels derived from central nervous system extracellular matrix. *Biomaterials*. 2013;34(4):1033–40.
31. Seif-Naraghi SB, Salvatore MA, Schup-Magoffin PJ, Hu DP, Christman KL. Design and characterization of an injectable pericardial matrix Gel- A potentially autologous scaffold for cardiac tissue engineering. *Tissue Eng Part A*. 2010;16(6).
32. Seif-Naraghi SB, Singelyn JM, Salvatore MA, Osborn KG, Wang JJ, Sampat U, Kwan OL, Strachan GM, Wong J, Schup-Magoffin PJ, Braden RL, Bartels K, DeQuach JA, Preul M, Kinsey AM, DeMaria AN, Dib N, Christman KL. Safety and efficacy of an injectable extracellular matrix hydrogel for treating myocardial infarction. *Sci Transl Med*. 2013;5(173):173ra25.

33. Wassenaar JW, Gaetani R, Garcia JJ, Braden RL, Luo CG, Huang D, et al. Evidence for mechanisms underlying the functional benefits of a myocardial matrix hydrogel for post-MI treatment. *J Am Coll Cardiol*. 2016;67(9):1074–86.
34. Singelyn JM, Sundaramurthy P, Johnson TD, Schup-Magoffin PJ, Hu DP, Faulk DM, et al. Catheter-deliverable hydrogel derived from decellularized ventricular extracellular matrix increases endogenous cardiomyocytes and preserves cardiac function post-myocardial infarction. *J Am Coll Cardiol*. 2012;59(8):751–63.
35. Ifkovits JL, Tous E, Minakawa M, Morita M, Robb JD, Koomalsingh KJ, et al. Injectable hydrogel properties influence infarct expansion and extent of postinfarction left ventricular remodeling in an ovine model. *Proc Natl Acad Sci U S A*. 2010;107(25):11507–12.
36. Dorsey SM, McGarvey JR, Wang H, Nikou A, Arama L, Koomalsingh KJ, et al. MRI evaluation of injectable hyaluronic acid-based hydrogel therapy to limit ventricular remodeling after myocardial infarction. *Biomaterials*. 2015;69:65–75.
37. Pérez-Luna V, González-Reynoso O. Encapsulation of biological agents in hydrogels for therapeutic applications. *Gels*. 2018;4(3):E61.
38. Mathew AP, Uthaman S, Cho KH, Cho CS, Park IK. Injectable hydrogels for delivering biotherapeutic molecules. *Int J Biol Macromol*. 2018;110:17–29.
39. Yi-Dong Lin C-YL, Yu-Ning H, Yeh M-L, Hsueh Y-C, Chang M-Y, Tsai D-C, Wang J-N, Tang M-J, Wei EIH, Springer ML, Hsieh PCH. Instructive nanofiber scaffolds with VEGF create a microenvironment for arteriogenesis and cardiac repair. *Sci Transl Med*. 2012;4(146):146ra109.
40. Eckhouse SR, Purcell BP, McGarvey JR, Lobb D, Logdon CB, Doviak H, et al. Local hydrogel release of recombinant TIMP-3 attenuates adverse left ventricular remodeling after experimental myocardial infarction. *Sci Transl Med*. 2014;6(223):223ra21.
41. Purcell BP, Lobb D, Charati MB, Dorsey SM, Wade RJ, Zellars KN, et al. Injectable and bioresponsive hydrogels for on-demand matrix metalloproteinase inhibition. *Nat Mater*. 2014;13(6):653–61.
42. Bastings MM, Koudstaal S, Kieltyka RE, Nakano Y, Pape AC, Feyen DA, et al. A fast pH-switchable and self-healing supramolecular hydrogel carrier for guided, local catheter injection in the infarcted myocardium. *Adv Healthc Mater*. 2014;3(1):70–8.
43. Vu TD, Pal SN, Ti LK, Martinez EC, Rufaihah AJ, Ling LH, et al. An autologous platelet-rich plasma hydrogel compound restores left ventricular structure, function and ameliorates adverse remodeling in a minimally invasive large animal myocardial restoration model: a translational approach: Vu and Pal “myocardial repair: PRP, hydrogel and supplements”. *Biomaterials*. 2015;45:27–35.
44. Sepantafar M, Maheronnaghsh R, Mohammadi H, Rajabi-Zeleti S, Annabi N, Aghdami N, et al. Stem cells and injectable hydrogels: synergistic therapeutics in myocardial repair. *Biotechnol Adv*. 2016;34(4):362–79.
45. Chen CH, Chang MY, Wang SS, Hsieh PC. Injection of autologous bone marrow cells in hyaluronan hydrogel improves cardiac performance after infarction in pigs. *Am J Physiol Heart Circ Physiol*. 2014;306(7):H1078–86.
46. Panda NC, Zuckerman ST, Mesubi OO, Rosenbaum DS, Penn MS, Donahue JK, et al. Improved conduction and increased cell retention in healed MI using mesenchymal stem cells suspended in alginate hydrogel. *J Interv Card Electrophysiol*. 2014;41(2):117–27.
47. Lin YD, Chang MY, Cheng B, Liu YW, Lin LC, Chen JH, et al. Injection of peptide nanogels preserves postinfarct diastolic function and prolongs efficacy of cell therapy in pigs. *Tissue Eng Part A*. 2015;21(9–10):1662–71.
48. Gaballa MA, Goldman S. Ventricular remodeling in heart failure. *J Card Fail*. 2002;8(6):S476–S85.



Regenerative Medicine for the Treatment of Congenital Heart Disease

11

Elda Dzilic, Stefanie Doppler, Rüdiger Lange,
and Markus Krane

Introduction

Congenital heart diseases (CHDs) originate from abnormal development of the cardiac structure and are present at birth. They are the most common birth defect affecting about 1% of all live births, and the leading cause of newborn death [1]. The spectrum of cardiac defects is ranging from simple CHDs, like atrial septal defect, to very complex malformations, like the tetralogy of Fallot or hypoplastic left heart syndrome. Hence, the spectrum of treatment options varies to a great degree: from medication to catheter procedures up to the often needed surgical repair. On February 25, 1939, Gross RE published the groundbreaking case report of the first

E. Dzilic · S. Doppler

Department of Cardiovascular Surgery, German Heart Center Munich at the Technische Universität München, Munich, Germany

Insure (Institute for Translational Cardiac Surgery), Department of Cardiovascular Surgery, German Heart Center, Technische Universität München, Munich, Germany
e-mail: Dzilic@dhm.mhn.de; doppler@dhm.mhn.de

R. Lange

Department of Cardiovascular Surgery, German Heart Center Munich at the Technische Universität München, Munich, Germany

DZHK (German Center for Cardiovascular Research), Partner Site Munich Heart Alliance, Munich, Germany
e-mail: lange@dhm.mhn.de

M. Krane (✉)

Department of Cardiovascular Surgery, German Heart Center Munich at the Technische Universität München, Munich, Germany

Insure (Institute for Translational Cardiac Surgery), Department of Cardiovascular Surgery, German Heart Center, Technische Universität München, Munich, Germany

DZHK (German Center for Cardiovascular Research), Partner Site Munich Heart Alliance, Munich, Germany

successful surgical treatment of a CHD, the ligation of a patent ductus arteriosus [2], paving the way forward to the future of congenital cardiac surgeries. Since then, the progress made in the treatment of CHDs, especially with regard to surgical approaches, has been tremendous. A nationwide cohort study in Norway showed that the 1-year mortality in children with CHDs undergoing heart surgery declined from 16.3% in 1994 to 3.7% in 2009 [3]. This progress also leads to an increased number of adults with CHD (ACHD) requiring specialized medical care [4].

However, deficiencies in the management of patients with CHD and ACHD remain. In contrast to adults with cardiac surgery, children undergoing cardiac repair often outgrow the implanted devices or grafts, because of lack of growth capacity of these devices. These children need repeated surgeries, thereby increasing morbidity and mortality. Van Dorn et al. were able to show that following the Fontan procedure, a complex surgical intervention for patients with single-ventricle physiology, 66% of patients required additional median sternotomies and 67% required further percutaneous cardiac interventions [5]. In addition, the resulting physiological and neurological effects on these young patients and their families are sometimes very difficult to assess. Furthermore, in spite of successful surgery to repair the congenital defect, patients with repaired complex CHDs often develop future complications such as heart failure, leaving heart transplantation as the only remaining option [6, 7]. In time of organ donor decline this last resort therapy has become less available. Therefore, new strategies to optimize the treatment of CHD patients are necessary.

For treating CHD beyond current surgical and percutaneous interventions, two main strategies within the field of regenerative medicine are considered promising: stem cell therapy and tissue engineering. Since Takahashi et al. published their pioneering protocol on the induction of human pluripotent stem cells (iPSCs) in 2007 the field of regenerative medicine prospered greatly [8]. This scientific milestone not only overcame the ethical problems of human embryonic stem cells (hESCs), but also offers the possibility to produce patient-specific cells. While autologous adult stem cell therapy so far has only shown modest improvements of cardiac function [9], stem cell therapy in neonates may offer potential for more successful treatment outcome due to the residual intrinsic regenerative ability of neonatal cardiomyocytes [10]. Besides, tissue engineering might be the key to the main shortcoming of implanted grafts used for the surgical treatment of CHD: the lack of growth capacity. Robert M. Nerem defined tissue engineering as “*the application of the principles and methods of engineering and the life sciences towards the development of biological substitutes to restore, maintain or improve functions*” [11]. The use of bioengineered tissue allows the conduit to react to biological stimuli, such as growth impulses [12].

In this chapter we focus on the achievements, limitations, and future prospects of regenerative medicine in the treatment of CHD. The chapter is divided into the three main categories according to the diseased tissue types: (1) blood vessel, (2) heart valve, and (3) heart muscle wall (Fig. 11.1).

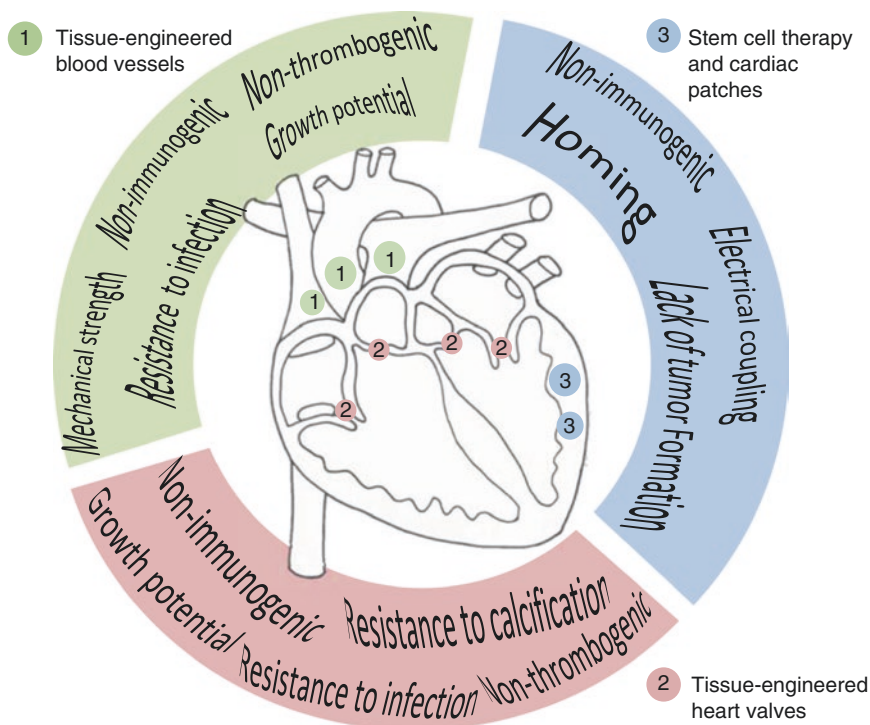


Fig. 11.1 Requirements of regenerative medicine in congenital heart disease

Tissue-Engineered Blood Vessels

As described above congenital heart disease arises from structural abnormalities of the normal cardiac tissue often leading to the necessity of surgical repair. The complexity of some of these cardiac malformations requires additional tissue to perform the reconstruction, for example, vascular grafts. Jean Kunlin opened the door to a new era of vascular surgery in 1948 after using a saphenous vein as graft for a femoropopliteal bypass surgery [13]. Since then the landscape of blood vessel repair and replacement has changed tremendously, including the use of artificial vascular grafts [14] and cryopreserved homografts [15]. In CHD currently used synthetic vascular grafts are made out of nondegradable materials, such as expanded polytetrafluoroethylene (Gore-Tex®) and polyethylene terephthalate (Dacron®). Unfortunately, these materials are associated with an increased risk of thrombosis, stenosis, infection, and calcification [16, 17]. In particular, the surgical treatment of CHD involving small-diameter vessels (<6 mm) is prone to poor rate of patency [18]. As mentioned above, in pediatric cardiac surgery, the most significant shortcoming is probably the lack of growth capacity of the grafted vessel conduit,

potentially resulting in multiple reoperations and thereby increasing morbidity and mortality. Some of these graft limitations were addressed via several modifications. Herring et al. harvested autologous endothelial cells out of subcutaneous veins and seeded them into the lumen of Dacron® prostheses in order to reduce thrombus formation [19]. Although this approach improved the patency of the grafts, it was not able to reach the standard of native tissue or avoid somatic overgrowth.

The criteria for the ideal vascular graft include the ability to withstand the mechanical strength of the blood pressure and to be non-thrombogenic, non-immunogenic, nontoxic, and resistant to infection. They need to be available in various sizes, and offer certain stability in order to endure the surgical handling. Most importantly, the grafts should be able to respond to intrinsic stimuli, and thereby be able to remodel, self-repair, and even grow [20]. Tissue-engineered vascular grafts (TEVGs) represent a promising tool to fulfill these criteria and to eliminate the abovementioned shortcomings of synthetic grafts. Tissue engineering can be subdivided into three components: (1) a scaffold, which provides a structure onto which neotissue can grow, (2) cells, and (3) biomatrices with or without signaling molecules that allow the cells to be seeded and the scaffold to be degraded over time [21]. The attempt to create TEVGs goes back to the 1980s, when Howard Greisler implanted woven absorbable polyglycolic acid (PGA) prostheses into adult rabbit aortas. After 7 months he was able to show that the grafts were remodeled containing smooth muscle-like myofibroblasts and dense fibroplasia [22]. Since then, multiple approaches to create TEVGs with various different types of scaffolds and cells have been demonstrated.

With regard to the use of TEVGs in CHD, Shinoka et al. were the first group to implement TEVGs in CHD cardiac surgery [23]. These investigators seeded ovine artery or vein cells onto a synthetic biodegradable tubular scaffold out of polyglactin and PGA. The construct was cultured for 1 week and then transplanted into lambs, replacing a segment of the pulmonary artery. The material was harvested after 6 months showing no residual scaffold material, no aneurysm formation, or signs of calcification. The grafts were lined with endothelial cells and resembled the morphology of native pulmonary arteries. In 1999 the group was able to perform the first clinical application of a TEVG in the surgical treatment of CHD [24]. A tubular scaffold made out of a 50:50 copolymer of ϵ -polycaprolactone–polylactic acid reinforced with woven PGA fibers was seeded with autologous cells obtained from an explanted vein. After 10 days the graft was implanted into a 4-year-old girl replacing a thrombosed segment of the pulmonary artery. After 7 months the graft was patent showing no signs of reocclusion or aneurysm. While this first clinical use of a TEVG was a success, the process to generate the graft is not feasible for routine application. This led the researchers to further investigate different cell and scaffold types in order to improve the feasibility of clinical TEVG transplantation. In 2001 they launched a clinical trial using poly-L-lactic acid/poly(ϵ -caprolactone/L-lactide) or polyglycolic acid/poly(ϵ -caprolactone/L-lactide) scaffolds seeded with autologous bone marrow cells enriched for the mononuclear fraction (BM-MNCs) [25]. BM-MNCs are able to differentiate into various cell types, including vascular endothelial cells, smooth muscle cells, and fibroblasts. After seeding the BM-MNCs

onto the scaffolds, the grafts were cultured for 2–4 h and then implanted into a total of 25 patients with single ventricle as conduits for an extracardiac total cavopulmonary connection. The long-term results with a mean follow-up of 11.1 years showed no graft-related mortality, but up to 28% of the patients had a graft stenosis that often was treated with balloon angioplasty or stent placement [26, 27]. Yet, in a further study, they showed that by modifying the process of generating TEVGs, the rate of stenosis could be reduced: Increasing the BM-MNC dose and reducing incubation time decreased stenosis and thereby increased the patency of the grafts. Interestingly, the researchers were also able to show that the seeded BM-MNCs disappeared completely, and the recellularization was carried out by smooth muscle cells and endothelial cells from the neighboring blood vessel wall [28, 29]. These results are very promising, but have yet to be translated into small-diameter conduits, because the abovementioned trials used TEVGs with internal diameters between 12 and 24 mm [30].

A different approach to create a TEVG is by using decellularized native vascular tissue. Decellularization removes the cellular components of a certain tissue, just leaving the extracellular matrix (ECM) as scaffold. So far this technique has not been used to treat CHD, neither in a preclinical nor clinical setting. However, Olausson et al. published an important case report of the transplantation of a decellularized deceased donor iliac vein that was recellularized with autologous stem cell-derived endothelial and smooth muscle cells into a 10-year-old girl with extrahepatic portal vein obstruction [31]. Initially, the graft showed good patency, but after 1 year the conduit was obstructed by surrounding tissue in the mesocolon, leading to reoperation to remove the obstruction and optimize the graft length by adding a second vein graft. This work shows that decellularized tissue is a potential option to create TEVGs. Unfortunately, further follow-up of the patient is not reported so far, leaving some questions open regarding the success rate of engrafting decellularized vascular tissue. One big concern with decellularized tissue is loss of ECM integrity due to the decellularization process, leading to potential graft failure [32]. Furthermore, the contribution of remaining donor cells triggering an immune response to the implanted graft remains [33].

Both the above described approaches so far, either with synthetic biodegradable or decellularized scaffolds, incorporate autologous cells. Syedain et al. proposed a new acellular technology to create TEVGs avoiding cell harvesting [34]. Tissue-engineered tubes were formed by injecting a suspension of fibrinogen, thrombin, and ovine dermal fibroblasts into tubular glass molds, which were cultured in a bioreactor over 2 weeks. Afterward, the grafts were transformed in a pulsed flow-stretch bioreactor for further 5 weeks using cyclic stretching. After decellularization the grafts were transplanted as pulmonary artery replacement into lambs. Ten months later, the grafts were harvested and further investigated. The researchers were able to show full recellularization of the grafts with smooth muscle and endothelial cells and increase in graft diameter and length. Also, there were no signs of calcification, aneurysm formation, or pathological immune response. This study suggests the real possibility of “off-the-shelf” TEVGs for the surgical treatment of CHD, but leaves the question open whether small-diameter grafts display the same patency rates,

because the used grafts had an inner diameter of 16 mm. However, the same study group conducted an investigation with 4 mm inner diameter grafts implanted into a sheep femoral artery [35]. The grafts were explanted after 24 weeks and showed full recellularization with no signs of dilatation or calcification. Recently, Bockeria et al. conducted a clinical trial using acellular grafts as conduits for total cavopulmonary connection [36]. They used grafts composed of bioresorbable supramolecular polyester that were implanted in five patients between the ages of 4 and 12 years with an inner diameter of 18–20 mm. Patients were followed up to 12 months and showed no signs of graft-related adverse events. The grafts showed good patency in echocardiography and MRI. The biomatrix on this graft is made out of polycaprolactone that is chain-extended with 2-ureido-4[1*H*]-pyrimidinone. In previous studies on sheep, the research group was able to show that the polymer is slowly degraded over time and fully replaced with neotissue, thereby eliminating all external material and avoiding adverse effects.

Instead of focusing on the scaffold, Itoh et al. made a scaffold-free graft utilizing multicellular spheroids (MCS) and a Bio-3D printer [37, 38]. MCS are spheroidal structure consisting of different cell types. They were composed of human umbilical vein endothelial cells (40%), human aortic smooth muscle cells (10%), and normal human dermal fibroblasts (50%). After printing the small-diameter grafts (inner diameter of 1.5 mm) and culturing them, they were implanted into the infrarenal abdominal aorta of rats. Five days after transplantation the conduits were harvested and showed already a layer of endothelial cells. Although these results are very promising in regard to engineering small-caliber vessels, the very short follow-up in this study precludes obtaining long-term outcome.

Another method to create TEVGs is to use ECM components like collagen or fibrin in order to create a biological scaffold. Using natural polymers has the advantage of already existing binding sites for cell adhesion, thereby enabling easier colonization and proliferation of the seeded or recruited cells. Collagen-based scaffolds were shown to lack sufficient biomechanical properties [39], so the focus shifted to fibrin-based conduits. Koch et al. reported the design of a fibrin scaffold supported by a poly(L/D)lactide 96/4 (P(L/D)LA 96/4) mesh and seeded with autologous arterial-derived cells [39]. After graft conditioning in a bioreactor over 28 days, the small-diameter grafts (5 mm) were implanted in the carotid artery position of sheep and harvested after 6 months. The grafts showed a good rate of patency with no aneurysm formation, no calcification, and no thrombus formation. The inner surface of the conduits was fully covered with endothelial cells. Unfortunately, one of the 6 examined grafts showed a significant stenosis after only 6 months.

As mentioned above researchers were able to show that the seeded cells in vascular conduits degrade over time [29]. The recellularization seems to be accomplished by the surrounding vasculature, potentially triggered by paracrine effects of the seeded cells [28]. This leads to the still unanswered question what cell type is optimal for TEVGs, and whether acellular concepts are to be favored or maybe just the cell-secreted bioactive products. There does not seem to be one right way to approach generating TEVGs, but rather finding a good combination of different methods in order to adopt a widespread clinical use.

Tissue-Engineered Heart Valves

Congenital heart diseases are often associated with functional and structural abnormalities of the valves requiring treatment like repair or replacement to prevent further cardiac damage due to volume and pressure overload. The mechanisms of valvular disease underlying different pathologies vary and therefore require different surgical approaches. Most commonly in CHD, the aortic and pulmonary valve are affected. In case of surgery the repair of the diseased heart valve is preferred instead of replacement. On the one hand because native tissue is more resistant to infection and calcification, on the other hand because implanted valves lack growth capacity. In some cases replacement is the only option left to treat the valvular disease, but it may not be possible due to a small annulus. Unfortunately, commercially available heart valves have limited sizes only starting from 15 mm [40]. Infants with CHD tend to need smaller conduits, leading to inoperability and potential death of these patients, if replacement is the only option left. One method to circumvent this problem is by using homografts. Homografts are processed cadaveric valves and were first implanted by Gordon Murray in 1956 [41]. Although, several publications have shown good long-term results using homografts [42–44], broad application could not be achieved because of limited availability.

Tissue-engineered heart valves (TEHVs) could solve major shortcomings of the present grafts in use. The ideal prosthesis for congenital valvular disease would be able to grow with the patient and be available in various sizes. The grafts need to be non-thrombogenic, non-immunogenic, nontoxic, and resistant to infection and calcification. Nowadays, utilizing computational modeling of the bioengineering approaches can help improve the design of the developed constructs [45]. In general two different approaches in creating a TEHVs can be distinguished: (1) generating a conduit that is already seeded with cells before implantation and (2) creating a scaffold that is populated with cells *in vivo*, meaning after implantation.

The first attempts to create TEHVs focused on selectively generating valve leaflets. In 1995, Shinoka et al. created valve leaflets by seeding fibroblasts and endothelial cells onto a synthetic biodegradable scaffold constructed from polyglactin and polyglycolic acid fibers [46]. The grafts were transplanted as right posterior leaflet of the pulmonary valve in lambs. After these first experiments research moved further to create fully TEHVs.

One of the first studies to create an entirely TEHV used decellularized pulmonary sheep valves, and seeded the conduits with autologous myofibroblasts and endothelial cells came from studies of carotid artery tissue [47]. The grafts were transplanted as pulmonary valve replacement into sheep. After a follow-up of 3 months histological examination revealed an intact endothelial cell surface with full repopulation of myofibroblasts. In 2002, Dohmen et al. went a step further and implanted a decellularized pulmonary allograft reseeded with autologous endothelial cells as pulmonary valve replacement into a 43-year old man suffering from aortic valve stenosis undergoing Ross procedure [48]. At the 1 year follow-up the TEHV showed no signs of calcification or thrombogenesis, and echocardiography revealed

regular valve function. In a different study, decellularized pulmonary allografts were reseeded with autologous endothelial progenitor cells and implanted into two pediatric patients with congenital PV failure. After 3.5 years of follow-up the implanted valves showed increase in size and no signs of valve degeneration [49]. Simon et al. took another approach and implanted commercially decellularized porcine heart valves (Synergraft™) without prior cell seeding into four children as pulmonary valve replacement [50]. Three patients died due to graft failure attributable to severe valve degeneration. The fourth valve was prophylactically explanted as a result of the observed fatal complications. All four valves showed severe inflammation, different degrees of calcification, and no cell repopulation. Also, examination of pre-implanted valves showed incomplete decellularization, potentially being the cause of the strong inflammatory reaction. This caused new decellularization protocols to be developed in order to avoid residual cell remnants [32, 51, 52]. In contrast to the case report from Dohmen et al., the Synergraft™ valves were not preseeded prior to implantation. The idea behind waiving the preseeding process is that the ECM is believed to function as a trigger for host cells to repopulate the scaffold. However, previous studies of decellularized heart valves have showed a lack of repopulation by the host [53, 54].

A very different approach to treat tricuspid valve disease was employed using small intestinal submucosa-derived extracellular matrix (SIS-ECM). The decellularized flat material is shaped into a tubular structure by suturing its edges and implanted as tricuspid valve replacement. Different animal models showed promising consistent results [55–57]. The TEHVs were competent, showed growth potential, and resembled native tissue structure after explantation without signs of inflammation or calcification. SIS-ECM, commercially available as CorMatrix™, was already used in the pediatric setting to treat atrioventricular valve disease. In one case report the tubular valve was implanted into an infant at the age of 128 days with a functionally univentricular heart undergoing atrioventricular valve replacement [58]. After 3 months the new valve was competent but showed a mild stenosis due to infection. Unfortunately, the patient developed sepsis unresponsive to antibiotics and died at the age 156 days. Another case report used the same conduit to replace the mitral valve of a 4-month-old infant with severe tricuspid and mitral valve disease. Unfortunately, the child died 8.5 months later due to pulmonary complications [59]. Both case reports represent examples where CorMatrix™ was used as last resort therapy, because no other strategy was possible for treatment. In contrast to infants and children, atrioventricular disease in adults has well-established devices for surgical treatment. These devices cannot be translated into pediatric patients due to their lack of growth capacity. Recently, Feins et al. developed prosthetic rings with the ability to grow [60]. They covered a degrading, biocompatible polymer poly(glycerol sebacate) (PGS) core with a braided, tubular sleeve that has the ability to elongate in response to native tissue growth. This new device was tested in female piglets for tricuspid valve annuloplasty. Echocardiography after 20 weeks showed a competent valve without any sign of tricuspid valve stenosis indicating the elongation of the device along with native tissue growth.

The rapid progress made in recent years in the field of heart valve tissue-engineered is highly promising, raising the hope that the existing deficiencies of conduits for pediatric patients can be remedied in the future.

Stem Cell Therapy and Cardiac Patches

Complex congenital heart diseases, like hypoplastic left heart syndrome (HLHS) or tetralogy of Fallot, often result in cardiac dysfunction. Especially with the improving treatment of CHDs the mortality is decreasing, thereby increasing the number of patients requiring treatment for heart failure. Current therapies are not sufficient to treat the long-term complications leading to an increased number of patients needing heart transplantation. Due to the existing lack of organ donors, new treatment for heart failure, especially in CHDs, needs to be developed. For decades researchers and physicians believed that the heart is a postmitotic organ. Recent studies, however, show that cardiomyocytes have regenerative potential that is at greatest during the neonatal phase and declines during adulthood [10, 61]. With this mind, new strategies to treat heart failure in CHDs are being developed. A lot of the current research in this area has been adapted from studies conducted in adult patients after myocardial infarction. Stem cell therapy using bone marrow mononuclear cells [62, 63], mesenchymal stem cells [64, 65], or cardiosphere-derived cells (CDCs) [66, 67] was already tested in clinical trials in adult patients showing disappointing results.

However, Liu et al. were able to show a positive outcome using human embryonic stem cell-derived cardiomyocytes (hESC-CMs) [68]. The group treated macaque monkeys with reduced left ventricular ejection fraction (LVEF) due to large transmural myocardial infarctions with ~750 million hESC-CMs via intramuscular injection into the infarct region or the border zone. The cells were administered 14 days after infarction, and the heart function was assessed 1 day before and 27 days after cell injection by MRI. The cell-treated group showed a significant increase in LVEF (~10%). Tracking of the injected cells revealed homing and electrical coupling with the host myocardium, leading the appearance of remuscularization of the infarcted areas. Unfortunately, the study raised concerns about the potential risk of arrhythmias after CM injection, which does not yet allow clinical trials with this approach. Another downside using hESC-CMs is the necessity of using immunosuppressive agents to avoid cell rejection. This obstacle has been overcome with the development of patient-specific induced pluripotent stem cells. However, creating personalized stem cells is very time- and cost-intensive, avoiding implementation as clinical routine. One way to allow widespread clinical use is by establishing HLA-haplotype banks of pluripotent stem cells [69, 70]. Nakatsuji et al. estimated that only 50 generated iPSC lines would provide a match for 90% of the entire Japanese population [70].

Stem cell therapy has already found its way into the clinical treatment of CHD patients. So far several case reports and small-case series utilizing stem cells in order to treat critically ill pediatric patients with heart failure have been published

[71–78]. Laciš et al. treated a 4-month-old infant with severe dilated cardiomyopathy by intramyocardial administration of autologous bone marrow mononuclear cells. The left ventricular ejection fraction increased from 20% to 40% after 4 months [71]. Another group treated nine children with terminal heart failure with an intracoronary infusion of autologous bone marrow-derived mononuclear cells as last resort therapy [73]. One patient died of hemorrhage unrelated to the procedure. Three patients got heart transplantations and the five remaining patients showed an increase in ejection fraction and an improvement of the New York Heart Association classification (greater than or equal to 1). Overall no adverse effects of the stem cell infusion were observed.

The first clinical trial using autologous cardiosphere-derived cells for cardiac regeneration in children with CHDs was conducted in 2015 [79]. CDCs were obtained from seven infants with HLHS undergoing cardiac surgery. They were cultured, expanded, and administered through intracoronary infusion in a dose of 3.0×10^5 cells/kg of body weight after 1 month. The patients showed no adverse effects afterward. After 18 months the infants with CDC injection had an increase in right ventricular ejection fraction from $46.9\% \pm 4.6\%$ to $54.0\% \pm 2.8\%$. Infants without CDC injection did not show an improvement in ejection fraction. Results from the 3-year follow-up show consistent heart function without complications or tumor formation [80]. This clinical trial shows that the intracoronary delivery of CDCs is safe and efficient. CDC delivery for the treatment of heart dysfunction in pediatric patients is further tested in clinical trials like PERSEUS [81], APOLLON, or HOPE [82, 83] with pending results.

One major shortcoming of stem cell injection is the low rate of cell homing and engraftment in the host myocardium due to washout and cell death [84]. As a result several groups designed cardiac patches in order to improve cell retention at the damaged area of the heart [84, 85]. Whether this approach is favorable is still unanswered. Levit et al. were able to show that human mesenchymal stem cells encapsulated in alginate and delivered by hydrogel patch increased cell retention, decreased scar formation, and improved cardiac function [86]. On the other hand, the comparison between injection of hESC-derived cardiomyocytes and epicardial delivery via tissue patch revealed an enhanced electrical integration of the cardiomyocytes into the host myocardium via injection [87]. The concept of cardiac patches improving heart function has been evaluated in multiple small animal [88–93] and large animal [94–96] models and is showing very promising results so far.

The first case report published to use cardiac patches in order to enhance heart function was performed by Sawa et al. [97] in 2012. A 56-year old man with severe heart failure (ejection fraction 11%) due to idiopathic dilated cardiomyopathy received a left ventricular assist device (LVAD) for treatment. Under LVAD therapy the heart function improved and the ejection fraction increased to 20%. In order to further improve heart function and to allow LVAD explantation, he received autologous myoblast cell sheet transplantation to the anterior to lateral surface of the dilated heart. After 3 months the heart function further improved, showing ejection fraction of 46% and thereby allowing the successful explantation of the LVAD. The patient did not experience any adverse effects after the transplantation. This case report led

to phase II clinical trial evaluating the safety and efficacy of autologous skeletal myoblast sheets in seven patients with severe chronic heart failure [98]. Five patients were classified as responders to therapy, which was defined as unchanged or increased LVEF. Two patients experienced further decline of the LVEF. No patient experienced any adverse effects. Another method to utilize cardiac patches in order to treat heart failure was introduced by Menasché et al. [99]. They performed the first clinical transplantation of human embryonic stem cell-derived cardiac progenitor cells embedded into a fibrin scaffold. The SSEA-1-positive cardiac progenitor cells strongly express the early transcription factor *Islet1* and should be able to develop in different cardiac lineages like cardiomyocytes, endothelial cells, and smooth muscle cells. The investigators implanted the tissue-engineered construct into a patient with heart failure undergoing coronary bypass surgery. They created a pocket between the pericardial flap and the epicardium across the infarction area for the cell-loaded patch. After 6 months they found no tumor growth and no occurrence of arrhythmia. The patient's LVEF improved substantially, but this effect is maybe due mostly, if not entirely, to the beneficial effect of the bypass surgery. This approach has already been evaluated in terms of safety and feasibility showing promising results. While these trials are major landmark studies toward implementing regenerative medicine into clinical practice, unfortunately, none of the trials have enrolled patients with CHD so far.

Conclusion

Conventional surgical treatment options for CHD patients have significantly improved over the last decades leading to improved survival of these patients. However, this leads to new treatment challenges, like lifelong anticoagulation, multiple reoperations, or severe heart failure. Therefore, there is an urgent need to develop new therapies where regenerative medicine comes into play. The progress made in stem cell therapy and tissue engineering within the last years is immense; first clinical trials with TEVGs and TEHVs already show promising results.

References

1. van der Linde D, et al. Birth prevalence of congenital heart disease worldwide: a systematic review and meta-analysis. *J Am Coll Cardiol*. 2011;58(21):2241–7.
2. Gross RE. Surgical management of the patent ductus arteriosus: with summary of four surgically treated cases. *Ann Surg*. 1939;110(3):321–56.
3. Jortveit J, et al. Trends in mortality of congenital heart defects. *Congenit Heart Dis*. 2016;11(2):160–8.
4. Marelli AJ, et al. Lifetime prevalence of congenital heart disease in the general population from 2000 to 2010. *Circulation*. 2014;130(9):749–56.
5. Van Dorn CS, et al. Lifetime cardiac reinterventions following the Fontan procedure. *Pediatr Cardiol*. 2015;36(2):329–34.
6. Voeller RK, et al. Trends in the indications and survival in pediatric heart transplants: a 24-year single-center experience in 307 patients. *Ann Thorac Surg*. 2012;94(3):807–15; discussion 815–6.

7. Lamour JM, et al. The effect of age, diagnosis, and previous surgery in children and adults undergoing heart transplantation for congenital heart disease. *J Am Coll Cardiol*. 2009;54(2):160–5.
8. Takahashi K, et al. Induction of pluripotent stem cells from adult human fibroblasts by defined factors. *Cell*. 2007;131(5):861–72.
9. Trounson A, McDonald C. Stem cell therapies in clinical trials: progress and challenges. *Cell Stem Cell*. 2015;17(1):11–22.
10. Simpson DL, et al. A strong regenerative ability of cardiac stem cells derived from neonatal hearts. *Circulation*. 2012;126(11 Suppl 1):S46–53.
11. Nerem RM. Tissue engineering in the USA. *Med Biol Eng Comput*. 1992;30(4):CE8–12.
12. Brennan MP, et al. Tissue-engineered vascular grafts demonstrate evidence of growth and development when implanted in a juvenile animal model. *Ann Surg*. 2008;248(3):370–7.
13. Menzoian JO, Koshar AL, Rodrigues N, Alexis Carrel, Rene Leriche, Jean Kunlin, and the history of bypass surgery. *J Vasc Surg*. 2011;54(2):571–4.
14. Blakemore AH, Voorhees AB Jr. The use of tubes constructed from vinyon N cloth in bridging arterial defects; experimental and clinical. *Ann Surg*. 1954;140(3):324–34.
15. Kieffer E, et al. Allograft replacement for infrarenal aortic graft infection: early and late results in 179 patients. *J Vasc Surg*. 2004;39(5):1009–17.
16. van Brakel TJ, et al. High incidence of Dacron conduit stenosis for extracardiac Fontan procedure. *J Thorac Cardiovasc Surg*. 2014;147(5):1568–72.
17. Robbers-Visser D, et al. Results of staged total cavopulmonary connection for functionally univentricular hearts; comparison of intra-atrial lateral tunnel and extracardiac conduit. *Eur J Cardiothorac Surg*. 2010;37(4):934–41.
18. Klinkert P, et al. Saphenous vein versus PTFE for above-knee femoropopliteal bypass. A review of the literature. *Eur J Vasc Endovasc Surg*. 2004;27(4):357–62.
19. Herring M, Gardner A, Glover J. Seeding human arterial prostheses with mechanically derived endothelium. The detrimental effect of smoking. *J Vasc Surg*. 1984;1(2):279–89.
20. Chlupac J, Filova E, Bacakova L. Blood vessel replacement: 50 years of development and tissue engineering paradigms in vascular surgery. *Physiol Res*. 2009;58(Suppl 2):S119–39.
21. Langer R, Vacanti JP. Tissue engineering. *Science*. 1993;260(5110):920–6.
22. Greisler HP. Arterial regeneration over absorbable prostheses. *Arch Surg*. 1982;117(11):1425–31.
23. Shinoka T, et al. Creation of viable pulmonary artery autografts through tissue engineering. *J Thorac Cardiovasc Surg*. 1998;115(3):536–45; discussion 545–6.
24. Shin'oka T, Imai Y, Ikada Y. Transplantation of a tissue-engineered pulmonary artery. *N Engl J Med*. 2001;344(7):532–3.
25. Naito Y, et al. Successful clinical application of tissue-engineered graft for extracardiac Fontan operation. *J Thorac Cardiovasc Surg*. 2003;125(2):419–20.
26. Hibino N, et al. Late-term results of tissue-engineered vascular grafts in humans. *J Thorac Cardiovasc Surg*. 2010;139(2):431–6, 436 e1–2.
27. Sugiura T, et al. Tissue-engineered vascular grafts in children with congenital heart disease: intermediate term follow-up. *Semin Thorac Cardiovasc Surg*. 2018;30(2):175–9.
28. Hibino N, et al. Tissue-engineered vascular grafts form neovessels that arise from regeneration of the adjacent blood vessel. *FASEB J*. 2011;25(8):2731–9.
29. Roh JD, et al. Tissue-engineered vascular grafts transform into mature blood vessels via an inflammation-mediated process of vascular remodeling. *Proc Natl Acad Sci U S A*. 2010;107(10):4669–74.
30. Lee YU, et al. Rational design of an improved tissue-engineered vascular graft: determining the optimal cell dose and incubation time. *Regen Med*. 2016;11(2):159–67.
31. Olausson M, et al. Transplantation of an allogeneic vein bioengineered with autologous stem cells: a proof-of-concept study. *Lancet*. 2012;380(9838):230–7.
32. Meyer SR, et al. Comparison of aortic valve allograft decellularization techniques in the rat. *J Biomed Mater Res A*. 2006;79(2):254–62.
33. Allaire E, et al. The immunogenicity of the extracellular matrix in arterial xenografts. *Surgery*. 1997;122(1):73–81.

34. Syedain Z, et al. Tissue engineering of acellular vascular grafts capable of somatic growth in young lambs. *Nat Commun.* 2016;7:12951.
35. Syedain ZH, et al. Implantation of completely biological engineered grafts following decellularization into the sheep femoral artery. *Tissue Eng Part A.* 2014;20(11–12):1726–34.
36. Bockeria LA, et al. Total cavopulmonary connection with a new bioabsorbable vascular graft: first clinical experience. *J Thorac Cardiovasc Surg.* 2017;153(6):1542–50.
37. Itoh M, et al. Scaffold-free tubular tissues created by a bio-3D printer undergo remodeling and endothelialization when implanted in rat aortae. *PLoS One.* 2015;10(9):e0136681.
38. Itoh M, et al. Correction: scaffold-free tubular tissues created by a bio-3D printer undergo remodeling and endothelialization when implanted in rat aortae. *PLoS One.* 2015;10(12):e0145971.
39. Weinberg CB, Bell E. A blood vessel model constructed from collagen and cultured vascular cells. *Science.* 1986;231(4736):397–400.
40. Pluchinotta FR, et al. Surgical atrioventricular valve replacement with melody valve in infants and children. *Circ Cardiovasc Interv.* 2018;11(11):e007145.
41. Murray G. Homologous aortic-valve-segment transplants as surgical treatment for aortic and mitral insufficiency. *Angiology.* 1956;7(5):466–71.
42. Musci M, et al. Homograft aortic root replacement in native or prosthetic active infective endocarditis: twenty-year single-center experience. *J Thorac Cardiovasc Surg.* 2010;139(3):665–73.
43. Yankah AC, et al. Homograft reconstruction of the aortic root for endocarditis with periannular abscess: a 17-year study. *Eur J Cardiothorac Surg.* 2005;28(1):69–75.
44. Gulbins H, et al. Mitral valve surgery utilizing homografts: early results. *J Heart Valve Dis.* 2000;9(2):222–9.
45. Emmert MY, et al. Computational modeling guides tissue-engineered heart valve design for long-term in vivo performance in a translational sheep model. *Sci Transl Med.* 2018;10(440):eaan4587.
46. Shinoka T, et al. Tissue engineering heart valves: valve leaflet replacement study in a lamb model. *Ann Thorac Surg.* 1995;60(6 Suppl):S513–6.
47. Steinhoff G, et al. Tissue engineering of pulmonary heart valves on allogenic acellular matrix conduits: in vivo restoration of valve tissue. *Circulation.* 2000;102(19 Suppl 3):III50–5.
48. Dohmen PM, et al. Ross operation with a tissue-engineered heart valve. *Ann Thorac Surg.* 2002;74(5):1438–42.
49. Cebotari S, et al. Clinical application of tissue engineered human heart valves using autologous progenitor cells. *Circulation.* 2006;114(1 Suppl):I132–7.
50. Simon P, et al. Early failure of the tissue engineered porcine heart valve SYNERGRAFT in pediatric patients. *Eur J Cardiothorac Surg.* 2003;23(6):1002–6; discussion 1006.
51. Iop L, et al. Decellularized cryopreserved allografts as off-the-shelf allogeneic alternative for heart valve replacement: in vitro assessment before clinical translation. *J Cardiovasc Transl Res.* 2017;10(2):93–103.
52. Cebotari S, et al. Detergent decellularization of heart valves for tissue engineering: toxicological effects of residual detergents on human endothelial cells. *Artif Organs.* 2010;34(3):206–10.
53. Mitchell RN, Jonas RA, Schoen FJ. Pathology of explanted cryopreserved allograft heart valves: comparison with aortic valves from orthotopic heart transplants. *J Thorac Cardiovasc Surg.* 1998;115(1):118–27.
54. Goffin YA, et al. Morphologic study of homograft valves before and after cryopreservation and after short-term implantation in patients. *Cardiovasc Pathol.* 1997;6(1):35–42.
55. Fallon AM, et al. In vivo remodeling potential of a novel bioprosthetic tricuspid valve in an ovine model. *J Thorac Cardiovasc Surg.* 2014;148(1):333–340 e1.
56. Zafar F, et al. Physiological growth, Remodeling potential, and preserved function of a novel bioprosthetic tricuspid valve: tubular bioprosthesis made of small intestinal submucosa-derived extracellular matrix. *J Am Coll Cardiol.* 2015;66(8):877–88.
57. Baker RS, et al. Tubular bioprosthetic tricuspid valve implant demonstrates chordae formation and no calcification: long-term follow-up. *J Am Coll Cardiol.* 2017;70(19):2456–8.
58. Guariento A, et al. Novel valve replacement with an extracellular matrix scaffold in an infant with single ventricle physiology. *Cardiovasc Pathol.* 2016;25(2):165–8.

59. Bibeovski S, Levy A, Scholl FG. Mitral valve replacement using a handmade construct in an infant. *Interact Cardiovasc Thorac Surg*. 2017;24(4):639–40.
60. Feins EN, et al. A growth-accommodating implant for paediatric applications. *Nat Biomed Eng*. 2017;1:818–25.
61. Bergmann O, et al. Evidence for cardiomyocyte renewal in humans. *Science*. 2009;324(5923):98–102.
62. Lunde K, et al. Intracoronary injection of mononuclear bone marrow cells in acute myocardial infarction. *N Engl J Med*. 2006;355(12):1199–209.
63. Schachinger V, et al. Intracoronary bone marrow-derived progenitor cells in acute myocardial infarction. *N Engl J Med*. 2006;355(12):1210–21.
64. Zhang S, et al. Impact of timing on efficacy and safety of intracoronary autologous bone marrow stem cells transplantation in acute myocardial infarction: a pooled subgroup analysis of randomized controlled trials. *Clin Cardiol*. 2009;32(8):458–66.
65. Hare JM, et al. Comparison of allogeneic vs autologous bone marrow-derived mesenchymal stem cells delivered by transcatheter injection in patients with ischemic cardiomyopathy: the POSEIDON randomized trial. *JAMA*. 2012;308(22):2369–79.
66. Makkar RR, et al. Intracoronary cardiosphere-derived cells for heart regeneration after myocardial infarction (CADUCEUS): a prospective, randomised phase 1 trial. *Lancet*. 2012;379(9819):895–904.
67. Malliaras K, et al. Intracoronary cardiosphere-derived cells after myocardial infarction: evidence of therapeutic regeneration in the final 1-year results of the CADUCEUS trial (Cardiosphere-Derived autologous stem Cells to reverse ventricular dysfunction). *J Am Coll Cardiol*. 2014;63(2):110–22.
68. Liu YW, et al. Human embryonic stem cell-derived cardiomyocytes restore function in infarcted hearts of non-human primates. *Nat Biotechnol*. 2018;36(7):597–605.
69. Wilmut I, et al. Development of a global network of induced pluripotent stem cell haplobanks. *Regen Med*. 2015;10(3):235–8.
70. Nakatsuji N, Nakajima F, Tokunaga K. HLA-haplotype banking and iPSCs. *Nat Biotechnol*. 2008;26(7):739–40.
71. Laciš A, Erglis A. Intramyocardial administration of autologous bone marrow mononuclear cells in a critically ill child with dilated cardiomyopathy. *Cardiol Young*. 2011;21(1):110–2.
72. Olgunturk R, et al. Peripheral stem cell transplantation in children with dilated cardiomyopathy: preliminary report of first two cases. *Pediatr Transplant*. 2010;14(2):257–60.
73. Rupp S, et al. Intracoronary bone marrow cell application for terminal heart failure in children. *Cardiol Young*. 2012;22(5):558–63.
74. Limsuwan A, et al. Transcatheter bone marrow-derived progenitor cells in a child with myocardial infarction: first pediatric experience. *Clin Cardiol*. 2010;33(8):E7–12.
75. Bergman I, et al. Follow-up of the patients after stem cell transplantation for pediatric dilated cardiomyopathy. *Pediatr Transplant*. 2013;17(3):266–70.
76. Burkhart HM, et al. Regenerative therapy for hypoplastic left heart syndrome: first report of intraoperative intramyocardial injection of autologous umbilical-cord blood-derived cells. *J Thorac Cardiovasc Surg*. 2015;149(3):e35–7.
77. Rupp S, et al. A regenerative strategy for heart failure in hypoplastic left heart syndrome: intracoronary administration of autologous bone marrow-derived progenitor cells. *J Heart Lung Transplant*. 2010;29(5):574–7.
78. Qureshi MY, et al. Cell-based therapy for myocardial dysfunction after Fontan operation in hypoplastic left heart syndrome. *Mayo Clin Proc Innov Qual Outcomes*. 2017;1(2):185–91.
79. Ishigami S, et al. Intracoronary autologous cardiac progenitor cell transfer in patients with hypoplastic left heart syndrome: the TICAP prospective phase 1 controlled trial. *Circ Res*. 2015;116(4):653–64.
80. Tarui S, et al. Transcatheter infusion of cardiac progenitor cells in hypoplastic left heart syndrome: three-year follow-up of the transcatheter infusion of cardiac progenitor cells in patients with single-ventricle physiology (TICAP) trial. *J Thorac Cardiovasc Surg*. 2015;150(5):1198–207. 1208 e1-2

81. Ishigami S, et al. Intracoronary cardiac progenitor cells in single ventricle physiology: the PERSEUS (cardiac progenitor cell infusion to treat univentricular heart disease) randomized phase 2 trial. *Circ Res.* 2017;120(7):1162–73.
82. Oh H. Cell therapy trials in congenital heart disease. *Circ Res.* 2017;120(8):1353–66.
83. Tsilimigras DI, et al. Stem cell therapy for congenital heart disease: a systematic review. *Circulation.* 2017;136(24):2373–85.
84. Dow J, et al. Washout of transplanted cells from the heart: a potential new hurdle for cell transplantation therapy. *Cardiovasc Res.* 2005;67(2):301–7.
85. Hirt MN, Hansen A, Eschenhagen T. Cardiac tissue engineering: state of the art. *Circ Res.* 2014;114(2):354–67.
86. Levit RD, et al. Cellular encapsulation enhances cardiac repair. *J Am Heart Assoc.* 2013;2(5):e000367.
87. Gerbin KA, et al. Enhanced electrical integration of engineered human myocardium via intramyocardial versus epicardial delivery in infarcted rat hearts. *PLoS One.* 2015;10(7):e0131446.
88. Zimmermann WH, et al. Engineered heart tissue grafts improve systolic and diastolic function in infarcted rat hearts. *Nat Med.* 2006;12(4):452–8.
89. Sekine H, et al. Endothelial cell coculture within tissue-engineered cardiomyocyte sheets enhances neovascularization and improves cardiac function of ischemic hearts. *Circulation.* 2008;118(14 Suppl):S145–52.
90. Sekine H, et al. In vitro fabrication of functional three-dimensional tissues with perfusable blood vessels. *Nat Commun.* 2013;4:1399.
91. Riegler J, et al. Cardiac tissue slice transplantation as a model to assess tissue-engineered graft thickness, survival, and function. *Circulation.* 2014;130(11 Suppl 1):S77–86.
92. Noguchi R, et al. Development of a three-dimensional pre-vascularized scaffold-free contractile cardiac patch for treating heart disease. *J Heart Lung Transplant.* 2016;35(1):137–45.
93. Ong CS, et al. Biomaterial-free three-dimensional bioprinting of cardiac tissue using human induced pluripotent stem cell derived Cardiomyocytes. *Sci Rep.* 2017;7(1):4566.
94. Ye L, et al. Cardiac repair in a porcine model of acute myocardial infarction with human induced pluripotent stem cell-derived cardiovascular cells. *Cell Stem Cell.* 2014;15(6):750–61.
95. Hata H, et al. Grafted skeletal myoblast sheets attenuate myocardial remodeling in pacing-induced canine heart failure model. *J Thorac Cardiovasc Surg.* 2006;132(4):918–24.
96. Miyagawa S, et al. Impaired myocardium regeneration with skeletal cell sheets--a preclinical trial for tissue-engineered regeneration therapy. *Transplantation.* 2010;90(4):364–72.
97. Sawa Y, et al. Tissue engineered myoblast sheets improved cardiac function sufficiently to discontinue LVAS in a patient with DCM: report of a case. *Surg Today.* 2012;42(2):181–4.
98. Sawa Y, et al. Safety and efficacy of autologous skeletal myoblast sheets (TCD-51073) for the treatment of severe chronic heart failure due to ischemic heart disease. *Circ J.* 2015;79(5):991–9.
99. Menasche P, et al. Human embryonic stem cell-derived cardiac progenitors for severe heart failure treatment: first clinical case report. *Eur Heart J.* 2015;36(30):2011–7.



Cardiovascular Regenerative Medicine: Challenges, Perspectives, and Future Directions

12

Sean M. Wu and Vahid Serpooshan

Cardiovascular regenerative medicine is an interdisciplinary field that utilizes the principles of engineering and life sciences to restore the structure and/or function of damaged or diseased heart. While current cardiovascular tissue and organ transplantation therapies suffer from scarce donor supply and various immune system complications [1], regenerative medicine approaches have enabled bypassing some of these obstacles and heal or replace tissues damaged by acquired or congenital disease [2, 3]. A broad range of regenerative strategies are currently being investigated in preclinical and clinical stages [3]. These methods can be classified to (a) the use of exogenous materials (e.g., scaffolds or cardiac patch systems [4]) and/or cells [5] to replace or salvage the damaged tissue structure and function and (b) leveraging the body's endogenous regenerative mechanisms [6, 7], although adult human heart possesses markedly restricted regenerative capacity. In many cases, a combination of these mechanisms is involved in healing the damaged tissue (e.g., paracrine effects or inducing innate therapeutic responses by implanted patch or cells) [8].

S. M. Wu (✉)

Cardiovascular Institute and Department of Medicine, Division of Cardiovascular Medicine, Stanford University, Stanford, CA, USA

e-mail: smwu@stanford.edu

V. Serpooshan

Department of Biomedical Engineering, Emory University School of Medicine and Georgia Institute of Technology, Atlanta, GA, USA

Department of Pediatrics, Emory University School of Medicine, Atlanta, GA, USA

Children's Healthcare of Atlanta, Atlanta, GA, USA

e-mail: vahid.serpoosahan@bme.gatech.edu

© Springer Nature Switzerland AG 2019

V. Serpooshan, S. M. Wu (eds.), *Cardiovascular Regenerative Medicine*,
https://doi.org/10.1007/978-3-030-20047-3_12

223

A variety of conventional and advanced tissue engineering methods are used to create cardiac patch systems including cell sheets [9], decellularized tissues [10], self- or wave-assembly techniques [11], and 3D bioprinting [12]. Although beneficial effects of engineered cardiac patch devices in a variety of *in vitro* and *in vivo* animal studies have been demonstrated, there still remain a number of challenges in their clinical applications. These challenges include (1) lack of sufficient vasculature in the patch, (2) precise control on the 3D scaffold structure, and (3) inadequate maturity/functionality of human cardiac muscle cells within engineered constructs [13, 14]. Additive manufacturing (i.e., 3D (bio)printing) technologies have emerged as powerful, versatile tools to manufacture 3D cardiac tissue constructs at remarkably greater precision, consistency, and reproducibility [14–16]. To date, a variety of bioprinted cardiovascular tissues/organs have been investigated including vasculature [17], cardiac patches [18, 19], coronary artery stents [20], and cardiac valves [21]. Despite the significant advances in cardiac tissue bioprinting, significant challenges remain, including but not limited to the need for large quantity of functional cardiac muscle cells and the necessity of incorporating functional vasculature in printed constructs [14]. Further work will be necessary to develop specialized bioink materials with biological and physiochemical properties that are optimized for cardiac tissue bioprinting [16].

While still in its infancy, the cardiovascular regenerative medicine field has made notable advances in recent years to enhance future applications to meaningfully regenerate damaged/diseased adult human heart [22, 23]. Efforts to understand the complexity of adult heart regeneration through basic sciences and translational studies in fields such as genetics, biomaterials and tissue engineering, nanotechnology, imaging, and cardiac cellular and molecular biology will pay dividends in the long run [23]. While the potential therapeutic benefits of many approaches to cardiac regenerative therapies have been examined thus far, their precise mechanisms of action are often unknown. For instance, while application of an epicardial patch, laden with the cardiogenic follistatin-like 1 protein, was recently shown to stimulate cardiomyocyte cell cycle re-entry and division, little is known about the cellular and molecular mechanisms underlying this regenerative effect [24, 25].

Looking ahead, the role for tissue engineering and regenerative therapy to treat patients with heart disease must contend and synergize with the large variety of device therapies that are currently being implemented in patients with cardiovascular diseases. For instance, while patients with sick sinus syndrome may benefit from implantation of biological pacemakers that are made from tissue engineered cells [26], the reliability and efficiency of these cells to maintain pacemaker function must be greater than that of an electronic pacemaker, which is the current standard of care [22]. It is expected that the future of regenerative therapies will focus on a selective number of cardiovascular diseases that are not served well by the current devices and treatments (e.g., genetic cardiomyopathies or acute myocardial infarction) [22]. Thus, economic, practical, and translational considerations must be more carefully taken into account in the future studies aiming at developing next-generation cardiovascular regenerative therapies.

References

1. Tansho M, et al. Heart transplantation: challenges facing the field. *Cold Spring Harb Perspect Med.* 2014;4(5):a015636.
2. Mao AS, Mooney DJ. Regenerative medicine: current therapies and future directions. *Proc Natl Acad Sci U S A.* 2015;112(47):14452–9.
3. Doppler SA, et al. Cardiac regeneration: current therapies-future concepts. *J Thorac Dis.* 2013;5(5):683–97.
4. Mahmoudi M, et al. Multiscale technologies for treatment of ischemic cardiomyopathy. *Nat Nanotechnol.* 2017;12(9):845–55.
5. Broughton KM, Sussman MA. Enhancement strategies for cardiac regenerative cell therapy: focus on adult stem cells. *Circ Res.* 2018;123(2):177–87.
6. Finan A, Richard S. Stimulating endogenous cardiac repair. *Front Cell Dev Biol.* 2015;3:57.
7. Xiang MS, Kikuchi K. Endogenous mechanisms of cardiac regeneration. *Int Rev Cell Mol Biol.* 2016;326:67–131.
8. Ye L, et al. Patching the heart: cardiac repair from within and outside. *Circ Res.* 2013;113(7):922–32.
9. Wang CC, et al. Direct intramyocardial injection of mesenchymal stem cell sheet fragments improves cardiac functions after infarction. *Cardiovasc Res.* 2008;77(3):515–24.
10. Wang B, et al. Fabrication of cardiac patch with decellularized porcine myocardial scaffold and bone marrow mononuclear cells. *J Biomed Mater Res A.* 2010;94a(4):1100–10.
11. Serpooshan V, et al. Bioacoustic-enabled patterning of human iPSC-derived cardiomyocytes into 3D cardiac tissue. *Biomaterials.* 2017;131:47–57.
12. Pati F, et al. Printing three-dimensional tissue analogues with decellularized extracellular matrix bioink. *Nat Commun.* 2014;5:3935.
13. Kolanowski TJ, Antos CL, Guan K. Making human cardiomyocytes up to date: derivation, maturation state and perspectives. *Int J Cardiol.* 2017;241:379–86.
14. Serpooshan V, et al. Bioengineering cardiac constructs using 3D printing. *J 3D Printing Med.* 2017;1(2):123–39.
15. Serpooshan V, et al. Chapter 8 – 4D printing of actuating cardiac tissue. In: Al’Aref SJ, et al., editors. *3D printing applications in cardiovascular medicine.* Boston: Academic Press; 2018. p. 153–62.
16. Hu JB, et al. Cardiovascular tissue bioprinting: physical and chemical processes. *Appl Phys Rev.* 2018;5(4):041106.
17. Lim GB. Vascular disease: treatment of ischaemic vascular disease with 3D-printed vessels. *Nat Rev Cardiol.* 2017;14(8):442–3.
18. Hu JB, et al. Bioengineering of vascular myocardial tissue; a 3D bioprinting approach. *Tissue Eng A.* 2017;23:S158–9.
19. Ong CS, et al. Biomaterial-free three-dimensional bioprinting of cardiac tissue using human induced pluripotent stem cell derived cardiomyocytes. *Sci Rep.* 2017;7:4566.
20. Misra SK, et al. 3D-printed multidrug-eluting stent from graphene-nanoplatelet-doped biodegradable polymer composite. *Adv Healthc Mater.* 2017;6(11).
21. Jana S, Lerman A. Bioprinting a cardiac valve. *Biotechnol Adv.* 2015;33(8):1503–21.
22. Lee RT, Walsh K. The future of cardiovascular regenerative medicine. *Circulation.* 2016;133(25):2618–25.
23. Matsuda H. The current trends and future prospects of regenerative medicine in cardiovascular diseases. *Asian Cardiovasc Thorac Ann.* 2005;13(2):101–2.
24. Wei K, et al. Epicardial FSTL1 reconstitution regenerates the adult mammalian heart. *Nature.* 2015;525(7570):479–85.
25. van Rooij E. Cardiac repair after myocardial infarction. *N Engl J Med.* 2016;374(1):85–7.
26. Mandel Y, et al. Human embryonic and induced pluripotent stem cell-derived cardiomyocytes exhibit beat rate variability and power-law behavior. *Circulation.* 2012;125(7):883–93.

Index

A

- Acellular bioactive scaffolds, 135
- Acoustic field-guided assembly, 109–111
 - bulk acoustic wave, 111
 - Faraday wave, 111, 112
 - surface acoustic wave (SAW), 113
- Additive manufacturing technologies, 224
- Adenovirus vector (Ad-HGF), 126
- Adipose-derived stem cells (ASCs), 128
- Adult cardiomyocytes, 22, 79, 173, 179
- Adult heart regeneration, 224
- Adult multipotent stem cells, 80
- Adult stem cells
 - bone marrow (BM)-derived, angiogenesis and cardiac regeneration, 178
 - heart regeneration
 - cardiac stem cells (CSCs), 178
 - cardiosphere-derived cells for, 178, 179
- Adults with CHD (ACHD), 208
- Alcain blue staining, 46
- Alginate, 187, 191–195
 - Algisyl-LVR, 193–195, 204
 - α -smooth muscle actin, 192
 - calcium crosslinked alginate hydrogel, 191, 192
 - Fib-Alg material, 191
 - fibrin, 191
 - IK-5001, 193, 195
 - leaky vasculature, 192
 - PRESERVATION-I, 193, 195
 - properties, 191
 - ST-elevation myocardial infarction, 193
- Algisyl-LVR, 187, 193–195
- α -smooth muscle actin (α SMA), 192

- Angiogenesis, 178
- Artificial intelligence, 28
- Artificial vascular grafts, 209
- AuNP, *see* Gold nanoparticles (AuNPs)
- Autologous adult stem cell therapy, 208

B

- Balloon catheter, 186, 192
- Barth syndrome, 24
- Bioassembly
 - acoustic field-guided assembly, 109, 111
 - bulk acoustic wave, 111
 - Faraday wave, 111, 112
 - surface acoustic wave, 113
 - arbitrary patterns of silicone particles, 118
 - cardiac physiological study, 117
 - cardiac regenerative therapy, 116, 117
 - challenges, 118
 - definition of, 108
 - drug screening, 117, 118
 - gravity-driven assembly, 109, 114
 - advantages, 114
 - hanging drop technique, 114
 - micromolding process, 115
 - magnetic field-guided assembly, 109, 113, 114
 - maturation and characterization, 116
 - merits and drawbacks, 110
 - molecular recognition-assisted self-assembly, 109, 115
 - types of, 109, 110
- Biocompatibility, 46, 48, 85, 111, 130, 131
- Biodegradability, 48, 153

- Bioengineering of three-dimensional (3D) cardiac microtissues
- bioassembly, 108
- acoustic field-guided assembly, 109, 111–113
- arbitrary patterns of silicone particles, 118
- cardiac physiological study, 117
- cardiac regenerative therapy, 116, 117
- challenges, 118
- definition of, 108
- drug screening, 117, 118
- gravity-driven assembly, 109, 114, 115
- magnetic field-guided assembly, 109, 113, 114
- maturation and characterization, 116
- merits and drawbacks, 110
- molecular recognition-assisted self-assembly, 109, 115
- types of, 109, 110
- biomaterial-free 3D bioprinting method, 108
- Biofabrication approaches, 108
- Bioinks, 108
- cardiac bioink kits, 71
- characteristics
- mass transfer properties, 68
- post-print processes, 67, 68
- printability, 65, 67
- printed tissue stability and controlled degradation, 68
- tissue-specific and chemically modifiable, 68, 69
- tunable mechanical properties, 69–71
- decellularized extracellular matrices, 52, 53
- definition of, 64
- features of, 65
- hydrogel bioinks, classification of, 66
- Biological pacemakers, 224
- Biomaterial-free 3D bioprinting method, 108
- Biomaterials, 190, 191, 224
- alginate, 191–195
- hyaluronic acid (HA), 197, 198
- mechanism of action, 190
- natural, 191
- synthetic, 191
- tissue derived ECM, 195, 196
- Bio-3D printer, 212
- BL-1040, 193
- Bone marrow cells enriched for the mononuclear fraction (BM-MNCs), 210
- Bone marrow-derived adult stem cell, 178
- Bone marrow-derived mesenchymal stem cells (BM-MSCs), 144
- Bone marrow-derived stem cells (BMSCs), 128
- Bone marrow hematopoietic stem cells (BM-HSC), 149
- Bulk acoustic wave, 111
- C**
- Calcium crosslinked alginate hydrogel, 192
- Calcium-induced calcium release (CICR), 22
- Cardiac cell therapy, 147–152
- Cardiac crescent, 3
- Cardiac extracellular matrix hydrogel (cECM), 36, 39–41, 49, 50, 52–55
- Cardiac fibroblasts (CFs), 113, 180
- Cardiac hypertrophy, 97
- Cardiac muscle patch based cell therapy, *see* Human cardiac muscle patch (hCMP)
- Cardiac patches, 133–135, 216, 217
- Cardiac physiological study, 117
- Cardiac stem cells (CSCs) for heart regeneration, 129, 178
- Cardiac tissue engineering, 109, 113
- Cardiogenic follistatin like-1 protein, 224
- Cardiometabolic diseases, 24
- Cardiomyocyte regeneration, 174, 175
- Cardiosphere-derived cells for cardiac regeneration, 216
- Cardiosphere-derived cells for heart regeneration, 178, 179
- Cardiotoxicity, 117, 118
- Cardiovascular network, 36
- Cardiovascular stem cell models, molecular maturity of, 5–7
- Cardiovascular tissue bioprinting, 63
- Cardiovascular tissue engineering technology
- cell sheets, 132, 133
- cytokines and growth factors (GFs), 126, 127
- hydrogels, 130–132
- stem cell therapy, 127–129
- 3D scaffolds/cardiac patches, 133–135
- cECM, *see* Cardiac extracellular matrix hydrogel (cECM)
- Cell-based regenerative therapy, 174
- adult stem cells
- bone marrow (BM)-derived, angiogenesis and cardiac regeneration, 178
- cardiac stem cells (CSCs) for heart regeneration, 178
- cardiosphere-derived cells for heart regeneration, 178, 179
- pluripotent stem cells (*see* Pluripotent stem cells (PSCs))

- proliferative cardiomyocytes
 - heart regeneration, gene modification for, 179
 - heart regeneration, small RNAs and signalings for, 179, 180
 - transdifferentiation from cardiac fibroblasts, 180
 - Cell reprogramming process, 174
 - Cell sheets, cardiovascular tissue engineering technology, 132, 133
 - Cell therapy, 80
 - Cellular imprinting, 89
 - Chemically crosslinked hydrogels, 186
 - Chronic heart failure (CHF), 193
 - Cisapride, 25
 - CM populated matrix (CMPM), 142
 - Collagen, 82, 90, 154, 177
 - Comprehensive in vitro Proarrhythmia Assay (CiPA), 26
 - Conductive nanomaterials, 89, 90
 - high-aspect ratio conductive nanomaterials, 93–95
 - spherical conductive nanoparticles, 90, 91, 93
 - Congenital heart diseases (CHDs), treatment of
 - cardiac patches, 216, 217
 - Fontan procedure, 208
 - patent Ductus arteriosus, ligation of, 208
 - stem cell therapy, 215, 216
 - tissue-engineered blood vessels, 209–212
 - tissue-engineered heart vessels, 213–215
 - CorMatrix™, 214
 - Coronary artery bypass grafting (CABG), 194
 - Coronary heart disease (CHD), 125
 - Cryopreserved homografts, 209
 - Cytokines, 126, 127
- D**
- Decellularized extracellular matrices, 35, 36, 191
 - characterization, 46–48
 - crosslinking and sterilization, 48, 49
 - formats
 - bioink, 52, 53
 - culture coating, 49
 - injectable materials, 50
 - patches, 50, 51
 - whole organ decellularization, 51
 - localized therapeutic delivery vehicles in non-ischemic diseases, 58
 - methods for decellularization
 - blood vessels, 42, 43
 - cardiac valves, 41, 42
 - cell-derived matrices, 44
 - myocardium and pericardium, characterization of, 36–41
 - of plant tissue, 44
 - myocardial application of
 - cardiac-derived matrices, 53, 54
 - hybrid scaffolds, 54–56
 - non-cardiac-derived matrices, 54
 - in pre-clinical and clinical trials, 56–58
 - repair of cardiac valves and blood vessels, 56
 - Decellularized pulmonary allograft, 213
 - Decellularized sheep pulmonary valve allografts, 57
 - Dilated cardiomyopathy (DCM), 4, 7
 - Direct protein therapy, 130
 - Droplet-based bioprinting, 64
 - Drug-induced cardiotoxicity, 107
 - Drug-induced tachyarrhythmias, 25
 - Drug screening, 117, 118
- E**
- Ejection fraction (EF), 186
 - Elasticity, 146
 - Electrospun polyurethane (PU) scaffolds, 85
 - Electrospun scaffolds, 5
 - Embryoid body (EB)-driven method, 12, 175
 - Embryonic stem cell (ESC), 2, 3, 144, 174, 175
 - Embryonic stem cell (ESC)-derived cardiomyocytes, 22
 - Embryonic stem cell (ESC)-derived cells, 150
 - Endothelial cells (ECs), 10, 11
 - Endothelial colony-forming cells (ECFC), 11
 - Engineered heart tissues (EHTs), 4, 6, 23, 24, 156, 157
 - application, 157
 - cell sources, 143–146
 - CM populated matrix (CMPM), 142
 - collagen-Matrigel matrix, 142
 - engineered heart tissue self-assembly, 5
 - ESCORT trial, 143
 - fibrous scaffolds, 5
 - hydrogel based engineered heart tissues, 4, 5
 - hypertrophic cardiomyopathy, 4
 - mechanisms, 153, 154
 - scaffolds, 146, 153
 - self-assembly, 5
 - Engineering nanocarriers for cardiac tissue repair, 95–98
 - CX-43 expression, 96
 - magic bullet, 96
 - magnetotactic bacteria, 96

- Engineering nanotopography of cardiac tissue scaffolds, 83
- cellular imprinting, 89
 - molecular imprinting, 89
 - nanofibrous scaffolds, 84–86
 - nanofibrous surfaces, 83, 84
 - nanoscale surface structures, 83, 84
 - surface nanostructures, 86, 88
- Enzymatic-based methods, 42
- Exogenous materials, use of, 223
- Expanded polytetrafluoroethylene (Gore-Tex®), 209
- Extracel-HP gel, 200
- Extrusion-based bioprinter, 64
- F**
- Fallot/hypoplastic left heart syndrome, 207
- Familial arrhythmogenic disorders, 24
- Faraday wave, 111, 112
- Femoro-popliteal bypass surgery, 209
- Fib-Alg material, 191
- Fibrin, 134, 154, 191
- Fibrotic remodeling, 54
- Fibrous scaffolds, 5
- Fluorescence activated cell sorting (FACS), 11
- Fontan procedure, 208
- Frank-Starling law, 185
- Functional tissue bioprinting, 64
- G**
- Gelatin methacrylate (GelMA), 113
- Gel-based design strategy, 4
- Gene modification for cardiomyocyte proliferation and heart regeneration, 179
- Genetic cardiac disorders, disease models of, 7–10
- Gold nanoparticles (AuNPs), 90, 91
- Gravity-driven assembly, 109, 110, 114
- advantages, 114
 - hanging drop technique, 114
 - micromolding process, 115
- Growth factors (GFs), 126, 127
- H**
- Hanging drop technique, 114
- Heart attack, *see* Myocardial infarction (MI)
- Heart failure (HF), 19, 79, 125–130, 153, 185, 186, 195, 215–217
- Heart regeneration
- cardiomyocyte proliferation
 - gene modification for, 179
 - small RNAs and signalings, 179, 180
 - cardiosphere-derived cells for, 178, 179
 - CSC for, 178
- Hepatic spheroids, 112
- Hepatocyte growth factor (HGF), 126
- High-aspect ratio conductive nanomaterials, 93–95
- High throughput (HT) instrumentation, 20
- HiPSCs, *see* Human induced pluripotent stem cells (HiPSCs)
- Human cardiac muscle patch (hCMP)
- engraftment rate, 158–160
 - functional assessment, 157
 - manufacturing, 155
 - patch implantation, 157, 158
 - patch size, 155, 156
 - poly(N-isopropyl acrylamide) (PIPAAm), 154
 - sheet-based patches, 154
 - vascularization, 156, 157
- Human embryonic stem cell-derived cardiac progenitor cells, 217
- Human embryonic stem cells-derived cardiomyocytes (hESC-CMs), 177, 215
- Human embryonic stem cells (hESCs), 80, 94, 208
- Human induced pluripotent stem cell-derived cardiac progenitor cells, 51
- Human induced pluripotent stem cell-derived cardiomyocytes (hiPSC-CMs), 112
- Human induced pluripotent stem cells (HiPSCs), 10, 94, 143
- endothelial cells (ECs), 10, 11
 - vascular smooth muscle cells (VSMCs)
 - from, 11–13
- Human PSCs (hPSCs), 175
- Human umbilical vein endothelial cells (HUVECs), 80, 115
- Hutchison-Gilford Progeria Syndrome (HGPS), 13
- Hyaluronic acid (HA), 187, 191, 197, 198
- Hydrogel-based bioinks, 63, 64, 71
- Hydrogels
- based engineered heart tissues, 4, 5
 - cardiovascular tissue engineering
 - technology, 130–132
 - definition of, 186
- Hydroxyethyl methacrylate (HEMA) hydrogel, 197, 199
- Hypertrophic cardiomyopathy (HCM), 4, 7, 9, 10
- Hypoplastic left heart syndrome (HLHS), 215
- I**
- I_{K1} deficiency, 22
- Induced pluripotent stem cells (iPSC), 2–5, 7–9, 80, 145, 174, 175, 208
- Induced pluripotent stem cells (iPSCs)-derived cardiomyocytes, 20

- to assess cardiotoxicity, 25, 26, 28
 - for disease modeling and drug discovery, 24, 25
 - drawbacks, 81
 - immaturity, 22, 23
 - Ca²⁺ handling, 22
 - engineered heart tissues (EHTs), 23, 24
 - β2 AR, 23
 - Induced pluripotent stem cells (iPSCs)-derived cells, 151
 - Interdigital transducer (IDT), 113
 - In vitro disease modeling, 2
 - Ischemic cardiomyopathy, 133
 - Ischemic heart diseases, 141
 - engineered heart tissues
 - cell sources, 143–146
 - CM populated matrix (CMPM), 142
 - collagen-Matrigel matrix, 142
 - ESCORT trial, 143
 - mechanisms, 153, 154
 - scaffolds, 146, 153
 - human cardiac muscle patch (hCMP)
 - engraftment rate, 158–160
 - functional assessment, 157
 - manufacturing, 155
 - patch implantation, 157, 158
 - patch size, 155, 156
 - poly(N-isopropyl acrylamide) (PIPAAm), 154
 - sheet-based patches, 154
 - vascularization, 156, 157
- K**
- Ki67 expression, 90
- L**
- Laser-based bioprinters, 64
 - Leaky vasculature, 192
 - Left ventricular assist device (LVAD), 128, 133, 216
 - Left ventricular ejection fraction (LVEF), 215, 216
 - Left ventricular end diastolic volume index (LVEDVI), 193
 - Left ventricular remodeling, 142, 186, 190, 193, 194, 199
 - Leveraging the body's endogenous regenerative mechanisms, 223
 - LipoPEG-PA13, 98
- M**
- Magnelles®, 96
 - Magnetic field-guided assembly, 109, 110, 113, 114
 - Magnetic-activated cell sorting (MACS), 11
 - Magnetotactic bacteria (MB), 96
 - Masson's trichrome staining, 46, 201
 - Matrigel®, 177
 - Matrix metalloproteinases (MMPs), 185, 199, 200
 - Matrix stiffness, 70, 146, 154
 - Mesenchymal stem cells (MSCs), 96, 144, 149, 153, 202, 203, 216
 - Metabolic diseases, 24
 - Methacrylate modified gelatin (gelMA), 67
 - Micromolding assembly, 115
 - Microscale, 82
 - Molecular imprinting, 89
 - Molecular recognition-assisted self-assembly, 109, 110, 115
 - Monolayer culture model, 12
 - Multicellular spheroids (MCS), 212
 - Multielectrode array (MEA), 26
 - Murine embryonic stem cell cardiomyocyte (mESC-CM), 177
 - Murine embryonic stem cell (mESCs), 177
 - Myocardial Assistance by Grafting a New Bioartificial Upgraded Myocardium (MAGNUM) trial, 134
 - Myocardial infarction (MI), 143
 - definition of, 185
 - stiff fibrous scar, 185
 - Myocardial infarction (MI), injectable hydrogel to
 - biologics delivered
 - benefits of, 198
 - Extracel-HP gel, 200
 - NFs, 198
 - PEG hydrogel, 200
 - PRP, 200, 201
 - rTIMP-3, 199, 200
 - TIMP-3 gel, 199
 - UPy-hydrogel, 200
 - VEGF, 199
 - biomaterials, 190, 191
 - alginate, 191–195
 - hyaluronic acid (HA), 197, 198
 - mechanism of action, 190
 - natural, 191
 - synthetic, 191
 - tissue derived ECM, 195, 196
 - cells delivered, 201–203
 - clinical trials, 189
 - encapsulating cells and biologic molecules, 203
 - large animal pre-clinical studies, 187–188
 - porcine or ovine models, 186
 - properties of, 186, 190
 - Myocardial matrix hydrogel, 195, 196
 - Myocardial patches, 56
 - Myocyte hypertrophy, 186

- Myocyte slippage, 186
 Myofibroblasts, 213
 Myostar catheter, 196
- N**
- Nano-biomaterials, 99
 bottom-up engineering strategies, 99
 conductive nanomaterials, 89, 90
 high-aspect ratio conductive nanomaterials, 93–95
 spherical conductive nanoparticles, 90, 91, 93
 engineering nanocarriers for cardiac tissue repair, 95–98
 engineering nanotopography of cardiac tissue scaffolds, 83
 cellular imprinting, 89
 molecular imprinting, 89
 nanofibrous scaffolds, 84–86
 nanofibrous surfaces, 83, 84
 nanoscale surface structures, 83, 84
 surface nanostructures, 86, 88
 nanoscale, heart at, 82, 83
 nanotechnology, 81, 82
 top-down strategies, 98
- Nanofibers (NFs), 198, 203
 Nanomaterials, 83
 Nanoparticulate systems, 83
 Nanopillars, 88, 95
 Nanoscale, 80, 82, 83
 Nanotechnology, 81, 82
 Natural biomaterials, 191
 Natural/fabricated solid scaffolds, 5
 Neonatal cardiomyocytes, 208
 Neovascularization, 156
 Neuregulin-1 (NRG-1), 127
 Neutral lipid storage disease (NLS D), 24
 Neutral lipid storage disease with myopathy (NLS D-M), 24
 NOGA™ mapping, 196, 200, 204
- O**
- Organoid technology, 5
- P**
- Patient-derived cardiomyocytes, 21, 107
 Percutaneous coronary intervention (PCI), 125, 193
 Phenotypic screening for iPSCs-derived cardiomyocytes, *see* Induced pluripotent stem cells (iPSCs)-derived cardiomyocytes
- Physical hydrogel, 186
 Picogreen assay, 46
 Piezoelectric (PZT) substrate, 113
 Platelet rich plasma (PRP), 200, 201
 Pluripotent stem cells (PSCs)
 definition, 2
 cardiomyocytes and their maturation
 PSC-CMs in regenerative cardiac therapy, 176, 177
 regeneration, 174, 175
 and their maturation, 175, 176
 Pluripotent stem cells-derived cardiomyocytes (PSC-CMs), 176
 Polycaprolactone diol (PCL) soft segment, 85
 Poly (di methyl siloxane) (PDMS), 89
 Polyethylene glycol (PEG), 155, 191, 201
 Polyethylene terephthalate (Dacron®), 209
 Polyglycolic acid (PGA), 154
 Poly (lactic-glycolic acid) (PLGA), 85, 86
 Polyurethane (PU), 154
 Ponatinib, 28
 Primary cardiac cells, 148
 Proliferative cardiomyocytes, heart regeneration
 gene modification for, 179
 small RNAs and signalings, 179, 180
 Protein-based materials, 191
 Pulmonary capillary wedge pressure (PCWP), 200
- R**
- Recombinant tissue inhibitor of matrix metalloproteinase-3 (rTIMP-3), 199, 200
 Right ventricle outflow tract (RVOT) stenosis, 57
 Ross procedure, 213
- S**
- Scanning electron microscopy (SEM), 46
 Shear-thinning hydrogel for injectable encapsulation and long-term delivery (SHIELD), 131
 Sibutramine, 25
 Silver (Ag) nanoparticles, 90
 Skeletal myoblast, 147
 Small RNAs and signalings, 179, 180
 Smooth muscle cells (SMCs), 132, 144
 Sodium dodecyl sulfate (SDS), 42, 49
 Sodium dodecyl sulfate (SDS)-based decellularization, 42
 Spatial modulation of magnetization (SPAMM), 197

- Spherical conductive nanoparticles, 90, 91, 93
 Standing surface acoustic wave (SSAW), 113
 ST-elevation myocardial infarction (STEMI), 193
 Stem cell therapy
 cardiovascular tissue engineering technology, 127–129
 for CHD, 215, 216
 Stromal cell-derived factor-1 α (SDF-1), 127
 Submucosa-derived extracellular matrix (SIS-ECM), 214
 Supravalvular aortic stenosis (SVAS), 14
 Surface acoustic wave (SAW), 113
 Synergraft™, 214
 Synthetic biomaterials, 191
 Synthetic polymers, 154, 191
- T**
 Target-centric drug discovery, 25
 Terfenadine, 25
 Three-dimensional (3D) engineered heart tissues (EHTs), 23
 3D bioprinting, 224
 bioink
 cardiac bioink kits, 71
 definition of, 64
 features of, 65
 hydrogel bioinks, classification of, 66
 mass transfer properties, 68
 post-print processes, 67, 68
 printability, 65, 67
 printed tissue stability and controlled degradation, 68
 tissue-specific and chemically modifiable bioinks, 68, 69
 tunable mechanical properties, 69–71
 droplet-based bioprinting, 64
 extrusion-based bioprinter, 64
 laser-based bioprinters, 64
 3D cardiac tissue engineered scaffolds, 155
 3D scaffolds/cardiac patches, 133–135
 Tissue derived extracellular matrix, 195, 196
 Tissue-engineered blood vessels (TEBVs), 13, 14, 209–212
 acellular grafts, 212
 Bio-3D printer, 212
 biomatrix, 212
 BM-MNCs, 210
 components, 210
 Dacron®, 209
 fibrin scaffold, 212
 Gore-Tex®, 209
 MCS, 212
 natural polymers, 212
 TEVG, 211
 TEVGs, 210, 211
 Tissue-engineered heart valves (TEHVs), 213–215
 Tissue engineered stem cell models
 cardiovascular disease models
 cardiovascular stem cell models, molecular maturity of, 5–7
 differentiation protocols, 3, 4
 engineered heart tissues (*see* Engineered heart tissues (EHTs))
 genetic cardiac disorders, disease models of, 7–10
 patient specific, 3
 induced pluripotent stem cells, 2, 3
 vascular disease models
 endothelial cells (ECs) from hiPSCs, 10, 11
 tissue engineered blood vessels (TEBVs), 13, 14
 vascular differentiation protocols, 10
 vascular smooth muscle cells (VSMCs) from hiPSCs, 11–13
 Tissue-engineered vascular grafts (TEVGs), 210–212
 Tissue engineering (TE), 58, 80, 142, 208, 224
 Tissue inhibitor of MMP-3 (TIMP-3), 199
 Titin truncating mutations (TTNtv), 8
 Triton X-100, 39, 42
 Two-dimensional (2D) cardiac monolayers, 118
 Two-dimensional (2D) cell culture methods, 2
 Two-dimensional (2D) monolayer culture, 107
- U**
 Ureido-pyrimid-ionine (UPy) hydrogel, 200, 201
- V**
 Vascular endothelial growth factor (VEGF), 10, 117, 126, 198, 199
 Vascular smooth muscle cells (VSMCs), 10–14
 Vascularization, 116, 156, 157
 VentriGel, 196
 Verhoeff-Van Gieson staining, 46
- W**
 Whole organ decellularization, 51
- Z**
 Zebrafish cECM, 53